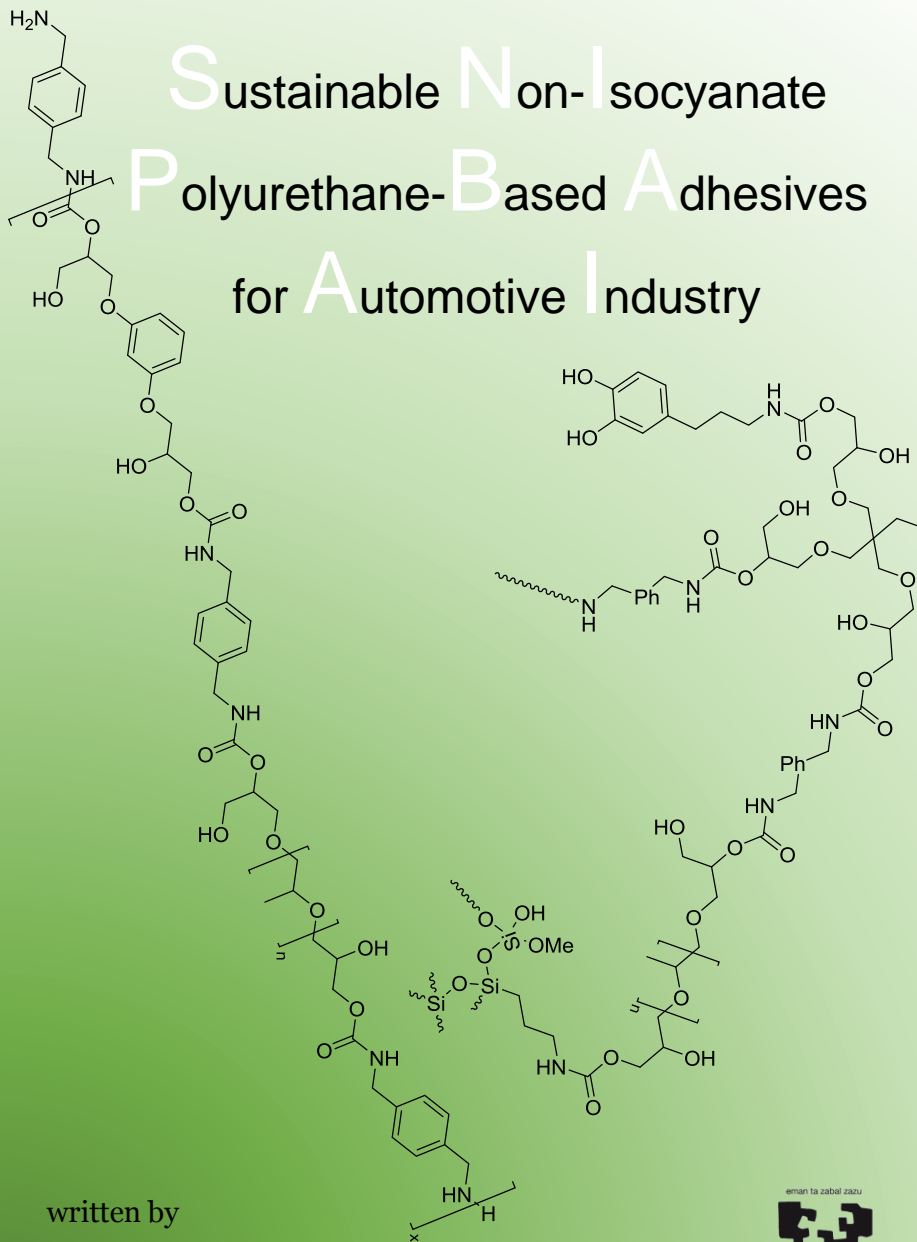


Sustainable Non-Isocyanate
Polyurethane-Based Adhesives
for Automotive Industry



written by

Álvaro Gómez López

PhD Thesis 2021

eman la zabal zaku

Universidad del País Vasco Euskal Herriko Unibertsitatea

Sustainable Non-Isocyanate
Polyurethane-Based Adhesives for
Automotive Industry

ÁLVARO GÓMEZ LÓPEZ

SUPERVISOR: HARITZ SARDON MUGURUZA

TESIS DOCTORAL OCTUBRE 2021

Sustainable Non-Isocyanate Polyurethane-Based Adhesives for Automotive Industry

A manuscript submitted to the

University of the Basque Country (UPV/EHU)

for the degree of

PhD in Applied Chemistry and Polymeric Materials

written by

Álvaro Gómez López

under the supervision of

Dr. Haritz Sardon (UPV/EHU)

with the collaboration of

Dr. Iñigo Calvo (Oribay Automotive Group)

Donostia/San Sebastián

October 2021

A btract

Conventional polyurethane (PU)-based adhesives are the main choice when high-performance applications are required since their excellent and tunable properties, which stems from the vast commercially available polyisocyanate and polyol precursors. Nevertheless, current trends for more sustainable and greener production of polymers have pushed researchers to develop new strategies of PU synthesis for avoiding the use of toxic isocyanate. Thus, in the last decade Non-Isocyanate Polyurethanes (NIPUs) have emerged as the most appealing alternative for the substitution of PUs. Among the different synthesis routes, polyaddition of poly(cyclic carbonate)s with polyamines, which produces poly(hydroxy urethane)s (PHUs), is usually the preferred option to prepare NIPUs since the reaction present 100% atom economy and the facile chemical [3+2] CO₂ insertion into epoxy resins to prepare 5-membered cyclic carbonate monomers. Nevertheless, the low reactivity of 5-membered cyclic carbonates gives rise to slow polymerizations, which requires elevate temperatures or catalysts to achieve high conversions with the consequent increment of side reactions. In this thesis, the combination of NIPU with other chemistries, such as sol-gel of alkoxy silanes and epoxy resins, was the main point to overcome the limitations of this family of polymers. Thus, a monocomponent adhesive was prepared by functionalization of a cyclic carbonate-terminated PHU prepolymer based on poly(propylene glycol) dicyclic carbonate (PPGdiCC) with 3-(aminopropyl)triethoxysilane (APTES). Incorporation of APTES allowed the curing at ambient conditions of the adhesive. Increasing of the curing temperature up to 100 °C and addition of 1 wt% of acetic acid not only decreased the gel time fivefold but also enhanced the PHU with better adhesion properties on stainless steel. The incorporation of greater amounts of hard monomer%, i.e. resorcinol dicyclic carbonate (RdiCC), up to 40 mol% resulted in adhesives with better cohesiveness increasing lap-shear strength values. In a second step, APTES was substituted by 3-(aminopropyl)trimethoxysilane (APTMS) for faster curing while dopamine hydrochloride (DOP) was added as adhesion promoter into new PHU formulations

based on trifunctional cyclic carbonate, trimethylolpropane tris(cyclic carbonate) (TMPTC) and aromatic diamine, *m*-xylylenediamine (MXDA). Combination of both additives kept adhesive properties while decreasing gel time quantitatively (fourfold) due to fast curing of APTMS. Best performance of 70/30 TMPTC/PPGdiCC molar ratios reasserted the requirement of well-balanced soft to hard ratios for obtaining better adhesion performance. Due to the requirement of high temperature (100 °C) during the curing step for obtaining good adhesion performance of these compositions, the incorporation of epoxy chemistry into the formulations was further considered in order to improve curing times as well as adhesion performance when curing process was carried out under ambient conditions. Amino-terminated PHU (A-PHU) based on 60/40 PPGdiCC/RdiCC molar ratio was combined with a viscous low-molar mass epoxy resin and a trifunctional thiol, trimethylolpropane tris(3-mercapto propionate) (TMPTMP), obtaining materials with excellent lap-shear strength as well as shear resistance under temperature and load. Adhesives based on 70/30 A-PHU/TMPTMP equivalent ratio was able to develop handle strength within 3 h. Finally, the curing process was accelerated by adding 0.875 mol% of a strong base, i.e. 1,1,3,3-tetramethylguanidine (TMG), decreasing greatly the gel time of the formulations. Seeking structural adhesives for automotive industry, compositions with hot-melt adhesive properties were also developed. Thus, an in-depth study of the influence of the monomers on the behavior of these adhesives is addressed combining mixtures of different dicyclic carbonates (PPGdiCC, RdiCC and 1,4-Butanediol dicyclic carbonate, BdiCC) with aromatic (*m*- and *p*-xylylenediamine), cycloaliphatic [1,3-cyclohexanebis(methylamine)] and aliphatic diamines (hexamethylenediamine and 1,12-diaminododecane). Incorporation of the aliphatic diamines into the formulations gave rise to materials, which exhibited rubbery behavior due to less steric hindrance and therefore, stronger hydrogen bonding of the chains. On the other hand, aromatic- and cycloaliphatic-based compositions presented stickiness at 100 °C to wet the surface of the adherends, while at

room temperature cohesiveness of the polymers was enough to keep substrates together up to 10.0 ± 1.2 MPa. Finally, hot-melt adhesives were endowed with higher service temperatures, up to 119 ± 12 °C, by adding 15 wt% of D.E.R.TM 671 epoxy resin. Thermo-reversibility of all hot-melt adhesives was demonstrated through subsequent re-bonding of the adherends without losing adhesion performance.

Resumen

Los adhesivos basados en poliuretanos convencionales (PUs) son la principal elección cuando se requieren aplicaciones con altas prestaciones gracias a sus excelentes y moldeables propiedades, que residen en la combinación de la amplia variedad comercial de poliisocianatos y polioles. Sin embargo, las tendencias actuales hacia rutas de producción de polímeros que sean más sostenibles y respetables con el medio ambiente han llevado a los investigadores al desarrollo de nuevas estrategias de síntesis para evitar el uso de los PUs basados en isocianatos, compuestos altamente tóxicos. Así, en la última década los poliuretanos libres de isocianato (NIPUs) han surgido como la opción más prometedora como alternativa a los poliuretanos convencionales. Dentro de las diferentes estrategias que existen, la poliadición de poli(carbonatos cíclicos) con poliaminas, la cual produce poli(hidroxi uretano)s (PHUs), es generalmente la opción preferida para la preparación de NIPUs debido a que la reacción de polimerización tiene lugar con un 100% de economía atómica, sin generarse productos no deseados, y la inserción química de CO₂ en resinas epoxi para la síntesis de los carbonatos cíclicos mediante procesos optimizados, resulta un proceso sencillo para la síntesis de los monómeros. No obstante, la baja reactividad de los carbonatos cíclicos de cinco miembros da lugar a polimerizaciones lentas, que requieren elevadas temperaturas o catalizadores para alcanzar conversiones altas, lo que conlleva reacciones secundarias no deseables. En esta tesis, para resolver este problema se ha llevado a cabo la combinación de la química de los NIPUs con otras como la química de sol-gel de compuestos alcóxidosilanos o epoxis. Por consiguiente, se preparó un adhesivo monocomponente a través de la funcionalización de un prepolímero basado en PHU de poli(propileno glicol) carbonato dicíclico (PPGdiCC) y resorcinol carbonato dicíclico (RdiCC) con 3-(aminopropil)trióxidosilano (APTES). La incorporación de APTES permitió el curado de los adhesivos bajo condiciones ambiente. El aumento de la temperatura y la adición de 1% en peso de ácido acético no solo redujo cinco veces el tiempo de gelación sino que también mejoró las propiedades adhesivas de los PHUs en acero inoxidable. La integración

de mayores cantidades de RdiCC, hasta el 40% en mol, resultó en una mejora de la cohesividad de los adhesivos incrementando los valores de lap-shear. En un Segundo paso, APTES fue remplazado por 3-(aminopropil)trimetoxisilano (APTMS) para un curado más rápido mientras que dopamina hidrociorada (DOP) se añadió como un promotor de la adhesión a las formulaciones basadas en un carbonato cíclico trifuncional (trimetilopropano tris(carbonato cíclico), TMPTC) y una diamina aromática (*m*-xililendiamina). La combinación de ambos aditivos fue capaz de mantener las propiedades adhesivas de las formulaciones base, mientras que redujo los tiempos de curado hasta 4 veces el de la formulación de referencia. La formulación de ratio molar 70/30 de TMPTC/PPGdiCC mostró el mejor rendimiento reafirmando el requisito de formulaciones que tengan un balance entre el segmento flexible y duro adecuado para desarrollar las mejores propiedades. Debido a que las composiciones ya mencionadas requirieron la utilización de altas temperaturas (100 °C) durante el curado para obtener buenas propiedades adhesivas, se tuvo en cuenta la integración de resinas epoxi en las formulaciones para la mejora de estas propiedades con un curado llevado a cabo a temperatura ambiente. PHUs basados en un ratio molar 60/40 PPGdiCC/RdiCC y terminados en grupos amino (A-PHU) fueron mezclados con una resina epoxi de bajo peso molar y un tiol trifuncional, trimetilopropano tris(3-mercaptopropionato) (TMPTMP), obteniendo materiales con excelentes valores de lap-shear así como resistencia a la cizalla soportando una carga de 1 kg y temperaturas de hasta 217 °C. El adhesivo basado en un ratio molar 70/30 de A-PHU/TMPTMP fue capaz de desarrollar fuerzas de manejo en tres horas después de la aplicación. Finalmente, el proceso de curado fue acelerado con la incorporación de 0.875% en mol de una base fuerte, i.e. 1,1,3,3-tetrametilguanidina (TMG), acortando el tiempo de gelación notablemente. En la búsqueda de adhesivos estructurales para la industria de la automoción, se desarrollaron también productos que presentaron propiedades de adhesivos hot-melt. Por ello, se presenta un estudio en profundidad de la influencia de los monómeros sobre el

comportamiento de estos adhesivos. Para ello se combinaron diferentes mezclas de carbonatos dicíclicos (PPGdiCC, RdiCC y 1,4-butanodiol carbonato dicíclico BdiCC) con aminas aromáticas (*m*- y *p*-xililendiamina), cicloalifáticas [1,3-ciclohexanobis(metilamina)] and alifáticas (hexametilendiamina and 1,12-diaminododecano). La incorporación de las diaminas alifáticas dio lugar a materiales cauchosos debido a el menor impedimento estérico y, por tanto, enlaces de puente de hidrógeno de mayor fuerza. Por otro lado, tanto las composiciones basadas en diaminas aromáticas como la cicloalifática presentaron pegajosidad a 100 °C siendo capaces de mojar la superficie de los substratos, mientras que a temperatura ambiente la cohesividad de los polímeros fue suficiente para mantener unida la junta hasta valores de 10.0 ± 1.2 MPa. Finalmente, la temperatura de servicio de los adhesivos hot-melt fue mejorada hasta 119 ± 12 °C con la adición de un 15% en peso de resina epoxi, D.E.R.TM 671. La termo-reversibilidad de todas las composiciones de adhesivos hot-melt se demostró a través de sucesivos ensayos de lap-shear, despegando y volviendo a pegar los substratos sin perder los adhesivos sus propiedades.

Table of Contents

List of Acronyms and Symbols.....	XXI
-----------------------------------	-----

Chapter 1 – Poly(Hydroxy Urethane) Adhesives: State-of-the-Art	1
1.1. Introduction	3
1.2. Main processing methods and applications of PU adhesives.....	6
1.3. Test for evaluating the performance of adhesives.....	9
1.4. Approaches for the preparation of NIPU-based adhesives	11
1.5. Motivation and objectives of the thesis	20

Chapter 2 – Monocomponent Non-Isocyanate Polyurethane Adhesives Based on a Sol-Gel Process.....	23
2.1. Introduction	25
2.2. Synthesis of triethoxysilane-terminated PHUs oligomers and their curing	27
2.3. Evaluation of the adhesive properties of the hybrid PHU products	35
2.4. Evaluation of the adhesive properties of the hybrid PHU at room temperature	39
2.5. Conclusions.....	40

Chapter 3 – Synergetic Synergetic Effect of Dopamine and Alkoxysilanes in Sustainable Non-Isocyanate Polyurethane Adhesives.....	43
3.1. Introduction	45
3.2. Influence of additives on PHU adhesive formulation	47
3.2.1. Synthesis and characterization of adhesives	47
3.2.2. Adhesive properties evaluation of initial compositions.....	50
3.3. Optimal hard/soft segment balance for well-designed adhesives.....	54
3.4. Effect of Dopamine and APTMS on balanced neat formulations	57
3.5. Conclusions	61

Chapter 4 – Fast-Curing Room Temperature Poly(Hydroxy Urethane)-Epoxy hybrid Adhesives	63
4.1. Introduction	65
4.2. Synthesis of amino-terminated PHUs oligomers	70
4.3. Synthesis of PHU-epoxy hybrid adhesives	72
4.4. Evaluation of the adhesive properties of the hybrid PHUs	78
4.4.1. Ultimate adhesive properties.....	79
4.4.2. Lap-shear strength evolution over time	82
4.5. Conclusions	83

Chapter 5 – Enhanced and Reusable Poly(Hydroxy Urethane)-Based Low-temperature Hot-Melt Adhesives 85

5.1. Introduction.....	87
5.2. PHU homopolymers: synthesis and rheology.....	90
5.3. Preparation of MXDA-based copolymer compositions.....	95
5.3.1. Synthesis and Characterization ...	95
5.3.2. Rheology of the copolymers ...	98
5.3.3. Adhesive properties of PHU hot-melt adhesives.....	103
5.4. Influence of the monomer structure in the rheological behavior and adhesives properties of the copolymers.....	108
5.4.1. Copolymers based on aliphatic dicyclic carbonates.....	108
5.4.1.1. Synthesis and characterization of 50/50BdiCC-MXDA.....	108
5.4.1.2. Rheology of 50/50BdiCC-MXDA.....	109
5.4.1.3. Adhesive properties of 50/50BdiCC-MXDA.....	110
5.4.2. Tuning PHU Hot-Melt adhesives by changing the diamine structure..	112
5.4.2.1. Synthesis and characterization of copolymers based on different diamines.....	112
5.4.2.2. Rheology of the copolymers based on different diamines.....	113
5.4.2.3. Diamine influence on adhesion properties of PHU Hot-Melt adhesives.....	117

5.4.2.4. Adhesive performance on different substrates.....	120
5.5. Enhanced hot-melt adhesives.....	121
5.6. Conclusions.....	124

Chapter 6 – Conclusions and Outlook 127

Appendix I – Methods 135

A-I.1. Instrumentation and characterization techniques.....	137
A-I.2. Materials.....	145
A-I.3. Experimental part.....	146
A-I.3.1. General.....	146
Typical procedure for the synthesis of cyclic carbonates.....	146
Titration of the cyclic carbonate by ¹ H NMR.....	146
A-I.3.2. Chapter 2.....	147
Typical procedure for PHU prepolymer preparation.....	147
Typical procedure for alkoxy silane prepolymer preparation.....	148
A-I.3.3. Chapter 3.....	148
Typical procedure for PHU adhesive preparation.....	148
A-I.3.4. Chapter 4.....	149
Typical procedure for amino-terminated PHU oligomer preparation.....	149
Titration of the A-PHUs by ¹ H NMR.....	150
Typical procedure for the synthesis of hybrid materials.....	150
A-I.3.5. Chapter 5.....	151

Typical procedure for PHU homopolymer preparation.....	151
Typical procedure for PHU copolymer preparation.....	152
Typical procedure for enhanced hot-melt adhesive preparation	152

Appendix II – Supporting Information 153

A-II.1. General	155
A-II.2. Chapter 2.....	160
A-II.3. Chapter 3.....	162
A-II.4. Chapter 4.....	167
A-II.5. Chapter 5.....	171

References..... 187

List of Publications, Collaborations and Contributions 205

List of Acronyms and Symbols

®	Registered mark
°C	Celsius degree
1,12-DAD	1,12-Diaminododecane
1,3-bis HFIB	1,3-Bis(2-hydroxyhexafluoroisopropyl)benzene
¹ H NMR	Proton Nuclear Magnetic Resonance
1K	One-component
2K	Two-component
AEW	Amine Equivalent Weight
AHEW	Active Hydrogen Equivalent Weight
Al	Aluminum
A-PHU	Amino-terminated Poly(Hydroxy Urethane)
APTES	3-(aminopropyl)triethoxysilane
APTMS	3-(aminopropyl)trimethoxysilane
ASTM	American Society for Testing and Materials
ATR	Attenuated Total Reflectance
BDGE	1,4-Butanediol diglycidyl ether
BdiCC	1,4-Butanediol dicyclic carbonate
BPA	Bisphenol-A
CBMA	1,3-cyclohexanebis(methylamine)
CDCl ₃	Deuterated Chloroform
CESBO	Carbonated-epoxidized soybean oil
CEW	Carbonate Equivalent Weight
CH ₃ OH-d ₄	Deuterated Methanol
d	Day
DBU	1,8-Diazabicyclo[5.4.0]undec-7-ene
DIN	German Institute for Standardization (Deutsches Institut für Normung)
DMSO-d ₆	Deuterated Dimethyl sulfoxide
DMTA	Dynamic Mechanical Thermal Analysis
DOP	Dopamine hydrochloride
DSC	Differential Scan Calorimetry
E'	Storage modulus
E''	Loss modulus

E _a	Activation Energy
EEW	Epoxy Equivalent Weight
EN	European Standard
eq	Equation
equiv	Equivalent
EWC	Equilibrium Water Content
FT-IR	Fourier Transform Infrared
g	Gram
G'	Storage modulus
G''	Loss modulus
GC	Gel Content
h	Hour
HAc	Acetic acid
HCl	Hydrochloric Acid
HMA	Hot-Melt Adhesive
HMDA	Hexamethylenediamine
H-NIPU	Hybrid NIPU
Hz	Hertz
K	Kelvin degree
min	Minute
mm ²	Square millimeter
M _n	Number-Average Molar Mass
MSA	Methanesulfonic acid
M _w	Weight-Average Molar Mass
MXDA	<i>m</i> -Xylylenediamine
N	Newton
N ₂	nitrogen
NaOH	Sodium Hydroxide
NCO	Isocyanate
NIPU	Non-Isocyanate Polyurethane
Pa	Pascal
PDI	Polydispersity Index
PDMS	Polydimethylsiloxane

PE-HD	High-density polyethylene
PHU	Poly(Hydroxy Urethane)
PHUdiCC	Cyclic carbonate-terminate PHU
pK _a	Negative Log of the acid dissociation constant
PMMA	Poly(methyl methacrylate)
PPG	Poly(propylene glycol)
PPGDE	Poly(propylene glycol) diglycidyl ether
PPGdiCC	Poly(propylene glycol) dicyclic carbonate
PSA	Pressure Sensitive Adhesive
PU	Polyurethane
PXDA	<i>p</i> -Xylylenediamine
RDGE	Resorcinol diglycidyl ether
RdiCC	Resorcinol dicyclic carbonate
REACH	Registration, Evaluation, Authorization and Restriction of Chemicals
rpm	Revolutions per minute
RT	Room temperature
SAFT	Shear Adhesion Failure Temperature
SEC	Size Exclusion Chromatography
SiO ₂	Silicon dioxide
SS	Stainless Steel
tan δ	Loss tangent
TBAI	Tetrabutylammonium iodide
T _{d5%}	Temperature at which sample lost 5 weight% during TGA
TEW	Thiol Equivalent Weight
T _g	Glass Transition Temperature
TGA	Thermogravimetric analysis
THF	Tetrahydrofuran
™	Trade Mark
TMG	1,1,3,3-Tetramethylguanidine
TMPTC	Trimethylolpropane tris(cyclic carbonate)
TMPTe	Trimethylolpropane triglycidyl ether
TMPTMP	Trimethylolpropane tris(3-mercaptopropionate)

TPU	Thermoplastic Polyurethane
UPV/EHU	University of the Basque Country
USD	United States Dollar
UV	Ultraviolet
VCO	Volatile Organic Component
w	week
WPU	Water-borne Polyurethane
wt%	Weight percentage
ZnO	Zinc oxide

Chapter 1.

Poly(Hydroxy Urethane) Adhesives: State-of-the-Art

1.1. Introduction

Polyurethanes (PUs) are highly versatile polymers that are widely employed in modern life as rigid or flexible foams, as well as in elastomers, composite materials, paints, coatings and adhesives. Currently, their annual worldwide production exceeds 20 million tons and accounts for about 7 wt% of all plastic production.¹ The polyurethane adhesives market size was estimated at USD 7.0 billion in 2019 and is projected to grow to USD 9.1 billion by 2024 (at a 5.6% compound annual rate growth).² The automotive and transportation industry represents the largest consumer/end-user application of polyurethane adhesives, which are also widely employed in the wood, furniture, building, construction, packaging and footwear industries. Nevertheless, since the first patent of Bayer³ in 1937, the chemistry behind PUs has remained largely unchanged, and the majority of commercially available PUs are fabricated by the step-growth copolymerization of polyisocyanates and polyols (Figure 1.1 a).

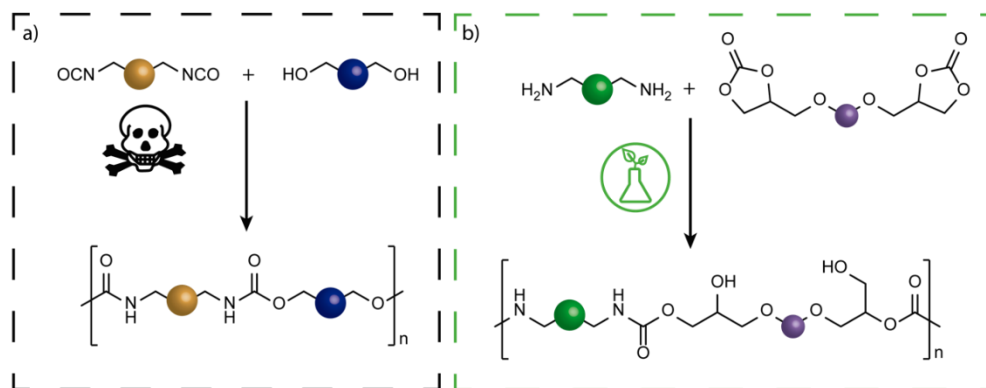


Figure 1.1. a) Conventional synthesis of polyurethanes through step-growth polymerization of polyisocyanate and polyol; b) synthesis of non-isocyanate polyurethanes by polyaddition of bis(cyclic carbonate) to diamine.

The physicochemical properties of PUs are largely guided by the nature, the stoichiometry and/or the functionality of the monomers, while their unique thermo-mechanical behavior

depends on the intrinsic tendency of the chains to phase segregate due to the strong hydrogen bonds between urethane moieties. On account of their diverse formulation options, PUs are the preferred choice when it comes to formulating high-quality coatings or adhesives with excellent adhesion, resistance to abrasion, chemical resistance and low temperature tolerance.⁴

Despite the good performance of PUs in a wide range of applications, the inherent toxicity of the isocyanates, which are known to cause asthma and dermatitis,⁵⁻⁷ as well as the chemicals used in their production, most notably the use of phosgene,⁸ are major drawbacks of this chemistry. In this context, the REACH regulation now restricts the use of isocyanates, and the quest for new, safer and greener alternatives to isocyanates is becoming one of the major challenges in the PU industry.

Non-Isocyanate polyurethanes (NIPUs) were initially discovered in 1957 by Dyer and Scott as a method to produce polyurethanes without using moisture sensitive isocyanates.⁹ At that time, they reacted amines with cyclic carbonates to form the urethane group (Figure 1.1 b). Nonetheless, the employment and the development of this synthesis was negligible until almost 10-15 years ago.^{10,11} The boost to this impressive development occurred probably due to the optimization on the complex chemical insertion of CO₂ in epoxy resins for the synthesis of cyclic carbonates (Figure 1.2), as well as the market demands to produce plastics not only based on their performance but also in their sustainability. The vast majority of industrially applied PUs are based on non-sustainable feedstocks including crude oil and gas. Therefore, there is a drive not just to limit the use of isocyanates, but also to substitute fossil resources by renewable ones in order to move towards a more sustainable industry.¹²

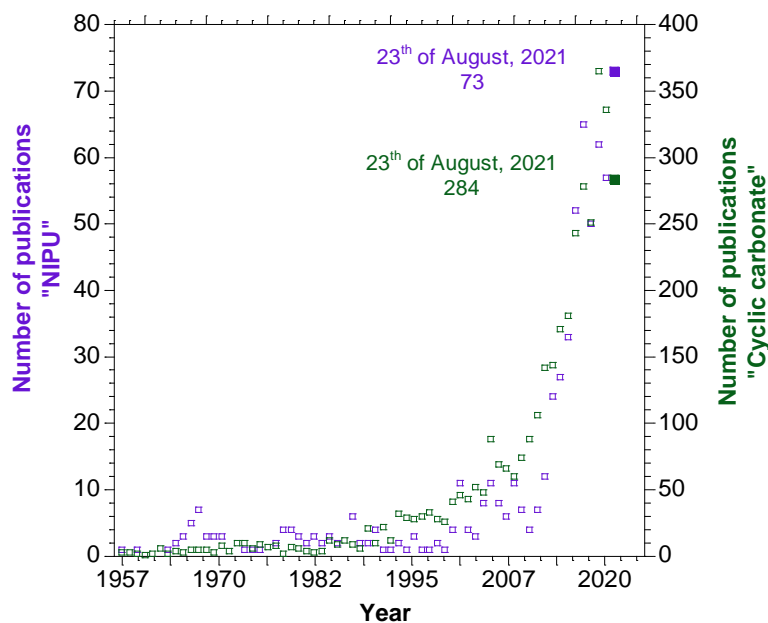


Figure 1.2. Evolution of the number of publications over the years on the topic of non-isocyanate polyurethanes (purple) and cyclic carbonates (green). Data were obtained searching in Scopus website in August, 2021 for the title, abstract and keywords "NIPU" or "non-isocyanate" or "nonisocyanate" or "poly(hydroxyurethane)" or "poly(hydroxy urethane)" or "hydroxyurethane" or "hydroxy urethane" for NIPU topic and "cyclic carbonate" for cyclic carbonates one. Different scale in the ordinate axis were employed to see more clearly the evolution of NIPU topic.

Various routes have been developed to synthesize NIPUs from a diverse range building blocks such as i) the ring-opening polymerization of carbamates, ii) the copolymerization of aziridines with CO₂, iii) the polycondensation of bis(dialkylcarbonate)s with diamines or bis(dialkylcarbamate)s with diols and iv) the polyaddition of poly(cyclic carbonate)s to polyamines. Of these, the latter pathway is by far the most popular and competitive approach.^{11,13} Indeed, this polyaddition provides poly(hydroxy urethane)s (PHUs) based on a 100% atom economy approach and a large portfolio of poly(cyclic carbonate)s, which is now easily accessible at low cost from multiple chemistries. The most popular is the facile chemical [3+2] CO₂ insertion into their corresponding (bio-based) epoxy precursors^{10,14-17} providing

materials with reduced/low carbon footprint, in line with the sustainability requirements of our society. Unlike isocyanates, cyclic carbonates are much less sensitive to moisture, enabling their facile long-term storage and manipulation.¹⁸

In the introduction of this thesis, a critical view of the current state-of-the-art of the PHUs in the field of adhesives will be discussed with a focus on the open literature and patents. The characteristics of conventional PU adhesives will be briefly introduced firstly to illustrate the scope of their application and to provide the guidelines to construct the next generation of PHU adhesives with equal, or even superior, performance.

1.2. Main processing methods and applications of PU adhesives

To design adhesives that compete with the performance of conventional PU materials, the formulation and processing of NIPUs should conform to certain characteristics. This necessitates the identification of the key features of conventional PU materials and the understanding of how they affect the final application. To fabricate PU adhesives that display an optimal balance between adhesive and cohesive forces, most systems are chemically crosslinked. Aromatic isocyanates are preferred as they possess a uniform reactivity of the reactive groups, lower volatility resulting in easier workplace handling, and lower prices than aliphatic isocyanates. Polyether polyols are usually chosen as comonomers as they offer improved low-temperature flexibility, are in a liquid state with acceptable viscosity at room temperature and are much less sensitive to hydrolysis than polyesters.¹⁹ Adhesives can be classified as either chemical reactive formulations, thermoplastics or solvent evaporation systems. Chemical reactive adhesives include two component systems and moisture-, heat- or UV-sensitive groups. Usually these are supplied in a low molar mass form and polymerization






occurs after application. Thermoplastics are basically hot-melt technologies, in which the adhesive flows at elevated temperature and solidifies when the temperature is decreased below their T_g or T_m . In solvent evaporation or diffusion type adhesives, polymers are applied in their final form, either dissolved or dispersed in a suitable solvent. In terms of sustainability, waterborne formulations are preferred than solvent-based ones. To date, the formulation and processing of polyurethane adhesives differ regarding the envisioned application and respond to one of the five technologies summarized in Table 1.1, each of which is suited for specific applications.

Table 1.1. General processing methods and applications of PU adhesives.

Technology	Description	Applications
Solvent-free	1K systems usually silane-terminated prepolymers with good adhesion to glass. 2K systems are applied when rapid curing is needed and for structural adhesives.	1K are typically used in automotive industry while 2K are more employed in the building sector or flooring applications.
Hot-melt	Reactive systems bearing low-percentage of free isocyanate which reacts with air moisture or functional moieties on the surface of the substrates.	Wood industry or shoe soles.
Solvent-based	High- molar mass prepolymers prepared with a slightly excess of NCO groups.	Shoes, food packaging, automotive and furniture industry.
Water-borne	Ionisable moiety is present to allow the dispersion of 1K as well as 2k formulations based on temperature sensitive reactive systems.	Footwears, bookbinding, furniture, textile laminates.
Radiation curable	Acrylate-tipped prepolymers endowing the adhesives with faster curing and higher stability.	Flexible and heat-sensitive substrates.

To avoid viscosity issues, polyurethane adhesives were initially formulated as two-component reactive systems by mixing low molar mass or oligomeric raw materials, which contained free isocyanates and/or alcohol moieties. Later, the addition of organic solvent was proposed to solve viscosity issues associated with the handling of high-molar mass prepolymers that are required to provide optimal end-use properties.²⁰

Table 1.2. Advantages and drawbacks for the different types of polyurethane adhesives and coatings.^{19,21-23}

	 Solvent-free	 Solvent-based	 Water-borne	 Hybrids	 Radiation curable
Low VOC emission	√√√	x	√√	~	√√√
Easily applicable	√	√√√	√√√	~	Need of external source of E
Presence of free-isocyanate	x	x (blocked isocyanate)	√	x (blocked isocyanate)/ √ acrylic or silane-ended prepolymers	√√
Curing time/T	Slow/ room T	Fast/ room or high T	Need of T	Need of T/ room T	Fast/ room T
Mechanical properties	√√	√√	√	√√√	√√

√√√: excellent; √√: good; √: slightly good; x: poor; ~: depends on the formulation.

Nevertheless, environmental concerns and new regulations from the European Union and the United States Environmental Protection Agency, which limit the amount of volatile organic components (VOC) that can be released into the atmosphere, have pushed scientists to explore new approaches to fabricate adhesives free of VOC and hazardous air pollutants. Thus, water-borne systems have emerged as competitive alternatives to solvent-borne ones. Water-borne polyurethanes (WPU) are usually prepared in a similar fashion to solvent-based PUs with the exception that hydrophilic groups are incorporated into the polymer backbone to ensure the dispersion of the chains in water.²⁴⁻²⁶ However, the hydrophilic moieties in WPUs result in a final material with lower water and weather resistance compared to their solvent-based counterparts.^{27,28} Another major drawback is the poor resistance of the WPU coatings towards mechanical strains and high temperatures. To improve the material

properties, additional curing is generally applied by incorporating radiation curable species, e.g. epoxides or acrylates, or moisture sensitive groups, e.g. alkoxy silanes. Table 1.2 summarizes the main advantages and drawbacks of each technology that should be taken into account when designing and processing formulations.

1.3. Test for evaluating the performance of adhesives

Adhesion is a complex process in which many factors govern the final adhesive performance. The combination of different adhesion theories explains this complex process.²⁹ In a simple way, the adhesive must wet the substrate and afterwards create either, chemical or mechanical interactions with the substrate to be adhered. For this reason, first, the adhesive has to present an ideal viscosity and surface tension to wet the substrate. According to wetting theory, good wettability is achieved when the surface tension of the adhesive is much lower than the surface energy of the substrate. Adhesives with low surface tension values wet the substrate surface easily. Regarding the interaction between adhesive and substrate, the nature, chemistry and morphology of the substrate substantially affect the adhesion process. According to mechanical theory, adhesion occurs when the adhesive penetrates the pores, cavities and other surface irregularities on the substrate. Based on the chemical bonding theory, some materials such as wood or glass contain hydroxyl groups that can react/interact with the adhesives by the formation of covalent bonds or hydrogen bonding, which increase the adhesion forces. On the other hand, covalent and ionic bonds provide much greater adhesion values than secondary forces (hydrogen bonding, dipole-dipole, ion-dipole or London dispersion forces). Thus, non-polar plastics such as polyethylene are more challenging to glue due to the poor interactions between them and the polar PHUs. A pre-treatment of these plastics is often required to increase the polarity at their outer surface, for instance by oxidation

by corona treatment.³⁰ Whatever the substrate, prior to coating or gluing, removal of dust and degreasing is a pre-requisite. Otherwise, the adhesive will bond to these pollutants establishing a weak boundary layer decreasing significantly the adhesion force of the joint. Quantification of these intermolecular forces is carried out through common test depicted in Figure 1.3.

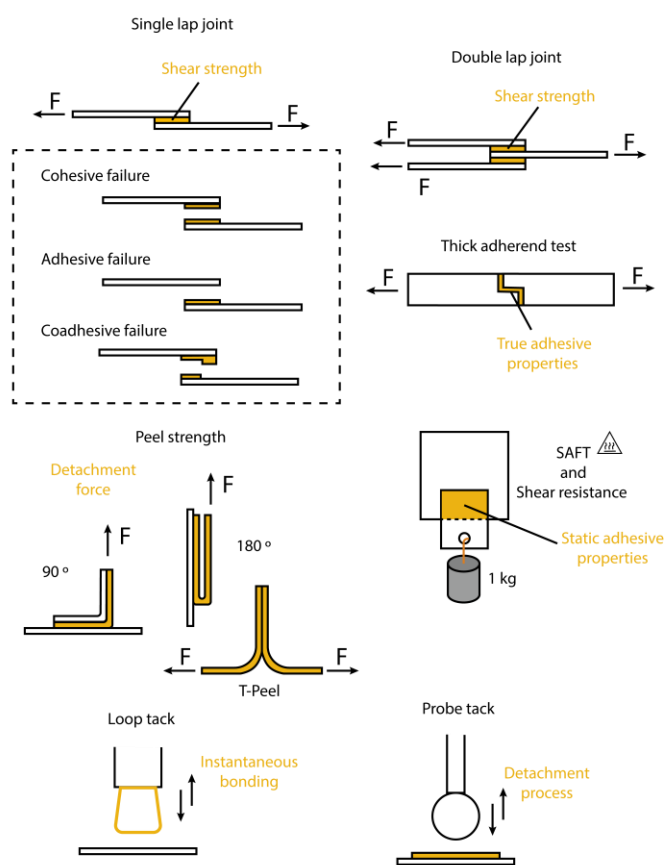


Figure 1.3. Schematic representation of the evaluation of adhesion for adhesives represented in yellow.

Briefly, lap-shear measurements employing single (ASTM D1002) or double (ASTM D3528) lap joints are the most common tests applied for comparison and quality control of adhesives. These tests determine the maximum shear strength of an adhesive together with

providing useful information about the bond failure mechanism (cohesive or adhesive). Cohesive failure indicates that the maximum strength in the joint is reached, while adhesive failure means the interaction force between the adhesive and the substrate is weaker than the cohesive forces in the polymer. Structural adhesives present high shear strength values, in the range of 15-30 MPa,³¹ while hot-melt adhesives are characterized by lower shear load capacity, usually 3-4 MPa.³²

Evaluation of static loads is carried out through shear resistance and Shear Adhesion Failure Temperature (SAFT) measurements (ASTM D4498 can serve as a guide for the preparation of test specimens). Specimens holding 1 kg are evaluated, determining the time or the temperature of failure, respectively. Information about service temperatures and resistance of the adhesive to creep, durability of the joint, are thus provided from these tests. Peel strength measures the required force per area to detach a flexible substrate from a rigid or another flexible one. Typically, rigid structural adhesives present very low peel strength in comparison with flexible adhesives. The test can be carried out with different angles between the adherends but T-peel, 180° and 90° are the most common experiments (ASTM D1876 and D3330).

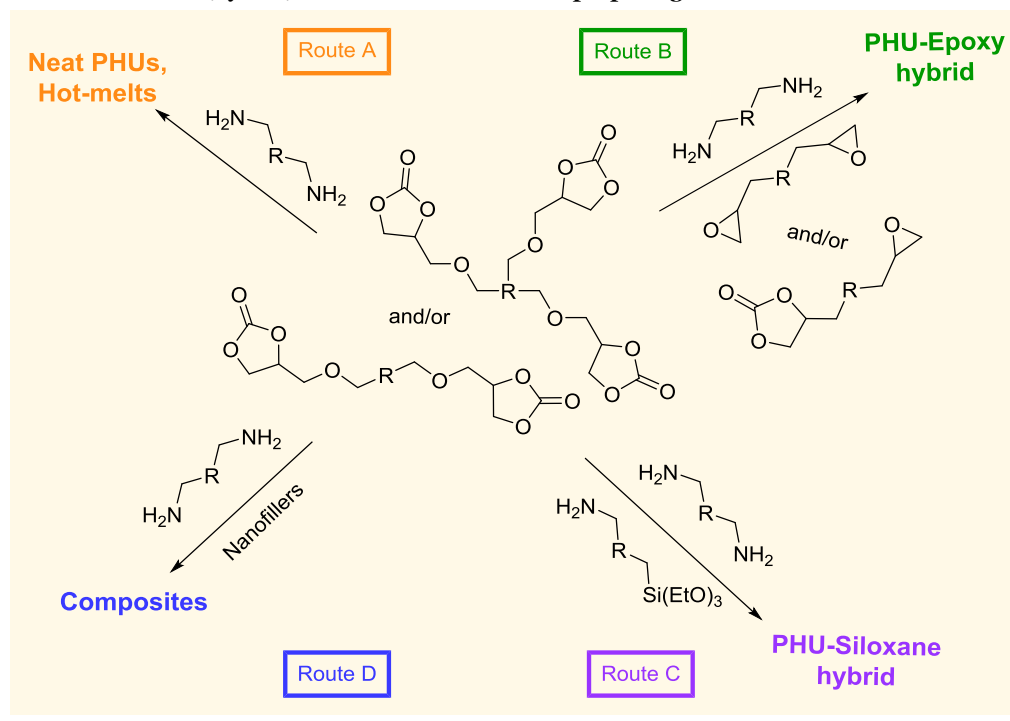
Another important property concerning adhesives, especially pressure sensitive adhesives (PSAs) and hot-melt adhesives, is the tackiness. Loop tack (ASTM D6195) or probe tack (ASTM D2979 or D3121) are the most common procedures to evaluate it. Loop tack is mostly employed for adhesive tapes, whereas probe tack can be performed for a wider range of adhesives.

1.4. Approaches for the preparation of NIPU-based adhesives

As PHUs are the most widely used NIPUs for adhesive applications, this section will be focused on this family of NIPU by describing the various processes used for their preparation.

PHUs materials that have been characterized by at least one of the standard evaluation tests discussed in section 1.3 are mainly reported. It is important to point out that PHUs differ from conventional PUs by the presence of hydroxyl groups along the polymer chain. While these groups participate in intramolecular and intermolecular hydrogen bonding,³³ such bonding with the substrate also enhances the adhesion forces. Nevertheless, they disfavor the phase separation present in conventional polyurethanes³⁴ and increase the adhesive hydrophilicity with the consequence of enhancing water uptake, which facilitates their wet delamination from the substrate.^{35,36} Various strategies have also been designed to overcome some of the limitations of PHU chemistry (slow reactivity, high temperature...) namely by developing orthogonal/hybrid chemistries in combination with the aminolysis of carbonates (Scheme 1.1).

Scheme 1.1. Main (hybrid) chemistries involved for preparing PHU adhesives.



Solvent-free formulations are certainly the most attractive route to prepare adhesives as no toxic solvent is released upon evaporation and shrinkage phenomena are limited during the curing process. However, this requires a suitable combination of poly(cyclic carbonate)s and polyamines for the preparation of a viscous formulation that can be applied to the substrate. Cornille et al.³⁷ were the first to report the application of neat PHUs as adhesives. Reactive formulations were made of bi- and trifunctional cyclic carbonates blends and (cyclo)aliphatic diamines and subsequently cured by thermal treatment for gluing similar substrates of beech wood, glass and aluminum (the latter was pre-covered by an epoxy paint) (Scheme 1.1, route A). The adhesive performance was evaluated and benchmarked with those of two conventional PUs derived from isocyanates. For glass, the substrate did not resist traction whatever the PHU formulation, underlying that the shear force required to break the adhesive was higher than that needed to break glass. For optimal PHU formulations made of a cycloaliphatic diamine, wood failure also occurred prior breaking the adhesive at a lap-shear strength greater than 15 MPa, while reference PUs only provided adhesion strength of 3 to 6 MPa. For both supports, the authors postulated that the presence of surface functional groups (silanol for glass or hydroxyl for wood) created additional Van der Waals/hydrogen bond interactions with the OH groups of PHUs that were responsible for the excellent adhesion. This hypothesis was further supported by the adhesion values and the predominant adhesive failure mode reported with painted Al. Much lower lap-shear strength values in the range of 2-3 MPa were measured for the various PHUs adhesives. Besides, the authors prepared further PU compositions employing diisocyanates and diols with identical backbone structures. Results showed lower lap-shear strength values than those for PHUs when gluing wood, evincing the stronger interaction of PHUs due to hydrogen bonds of hydroxyl groups.

Detrembleur et al.³⁸ reported the synthesis of biomimetic PHU adhesives by adding an amino functional catechol, dopamine (DOP), as an adhesion promoter to a PHU formulation made of a trifunctional cyclic carbonate (trimethylolpropane tris(cyclic carbonate), TMPTC) and a diamine (hexamethylene diamine, HMDA). At a low DOP loading (3.9 mol%), lap-shear strength values as high as 24 and 28 MPa for Al and wood substrates, respectively, were measured. Interestingly, lap-shear adhesions up to 4.76 MPa were obtained on PE-HD. Furthermore, this formulation was also efficient for gluing dissimilar substrates (e.g. Al to SS or plastics) with a similar range of forces between 6.7-25.0 MPa. These biomimetic adhesives were found to be competitive to commercial formulations (Teromix-6700 and Araldite®2000), provided that the appropriate thermal curing was applied to the PHU formulation.

Hot-melt PHU adhesives are solvent-free systems that are employed by melting thermoplastic polymers on a substrate.³⁹⁻⁴³ Tryznowski et al.,^{39,40} fabricated hot-melt PHU adhesives for birch wood. Amino telechelic oligoamides made by the condensation of 1,3-diaminopropane with diethyl tartrate³⁹ or dimethyl succinate⁴⁰ were chain extended with diglycerol dicarbonate providing PHUs containing polyamide segments. For bonding wood joints, the thermoplastic PHU was melted at 130 °C on both surfaces of the substrates, followed by cooling to solidify the adhesive. This methodology provided moderate adhesion values up to 3.19 MPa. Along the same lines, recent work of Xi et al.^{41,42} has reported the application of saccharide-based NIPUs onto wood joints. Under optimized conditions, pressing the samples at 230 °C for 12 minutes, sucrose-based NIPUs presented internal bond strength values around 1.02 MPa, 3 times higher than the standard requirement (≥ 0.35 MPa).⁴⁴

Nair et al.⁴³ described the preparation of thermo-reversible hot-melt PHU adhesives based on homo- and copolymers of aromatic, bisphenol A-based, and cycloaliphatic, Araldite® CY

230-based, bis(cyclic carbonate)s and aminotelechelic oligo(propylene glycol). Beside the good adhesion values up to 9 MPa on aluminum and 2 MPa on high-density polyethylene, the authors showed that the substrates could be debonded manually after thermal treatment up to 100 °C for 0.5 h and then rebonded with no noticeable loss of the shear strength values. Additional examples of hot-melt PHU adhesives may be found in the patent literature⁴⁵⁻⁴⁷ and mainly differ by the composition and application/curing temperatures of the thermoplastic.

The low reactivity of cyclic carbonates with amines is a major hurdle to the development of PHU adhesives, particularly in applications that require fast curing at room temperature. Therefore, hybrid systems combining PHU with other chemistries (epoxy, sol-gel or composites) have been used to enhance the competitiveness of the adhesives (Scheme 1.1, routes B, C and D).³³

Two decades ago, Figovsky et al.⁴⁸ briefly introduced a series of PHU-epoxy hybrid coatings and adhesives using cyclic carbonates, epoxy oligomers and amine hardeners for potential application in microelectronics. Curing was performed at room temperature for 24 h on Al or SS and the authors claimed a 1.5 to 1.7-fold increase of the lap-shear adhesion strength of the hybrid system onto aluminum and steel (12 and 16.7 MPa, respectively) compared to an epoxy-based adhesive. The adhesive was cured by the combined use of the epoxy resin (by the amine/epoxide reaction) and PHU. The same authors⁴⁹ also reported another PHU-epoxy hybrid adhesive curable at room temperature (for 7 days) by mixing an epoxy resin (DER[®] 331) with carbonated-epoxidized soybean oil (CESBO), and Vestamin TMD as amine hardener. The shear strength of the hybrid adhesives evolved with the carbonate content and reached maximum of ~10 MPa and 7 MPa, respectively for carbon steel and aluminum, when the CESBO percentage was increased up to 10 mol%. Similarly, Stroganov et al.⁵⁰ evaluated the

adhesive properties of a PHU combined with a BPA-based epoxy resin following Figovsky's curing protocol (r.t, 7 days). They found that the addition of the cyclic carbonate to the formulation improved the lap-shear strength up to 15.8 MPa when room temperature curing was applied. However, a post-treatment of 10 h at 100 °C incremented this value up to 22.8 MPa.

Recently, Lambeth et al.⁵¹ revisited this chemistry to optimize the fabrication of hybrid PHU-epoxy hybrid adhesives by understanding the reactivity of the epoxide and carbonate chemistries. The authors showed that the aminolysis of the epoxide was slightly faster than the cyclic carbonate counterpart, thus forming PHU-epoxy hybrid networks that were fairly uniform with a slight preference for the epoxide ring-opening compared to the cyclic carbonate in the early stage of the adhesive formation. They also showed that the secondary amines formed by aminolysis of epoxides did not contribute to the network construction. They formulated thermoset PHU-epoxy hybrid adhesives for bonding Al plates from trimethylolpropane triglycidyl ether (TMPTGE), trimethylolpropane tris(cyclic carbonate) (TMPTC) and 4,4'-methylenebis(cyclohexylamine), and evaluated the performance of the adhesives for various compositions cured at 80 °C. Remarkably, the epoxy and hydroxyurethane moieties operated in synergy to create high performance adhesives with a maximum lap-shear adhesion value of 27 MPa for a 50/50 TMPTGE/TMPTC molar composition that is ~1.7 or ~1.3 higher than pure epoxy or PHU formulations, respectively. The benefit of merging epoxies chemistries with PHU was further confirmed by Anitha et al.⁵² who introduced hydroxyurethane moieties within amine-cured epoxy systems by utilizing a monofunctional cyclic carbonate additive. At cyclic carbonate content as low as 1 to 4 mol%, the adhesive performance of epoxy adhesives made of Jeffamine T403 and diglycidyl ether bisphenol A were significantly increased with lap-shear adhesion strength value up to 22 MPa

for Al substrate, surpassing the value for the neat epoxy analogue (17 MPa). It has to be noted that many patents have been filed on PHU-epoxy hybrid formulations for (structural) adhesives among other applications.⁵³⁻⁵⁸

Alkoxysilanes can undergo condensation reaction and cross-link to form a siloxane-linked network by a sol-gel process.⁵⁹ They are also able to react with the functional groups at the surface of glass and metallic substrates creating -Si-O-Si- and -Si-O-M- covalent bonds that are beneficial for the adhesive performance. Rossi de Aguiar et al.⁶⁰ combined this sol-gel chemistry with PHUs to prepare hybrid thermoset adhesives. Cyclic carbonate-terminated PDMS (CC-PDMS) was reacted with (3-aminopropyl)triethoxysilane (APTES) as a sol-gel precursor or with blends of APTES and isophorone diamine. After thermal curing at 60 °C, the hybrid adhesives displayed an adhesive strength ranging from 0.9 to 1.3 MPa or 3 MPa for Al-to-glass and glass-to-glass adhesion, respectively. The adhesion was maximum for a composition containing only APTES. Increasing the curing temperature from 60 to 180 °C to favor the sol-gel process was found to be detrimental with respect to the adhesive performance, with a loss of the adhesion strength of ~50 % between 100 to 160 °C and a loss of around 70 % at 180 °C.

Detrembleur et al. revisited the formulations for gluing Al substrates and highlighted the importance of the thermal curing conditions on the adhesion performance. They showed that the adhesives underwent facile wet delamination due to the hydrophilic nature of PHUs, which favored water absorption.⁶¹ To limit this delamination, hydrophobic segments (PDMS)⁶¹ or biorenewable hydrophobic cyclic carbonates (issued from vegetable oils)⁶² were used in the formulations (Scheme 1.1, route D). By loading the formulations with SiO₂ or ZnO nanofillers, water uptake was strongly decreased and a remarkable enhancement of the adhesive

performance and mechanical properties was noted. These improvements were optimal when using 5 wt% ZnO nanoparticles functionalized by cyclic carbonate groups, with an increase of lap-shear strength from 11.2 to 16.3 MPa when the functionalized ZnO nanofillers were incorporated in the formulation. All these benefits were attributed to the higher crosslinking density of the adhesive that resulted of the aminolysis of the cyclic carbonate at the nanoparticles surface. Interestingly, while composites NIPU adhesives made of native or epoxy-functional ZnO fillers resulted in cohesive failure, formulations made from cyclic carbonate-functional fillers presented an adhesive failure mechanism due to the higher mechanical resistance of the material. Similar formulations were developed by the same group by using carbonated soybean oil as the poly(cyclic carbonate) to design partly bio-based composite PHUs. High adhesion values up to 12 MPa were obtained for adhesion of Al-Al and SS-SS substrates observing mostly a cohesive failure.⁶²

Table 1.3. Summary of the principal properties of the PHU-based adhesives reported in academia.

Type of adhesive	Substrates	Curing conditions	Speed of test (mm·min ⁻¹)	Lap-Shear strength (MPa)	Reference
Solvent-free	Wood	80 °C, 12 h + 150 °C, 30 min	100	15.0 ± 1.5	37
	Aluminum (Al) ^a			2.0–3.0	
Solvent-free	Al	100 °C, 18 h	2	24.1 ± 1.7	38
	Stainless Steel (SS)			22.1 ± 0.9	
	Beech			28 ± 1.7	
	PMMA			17.9 ± 1.3	
	PE-HD			4.76 ± 2.5	
	Dissimilar substrates			6.7–25.0	
Hot-melt	Birchwood	130 °C, 1.18 MPa, 30 min	10	0.67 ^b	40

Type of adhesive	Substrates	Curing conditions	Speed of test (mm·min ⁻¹)	Lap-Shear strength (MPa)	Reference
				3.19 ^b	39
Hot-melt	Pine	220 °C, 2.75 MPa, 6 min	2	3.16 ± 0.05 3.62 ± 0.02 ^c 3.38 ± 0.04 ^d	41
				2.76 ± 0.09 1.32 ± 0.08 ^e 1.24 ± 0.04 ^d	
Hot-melt	Beech	230 °C, 12 min ^e	f	1.02 ^g	42
Hot-melt	Al	T not reported, 24 h	50	9 ^h	43
	PE-HD			< 2 ^h	
	Polyimide			>1.5 kg/cm ⁱ	
PHU- Epoxy hybrid	Al	r.T., 24 h	Not reported	12	48
	Steel			16.7	
PHU- Epoxy hybrid	Carbon Steel	r.T., 7 days	5	10	49
	Al			7	
PHU- Epoxy hybrid	Not reported	22 °C, 7 days	Not reported	15.8	50
		22 °C, 7 days + 100 °C, 10 h		22.8	
PHU- Epoxy hybrid	Al 2024-T3	80 °C, 48 h	ASTM D1002	27	51
PHU- Epoxy hybrid	Al	30 °C, 18 h + 80 °C, 1 h + 100 °C, 2 h	10	22	52
PHU-siloxane hybrid	Glass	60 °C, 24 h	1	3 ^j	60
Composite	Al	70 °C, 12 h + 100 °C, 3 h	2	16.3 ± 1.4	61
	Al, SS			3.7–11.7	62

^acover of epoxy paint; ^bcohesive forces investigated through mechanical testing of the NIPU-wood joints; ^c24 h cold water; ^d2 h boiling water; ^ethree-stage hot pressing cycle (pressure: 33 kg cm⁻², 4 min – 15 kg cm⁻² 5 min – 5 kg cm⁻², 3 min); ^fUniformly load making the specimen damaged within (60 ± 30)s according to China National Standard GB/T 17657-1999; ^gInternal Bond strength; ^hNo remarkable differences after

thermoreversible adhesion at 100 °C of the materials; ⁱpeel strength values; ^jkept adhesive performance above the 50% after 10 days at 160 °C; ^kkept adhesive performance after 4 days immersed in water

1.5. Motivation and objectives of the thesis

In light of the foregoing, polyurethanes (PUs) can be considered the preferred option when high-performance materials such as foams, elastomeric thermoplastics, coatings and adhesives are required. Nevertheless, guided by environmental concerns and legal obligations, greener and safer alternatives to conventional PUs are now being sought in order to avoid the use of toxic isocyanates that are one of the primary components used in their formulation.

Bearing this in mind, this thesis was born from the collaboration between the POLYMAT Institute at the University of the Basque Country (UPV/EHU) and ORIBAY Group Automotive, specifically with the R&D Department. ORIBAY is a company located in Donostia-San Sebastián, which is focused, among other projects, on manufacturing structural adhesives for automotive industry, mainly for windshields and the pieces thereof. Apart from their own adhesives, the use of isocyanate-based polyurethane adhesives is widespread in the company. In a further step of development, this thesis has been focused on furnishing new relevant sustainable non-isocyanate polyurethane adhesives for its implementation in the automotive industry.

For this purpose, the research was based on poly(hydroxy urethane)s, formed by the polyaddition of poly(amine)s with poly(cyclic carbonate)s, which have emerged as the most appealing and versatile non-isocyanate polyurethanes for adhesive applications.

Thus, Chapter 2 focuses on the improvement and application of these materials as adhesives through the combination with a sol-gel process that allows for curing by atmospheric

humidity. The synthesis of PHU prepolymers functionalized with (3-aminopropyl)triethoxysilane (APTES) is demonstrated, and their curing behaviour and adhesion performance are investigated by means of rheological experiments and lap-shear test, respectively. The use of catalyst and elevated temperatures speeds up the curing process and leads to improved adhesion properties. Hence, it is demonstrated that the fastest curing and the best performance are achieved at 100 °C when acetic acid is employed as catalyst. Finally, it is established the importance of the soft (poly(propylene glycol) dicarbonate) to hard (resorcinol dicarbonate) ratio to achieve superior cohesion and adhesion properties in PHU adhesives.

Chapter 3 will depict the synergetic effect of a fast curing, i.e. (3-aminopropyl)trimethoxysilane (APTMS), and an adhesion promoter, i.e. dopamine hydrochloride (DOP), in a non-isocyanate polyurethane adhesive formulation. Initial hard compositions are endowed with better adhesives properties taking into account the importance of balancing soft to hard ratios described in Chapter 2. The addition of APTMS allows speeding up the curing process of the adhesive and enhances the adhesion performance under high temperature conditions of the polymers. For enlarging the PHU adhesive applicability, adhesion on wood, aluminium, poly(methyl methacrylate), high-density polyethylene and polyamide are evaluated in this chapter.

In Chapter 4 the main drawback of the previous chapters, i.e. the necessity of curing at high temperature for obtaining outstanding performance, is tackled. Incorporation of an epoxy resin improves the adhesion performance when curing at room temperature as well as the retention of this performance under load and elevated temperature adhesion when elevated temperatures are applied. Moreover, a thiol compound, i.e. trimethylolpropane tris(3-mercapto propionate) (TMPTMP), is added to the formulation for speeding up the curing process through

fast reaction with the epoxy resin. Curing times are largely decreased by adding a strong base, 1,1,3,3-tetraethylguanidine, as catalyst, although an appropriated system of application of the adhesives has to be found since pot life is not enough for one-pot system.

Finally, another kind of adhesives are presented in Chapter 5: poly(hydroxy urethane) low-temperature hot-melt adhesives. In this chapter, the synthesis of thermoplastic PHUs that present adhesion at elevated temperatures and cohesiveness when they are cooled down is discussed. FTIR-ATR and ¹H NMR characterization of the copolymers are provided to confirm the PHU structures. Rheological characterization of the materials as well as adhesion tests such as probe tack, lap-shear, shear adhesion failure temperature and shear resistance are performed to evaluate the influence of the cyclic carbonate molar ratios, the substitution of the aromatic for an aliphatic cyclic carbonate and the diamine structure. Hence, it is highlighted again the importance of a balanced hard to soft ratio, along with the relevance of the chain extender in the final properties. Enhancement of these adhesives is presented with the addition of 15 wt% of an epoxy resin as crosslinker, which endowed the adhesives with greater service temperatures.

Chapter 2.

Monocomponent Non-Isocyanate Polyurethane Adhesives Based on a Sol-Gel Process



2.1. Introduction

As mentioned in Chapter 1, the preparation of non-isocyanate polyurethanes (NIPUs) by the step-growth polyaddition of diamines with dicyclic carbonates was postulated as the most promising alternative to toxic conventional polyurethanes (PUs).^{63,64} 5-membered cyclic carbonates are preferred over bigger cyclic carbonates since their easy and big scale preparation (from grams to kilos) by the (organo)catalysed cycloaddition of CO₂ to epoxides.¹⁴ Nonetheless, the low reactivity of 5-membered cyclic carbonates typically leads to slow polymerizations as well as side-reactions that can limit the NIPU molar mass. Furthermore, materials with poor mechanical properties are often obtained. In this regard, different approaches have been applied to improve the properties of NIPU based on 5-membered cyclic carbonates such as the production of more reactive monomers,^{11,13,65,66} the use of catalysts,^{67,68} using trifunctional or polyfunctional carbonates,^{38,62,69,70} the incorporation of inorganic compounds,^{62,71} and the preparation of hybrid polymers in combination with acrylates,⁷⁰ methacrylates⁷² or with partially carbonated epoxide monomers⁷³. In spite of the significant improvements in terms of properties and polymerization kinetics, in all the cases where the properties are optimal for industrial implementation (e.g. using polyfunctional carbonates or epoxy comonomers) a crosslinked material is formed in-situ at the initial stages of the polymerization, which limits practical use of the adhesive.

One potential method employed in PU chemistry in order to improve mechanical properties and applicability of polyurethane adhesives is devoted to the reaction of PU prepolymers with alkoxy silane compounds in order to obtain a stable, yet curable material. Alkoxy silane groups can undergo crosslinking reactions to form a siloxane linked network by a

sol-gel process, which results in the improvement of the properties of the PU due to the incorporation of nanoscale inorganic domains.^{74,75}

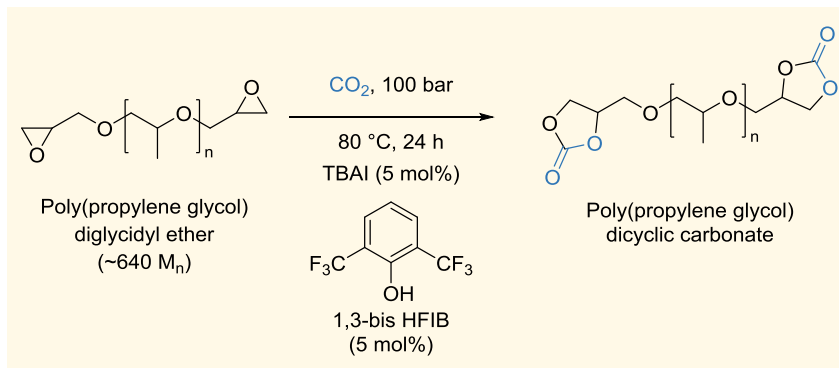
There are few examples of hybrid sol-gel NIPUs in the literature.^{76–78} For instance, Caillol et al.⁷⁸ carried out the synthesis and characterization of different hybrid poly (hydroxy urethane)-siloxane thermosets, crosslinked by a sol-gel process. They evaluated the effect of trifluoroacetic acid on the final properties of the materials. The insertion of alkoxy silane groups in the NIPUs allowed the polymer to be cured using atmospheric moisture at elevated temperatures.

In this chapter, in order to prepare an industrially relevant moisture curable poly(hydroxy urethane) (PHU), we synthesized a range of hybrid non-isocyanate polyurethanes utilizing bio-based Priamine™ 1074, different contents of dicyclic carbonates, poly(propylene glycol dicyclic carbonate) (PPGdiCC) and resorcinol dicyclic carbonate (RdiCC), and an organosilane compound ((3-aminopropyl)triethoxy silane, APTES) as crosslinker. Films for physical characterization and adhesives were prepared through a sol-gel process by hydrolysis and condensation of the triethoxysilanes. As the curing process was not sufficiently fast at room temperature in the absence of catalyst, we explored the impact of temperature and different organocatalysts [methanesulfonic acid (MSA), acetic acid (HAc), 1,8-Diazabicyclo[5.4.0]undec-7-ene (DBU)] on the curing step. Moreover, water uptake and gel content were measured, and lap-shear strength tests were performed to evaluate the adhesive performance of the products.

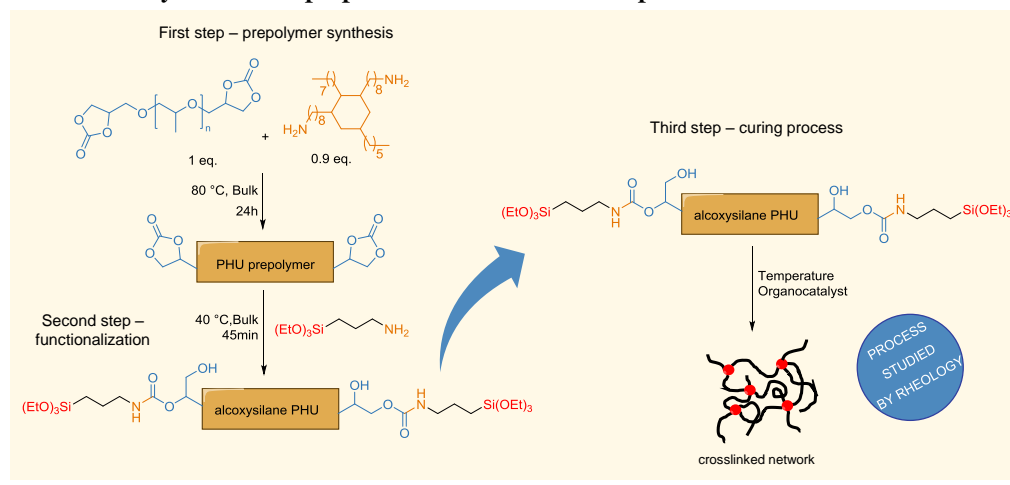
2.2. Synthesis of triethoxysilane-terminated PHUs oligomers and their curing

Poly(propylene glycol) dicyclic carbonate (PPGdiCC) was synthesized at the kilogram scale by the quantitative organocatalyzed coupling of CO₂ to poly(propylene glycol) diglycidyl ether for 24 h following a previously reported procedure (Scheme 2.1).⁷⁹ The completion of the reaction was noted by ¹H NMR spectroscopy by the complete disappearance of epoxy group signals at 3.14, 2.78 and 2.61 ppm and the appearance of peaks related to the carbonate group at 4.78 and 4.66 ppm (Figure A-II.1).

Scheme 2.1. Synthesis of PPGdiCC from [3+2] CO₂ insertion into poly(propylene glycol) diglycidyl ether precursor. Tetrabutylammonium iodide (TBAI) and 1,3-Bis(2-hydroxyhexafluoroisopropyl)benzene (1,3-bis HFIB) were employed as catalysts and activator, respectively, for the reaction.



The preparation of poly(hydroxy urethane) hybrids was then performed following an adapted procedure from previous work,⁷⁷ consisting of a three-step strategy as illustrated in Scheme 2.2: a) synthesis of cyclic carbonate-terminated PHU prepolymer (PHUdiCC), b) functionalization of the prepolymer by aminolysis of the cyclic carbonates with (3-aminopropyl)triethoxysilane (APTES) and c) curing by hydrolysis and condensation of the ethoxysilane functionalized PHUs.

Scheme 2.2. Synthesis and preparation of PHU monocomponent adhesives.

For the first step, the preparation of the PHUdiCC was carried out using an excess of PPGdiCC relative to the diamine, with a cyclic carbonate to amine molar ratio of 1/0.9 (Scheme 2.2; first step). PPGdiCC was selected because PPG is one of the most commonly employed soft segments in polyurethane adhesives as it provides good adhesion to different substrates and also presents good hydrolysis resistance and hydrophobicity⁸⁰. Priamine™ 1074 was used as it is a commercially available bio-based diamine, which also confers hydrophobicity to the materials.⁸¹ The reaction was carried out at 80 °C for 24 h without catalyst and solvent. The monomer conversion was monitored by FTIR-ATR by following the decrease of the relative intensity of the carbonyl stretching vibration band of the carbonate at 1798 cm^{-1} (Figure 2.1). The intensity of the bands at 3035-2800 cm^{-1} (corresponding to C-H and $\text{CH}_2\text{-O}$ stretching band of alkanes and ether, respectively), whose intensities did not change with reaction time, were used to normalize the areas. After 24 h, a new band at 1700 cm^{-1} characteristic of the carbonyl of the urethane group was clearly observed, together with the disappearance of the carbonyl band of the cyclic carbonate (1798 cm^{-1}) at the PHU ends. $^1\text{H-NMR}$ spectroscopy of the

PHU prepolymer (Figure 2.2, red spectrum) showed the characteristic resonance of the PPG repeating units at 3.3-3.8 and 1.12 ppm, as well as a signal at 3.13 ppm associated with the methylene group next to the reactive amine group of the priamine and the characteristic resonance of the aliphatic chains of the diamine at 1.46, 1.24 and 0.86 ppm. Average molar mass values were characterized by SEC measurements (Table 2.1). Low molar masses were obtained in agreement from typical values for NIPUs.⁸²

Table 2.1. Average molar masses of the different compositions of the synthesized PHU prepolymers.

Composition (PPGdiCC/RdiCC)	M _n ^a (kg mol ⁻¹)	M _w ^a (kg mol ⁻¹)	PDI ^a
100/0	4.4 ± 0.4	10.7 ± 1.2	2.5 ± 0.4
95/5	3.8 ± 0.4	10.4 ± 1.1	2.7 ± 0.6
90/10	4.5 ± 0.3	10.9 ± 0.5	2.4 ± 0.3
80/20	4.4 ± 1.3	11.3 ± 0.7	2.7 ± 0.7
60/40	6.5 ± 1.2	18.6 ± 5.1	2.8 ± 0.3

^aAverage molar masses based on calibration with polystyrene standards ranging from 0.573 to 3,848 kg mol⁻¹.

For the second step, the majority of the unreacted carbonate groups was reacted with APTES for 40 minutes at 40 °C, giving rise to an alkoxy silane end-capped NIPU. The reaction temperature was reduced in order to avoid undesired condensation during the functionalization step. The effectiveness of the reaction was confirmed by the appearance of new bands at 959 and 1083 cm⁻¹ attributed to the CH₃ rocking and C-O symmetric stretching of APTES, respectively.⁸³ ¹H NMR spectroscopy also showed the appearance of new signals at 3.78, 2.68 and 0.60 ppm, corresponding respectively to the -O-CH₂-CH₃, -NH-CH₂- and -CH₂-Si- of the reacted APTES (Figure 2.2).

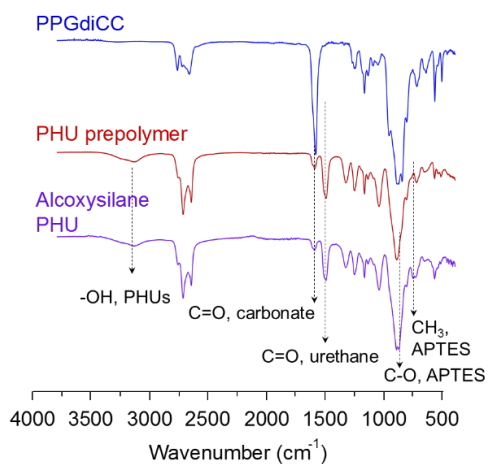


Figure 2.1. FTIR-ATR characterization of NIPUs before preparation of the film.

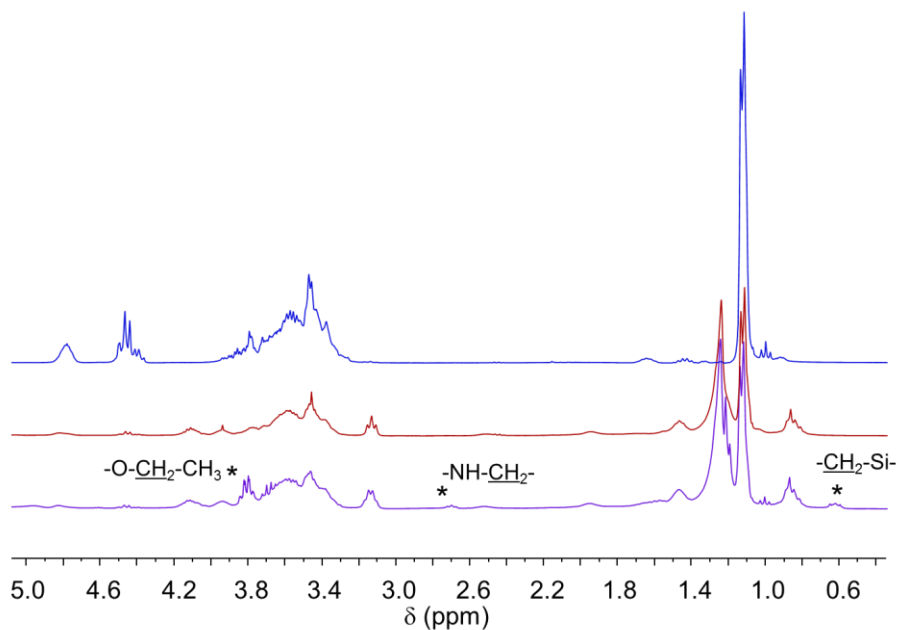


Figure 2.2. ^1H NMR characterization of NIPUs before preparation of the film. Blue spectrum corresponds to PPGdiCC; red spectrum corresponds to PHUdiCC prepolymer; and purple spectrum corresponds to alcoxysilane-terminated PHU. New signals are marked with * confirming the reaction with APTES.

One of the greatest advantages of alkoxy silane-functionalized formulations is their ability to cure under ambient conditions by a sol-gel process. In order to investigate the curing ability of this telechelic PHU oligomer, the curing was followed by FTIR-ATR and rheological measurements. The rheological measurement was performed to determine the gel time ($G' = G''$, therefore, $\tan \delta = 1$) at a single frequency and amplitude. The PHU alkoxy silane was first cured under ambient conditions for 15 h. Although FTIR-ATR spectra (Figure 2.3 a) showed the disappearance of the characteristic bands of CH_3 rocking and C-O symmetric stretching of APTES centred at 959 cm^{-1} and 1083 cm^{-1} respectively, the loss modulus (G'') remained higher than the storage modulus (G'), confirming that PHU was not cross-linked (Figure 2.3 b). No gel point (assigned when G' crosses G'') was observed, even after 15 h of reaction, suggesting the low capability of the APTES-terminated PHU oligomers to cure under ambient conditions.

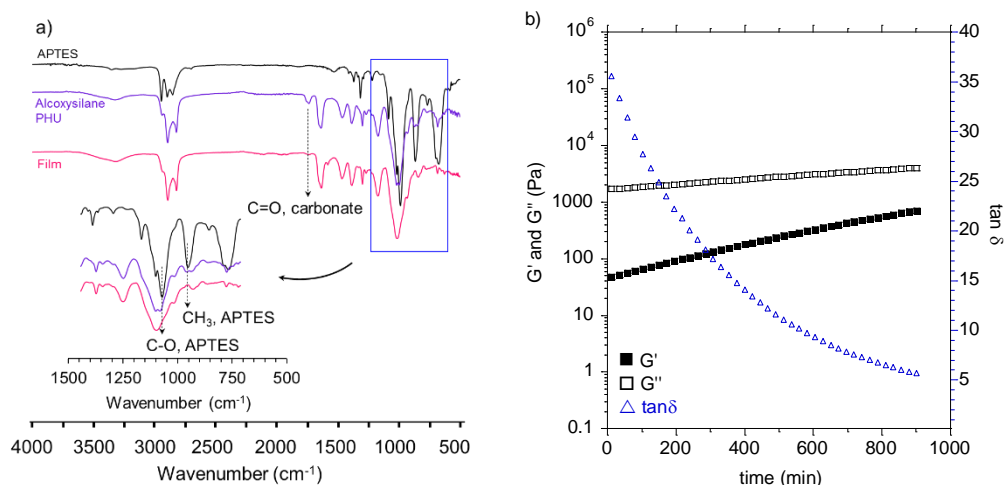


Figure 2.3. a) FTIR-ATR spectra for the following of the curing process; b) storage (G'), loss (G'') moduli and $\tan \delta$ values for the sample at $25 \text{ }^\circ\text{C}$.

In order to favor PHU curing, we investigated the effect of temperature and the use of a catalyst. Figure 2.4 a shows the values of G' and G'' at different temperatures. It is clear that the

gelation process is highly temperature dependent. The gelation time (t_{gel}) was decreased considerably by raising the temperature, with a gel time of 20 min at 120 °C, while no crosslinking was noted at 25 °C after 15 h. The curing was then performed at different temperatures (100, 80 and 60 °C) and the temperature dependence of the gel time was calculated by the Arrhenius equation⁵⁹ and plotted in Figure 2.4 b. This linear plot allowed for the calculation of the activation energy (E_a) of the process. As the sol-gel process implies two steps (hydrolysis and condensation of the ethoxysilanes), E_a was referred to the whole reaction. Without catalyst, the activation energy value was 50 kJ mol⁻¹, which is in the range of the typical E_a for silica gels (~40-80 kJ mol⁻¹).⁸⁴⁻⁸⁶

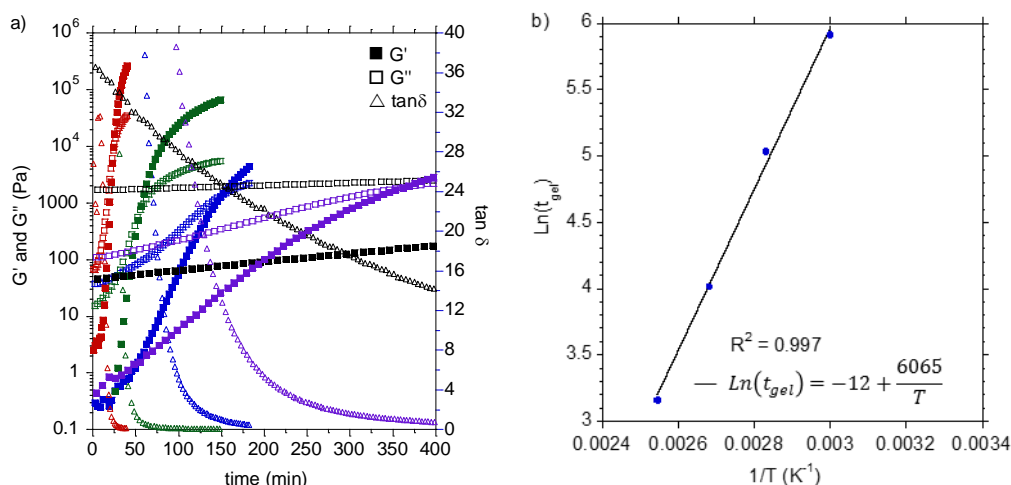


Figure 2.4. a) Storage (G') and loss (G'') modulus values of the rheological measurements of the monocomponent PHU adhesive system depending on temperature, b) plot representation of $\ln(t_{gel})$ vs. $1/T$ for the measurements presented in a).

The addition of a catalyst was then considered in order to accelerate the curing of the ethoxysilane moieties (Figure 2.5 a). As both hydrolysis and condensation reactions of the ethoxysilane group can be promoted by acids and bases,⁵⁹ a strong base (1,8-Diazabicyclo[5.4.0]undec-7-ene, DBU; $pK_a = 13.5$ ⁸⁷), a strong acid (methanesulfonic acid, MSA;

$pK_a = -1.9^{88}$) and a mild weak acid (acetic acid, HAc; $pK_a = 4.75^{89}$) (Figure 2.5 b) were tested as catalysts added at 1 wt% for reactions performed at 100 °C.

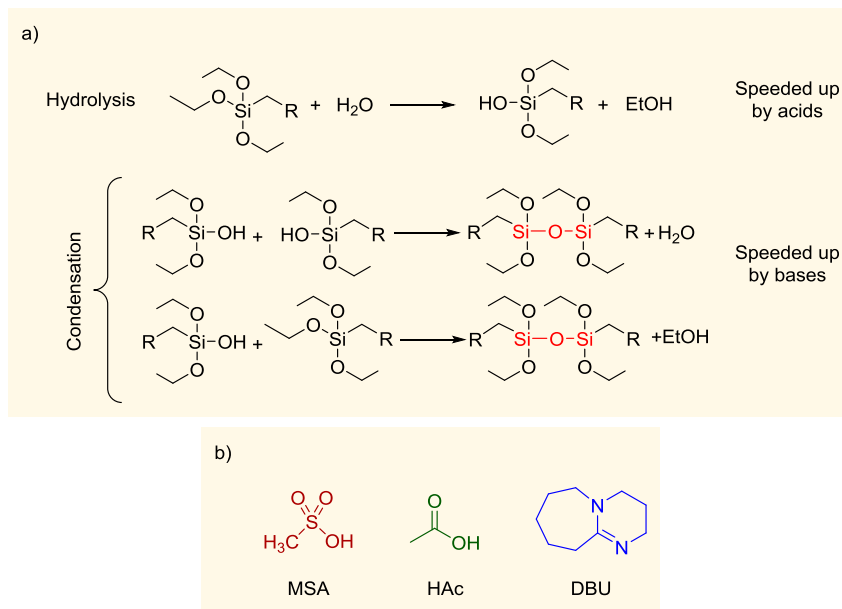


Figure 2.5. a) Hydrolysis and condensation scheme of alkoxy silane derivatives during the sol-gel process and b) structures of acids (MSA, HAc) and base (DBU) employed for speeding up the curing process.

While the strong acid and strong base slightly enhanced the curing rate (t_{gel} of about 40 min vs 56 min, Table 2.2, comparison of entries 2, 6, and 8), the mild acid led to a much faster curing ($t_{\text{gel}} = 10$ min; Table 2.2, entry 7; Figure 2.6 a). This faster curing with HAc agrees with results from Coltrain et al.⁹⁰ who found that a compromise is required in terms of hydrolysis and condensation to promote fast curing. When using a higher HAc concentration (5 wt%), a gel time of 20 min was obtained at a lower temperature, i.e. 60 °C, (Figure 2.6 b).

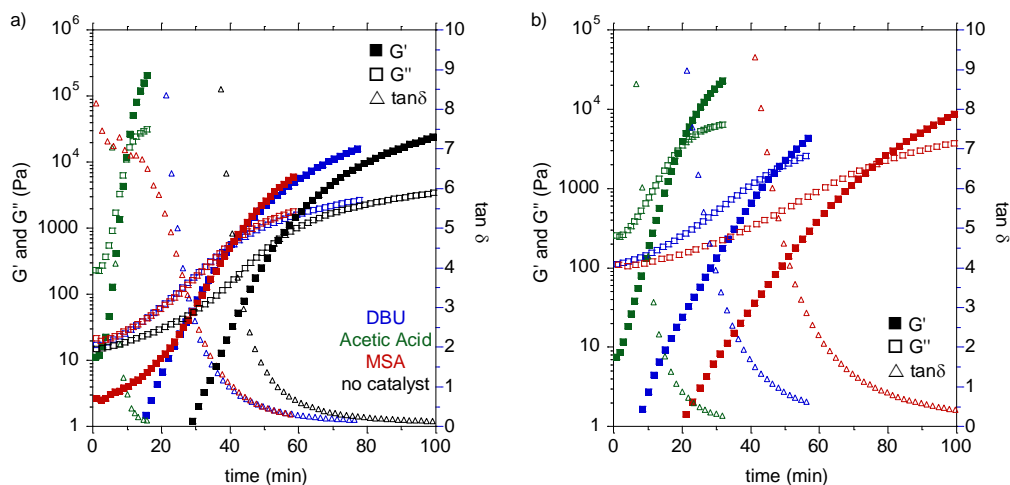


Figure 2.6. a) G' , G'' and $\tan \delta$ values for rheological measurements carried out at 100 °C in the presence of the different catalysts and b) G' , G'' and $\tan \delta$ values for rheological measurements employing 1 (red), 2.5 (blue) and 5 (green) wt% of acetic acid at 60 °C.

Table 2.2. Gel time values for all the different studied compositions and conditions.

Entry	Composition (PPGdiCC/RdiCC)	Temperature (°C)	Catalyst	t_{gel}^b (min)
1	100/0	120	no catalyst	23.5 ± 0.7
2		100		55.8 ± 2.5
3		80		153.5 ± 4.9
4		60		369.5 ± 12
5		25		^a
6	100/0	100	DBU (1 wt%)	42.8 ± 4.0
7			HAc (1 wt%)	9.8 ± 0.4
8			MSA (1 wt%)	39.7 ± 5.6
9	95/5	100		46.8 ± 4.0
10	90/10			32.1 ± 0.8
11	80/20		no catalyst	33.3 ± 1.7
12	60/40			18.6 ± 1.9

^aNo crossover after 15 h of measurement. ^bGel times values from the crossover between G'' and G' ($\tan \delta = 1$).

2.3. Evaluation of the adhesive properties of the hybrid PHU products

The adhesive properties of the hybrid PHU products (cured at 100 °C with 1 wt% HAc) on stainless steel were evaluated by lap-shear strength measurements. In order to ensure complete curing of the samples, materials were kept for 24 h at this temperature before measurement. Shear stress-displacement curve of the sample based on triethoxysilane-terminated PPG is depicted in Figure 2.7 a (blue curve). This formulation was characterized with low lap-shear strength of 1.1 ± 0.2 MPa. Moreover, the failure in this sample was cohesive, indicating that the internal forces of the adhesive were not strong enough (Figure A-II.7). We envisioned that an increase in the rigidity of the adhesive might enhance these cohesive forces and, therefore, the lap-shear strength of the material.

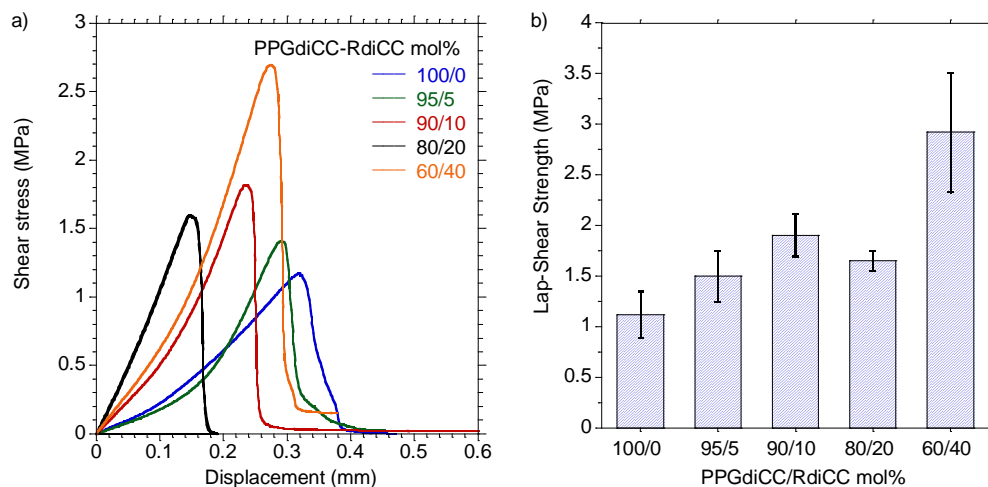
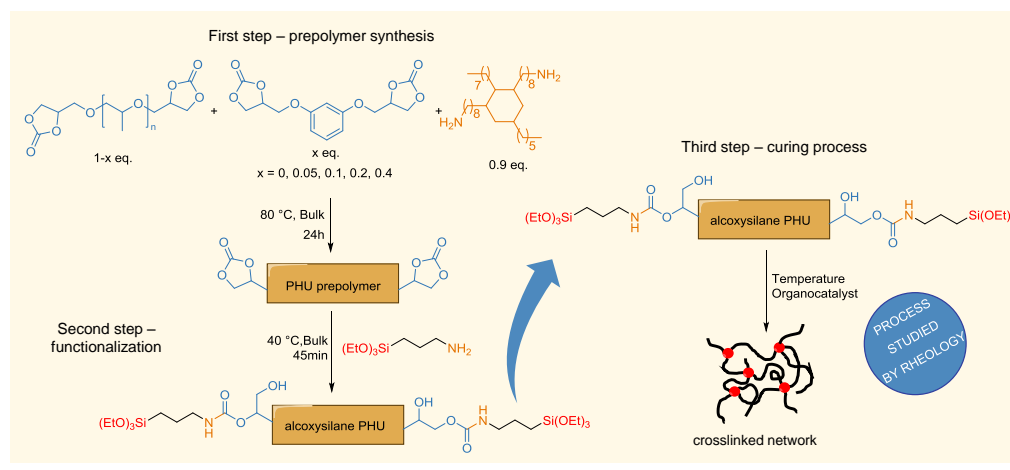


Figure 2.7. a) Representative curves of the lap-shear strength for each composition; b) values with error bars, representing standard deviation for each sample set.

Thus, in order to increase the cohesive strength, dicyclic carbonate-terminated PHU oligomers were prepared by substituting part of PPGdiCC by a more rigid resorcinol-based

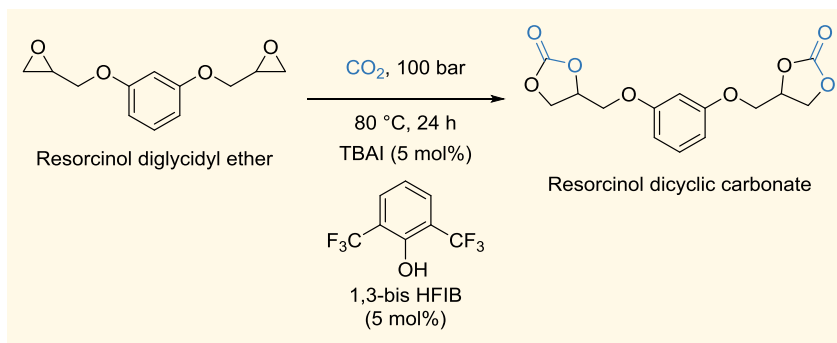
dicyclic carbonate (RdiCC; Scheme 2.3). RdiCC was previously synthesized by chemical insertion of CO₂ in resorcinol diglycidyl ether precursor at 80 °C for 24 h (Scheme 2.4). Although resorcinol production is mainly petrol based, it can also be prepared from bioresources, e.g. from catechins by fermentation or from glucose.⁹¹

Scheme 2.3. Synthesis of adhesives based on a mixture of soft (PPGdiCC) and hard (RdiCC) dicarbonates.



The curing process of the corresponding PHU oligomers was also investigated by rheology for four different PHU compositions at 100 °C without catalyst (Table 2.2, entries 9-12). Importantly, the gel time decreased progressively and significantly by increasing the RdiCC content in the PHU composition, from 56 min for the RdiCC-free PHU to 19 min for the RdiCC richest one.

Scheme 2.4. Synthesis of RdiCC from [3+2] CO₂ insertion into resorcinol diglycidyl ether precursor. TBAI and 1,3-bis HFIB were employed as catalysts and activator, respectively, for the reaction.



While similar lap-shear adhesion strengths were obtained for cured hybrid PHUs prepared with up to 20 mol% RdiCC (Table 2.3), better performance (2.9 ± 0.6 MPa) was obtained with 40% of the comonomer. A possible explanation for this could be that the cohesive forces were enhanced via non-covalent interactions of the resorcinol moiety as observed by Detrembleur et al.³⁸ No further addition of RdiCC into the formulation was performed due to the high viscosity of the samples, which led to practical difficulties in efficient mixing of the components.

Table 2.3. Values of shear strength for the different formulations and the type of failure.

Entry	Composition (PPGdiCC/RdiCC)	Lap-Shear strength (MPa)	Nature of adhesive failure
1	100/0	1.1 ± 0.2	Cohesive
2	95/5	1.5 ± 0.2	Cohesive
3	90/10	1.9 ± 0.2	Cohesive
4	80/20	1.6 ± 0.1	Cohesive
5	60/40	2.9 ± 0.6	Cohesive
6	60/40 ^a	2.8 ± 0.8^a	Cohesive

^aLap-shear measurement was performed after 96 h immersed in water.

Gel content measurements for all samples containing different soft to hard ratios were carried out in order to understand the impact of the crosslinking degree on the adhesion properties. The gel content for all compositions remained at around 70% (Figure A-II.8), except for the adhesive prepared from the PHU oligomer synthesized with 40 mol% RdiCC. In this latter case, the gel content was around 80%. Therefore, both the covalent (gel content) and non-covalent interactions (π - π interactions of the aromatic rings) of the sample are assumed to be responsible to some extent for the increase in the lap-shear strength of the specimens.

Aside from the shear strength, there are other properties that are important to study in order to evaluate the potential of an adhesive, including the water uptake and the thermal properties (the glass transition temperature, T_g , and the degradation temperature, T_d). Most adhesives should have a low water uptake in order not to swell during use and to avoid the delamination from the substrate.⁶² Due to the presence of primary and secondary alcohols in their structure, PHUs and, therefore, PHU adhesives are typically considered to be high water uptake materials.^{61,92} In agreement with these works, the adhesives based on PPGdiCC only or PPGdiCC and RdiCC (with up to 20 mol% RdiCC) had a water uptake of around 11% (Table 2.4, entries 1-4). Increasing the resorcinol content in the PHU to 40 mol% decreased this water uptake, owing to the introduction of hydrophobic aromatic groups within the polymer chain (Table 2.4, entry 5). It may be noted that the water uptake values for all compositions are much lower compared to other PHUs employed as adhesives in the literature^{38,61} and are comparable to NIPUs in which hydrophobic cyclocarbonated soybean oil was employed as part of the formulation.⁶² Furthermore, lap-shear strength measurements were carried out after immersing the specimens 96 h in water to evaluate the performance of the most hydrophobic adhesive. Interestingly, even after 4 days in water the lap-shear strength, 2.8 ± 0.8 MPa, of the adhesive was unaffected (Table 2.3, entry 6).

Table 2.4. Summary of results for the different formulations prepared. Curing conditions were set as 24 h at 100 °C.

Entry	Composition (PPGdiCC/RdiCC)	Catalyst	EWC ^a (%)	GC ^b (%)	T _g ^c (°C)	T _{d5%} ^d (°C)
1	100/0	HAc (1 wt%)	11.3 ± 0.5	68.7 ± 0.7	-32	273
2	95/5		10.1 ± 1.3	65.8 ± 3.5	-33	270
3	90/10		12.0 ± 1.6	64.8 ± 2.5	-32	265
4	80/20		12.2 ± 0.6	70.7 ± 3.5	-32	272
5	60/40		6.0 ± 0.4	79.6 ± 0.5	-23	265

^aEquilibrium water content measured after 96 h immersed in water; ^bgel content after Soxhlet extraction in refluxing THF for 24 h; ^cglass transition temperature; ^dtemperature at which sample lost 5 weight%.

On the other hand, the glass transition temperature defines at which temperature the adhesive is in its glassy state and becomes stiff and brittle.⁹³ The T_g for the adhesives was in the range of -32 to -23 °C (Table 2.4) allowing a low service temperature for all compositions. In addition, the thermal stability of the PHUs was investigated by thermogravimetric analysis (TGA) and no significant difference between the formulations was observed, with a degradation temperature at 5% (t_{d5%}) above 265 °C (Table 2.4) in all cases, in accordance with previous results using polyurethanes based on APTES.⁷⁴

2.4. Evaluation of the adhesive properties of the hybrid PHU at room temperature

One of the greatest assets of alkoxy silane groups is their potential to undergo crosslinking reactions at ambient conditions in the presence of an appropriate catalyst.⁹⁴ Therefore, the optimal composition containing 60/40 PPGdiCC/RdiCC was cured at 25 °C for 24 h employing 2.5, 5 and 7.5 wt% of HAc catalysis and the adhesive properties were investigated. Rheological measurements proved that even at the lowest catalysts concentrations, crosslinking occurred in 326 ± 84 min (Figure A-II.9). Nevertheless, the adhesion values in all cases were 3 times lower (Table 2.5) than in the case of curing the material at 100 °C which is related to the low values

obtained of gel content for these compositions (Table 2.5). The room temperature for curing affected detrimentally to the curing kinetics and therefore to the the cohesiveness of the adhesives.

Although the T_g values of the compositions cured at 25 °C (Table 2.5) remained similar to the previous ones allowing a low service temperature, equilibrium water content of these films increased significantly (up to 30%, Table 2.5) decreasing the resistance against delamination.

Table 2.5. Summary of results for the composition 60/40 PPGdiCC/RdiCC cured at 25 °C for 24 h with different amounts of HAc.

Entry	Composition (PPGdiCC/RdiCC)	HAc (wt%)	Lap-Shear Strength (MPa)	EWC ^a (%)	GC ^b (%)	T_g^c (°C)	Td5% ^d (°C)
1	60/40	2.5	1.1 ± 0.3	28.8 ± 0.4	40.9 ± 1.1	-30	215
2		5	1.1 ± 0.4	30.0 ± 3.3	18.6 ± 3.6	-26	222
3		7.5	0.8 ± 0.0	27.2 ± 2.3	*	-29	202

^aEquilibrium water content measured after 96 h immerse in water; ^bgel content after soxhlet extraction in refluxing THF for 24 h; ^cglass transition temperature; ^dtemperature at which sample lost 5 weight%. *No gel content, all sample was dissolved in THF.

2.5. Conclusions

Monocomponent non-isocyanate polyurethane adhesives were synthesized by adding (3-aminopropyl)triethoxysilane to a previously prepared PHU prepolymer based on 5-membered cyclic carbonates and Priamine™ 1074, allowing the curing process to proceed under ambient conditions through a sol-gel process in the presence of a mild acid. The activation energy of the sol-gel process was determined to be 50 kJ mol⁻¹ by rheological measurements conducted at different curing temperatures. In order to speed up the curing, the addition of catalyst and the increase of the reaction temperature were considered. By using 1 wt% of acetic acid at 100 °C the curing time was decreased fivefold. Furthermore, the use of 2.5

wt% of acetic acid allowed for curing to occur under ambient conditions, although the adhesive properties were slightly compromised. Finally, we found that the incorporation of 40 mol% of resorcinol dicarbonate hard comonomer increased the lap-shear strength more than 2.5 times, thus demonstrating the importance of the hard to soft ratio to obtain adhesives with good cohesion and adhesion properties.

Chapter 3.

Synergetic Effect of Dopamine and Alkoxysilanes in Sustainable Poly(Hydroxy Urethane) Adhesives

3.1. Introduction

Although a monocomponent NIPU adhesive based on a sol-gel process was successfully prepared, the materials presented moderated lap-shear strengths and curing times still far from been competitive in industry regarding to conventional PU adhesives (5 MPa, safe drive away time of 60 min).^{93,95,96} The preparation of polyurethane hybrid systems is widespread in the industry since they provide tunable speed of curing, which can be adjusted by the reactivity of the monomers and catalysts in the formulation. Moreover, it has been demonstrated that the incorporation of additives within the formulations, such as fillers^{61,62} or adhesion promoters such as dopamine strongly improved the adhesive performance.^{38,97} Incorporation of functionalized fillers enhances the adhesive performance of the PHU adhesives increasing their crosslinking density,⁶² whilst dopamine possess the ability to establish a large variety of chemical interactions and to self-crosslink, showing high affinity to different surfaces.^{98,99}

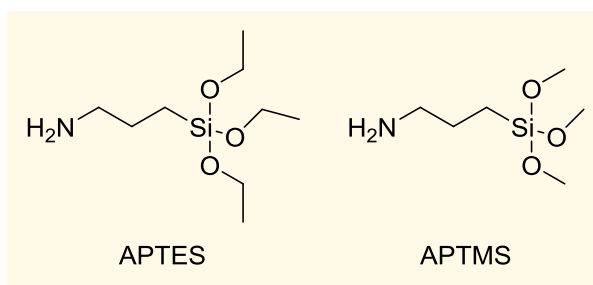


Figure 3.1. Structures of the alkoxysilane compounds employed as crosslinker agents in Chapter 2 (APTES) and in this Chapter (APTMS).

On the other hand, as it has been demonstrated in Chapter 2, alkoxysilane compounds creates a three-dimensional network through a sol-gel process. This process is not only accelerated by the addition of acid or base catalysts⁵⁹ and temperature,^{85,100} as it was demonstrated in Chapter 2, but also by factors such as the ratio water to alkoxyde,^{84,101} concentration of the alkoxysilane compound⁸⁴ and the size of the alkoxy group.¹⁰² Taking into

account these factors, we think that the size of the alkoxy group is the easiest one to control or change in the system presented in Chapter 3. The sol-gel process is speeded up with smaller alkoxy groups in the molecule.¹⁰² Thus, in order to obtain faster curing process we have change the 3-(aminopropyl)triethoxy silane (APTES) employed in Chapter 2 for 3-(aminopropyl)trimethoxy silane (APTMS) (Figure 3.1).

Therefore, in this chapter these two chemistries were combined with non-isocyanate polyurethane chemistry with the goal to enhance the adhesion performance while presenting fast curing rates. To do so we incorporated dopamine hydrochloride (DOP) as an adhesion promoter and 3-(aminopropyl)trimethoxy silane (APTMS) as a fast-curing promoter in the formulation. While these two chemistries have already been combined separately with NIPU chemistry, we take advantage of the orthogonal effect to implement adhesives on different substrates such as metals (stainless steel, aluminium), wood and plastics (PMMA, polyamide, PE-HD). Adjustment of the cyclic carbonate-based soft and hard segment molar ratios were performed in order to obtain best adhesion performance.

3.2. Influence of additives on PHU adhesive formulation

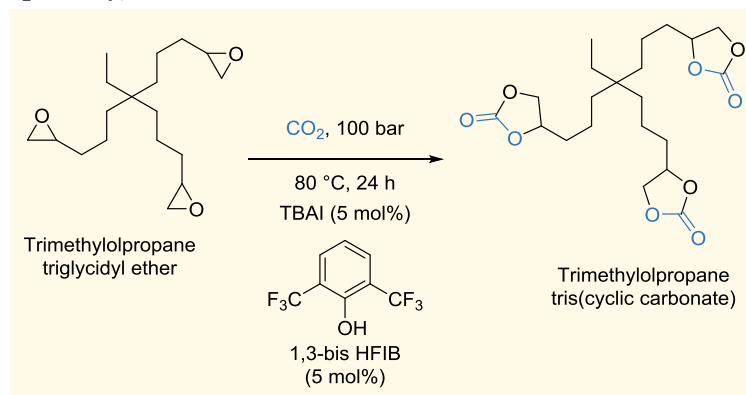
3.2.1. Synthesis and characterization of adhesives

In order to prepare suitable formulations we took as starting point one of the formulations with the best adhesion values from the literature, based on trifunctional cyclic carbonate (Trimethylolpropane tris(cyclic carbonate), TMPTC) and DOP³⁸ and we evaluated the effect of the addition of APTMS.

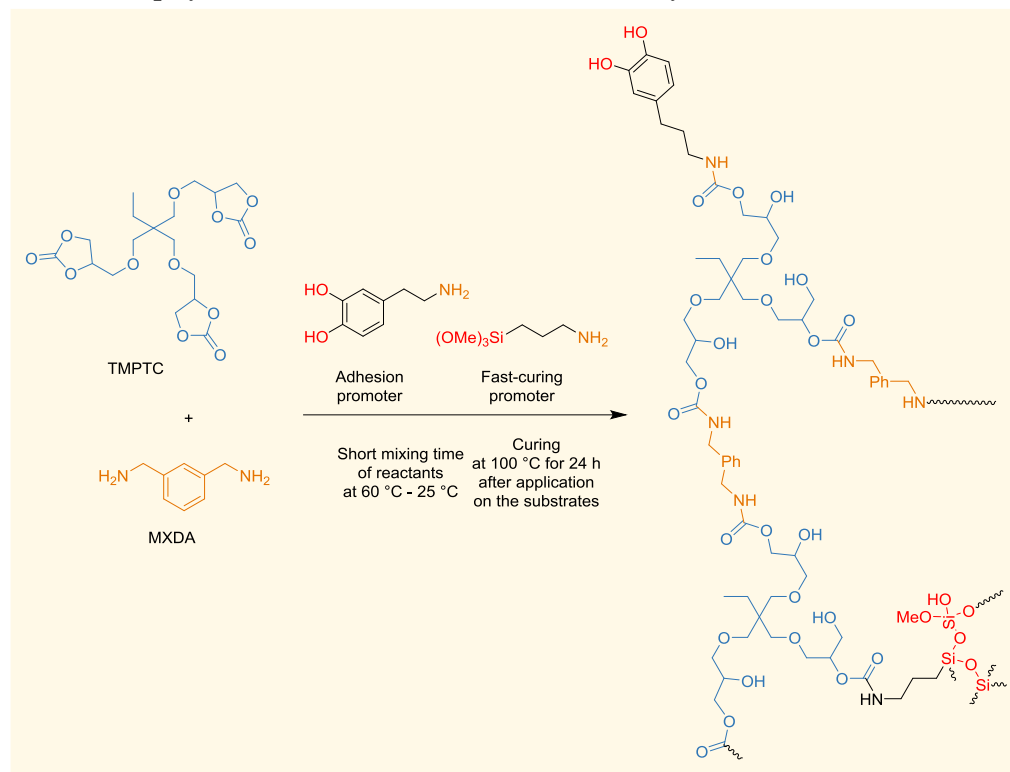
TMPTC was synthesized following the procedure presented in Chapter 2 for the synthesis of cyclic carbonates. Quantitative conversion of trimethylolpropane triglycidyl ether (TMPTE) was reached after 24 h of reaction at 80 °C passing a pressure of 100 bar of CO₂ (Scheme 3.1).

PHU adhesives were prepared by the reaction of an aromatic (MXDA) diamine, TMPTC and DOP in the presence of APTMS (Scheme 3.2). The viscous materials were applied onto the substrates and cured at 100 °C for 24 h to ensure complete reaction.

Scheme 3.1. Synthesis of TMPTC from [3+2] CO₂ insertion into trimethylolpropane triglycidyl ether precursor. Tetrabutylammonium iodide (TBAI) and 1,3-Bis(2-hydroxyhexafluoroisopropyl)benzene (1,3-bis HFIB) were employed as catalysts and activator, respectively, for the reaction.



Scheme 3.2. Synthesis for the preparation of the non-isocyanate polyurethane adhesives based on the polyaddition of an aromatic diamine with a tricyclic carbonate.



Completion of the reaction was followed by FTIR-ATR through the disappearance of the carbonyl stretching vibration band of the carbonate at 1781 cm^{-1} (Figure 3.2 a) and the appearance of new signals at 3320 (O–H, N–H), 1690 (C=O, urethane group), 1533 (δ N–H), 1412 (C–C, ph), 1332 (C=C, ph), 1456 and 1248 (C–O), 1165 (CH₃, rocking APTMS), 1096 and 1044 (C–O–O overlapped with Si–O–C) and 867 cm^{-1} (C–H, ph) confirming the formation of the urethane bond as well as the presence of DOP and APTMS in the polymer structure. Three-dimensional network of the materials was confirmed by rheological measurements, in which the storage moduli (G') remained over the loss moduli (G'') over the temperature (Figure 3.2 b). In addition, crosslinking degree of the samples were determined through soxhlet extractions in

refluxing THF for 24 h and after immersion for four days in deionized water. For all compositions, hybrid PHUs showed a high degree of crosslinking, giving gel contents above 99% when measured in THF while slightly lower values were obtained in water (Table 3.1), indicating more solubility of the extractable species in water.

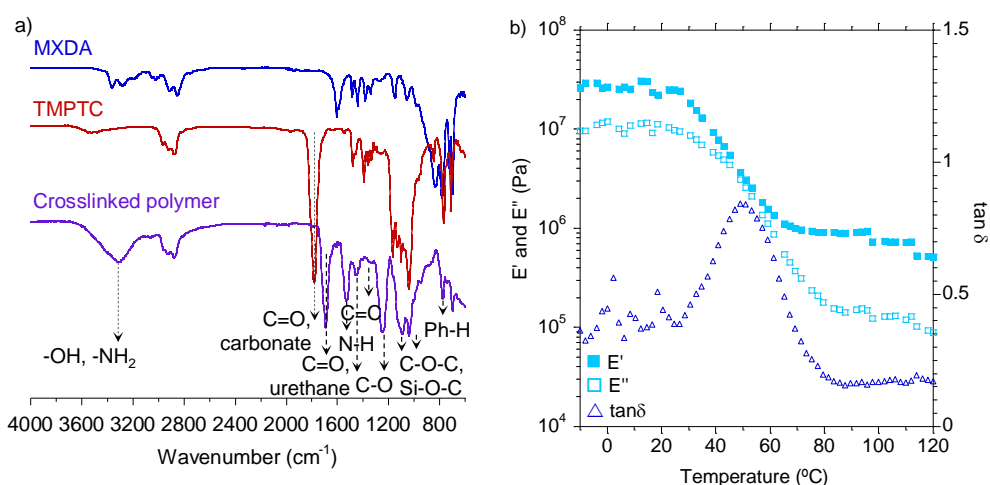


Figure 3.2. a) FTIR-ATR and b) storage (E') and loss (E'') moduli and $\tan \delta$ values from temperature sweep measurement of the doped aromatic diamine-based composition.

Table 3.1. Summary of results for the different formulations based on MXDA aromatic diamine. Curing conditions were set as 24 h at 100 °C.

Entry	Composition	EWC ^a (%)	GC (%)		T _g ^d (°C)		LSS ^e (MPa)	SAFT ^f (°C)
			THF ^b	Water ^c	DSC	DMA		
1	Neat	17.8 ± 1.6	>99%	96.5 ± 0.8	29; 62 ^h	76	10.7 ± 0.7	192 ± 16
2	DOP ^g	29.5 ± 0.9	>99%	92.5 ± 0.7	19; 58 ^h	63	12.3 ± 1.6	175 ± 8
3	APTMS ^g	24.1 ± 1.6	>99%	93.5 ± 0.2	52	70	10.0 ± 0.9	217 ± 0 ⁱ
4	DOP&APTMS ^g	25.0 ± 2.2	>99%	94.8 ± 0.8	13; 58 ^h	66	12.4 ± 1.6	188 ± 19

^aEquilibrium water content measured after 96 h immersed in water; ^bgel content after Soxhlet extraction in refluxing THF for 24 h; ^cgel content after 96 h immersed in water; ^dglass transition temperature; ^eLap-Shear strength; ^fShear Adhesion Failure Temperature; ^g3.9 mol% regarding monomers; ^hfirst and second T_g, respectively; ⁱkept the adhesive properties at this temperature for more than 7 hours.

3.2.2. Adhesive properties evaluation of initial compositions

The adhesive properties (shear strength and shear resistance) of these hybrid PHUs were addressed on stainless steel for the neat and modified formulations through single lap-shear and shear adhesive failure temperature (SAFT) experiments, respectively (Figure 3.3 and Table 3.1). Lap-shear strength of a reference NIPU formulation simply made of MXDA and TMPTC resulted in similar values (10.0 ± 0.9 MPa) to the ones reported by some of us using hexamethylene diamine instead of MXDA (9.1 ± 3.1 MPa).³⁸ When 3.9% mol of DOP was included into the formulation, lap-shear strength were raised up to 12.3 ± 1.6 MPa, in agreement with the trend and values of the literature. Adhesive failure of the samples was predominantly observed, therefore, we can conclude that dopamine increase the adhesion strength by the increase of the interaction forces with the adherend.¹⁰³ The further incorporation of APTMS within TMPTC/MXDA/DOP formulations had no impact on the adhesive performances with similar lap-shear strength values to the reference formulations (Table 3.1).

Dopamine and APTMS can establish covalent interactions contributing to reach shear strength values as high as the TMPTC/MXDA/DOP composition.^{98,104} Moreover, this compound can accelerate the curing process as reported in Chapter 2. In order to confirm this fact, gel times were determined through rheological measurements at 100 °C when crossover between G' and G'' ($\tan \delta = 1$) occurred over time (Figure 3.4). While gel time was not observed after 3 hours for the composition TMPTC/MXDA/DOP, the incorporation of APTMS decreased the gel time below 45 minutes, more than fourfold times.

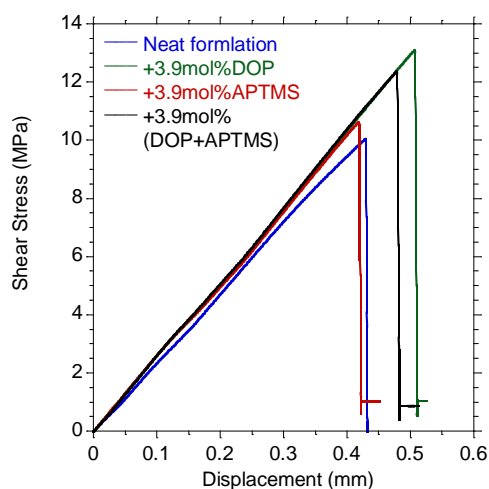


Figure 3.3. Representative shear stress-displacement curves for each composition based on MXDA diamine and TMPTC.

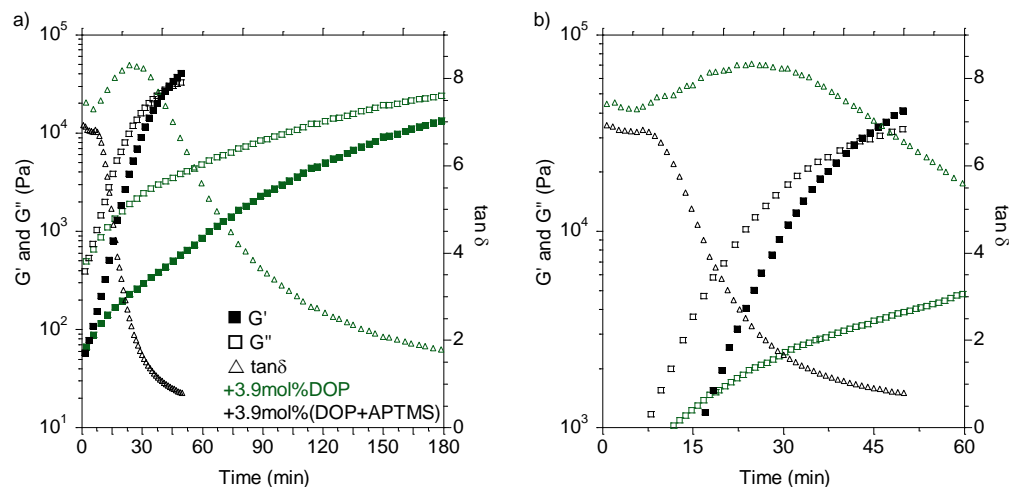


Figure 3.4. a) Storage (G') and loss (G'') modulus and $\tan \delta$ values for rheological measurements at 100 °C of 100/0 compositions adding 3.9 mol% of DOP (green) or +3.9 mol% of DOP and APTMS (black); b) zoom between 0 and 60 minutes of the previous graphic.

Interestingly, the combination of both additives, DOP and APTMS, kept adhesive properties of the materials at the same level when using just DOP. Adhesive failure was also predominant for these compositions (Figure A-II.10). Another reported benefit of siloxane

linked networks is their improvement of the service temperature.⁷⁷ To highlight this effect, Shear Adhesion Failure Temperature (SAFT) was determined. We found that the addition of APTMS endowed the materials with higher temperature resistance under load, even keeping adhesive properties more than 7 hours at 217 °C (Table 3.1). We believe that APTMS promotes more nodes of crosslinking in the polymer network improving cohesive strength as well as a better thermal resistance due to the inorganic nature of the compound.⁷⁴ Incorporation of APTMS combined with DOP slightly improved SAFT performance of just DOP as additive.

Aside from the lap-shear strength and SAFT properties, the water uptake and glass transition temperature of the adhesives were evaluated. On the one hand, water uptake of the materials will provide information about the potential use in damped atmospheres. Water absorption reduces the mechanical properties induced by plasticization of the adhesive and may induce interfacial failure (wet delamination of the adhesive).¹⁰⁵ The addition of the DOP substantially increased the water uptake from 17.8 ± 1.6 to 29.5 ± 0.9 . Nonetheless, we found that when DOP was combined with APTMS the water uptake increase was not as pronounced (25.0 ± 2.2). We think that this increase in the water uptake of the samples was related to the incorporation of more hydroxyl groups of DOP (hydrophilic pendant groups) to the polymers. On the other hand, the glass transition temperature indicates when the adhesive turns into a glassy state, increasing its stiffness and brittleness.⁹³ A T_g higher than the room temperature, confirmed the rigidity of the hybrid PHU materials. Broad T_g values were observed for neat and DOP-containing formulations, which can be associated with different densities of crosslinking inside the material. The greater T_g was associated to regions with higher density of crosslinking. In the samples with dopamine was observed a lower T_g , since dopamine does not contribute directly in the crosslinked network, while incorporation of APTMS showed a more defined and higher T_g as results of the greater homogeneity in the 3d network. For a further study dynamic

mechanical thermal analysis (DMTA) was employed for determining crosslinking densities (v_e) and glass transition temperatures of the cured formulations. Table 3.1 show T_g values of the formulations while storage moduli in the rubbery plateau (E') (T_{g+50} °C) and v_e are collected in Table 3.2.

Table 3.2. Values of storage modulus (E') at T_{g+50} °C and crosslinking densities of the different formulations.

Entry	Composition	E'^a (MPa)	v_e^b (10^2 mol m^{-3})
1	Neat	1.1	1.1
2	+3.9 mol% DOP	0.6	0.6
3	+3.9 mol% APTMS	2.3	2.4
4	+3.9 mol% DOP&APTMS	1.2	1.2

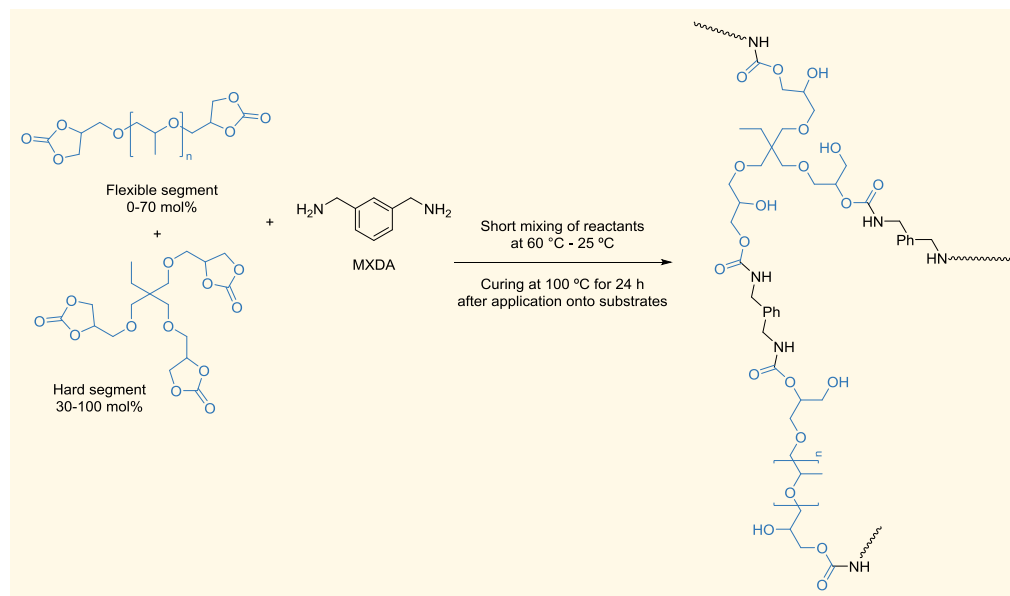
^aStorage Modulus in the rubbery region of the material (T_{g+50} °C); ^bcrosslinking density calculated from eq 7.

Raw data obtained from the temperature sweep measurements are depicted in Figure A-II.11. T_g values higher than room temperature were observed confirming results of DSC measurements and the rigidity of the materials. Crosslinking density was calculated from eq 7. Addition of dopamine into the formulation decreased the crosslinking density of the neat composition, corroborating it less participation of this compound to the three-dimensional network. On the other hand, the incorporation of APTMS to the neat composition increased twofold v_e due to the greater nodes of crosslinking that provide the siloxane compound. Combination of both additives resulted in a slightly higher v_e than neat formulation one.

3.3. Optimal hard/soft segment balance for well-designed adhesives

Despite the good results obtained for shear strength and SAFT, the hybrid PHU recipes were made of reactants affording hard materials. To design adhesives with optimal properties, the balance between hard and soft segments within the chains/network has to be properly adjusted as it is reported in literature^{37,51} and demonstrated in the Chapter 2 of this thesis. Therefore, the bifunctional cyclic carbonate based on a flexible aliphatic chain containing ether links use in the Chapter 2, i.e. poly(propylene glycol) dicyclic carbonate (PPGdiCC), was blended with TMPTC at different TMPTC/PPGdiCC molar ratios (Scheme 3.3).

Scheme 3.3. Synthesis of hybrid adhesives incorporating a flexible monomer to the formulation.



Incorporation of PPGdiCC decreased the formulation viscosity before application. Before analysing the effect of the soft segment on the adhesive properties, the mixing time of the

formulation (prior to application and curing) on the final adhesive performance of PHU was optimized (Figure A-II.12). This experiment was carried out for a 70/30 TMPTC/PPGdiCC formulation for 1.5, 5, 10 and 20 min of mixing times. Figure A-II.12 shows that increasing the mixing time substantially raised the lap-shear strength, from 13 MPa for 1.5 min of mixing to 19 MPa for 20 min. Mixing times of 20 min were therefore applied for the following experiments.

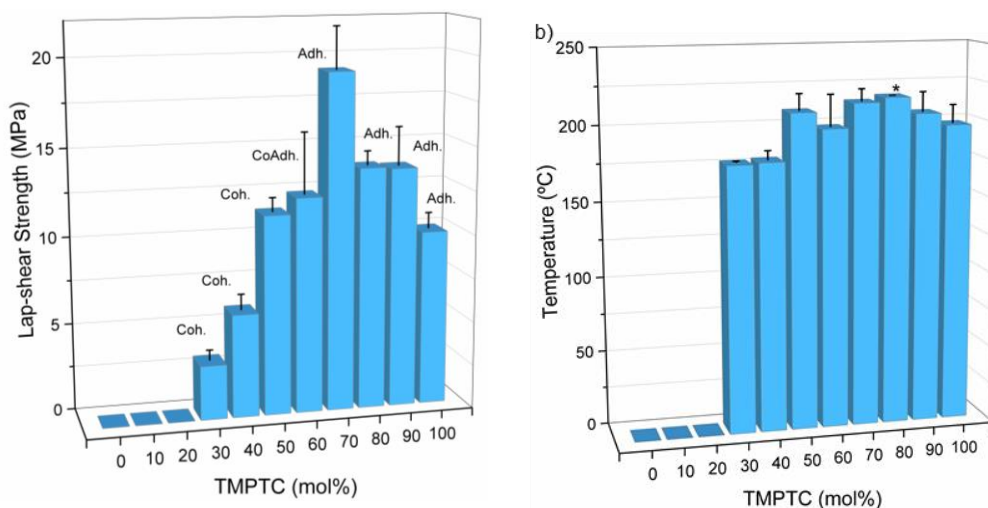


Figure 3.5. a) Lap-shear strength values on stainless steel obtained from single-lap-shear measurements as function of the incorporated mol% of hard segment (TMPTC) into the formulation and b) Shear adhesion failure temperatures as function of the incorporated mol% of hard segment (TMPTC) into the formulation. Adh.: adhesive failure; Coadh.: coadhesive failure; Coh.: cohesive failure. *80/20 mol% (TMPTC/PPdiCC) based-formulation kept the adhesive properties at 217 °C for more than 7 hours.

Figure 3.5 a shows that below 30 mol% of TMPTC, it was not possible to perform free standing films and the corresponding lap-shear strength values were negligible. The lap-shear strength strongly increased when raising the TMPTC content from 30 to 70 mol%, with the highest value obtained at 70 mol% (19.2 ± 2.4 MPa). Higher contents of TMPTC were detrimental to the adhesion. This progressive increase of the adhesive performance with the content of TMPTC (in the 30-70 mol% range) correlates with the higher degree of crosslinking of the materials (Table 3.3), which reinforced the cohesive forces. The nature of the adhesive

failure supported the increment of the cohesive forces, changing from cohesive (Figure A-II.13 e-h) to adhesive failure (Figure A-II.13 a-d). At low percentages of hard segment, forces between adhesive and the adherend were higher than the internal forces of the glue, while at higher content of the hard segment, intermolecular forces became enough strong to keep the adhesive together and break the linkage with the surface primarily. Beyond 70 mol% of TMPTC, the adhesives became too brittle and stiff (T_g substantially increased with the TMPTC content in the formulation as reported in Table 3.3), and are thus not able to withstand high deformation forces. Premature break was thus observed for high contents of TMPTC (> 70 mol%) (Figure 3.5 a).

Table 3.3. Characterization values for the compositions based on different molar ratios of TMPTC and PPGdiCC mixed with MXDA.

Composition TMPTC/PPGdiCC (mol%)	EWC ^a (%)	GC (%)		T_g^d (°C)	LSS ^e (MPa)	SAFT ^f (°C)
		THF ^b	Water ^c			
100/0	17.8 ± 1.6	>99	96.5 ± 0.8	29; 62 ^g	10.0 ± 0.9	198 ± 12
90/10	20.4 ± 0.6	>99	97.1 ± 0.6	25; 51 ^g	13.7 ± 2.2	206 ± 13
80/20	20.2 ± 1.0	98.4 ± 1.2	98.3 ± 0.1	15	13.8 ± 0.8	217 ± 0 ^h
70/30	31.8 ± 4.0	91.7 ± 3.4	96.7 ± 0.4	10	19.2 ± 2.4	214 ± 8
60/40	43.3 ± 2.0	84.5 ± 0.7	96.9 ± 0.3	9	12.3 ± 3.5	198 ± 21
50/50	68.2 ± 4.1	76.0 ± 1.2	95.2 ± 0.5	1	11.4 ± 0.8	209 ± 11
40/60	75.6 ± 2.5	64.4 ± 0.9	92.0 ± 0.5	0	5.9 ± 0.8	178 ± 6
30/70	86.0 ± 2.4	44.0 ± 1.1	93.0 ± 0.8	-8	3.1 ± 0.6	177 ± 1

^aEquilibrium water content measured after 96 h immersed in water; ^bgel content after Soxhlet extraction in refluxing THF for 24 h; ^cgel content after 96 h immersed in water; ^dglass transition temperature; ^eLap-Shear strength; ^fShear Adhesion Failure Temperature; ^gfirst and second T_g , respectively; ^hkept the adhesive properties at 217 °C for more than 7 hours.

The adhesive properties under load and temperature were evaluated through shear adhesion failure measurements, determining the temperatures of the samples at which breaking of the bonding occurs (Figure 3.5 b). The formulations with 40/60 and 30/70 mol%

TMPTC/PPGdiCC withstood creep forces up to 178 ± 6 °C and 177 ± 1 °C, respectively. Similarly to shear strength, SAFT reached a maximum value for a composition of 70/30 and 80/20 TMPTC/PPGdiCC. Importantly, the PHU with the 80/20 TMPTC/PPGdiCC formulation kept adhesive properties more than 7 h at 217 °C. When high adhesive performances have to be maintained at high temperature (>200 °C), a minimum of 50 mol% of TMPTC is required in the formulation (Table 3.3).

Complementary to the adhesive properties, water uptake and glass transition temperatures were determined for all cured formulations. Despite the hydrophobic nature of PPGdiCC, the incorporation of the flexible monomer into the formulation had a detrimental effect into water uptake of the materials. Long hydrophilic chains of PPGdiCC allowed the adhesive to swell and absorb more water. On the other hand, a decreasing trend in T_g values was observed at higher PPGdiCC molar ratios. The higher mobility of the PPG chains decreased these values making adhesive more suitable for lower temperatures.

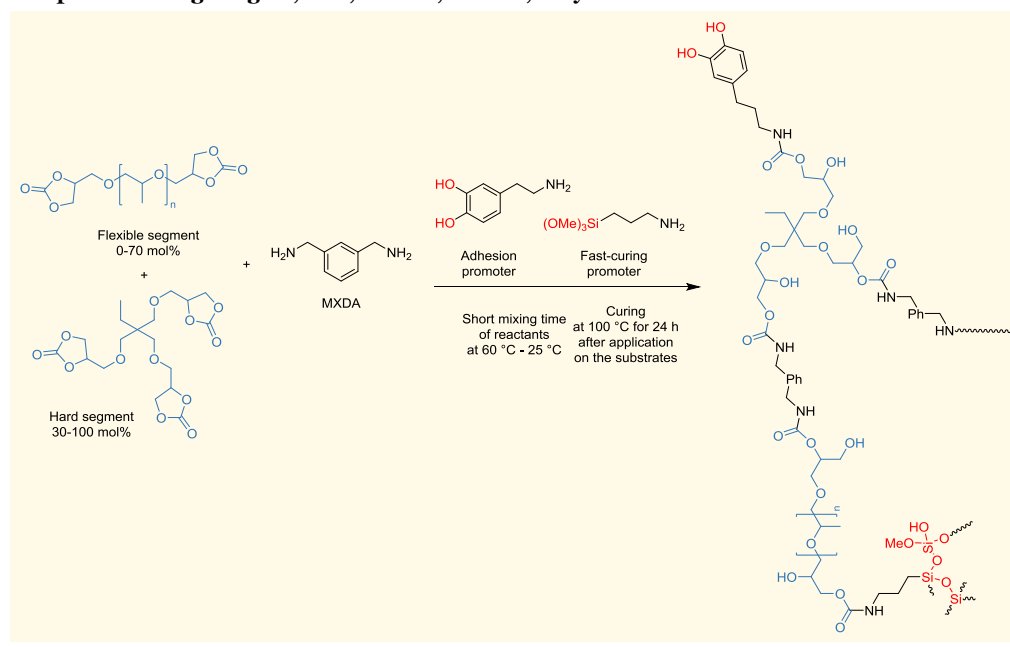
3.4. Effect of Dopamine and APTMS on balanced neat formulations

We carried out a further evaluation of the influence of the addition of DOP and APTMS on the adhesion properties of PHUs prepared from 50/50, 60/40 and 70/30 TMPTC/PPGdiCC formulations (Scheme 3.4).

Formulations were selected according to best lap-shear strengths among adhesive and cohesive failures since compositions were able to withstand similar SAFTs. Only in the case of 70/30 composition an improvement was achieved when 3.9 mol% of DOP and APTMS were introduced into the formulation (21.6 ± 0.7 MPa). In the two other cases, the incorporation of

the additives was not favorable to the shear strength (Figure 3.6). We think that in these two cases, cohesive forces were not enough enhanced and only adhesive properties of high cohesive materials were improved thanks to DOP. The importance of the combination of soft and hard segment were demonstrated as 70/30 mol% ratio surpassed shear strengths of fully tricyclic carbonate based formulation.

Scheme 3.4. Synthesis scheme of the doped 70/30 mol% hard/segment ratio PHU adhesive composition for gluing SS, Oak, PMMA; PE-HD, Polyamide and Aluminum.



The ability of the adhesive for gluing different substrates and the influence of the additives, i.e. DOP and APTMS, were addressed by lap-shear measurements on oak wood, polyamide, PMMA, PE-HD and aluminum (Figure 3.7). 70/30 TMPTC/PPGdiCC compositions were characterized with low lap-shear strength values (0.7 – 2.8 MPa, Table A-II.2) when polymeric substrates were glued. Polyamide showed the strongest interactions with the adhesive among polymeric substrates due to its greater surface energy.¹⁰⁶ The higher surface

energy, the easier wettability of the substrate and therefore stronger attractive forces are created between the adhesive and the adherend.⁴ In addition, polyamide can establish hydrogen bonding interactions with the polymer, while PE-HD is not able to do it. For all polymeric substrates adhesive failure was observed, showing the low affinity between adherend and adhesive (Figure A-II.14). When polar substrates, i.e. wood and aluminium, were bonded, much higher shear strength values were obtained. For instance, hybrid PHU provided values up to 18.9 ± 1.5 MPa on aluminum. This demonstrates a higher interaction of dopamine with polar substrates, since the stronger interaction of hydroxyl groups with these surfaces.

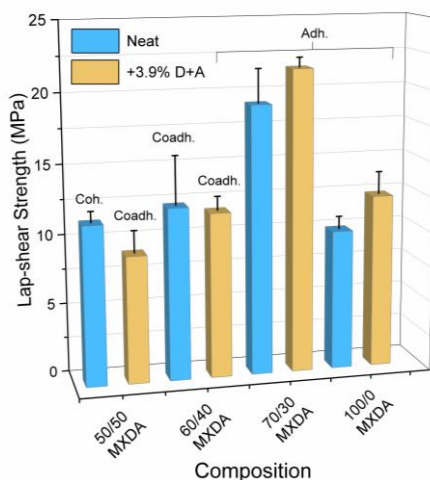


Figure 3.6. Lap-shear strength values comparison between neat and DOP-APTMS (3.9 mol%) of 50/50, 60/40 and 70/30 mol% hard/soft segment ratio compositions and full TMPTC composition.

All substrates tested above were cleaned prior to testing by immersing them in solvents and water as detailed in the experimental section. Nevertheless, due to the porosity of oak wood, these immersion steps could be detrimental to the shear strength. In order to investigate the effect of these cleaning treatments on the adhesive performance of PHU on this substrate, the specimens were kept overnight at 70 °C in order to eliminate humidity before applying the

adhesive. This treatment greatly enhanced the adhesion values from 5.0 ± 1.5 to 10.0 ± 2.7 MPa (entries 2 and 3, Table A-II.3). In order to evaluate if other treatments can enhance even more the adhesion due to a weak boundary layer or poor wetting of the surface, the wood substrate was treated with sandpaper and wiped with a paper wet with acetone (entry 1, Table A-II.3).³⁰ This value was inferior (7.1 ± 0.6 MPa) to treating the sample with solvent + heating. The application of a higher amount of PHU formulation enhanced the adhesion performances from 10.0 ± 2.7 MPa (~35 mg of adhesive) to 12.8 ± 2.4 MPa (~80 mg of adhesive) (Figure 3.7 b). Indeed, in both cases wood was destroyed during the measurement suffering substrate failure (Figure A-II.15 d-g). Therefore, the collected values were minimum shear strength values for bonding oak wood.

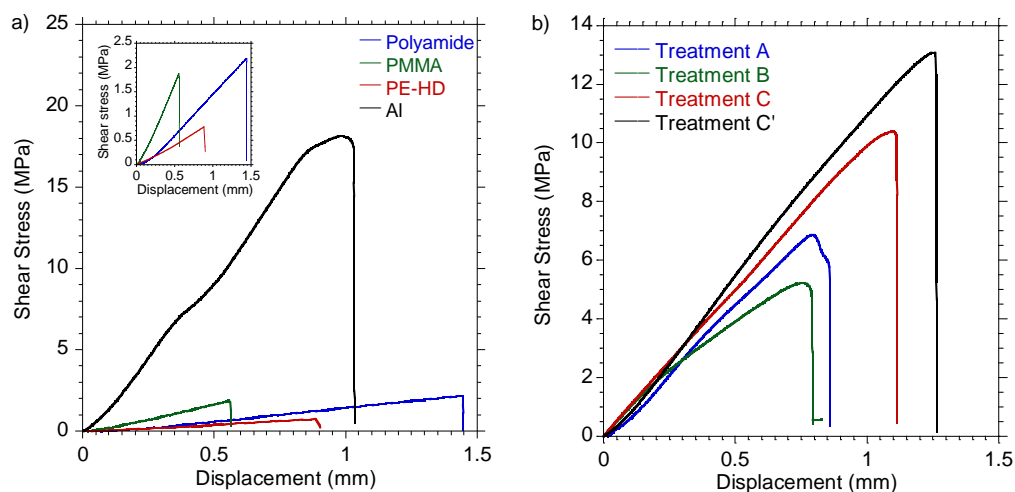


Figure 3.7. Representative shear stress-displacement curves of the neat 70/30 mol% hard/segment ratio composition for a) polyamide, PMMA, PE-HD and aluminum substrates and d) depending on the different surface treatments applied to oak wood. Treatment A: sanded with sandpaper and wiped with a paper wet in acetone; Treatment B: common treatment for the other substrates; Treatment C: same as treatment B with an additional overnight at 70 °C; Treatment C': same as treatment C but applying a greater amount of adhesive (~80 mg).

In all cases the adhesion performance of the pure PHU was compared to hybrid PHUs. We found that only in the case of aluminium a small improvement of the adhesion performance was observed (Table A-II.2). Nevertheless, it should be pointed out that the incorporation of APTMS could greatly improve the initial curing process of PHUs to facilitate their potential industrialization as previously demonstrated.

3.5. Conclusions

To conclude, non-isocyanate hybrid polyurethane adhesives were synthesized by reacting a trifunctional 5-membered cyclic carbonate (TMPTC), a hard monomer, with an aromatic diamine, an adhesion (dopamine hydrochloride) and a fast-curing (aminopropyl trimethoxysilane, APTMS) promoters. The incorporation of 3.9 mol% of DOP and APTMS into the compositions showed a synergetic effect of the additives enhancing lap-shear strength on stainless steel as dopamine alone did and reducing gel time fourfold times. Furthermore, the use of APTMS endowed adhesives with outstanding resistance to creep under temperature and 1 kg load. We found that the incorporation of 30 mol% of PPGdiCC as soft monomer significantly improved the lap-shear strength, surpassing the performance obtained when using 100 mol% hard monomer-based doped formulation. The incorporation of both additives (dopamine and APTMS) to this formulation provided PHUs adhesives that retain adhesion to different substrates, showing better performance with metals (SS and Al) and wood than for polymeric substrates (polyamide, PMMA, PE-HD). The incorporation of APTMS could facilitate the implementation of PHU adhesives in the industry due to its well reported fast curing in ambient conditions.

Chapter 4.

Fast-Curing Room Temperature Poly(Hydroxy Urethane)-Epoxy hybrid Adhesives



4.1. Introduction

In any industry and particularly in automotive industry, processing times are crucial. On these production lines, the assembly of different parts of the vehicle is performed using adhesives thanks to the reduction of weight as well as increasing of safety, in terms of energy absorption, compared to spot welding, riveting or clinching.^{107,108} Liquid structural adhesives are widely used for this purpose although an increase of the process time is suffered or assumed due to long curing times. It is worth to point out that during the curing process of liquid structural adhesives two main stages must to be considered. On the one hand, the time to achieve enough strength in order to hold the parts of the ensemble together (handle strength), that is related to the gel time of the adhesive. On the other hand, in the second stage is considered the time to reach the ultimate strength of the adhesive joint related to the final application properties. Some technologies have decreased cycle times from hours to minutes, especially when (high) temperatures can be applied, making adhesives more cost-effective. It has to be noted that the automotive parts manufacturers' process has not been adapted to the adhesive curing conditions, but it is the adhesive, which has been designed to fit in the automotive production lines. Therefore, despite the good adhesive performance showed by doped formulations of PHU adhesives in the range of 10-22 MPa and services temperatures up to 200 °C, the need of high temperature (100 °C), which for some applications ruins their industrial implementation. Thus, the main target for our adhesive is to cure under ambient conditions and within one hour of time, developing enough strength to keep the substrates together.

The employment of other chemistries such as epoxy, sol-gel or composites, has been widespread for enhancing PHU performance.³³ The creation of hybrid systems through the

combination with epoxy chemistry is one of the most popular, being widely used not only for endowing PHUs with better adhesion performance^{48,50–52,109} but also to improve other applications, mainly coatings.^{110–114}

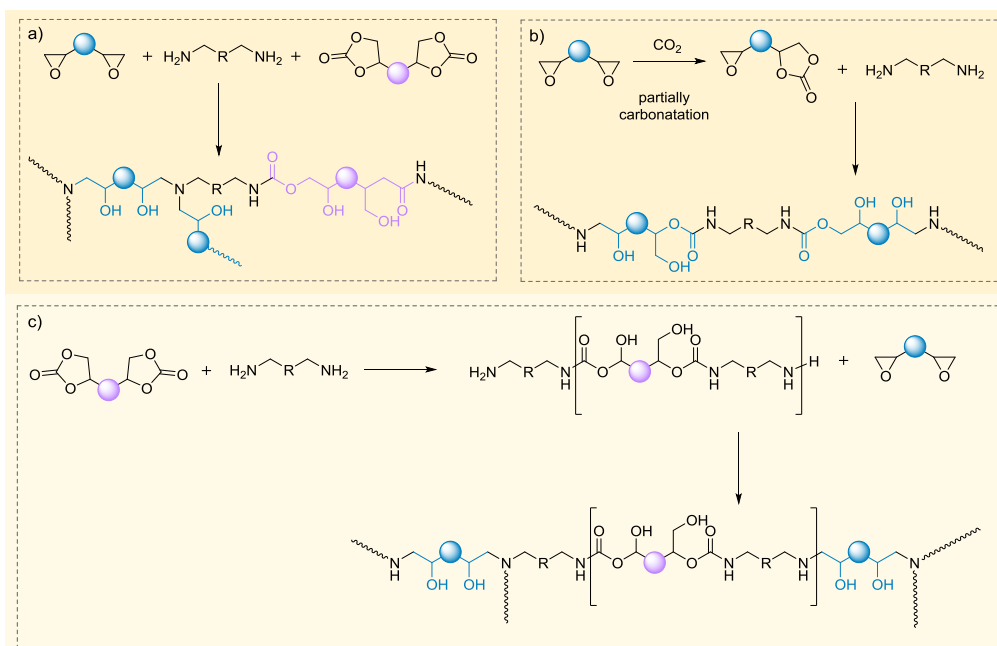


Figure 4.1. Strategies for the preparation of PHU-epoxy hybrids. One-step co-polymerization of epoxy resins and cyclic carbonates with amines through a) direct mixing of amine, epoxy resin and cyclic carbonates and b) partial conversion of epoxy into cyclic carbonates with reacted with amines. c) prepolymer synthesis of poly(hydroxy urethane)s and curing with epoxy resins.

Two are the main strategies for the production of PHU-epoxy hybrids:^{33,115} i) one step co-polymerization of epoxy and cyclic carbonates with amines (Figure 4.1 a and b); ii) amino-terminated PHU (A-PHU) prepolymer synthesis and further reaction with the epoxy resin (Figure 4.1 c). The one-step co-polymerization can be divided in two strategies: a) straight mixing of amine, cyclic carbonate and epoxy resin (Figure 4.1 a) or b) partial conversion of epoxy resins into cyclic carbonates to access to hybrid oligomers, which are further reacted with

amines to prepare the hybrid materials (Figure 4.1 b). None of them solves the low reactivity of cyclic as in the majority of the cases long periods (7 days) or high curing temperatures (at least 80-100 °C) are needed to achieve good adhesion performance. On the other hand, in the prepolymer synthesis an excess of amines is employed to reach full conversion of cyclic carbonates in a first step (Figure 4.1 c). The amino-terminated prepolymer as well as the excess of amine, which acts as reactive diluent, further react with the epoxy in the second step without the necessity of temperature and in shorter times than previous strategies (Figure 4.2 a).^{116,117} Considering the two active hydrogen that possess primary amines, is not mandatory the addition of additional crosslinker to the formulation since the created secondary amine undergoes a second reaction with another epoxy group forming a three-dimensional network (Figure 4.2 b).^{118,119} Thus, strategy ii (A-PHU synthesis and further reaction with epoxy resin) was selected for the preparation of PHU-epoxy hybrid adhesives at room temperature.

Moreover, taking advantage of the incorporation of epoxy groups into the formulation we hypothesized that the curing process may be speeded up by adding a new component to the formulation, thiol to promote thiol-epoxy 'click' chemistry. Thiol-epoxy polymerizations have industrial relevance in the area of adhesives, high-performance coatings and composites.¹²⁰ The reaction is rapid, selective, 100% atom economy and takes place in bulk and quantitatively under mild conditions.^{120,121} It is well established that the base-catalyzed thiol-epoxy condensation takes place by simple nucleophilic addition between thiolate and epoxy groups.^{122,123} When strong bases such as imidazole and TMG are employed as catalyst, deprotonation of the thiol occurs in a first step followed by the nucleophilic attack of the formed thiolate to the epoxy ring (Figure 4.2 c and d). The protonation of the alcoholate anions via either the base catalyst (Figure 4.2 c) or the thiol (Figure 4.2 d) gives rise to the final thiol-epoxy structure. We hypothesize that the thiol-epoxy reaction will be faster than the

amino-epoxy reaction, contributing to accelerate the initial hardening of the adhesive decreasing the time to reach handle strength. Meanwhile, A-PHU will react more gradually and will contribute to the final mechanical properties of the adhesive.

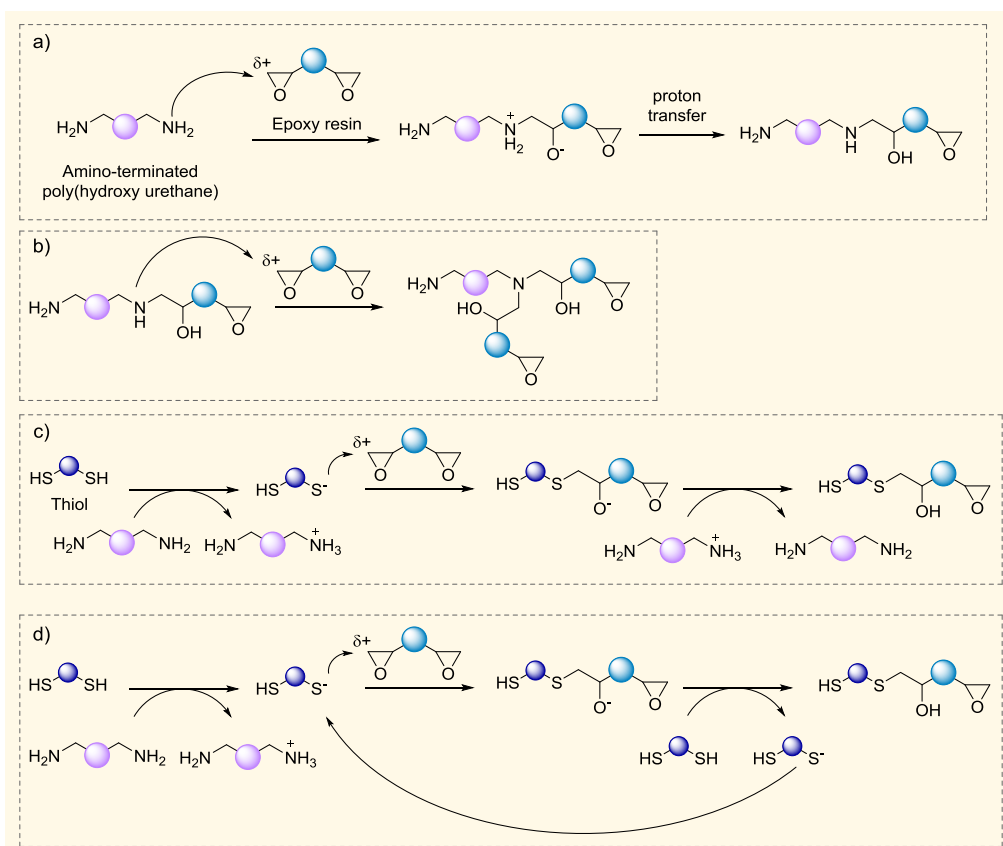


Figure 4.2. a) Reaction between a primary amine and an epoxy resin; b) further reaction of the created secondary amine from reaction a) with another epoxy group; c) base-catalyzed reaction of thiol with epoxy group with regeneration of the base catalyst/A-PHU. It is depicted just A-PHU as catalyst for making clear the figure and d) same reaction as c) with the generation of the thiolate in the proton transfer step.

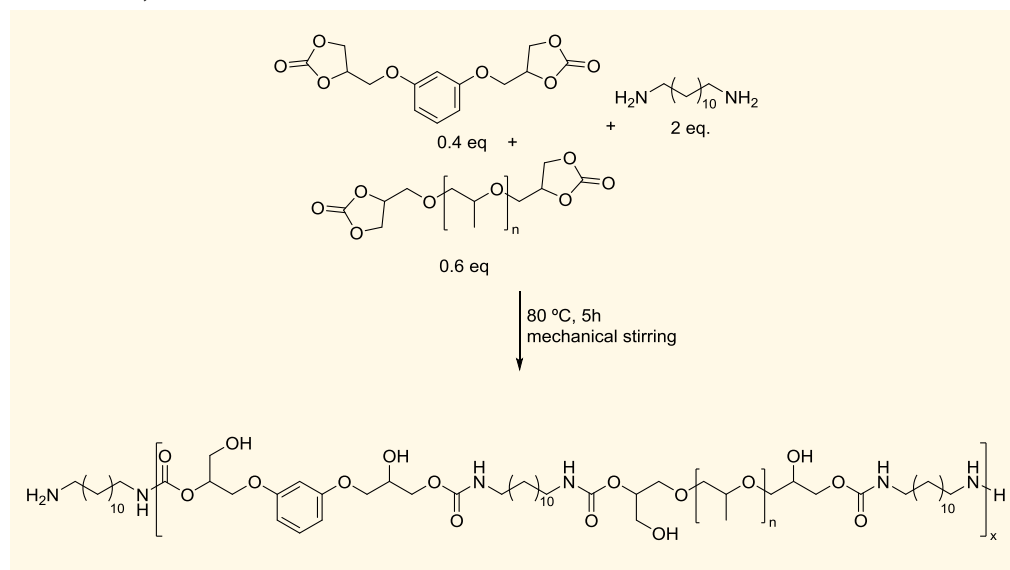
Thus, in this chapter a complex system combining an amino-terminated poly(hydroxy urethane), an epoxy resin, a thiol compound and a strong base was employed aiming to develop PHU-epoxy hybrid adhesives at room temperature, which were able to reach handle strength in

short times. Therefore, A-PHU was synthesized through copolymerization of a 60/40 molar ratio of poly(propylene glycol)/resorcinol dicyclic carbonates with 1,12-diaminododecane. Afterwards, the A-PHU was mixed with a BPA-based epoxy resin for the preparation in bulk conditions of structural adhesives cured at room temperature with good lap-shear strength and shear resistance under static load and temperature. Influence of the incorporation of the thiol compound, trimethylolpropane tris(3-mercapto propionate) (TMPTMP), on the curing process and the adhesive properties was addressed. Integration of a trifunctional thiol compound allowed a faster curing in the presence of 0.875 mol% based on total equivalents of epoxy groups of a strong base as catalyst, 1,1,3,3-Tetramethylguanidine (TMG). Moreover, combination of A-PHU and TMPTMP as curing agents for the epoxy resulted in adhesives with superior toughness without losing ultimate lap-shear strength nor shear resistance under load and temperature.

4.2. Synthesis of amino-terminated PHUs oligomers

Amino-terminated poly(hydroxyurethane) was prepared reacting a mixture of dicyclic carbonates, PPGdiCC/RdiCC, in 60/40 molar ratio with 2 equivalents of 1,12-diaminododecane at 80 °C for 5 h under continuous mechanical stirring (Scheme 4.1).

Scheme 4.1. Synthesis of amino-terminated PHU (A-PHU) for the polyaddition of PPGdiCC, RdiCC and 1,12-DAD.



Reaction was monitored by FTIR-ATR by following the decrease of the relative intensity of the carbonyl stretching vibration band of the carbonates. After 5 h, the carbonyl stretching vibration bands of the carbonates (1790 and 1782 cm^{-1} of PPGdiCC and RdiCC, respectively) were totally disappeared and a new band at 1701 cm^{-1} characteristic of the carbonyl of the urethane group was clearly observed (Figure 4.3). Then, the reaction was cold down and the polymer was stored for further mixing with the epoxy resin and the thiol. Additionally, vibration bands at 3304 (O-H, N-H), 1593 (C=C, ph), 1536 (δ N-H), 1492 (C=C, ph), 1463

(C-O), 1254 (C-O-C, as), 1101 cm^{-1} (C-O-C, sy) overlapped with C-O stretching vibration bands of primary and secondary alcohols and at 772 and 721 cm^{-1} (C-H out of plane bending vibrations of the aromatic rings, meta substitution) confirmed the structure of the prepolymer. $^1\text{H-NMR}$ spectroscopy of the A-PHU (Figure 4.4) showed the split in two of the signal at 2.65 ppm ($\text{NH}_2\text{-CH}_2\text{-}$), appearing a new signal at 3.11 ppm ($\text{CH}_2\text{-NH-C(O)-O}$) confirming the functionalization of the A-PHU. The amine equivalent weight (AEW) was determined by ^1H NMR titration (Figure A-II.16) in a standard solution of toluene in CD_3OD as described in the experimental section. The A-PHU was characterized with an amine equivalent weight of $520.4 \pm 5.5 \text{ g equiv}^{-1}$.

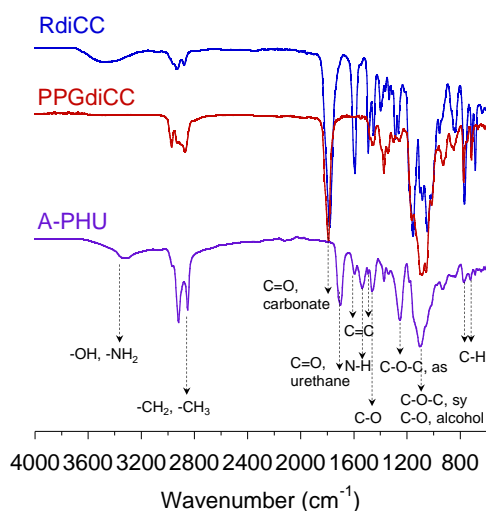
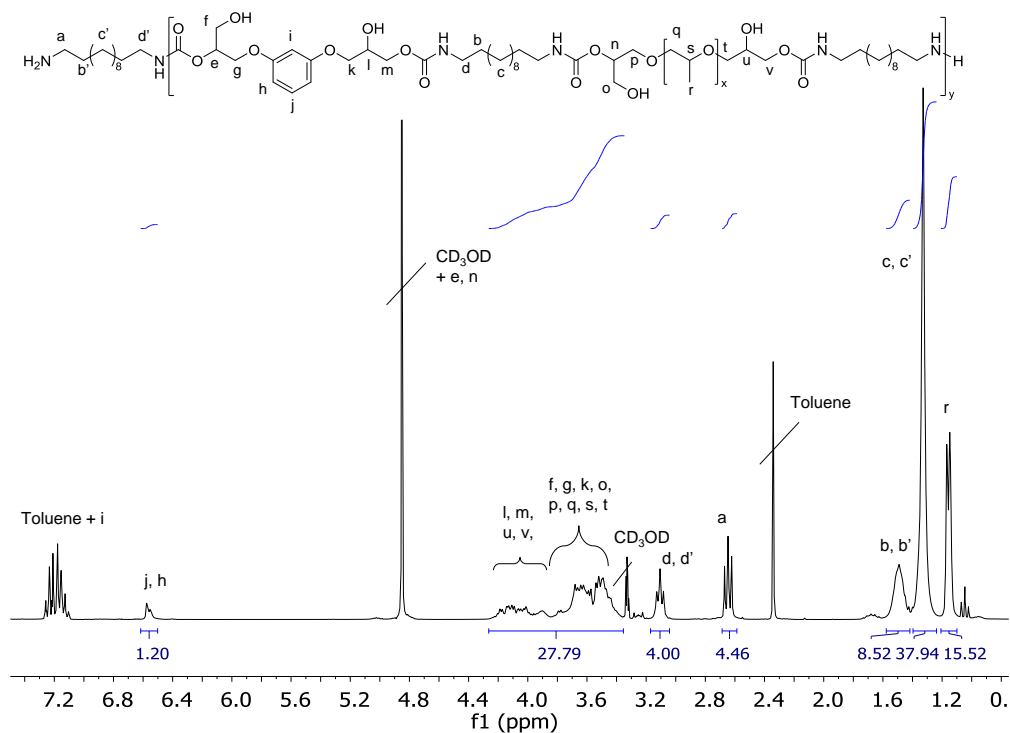


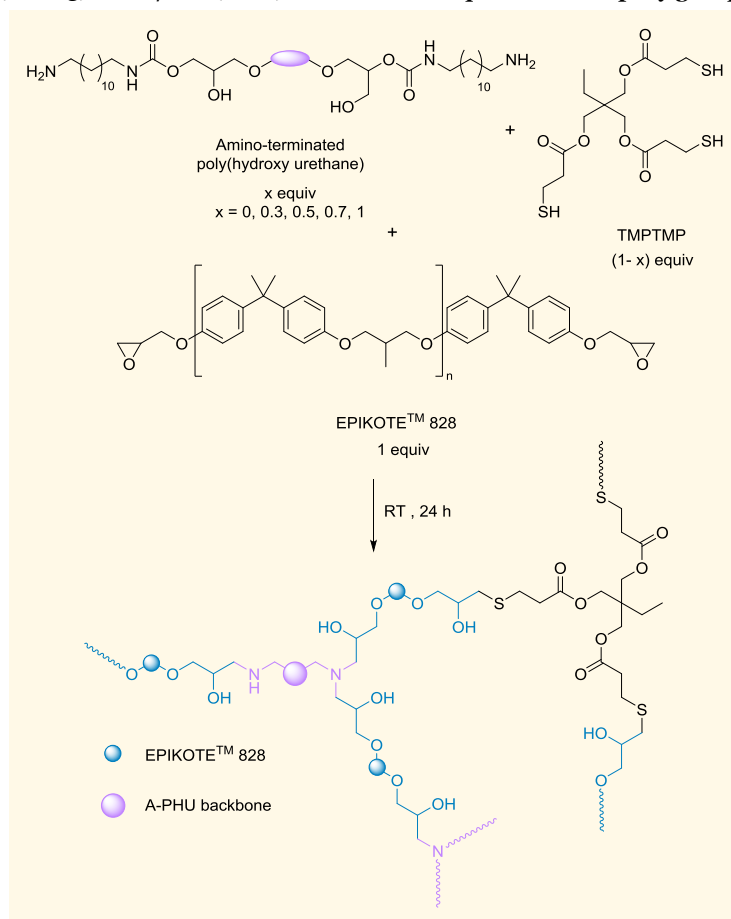
Figure 4.3. FTIR spectrum of the amino-terminated poly(hydroxy urethane).

Figure 4.4. ^1H NMR spectrum of the A-PHU.

4.3. Synthesis of PHU-epoxy hybrid adhesives

The synthesis of PHU-epoxy hybrid materials was performed as showed in Scheme 4.2. A-PHU and TMPTMP were employed in different equiv ratios as curing agents of EPIKOTETM 828 resin (epoxy resin) (Scheme 4.2). Thus, the sum of equiv of amine (taking into account the two active H that the amine posses) and thiol groups matched the equiv number of epoxy group for all compositions. Reagents were mixed at 50 °C for 2 minutes followed by 1 minute at room temperature for preparing and homogeneous viscous mixture. Completion of the reaction after 24 h was followed by FTIR-ATR through the total disappearance of the stretching vibration

Scheme 4.2. Preparation of hybrid PHU-epoxy adhesives mixing A-PHU prepolymer with TMPTMP and a commercial epoxy viscous resin, EPIKOTE™ 828. Equiv ratios between A-PHU and TMPTMP were employed as followed: 100/0 ($x = 1$), 70/30 ($x = 0.7$), 50/50 ($x = 0.5$), 30/70 ($x = 0.3$) and 0/100 ($x = 0$) to match with equivalents of epoxy groups.



band of the thiol at 2569 cm^{-1} (Figure 4.5 a) and the decreased in the intensity of the asymmetric C-O-C stretching vibration band of the epoxy at 914 cm^{-1} (Figure 4.5 b).

The remaining signal of the band related to the epoxy ring could be due to the reduction of the polymer chains mobility when the gel point is reached, slowing down the curing kinetics

and probably the reaction of secondary amines with these rings. Nonetheless, three-dimensional network of the materials was confirmed by DMTA experiments, in which the storage moduli (E') remained over the loss moduli (E'') over temperature (Figure 4.6) and high crosslinking degrees were achieved (Table 4.1). The appearance or intensity increment of the signal at 3413 cm^{-1} associated to the stretching O-H vibration band also confirmed the new formation of hydroxyl groups due to ring opening of the epoxy.

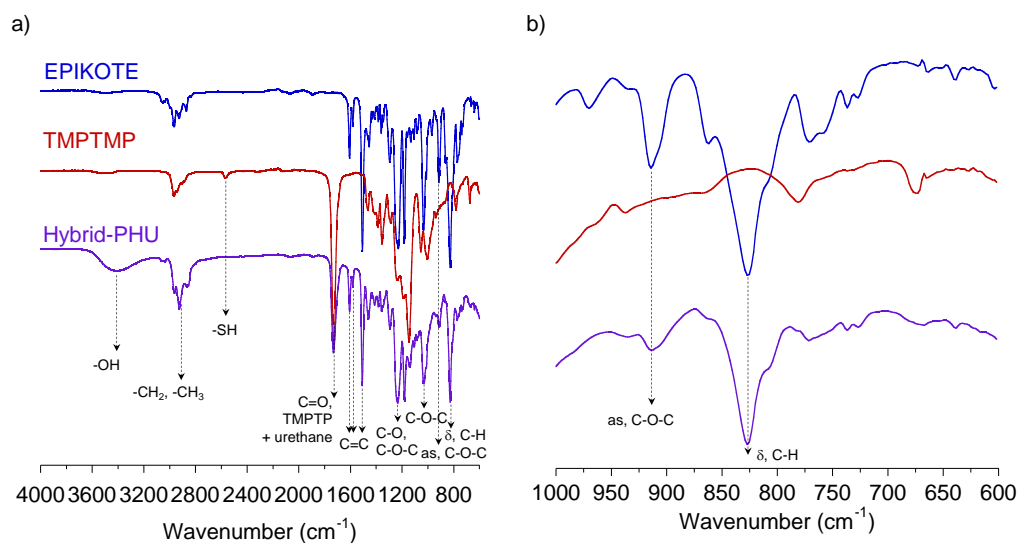


Figure 4.5. a) FTIR-ATR spectra of EPIKOTE, TMPTMP and the hybrid-PHU material after curing step at room temperature for 24 h and b) zoom of the spectra from 600 to 1000 cm^{-1} showing the decreased of the asymmetric C-O-C stretching vibration band of the epoxy ring.

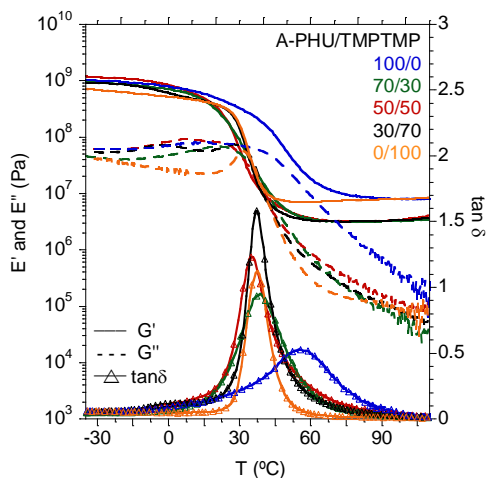


Figure 4.6. E' , E'' and $\tan \delta$ values for the compositions of the hybrid-PHUs.

The capacity of the materials to cure at room temperature was addressed by rheological measurements in parallel plates determining gel times ($G' = G''$) of the compositions. Compositions without catalyst were characterized with gel times higher than 2 hours when A-PHU was employed, independently of the ratio of curing agents (Figure 4.7 a). Despite the lower initial viscosity of the 30/70 composition, it presented a faster evolution of the moduli, meaning a faster curing. This fact can be attributed to the higher reactivity and functionality of the thiol. The amine has to react twice with the epoxy to create a three-dimensional network. The formed secondary amine is sterically hindered and possesses a lower reactivity, being slower the formation of the crosslinked network.⁵¹ 0/100 equiv ratio composition was not able to cure without adding a catalyst. Moduli as well as stretching vibration bands of the S-H (2569 cm^{-1}) and C-O-C of the epoxy (914 cm^{-1}) remained unaffected after 2 h (Figure 4.7 a, curve black) and 1 week (Figure A-II.17), respectively. Therefore, A-PHU acted as initiator or catalyst of the thiol/epoxy reaction.

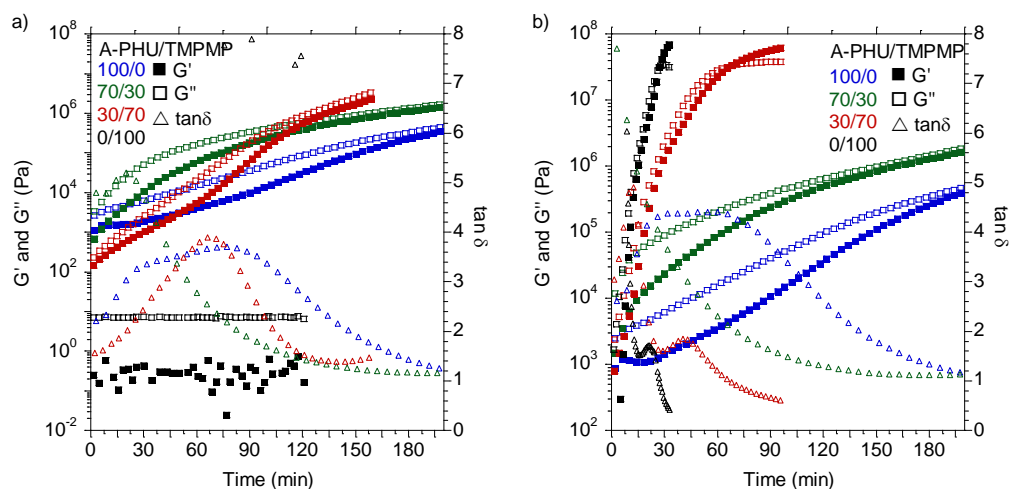


Figure 4.7. a) Evolution of G' and G'' values with time during rheological measurements carried out at 25 °C without catalyst and b) evolution of G' and G'' values with time during rheological measurements carried out at 25 °C in the presence of 0.875 mol% of TMG.

The addition of 0.875 mol% of TMG regarding equiv of epoxy group was then considered in order to accelerate the curing process (Figure 4.7 b). Results showed the ability of the 0/100 composition to cure in less than 30 minutes (Figure 4.7 b, curve black). Integration of TMG catalyst into the 100/0 formulation did not accelerated the curing process, showing similar G' and G'' evolution over time that when no TMG was added (Figure A-II.18 a), while 70/30 composition showed an increment in the slope of the moduli as well as faster decay of $\tan \delta$ during the first 15 min (Figure A-II.18 b). In this case, the amount of thiol is not enough to speed up the curing process more than in the initial stages. However, composition containing 70 mol% of TMPTMP, exhibited a huge decrease in gel time (76 min) when the catalyst was employed (Figure 4.7 b, red curve; Figure A-II.18 c). Thus, rheological measurements demonstrated that TMG catalyzed the thiol-epoxy reaction, whereas formulations with higher amounts of A-PHU exhibited similar behavior in the presence and absence of catalyst.

Table 4.1. Summary of results for the different formulations prepared. Curing conditions were set as 24 h at room temperature.

Entry	Composition (A-PHU/ TMPTMP equiv ratio)	EWC ^a (%)	GC ^b (%)	SI ^c (%)	T _g ^d (°C)	E' ^e (MPa)	v _e ^f (10 ² mol m ⁻³)
1	100/0	2.4 ± 0.7	98.2 ± 0.0	83.9 ± 3.9	54.1 ± 1.5	8.3 ± 0.4	8.8 ± 0.4
2	70/30	3.5 ± 0.3	99.0 ± 0.6	94.0 ± 3.0	38.9 ± 0.1	3.6 ± 0.6	4.0 ± 0.7
3	50/50	3.2 ± 0.1	86.0 ± 0.3	179.3 ± 10.2	34.4 ± 1.8	2.3 ± 1.2	2.6 ± 1.3
4	30/70	2.7 ± 0.3	88.4 ± 0.8	122.0 ± 1.6	37.2 ± 0.2	2.9 ± 0.5	3.2 ± 0.5
5	0/100	1.1 ± 0.2	>99%	80.6 ± 3.4	36.7 ± 0.8	8.1 ± 2.1	9.0 ± 2.4

^aequilibrium water content measured after 96 h immersed in water; ^bgel content and ^cswelling index after Soxhlet extraction in refluxing THF for 24 h; ^dglass transition temperature from DMTA measurements; ^eStorage Modulus in the rubbery region of the material (T_g+50 °C); ^fcrosslinking density calculated from the rubbery plateau using eq 7.

Physical characterization of the 3D-networks of the materials were further investigated through dynamic mechanical thermal analysis and soxhlet extractions (Table 4.1). Glass transition temperatures were calculated from the maximum value of tan δ. T_g values for all compositions were above room temperature, confirming the rigidity of the materials. When just A-PHU was used as curing agent in the formulation, a broader T_g was observed meaning more heterogeneity of the adhesive that can be due to immiscibility between polar A-PHU and non-polar epoxy resin regions. Crosslinking densities were calculated at a temperature of 50 K above the T_g since is well accepted to be already in the rubbery plateau.^{124,125} Interestingly, a minimum of v_e for 50/50 equiv ratio composition was observed, correlated with a maximum in swelling index. The higher the crosslinking density the lower the swelling index since penetration of the solvent into the network is more difficult to occur. Our hypothesis is that two different kind of interactions are taking place to observe this behavior. On the one hand, when 0/100, 30/70 and 50/50 A-PHU/TMPTMP equiv ratio compositions are compared, substitution of small TMPTMP molecules by longer A-PHU polymer chains resulted in a decrease in crosslinking density and an increase in swelling. Distance between covalent

crosslinked points increased lowering the crosslinking density. Thus, solvent penetrated easier through the polymer chains and therefore, swelling of the adhesive increased. Taking into account this explanation, 50/50 composition would be expected to present higher crosslinking density and lower swelling index than 70/30 and 100/0 compositions. Nonetheless, an opposite behavior was observed and 100/0 equiv ratio formulation presented more than twofold crosslinking density. Our thought is that physical inter- and/or intramolecular hydrogen bonding between A-PHU chains were occurring and created strong interactions that enhanced crosslinking density and decreased swelling of the polymer. Gel content showed a similar trend, in which 50/50 equiv ratio presented higher amounts of soluble species trapped in the 3D-network. Finally, equilibrium water content after 96 h immersed in water showed that the incorporation of the epoxy resin into the formulations conferred a higher hydrophobic behavior to the polymer. Regardless the A-PHU/TMPTMP equivalent ratio, EWC values were by far lower than the best EWC values of PHU adhesives prepared in Chapter 2 (60/40 PPGdiCC/RdiCC-based PHU, 6.0 ± 0.4 %, Table 2.4) and in Chapter 3 (TMPTC-MXDA-based PHU, 17.8 ± 1.6 , Table 3.1). Thus, the PHU-epoxy hybrid adhesives are more appropriate for wet environments.

4.4. Evaluation of the adhesive properties of the hybrid PHUs

As mentioned in the introduction of this chapter, liquid structural adhesives are characterized by two stages after application. The first is achieved when the adhesive possess enough strength to hold together the parts to be adhered, whereas the second stage is reached when the adhesive has developed the ultimate adhesive properties. In order to analyze both stages, lap-shear strength measurements were accomplished. For the ultimate properties,

lap-shear tests after long times of curing were performed, whereas the first stage was evaluated by lap-shear measurements at different curing times.

4.4.1. Ultimate adhesive properties

Aiming at addressing ultimate adhesion performance of the hybrid compositions lap-shear tests were carried out on dissimilar substrates [poly(methylmethacrylate)-stainless steel] after 24 h and 1 week of curing at room temperature for the intermediated compositions, i.e. 70/30, 50/50 and 30/70 A-PHU/TMPTMP equivalent ratios, was addressed by lap-shear measurements. Representative stress-displacement curves for the compositions are depicted in Figure 4.8 a. The increment of TMPTMP in the composition enhanced adhesion of the materials due to the less polarity of the polymer. Substitution of A-PHU by TMPTMP reduced the number of hydroxyl groups in the polymer chain and, therefore, the polarity. Adhesive failure was observed regardless the composition, remaining the adhesive in the stainless steel, which supported the less affinity of the richer composition in A-PHU for the PMMA substrate (Figure A-II.19). The additional curing of 1 week at room temperature (dashed lines in Figure 4.8 a) did not improved the lap-shear strength values of the compositions, confirming the total curing and ultimate lap-shear strength development in 24 h.

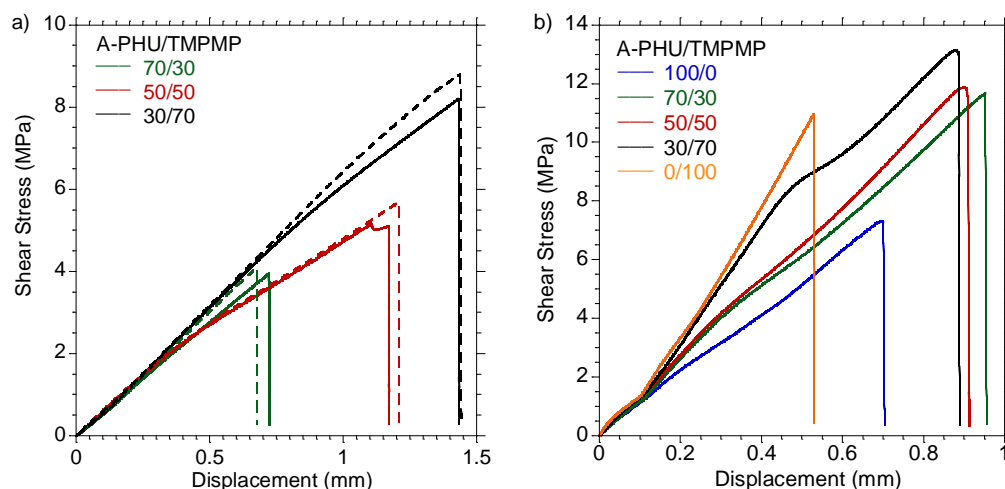


Figure 4.8. a) Representative shear stress-displacement curves for 70/30 (green), 50/50 (red) and 30/70 (black) A-PHU/TMPMP equiv ratios after 24 h (solid line) and 1 week (dashed line) of curing at room temperature and b) representative curves of the lap-shear strength for each composition on stainless steel adherends.

After confirming that the evolution of lap-shear strength reached a maximum after 24 h, the adhesive properties of the hybrid PHUs cured at room temperature for 24 h on stainless steel were evaluated by lap-shear strength (Figure 4.8 b). Stainless steel adherends were selected to compare the results with compositions of Chapter 2 and 3. A-PHU and epoxy resin composition (Figure 4.8 b, blue curve) was characterized with a lap-shear strength of 7.6 ± 0.9 MPa, while for the thiol-epoxy mixture (Figure 4.8 b, orange curve) lap-shear strength was increased up to 11.4 ± 1.1 MPa. In both cases adhesive failures, the adhesive remained in just one of the substrates after bond breaking, were observed meaning a greater cohesiveness of the polymer chains than adhesion forces with the adherend (Figure A-II.20 a and e, respectively).

For the compositions in which A-PHU and TMPMP were combined to cure the epoxy resin, close values of lap-shear strength were achieved compared to the 0/100 equivalent ratio formulation and, therefore, greater than 100/0 composition value. This indicates that the

addition of the TMPTMP to the formulations increased the ultimate lap-shear strength, even at low equiv amounts. On the other hand, combination of curing agents exhibited a synergetic effect increasing the elongation at break of the adhesives. This indicates an enhancement of the toughness, without losing maximum force resistance, making the adhesive joining less brittle. It is worth to point out that this property is important to improve in structural adhesive, making the adhesive joint more resistance to vibrations and shock impacts. The increment of the elongation at break can be related to the lower crosslinking densities (Table 4.1) of the formulations with combination of curing agents (70/30, 50/50 and 30/70 A-PHU/TMPTMP), which makes the adhesive more elastic. Cohesive failures were observed for 50/50 and 30/70 compositions meaning greater adhesion forces to the substrate than internal cohesive forces of the polymer.

Table 4.2. Lap-shear strength and SAFT values of the compositions cured at room temperature for 24 h.

Entry	Composition (A-PHU/ TMPTMP equiv ratio)	Lap-shear strength (MPa)	SAFT ^a (°C)
1	100/0	7.6 ± 0.9	217 ^b
2	70/30	11.6 ± 0.8	217 ^b
3	50/50	11.8 ± 1.0	217 ^b
4	30/70	12.8 ± 1.0	217 ^b
5	0/100	11.4 ± 1.1	217 ^b

^ashear adhesion failure temperatures at 1 kg/625 mm²; ^bkept the adhesive properties at this temperature for more than 7 h.

Besides shear strength under dynamic deformations (lap-shear tests), it is also relevant the evaluation of structural adhesives under the effect of static load and temperature, which will proportionate information about resistance of the material to creep and service temperatures of the adhesives. In consequence, shear adhesion failure temperature (SAFT) measurements were carried out (Table 4.2). Samples were prepared following the same procedure as in Chapter 3,

gluing 625 mm² (25 x 25 mm x mm) of two stainless steel substrates and allowing them 24 h at room temperature for curing. Then, the specimens were put in an oven with 1000 g hanging and a heating ramp of 1 °C min⁻¹ was started. In all cases, adhesives were able to withstand 217 °C more than 7 hours, showing the excellent resistance to creep of these materials under high temperature. Incorporation of the epoxy resin into the formulations improved greatly this resistance comparing with PHU adhesives of Chapter 3 even the PHU-epoxy hybrid adhesives were cured at room temperature.

4.4.2. Lap-shear strength evolution over time

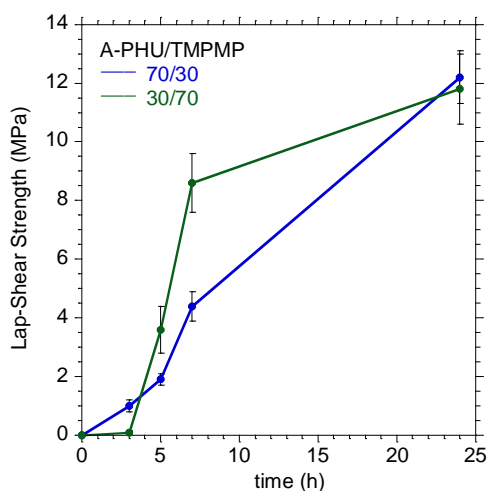


Figure 4.9. Evolution over time of the lap-shear strength values for the 70/30 and 30/70 compositions. Error bars represents standard deviation for each sample set.

A fast development of a minimum lap-shear strength is mandatory to be competitive in the industrial manufacturing process (1.2 MPa¹²⁶ as value for handling). Therefore, adhesive strength over the time was set for evaluating the development of lap-shear strength for 70/30 and 30/70 A-PHU/TMPMP equivalent ratio compositions. Figure 4.9 are depicted the values

for both compositions. The 70/30 composition showed a more smooth evolution of the shear strength (Figure 4.9, green curve), developing 1 MPa of adhesion after 3 h. On the other hand, a sharper evolution was observed for 30/70 composition (Figure 4.9, black curve). It need greater time to reach the minimum lap-shear strength for handling but afterwards it surpassed the values of the 70/30 equivalent ratio formulation. After 7 h of curing it reached up to 72.9% of the ultimate lap-shear strength. Evolution of adhesive properties met with evolution of storage and loss moduli from the rheological measurements (Figure 4.7 a, curves green and red), presenting a faster initial evolution for the 70/30 composition and a sharper curve when higher amount of TMPTMP was employed (30/70 composition), while ultimate lap-shear strengths for both compositions were similar as previously reported in section 4.4.1.

In the way to prepare an adhesive able to acquire enough shear strength within one hour, TMG must be incorporated to the formulation based on the rheological measurements. Despite the excellent results obtained in these experiments, the preparation of these formulations in one-pot systems was not possible due to these fast curing rates when the catalyst was added. Strategies such as the use of a 2K syringe, the use of light to generate TMG or the addition of other bases are under investigation to improve the pot-life of the adhesive.

4.5. Conclusions

In this chapter, PHU-epoxy hybrid adhesives able to cure at room temperature were prepared by mixing amino-terminated PHU (based on 60/40 molar ratio mixture of PPGdiCC and RdiCC reacted with excess of MXDA) with a viscous epoxy resin, EPIKOTE™ 828 and trifunctional thiol (TMPTMP). Similar adhesion values for gluing dissimilar adherends, i.e. PMMA-SS, were obtained after 24 h as well 1 week at room temperature, demonstrating the

capacity of the materials to cure in short times. 30/70 A-PHU/TMPTMP exhibited better adhesion to these adherends since the less polarity of the polymers. On the other hand, when stainless steel substrates were bonded, the fully based A-PHU-epoxy hybrids cured at room temperature showed 7.6 ± 0.9 MPa surpassing largely the results obtained in Chapter 2, even when the latest were cured at 100 °C. Integration of trifunctional thiol, TMPTMP, improved lap-shear strength values up to 12.8 ± 1.0 MPa and more importantly, toughness of the adhesives. Higher elongation at breaks were related to lower crosslinking densities and therefore, greater elasticity of the adhesives. Thus, adhesives with enhanced resistance to vibrations and shock impacts were developed without losing adhesion performance. Adhesives also exhibited excellent resistance to shear under static load and high temperatures, tolerating 1 kg-shear load under 217 °C for more than 7 h. Lap-shear evolution over time showed that 70/30 A-PHU/TMPTMP compositions was able to developed handling strength within only 3 h at room temperature. However, this value does not fulfill industrial requirements (safe drive away times of 60 min). In order to speed up the curing process a base, TMG, was added to the formulation to enhance the kinetics of the thiol-epoxy “click” chemistry reaction. Despite rheological measurements demonstrate the faster curing when 0.875 mol% of TMG was added to 30/70 composition, gel point were reached in 76 min, we are still searching an appropriate application technique due to the low pot life when adhesives are one-pot formulated.

Chapter 5.

Enhanced and Reusable Poly(Hydroxy Urethane)- Based Low-temperature Hot-Melt Adhesives

5.1. Introduction

Up to now, this dissertation has been focused on the development of structural adhesives, which was the initial goal. However, during the development of these adhesives some formulations with potential as hot-melt adhesives (HMAs) were found. The global hot-melt adhesive market is projected to reach USD 9.46 billion by 2022.¹²⁷ Hot-melt adhesive applications range from automotive industry, packaging, bookbinding, shoe making and textile binding to other pressure-sensitive application such as labelling of bottles, disposable products, stamps and envelopes.^{93,128,129} This kind of adhesives are solvent-free thermoplastic materials, which are characterized by their solid state at low temperatures, i.e. below 80 °C, while present low viscosity and flow at high temperatures, typically above 80 °C. They quickly set upon cooling, developing great bond strengths in short periods, which makes them very attractive when fast processing is required. Moreover, they are relatively easy to handle, economic and clean running. The main limitation is the high temperatures (170-180 °C) that are often required for application.¹³⁰ These temperatures may cause health and safety risk to plant operators or the degradation of the adhesive when are maintained for prolonged periods. The reduction of application temperatures to 100-130 °C can significantly decrease energy consumption and the carbon footprint of the operation as well as improve safety and prolong the lifetime on line machinery.

Typical formulations of HMAs consist of polymers (~33%), resins (~33%), waxes (~32.5%) and antioxidants (~0.5%).¹³⁰ Polymers impart strength and hot tack, resins provide a lower viscosity improving wettability and adjust T_g of the system as well and waxes enhance setting speed and provide heat resistance.¹³¹ Among the polymers used for HMAs, thermoplastic polyurethanes (TPUs) possess high popularity as they show better low-temperature properties

and greater flexibility than those based on ethylene vinyl acetate and polyamide.¹³² Moreover, they present excellent adhesion on difficult surfaces to adhere, such as non-porous materials. Aforementioned toxicity of the isocyanate-based PUs in unison with current greener trends in the development of hot-melt adhesives¹³³ has motivated researchers to develop non-isocyanate polyurethane-based hot-melt adhesives. TPUs are synthesized in two steps: first an isocyanate-terminated prepolymer is prepared reacting a long chain polyol with an excess of diisocyanate, which is further reacted in a second step with a low molar mass alcohol, known as a chain extender. The resulting polymer comprises alternating soft segments, mainly containing the polyol, and hard segments, formed through the reaction of the isocyanate and the short chain diols. The incompatibility between the two phases leads to a phase-separated structure consisting of soft and hard domains. This phase separation, which is brought about by hydrogen bond-based physical cross-linking of the hard segment, imparts unusual morphological and physical properties.¹³⁴ When the polyaddition of polycyclic carbonates and polyamines is employed to prepare NIPUs, the opening of the cyclic carbonate generates hydroxyl groups along the polymeric chain. These hydroxyl groups can establish strong hydrogen bonds with the soft segment, enhancing the miscibility between both phases and suppressing the distinctive phase separation of conventional PUs, thus hindering the potential of NIPUs as substitutes for TPUs.³⁴ Some authors have tackled this issue employing different approaches, selecting carefully the monomers¹³⁵⁻¹³⁷ or synthesis conditions.⁶⁷ However, the resulted polymers showed elastomeric-like behavior and adhesion performance was not reported.

The most interesting work of NIPU-based hot-melt adhesives was addressed by Nair et al.⁴³ They detailed the synthesis of thermo-reversible hot-melt PHU adhesives based on homo- and copolymers of aromatic and cycloaliphatic bis(cyclic carbonate)s and amino-terminated

oligo(propylene glycol) (Figure 5.1). In addition to the high lap-shear strength values up to 9 MPa on aluminum and 2 MPa on high density polyethylene, the authors demonstrated the thermo-reversibility of the materials after debonding manually (a previous thermal treatment up to 100 °C for 0.5 h was applied) and then re-bonding the substrates with no noticeable loss of the adhesion values. ¹H NMR and FTIR characterization showed the reversible hydrogen bonding and debonding as function of temperature.

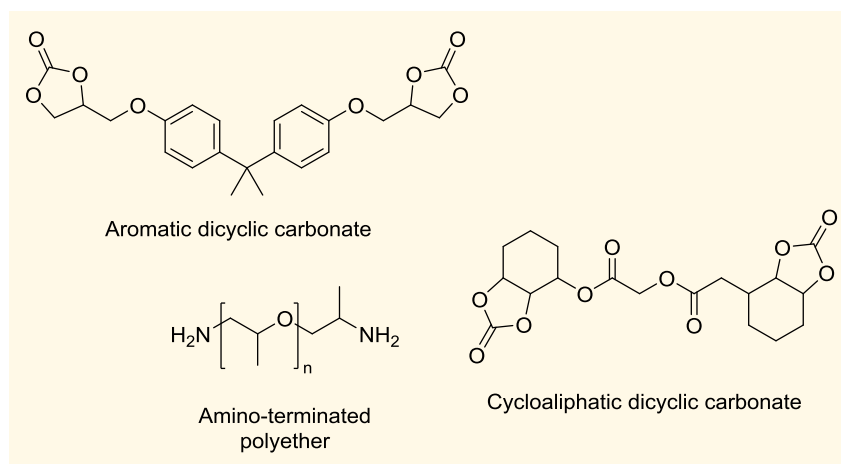


Figure 5.1. Structures of the monomers used by Nair et al.⁴³ employed for the synthesis of thermo-reversible PHU adhesives.

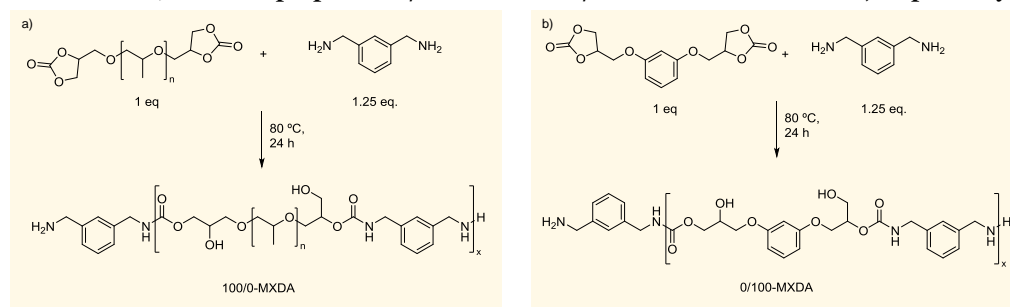
Hence, in this chapter the hot-melt adhesion performance of new PHU formulations was explored. Solvent-free synthesis of PHU was carried out through copolymerization of hard (resorcinol-based) and soft (PPG-based) dicyclic carbonates with diamines. Hot-melt adhesives were applied at low temperatures showing good adhesion performance. Moreover, influence of the molar ratio of dicyclic carbonates, as well as nature of thereof, on adhesion properties was addressed by rheology, probe tack, lap-shear, shear adhesion failure temperature and shear resistance measurements. An in-depth study of the influence on this behavior of the diamine structure was addressed employing two different aromatic diamines, *m*- and

p-xylylenediamine, a cycloaliphatic diamine, 1,3-cyclohexanebis(methylamine), and two aliphatic diamines, hexamethylenediamine and 1,12-diaminododecane. Finally, low-temperature hot-melt adhesives were endowed with higher resistance to creep under static load and temperature combining formulations with an epoxy resin.

5.2. PHU homopolymers: synthesis and rheology

Homopolymers were synthesized through the polyaddition of *m*-xylylenediamine with poly(propylene glycol) dicyclic carbonate or resorcinol dicyclic carbonate at 80 °C in bulk for 24 h giving under mechanical stirring (Scheme 5.1 a and b, respectively).

Scheme 5.1. Synthesis of PHU homopolymers reacting 1.25 equiv of MXDA with 1 equiv of a) PPGdiCC or b) RdiCC to prepare 100/o-MXDA and o/100-MXDA formulations, respectively.



Completion of the reaction was followed by FTIR-ATR, through the disappearance of the carbonyl stretching vibration band of the carbonates at 1791 cm^{-1} (PPGdiCC) and 1782 cm^{-1} (RdiCC) and the appearance of the carbonyl stretching vibration band of the urethane at 1699 cm^{-1} in (100/o-MXDA) and 1694 cm^{-1} (o/100-MXDA) (Figure 5.2). Additionally, common signals at 3320 cm^{-1} (-OH, -NH₂ stretching), 2930-2970 cm^{-1} (-CH₂, -CH₃) stretching, at 1592, 1491 and 1450 cm^{-1} (C=C stretching of the aromatic rings), at 1531 cm^{-1} (N-H bending), at 1240 cm^{-1} (C-O stretching) and at 775 and 700 cm^{-1} (C-H out of plane bending vibrations of the

aromatic rings) confirmed the structure of the homopolymers. More specifically, for 100/0-MXDA composition were observed the signals at 1374 cm^{-1} (CH_3 bending (umbrella band) and at 1086 cm^{-1} (overlapped C-O-C stretching and secondary alcohol bands), while for 0/100-MXDA appeared at 1181 cm^{-1} (C-O-C stretching bands), at 1131 cm^{-1} (C-O secondary alcohol bands) and at 1038 cm^{-1} (C-O primary alcohol band).

$^1\text{H-NMR}$ spectrum of the 100/0-MXDA formulation is depicted in (Figure 5.3). The disappearance of the signals at 4.89, 4.51 and 4.27 ppm corresponding to the cyclic carbonates as well as the appearance of new signals at 7.64 ppm and 4.15 ppm corresponding to $-\text{NH}-\text{C}(\text{O})\text{O}-$ of the urethane group and $-\text{CH}_2\text{NH}-$ methylene group of the amine, respectively, confirmed the formation of the homopolymer. In Figure 5.4 is showed the $^1\text{H-NMR}$ spectrum of the 0/100-MXDA composition, in which the disappearance of the signals of the cyclic carbonate (5.02, 4.62-4.53 and 4.23-4.13 ppm) and the appearance of the signals at 7.72 ($-\text{NH}-\text{C}(\text{O})\text{O}-$, urethane) and at 4.16 ppm (methylene group of the amine), confirmed the formation of the RdiCC-based homopolymer.

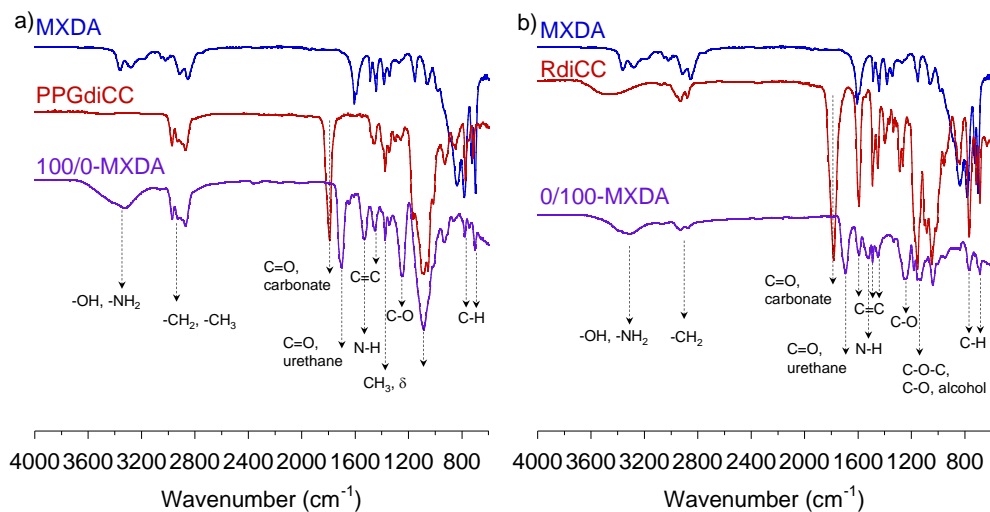


Figure 5.2. FTIR-ATR spectra of a) 100/o-MXDA and b) o/100-MXDA

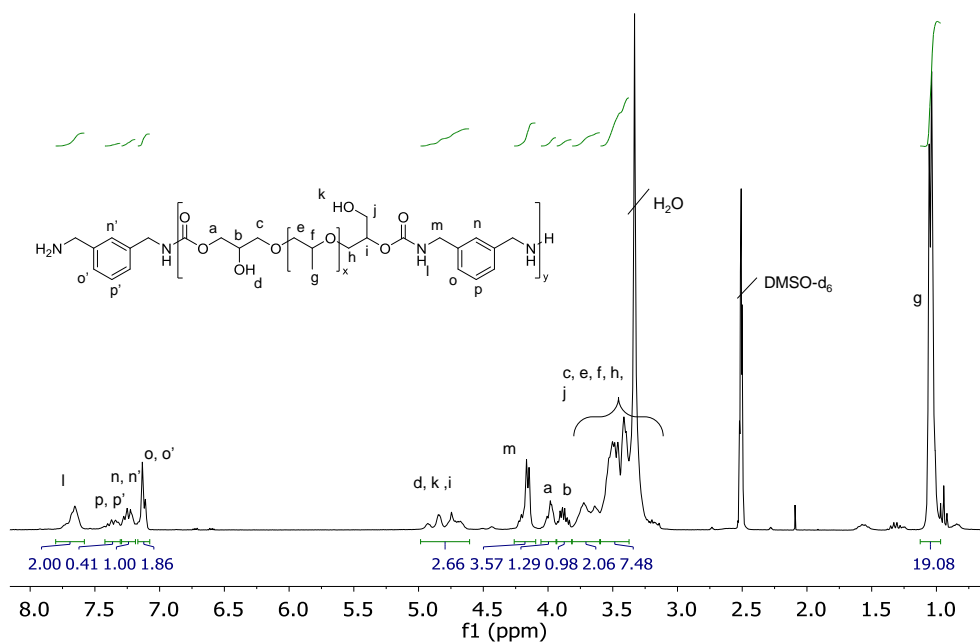


Figure 5.3. NMR spectrum of the 100/o-MXDA composition.

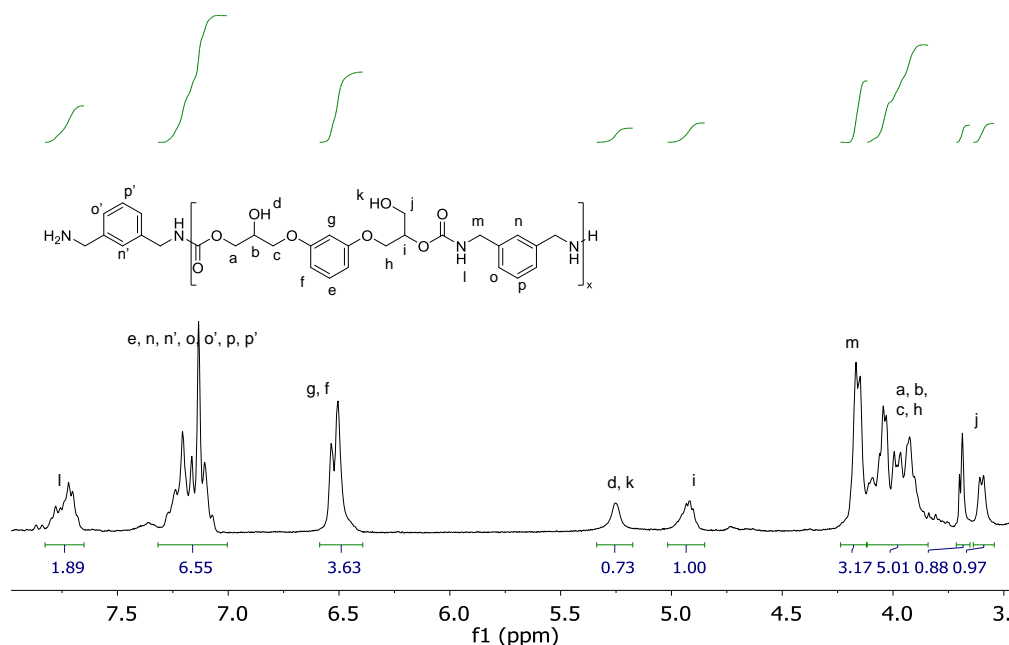


Figure 5.4. NMR spectrum of the o/100-MXDA composition.

Thermal characterization of the materials was performed by differential scanning calorimetry (DSC). In Figure 5.5 are depicted the curves from -70 to 120 °C for the compositions. Glass transition temperatures were calculated from the second heating scan. 100/o-MXDA composition showed a low T_g of -11 °C being viscous at room temperature, while o/100-MXDA presented a T_g of 51 °C, presenting high rigidity at ambient conditions. Therefore, none of the compositions was useful as an adhesive, as 100/o-MXDA was excessively soft, whereas o/100-MXDA was too rigid. As it was concluded in chapter 2 and 3, the balance between hard and soft segments is mandatory for designing adhesives with optimal properties. Therefore, in order to prepare relevant hot-melt PHU-based adhesives, copolymers of PPGdiCC and RdiCC were formulated.

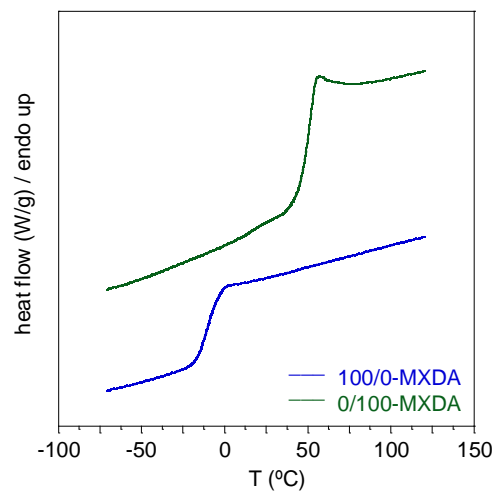
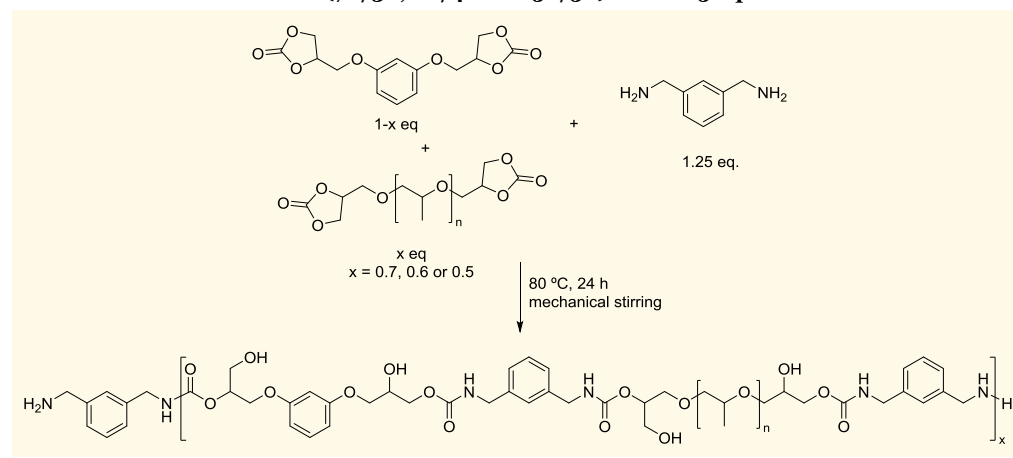


Figure 5.5. DSC thermograms of the PPGdiCC- (blue curve) and RdiCC-based (green curve) poly(hydroxyl urethane)s.

5.3. Preparation of MXDA-based copolymer compositions

5.3.1. Synthesis and Characterization

Scheme 5.2. Preparation of PHU copolymer compositions reacting three different molar ratio of PPGdiCC and RdiCC (70/30, 60/40 and 50/50) with 1.25 equiv of MXDA.



Three molar ratios of PPGdiCC:RdiCC (70/30, 60/40 and 50/50) were reacted with MXDA at 80 °C for 24 h with continuous mechanical stirring to prepare compositions 70/30-MXDA, 60/40-MXDA and 50/50-MXDA (Scheme 5.2). As previously reported for homopolymer compositions, completion of the reaction was followed by FTIR-ATR. The disappearance of the carbonyl stretching vibration band of the cyclic carbonates at 1790 cm^{-1} for PPGdiCC and 1782 cm^{-1} for RdiCC and the appearance of the carbonyl stretching vibration band of the urethane bond at 1696 cm^{-1} , confirmed the completion of the reaction. Additionally, the appearance of O-H stretching bands at 3315 cm^{-1} supported the ring opening of the cyclic carbonate. The FTIR of the 50/50-MXDA is showed in Figure 5.6 and signals are assigned as follows: below 3000 cm^{-1} C-H stretching, C=C stretching of the aromatic rings at 1592, 1492 and 1450 cm^{-1} , N-H bending at 1532 cm^{-1} ; CH_3 bending (umbrella band) at 1374 cm^{-1} ;

asymmetric C-O-C stretching at 1257 cm^{-1} ; overlapped symmetric C-O-C stretching with C-O stretching of primary and secondary alcohols at 1086 and 1041 cm^{-1} ; C-H out of plane bending vibrations at 775 and 700 cm^{-1} (meta substitution in aromatic rings).

Further characterization of the copolymer by ^1H NMR is depicted in Figure 5.7. Signal at 7.6-7.8 ppm, which corresponds to the proton of the $-\text{NH}-\text{C}(\text{O})\text{O}$ of the carbamate linkage, confirmed the formation of urethane bond. Additional signals at 5.3 ppm, which belong to OH groups, and at 4.15 ppm ($-\text{CH}_2\text{NH}-$) supported the ring opening of the cyclic carbonates.

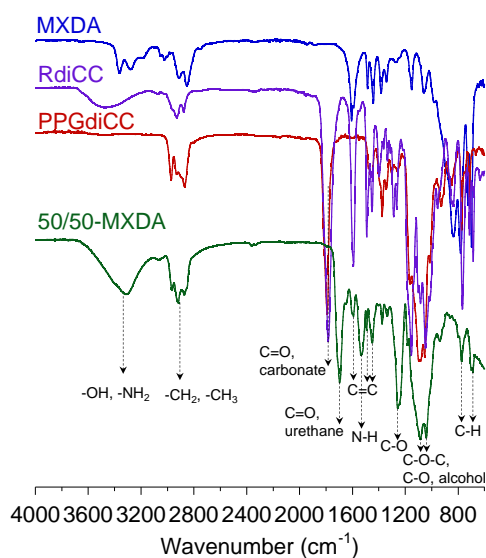


Figure 5.6. FTIR-ATR spectrum of 50/50-MXDA. MXDA, RdiCC and PPGdiCC spectra were added for a clearer comparison of the new bands after reaction. Spectra of 70/30-MXDA and 60/40-MXDA are depicted in Figure A-II.21.

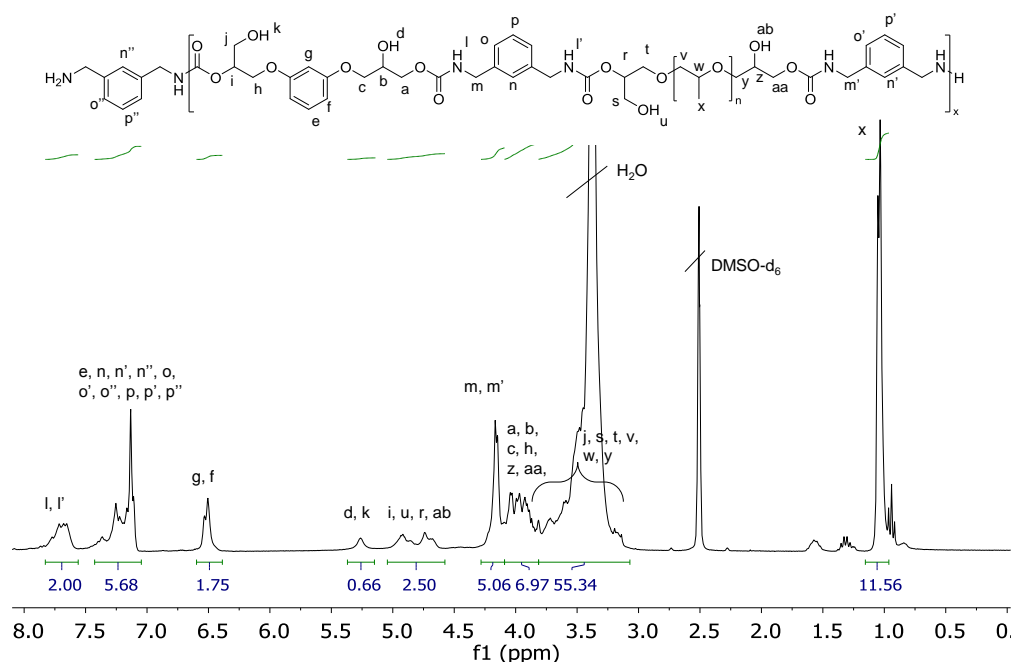


Figure 5.7. ^1H NMR spectrum of the 50/50-MXDA copolymer. Spectra of 60/40- and 70/30-MXDA copolymers are depicted in Figure A-II.22 and Figure A-II.23, respectively.

Size exclusion chromatography (SEC) was employed for the characterization of the average molar masses of the copolymers (Table 5.1). The compositions presented very similar weight-average molar masses and polydispersities, in the typical values for step-growth polyaddition of dicyclic carbonates with diamines. The low M_w are commonly obtained for PHU polymers due to the strong hydrogen bonds that are form between carbonyl groups, NH of the carbamate group and the hydroxyl group form during ring opening of the cyclic carbonates.⁸²

Table 5.1. Average molar masses and glass transition temperatures of the copolymers based on the polyaddition of MXDA with three PPGdiCC/RdiCC molar ratios.

Composition PPGdiCC/RdiCC (mol%)	Code	M_n^a kg mol ⁻¹	M_w^a kg mol ⁻¹	PDI ^a	T_g^b (°C)
70/30	70/30-MXDA	2.8 ± 0.0	6.4 ± 0.2	2.3 ± 0.0	10.3
60/40	60/40-MXDA	2.5 ± 0.2	6.3 ± 0.4	2.5 ± 0.0	20.4
50/50	50/50-MXDA	2.6 ± 0.1	6.4 ± 0.3	2.5 ± 0.0	30.5

^aAverage molar masses based on calibration with polystyrene standards ranging from 573 to 3,848,000 g mol⁻¹; ^b T_g values from rheological temperature sweep measurements done in parallel plates

5.3.2. Rheology of the copolymers

Dynamic rheological measurements are an important tool to understand the viscoelastic response of the adhesive.¹³⁸ Therefore, temperature sweep as well as frequency sweep experiments were carried out to elucidate the behavior of the adhesives. Figure 5.8 shows the evolution over temperature of the storage and loss moduli and the $\tan \delta$ of the copolymer compositions.

It was observed an earlier decay of G' and G'' for the composition with a higher percentage of PPGdiCC due to the longer flexible chains of this monomer. Incorporation of greater amounts of RdiCC restricted the mobility of the polymer chains, showing higher moduli values over the whole temperature range. This restriction of the mobility was also noticed in the glass transition temperatures. Thus, 70/30-MXDA composition presented a T_g value of 10.3 °C increasing up to 30.5 °C when an equimolar ratio of dicyclic carbonates were employed (50/50-MXDA). Moreover, 50/50-MXDA formulation showed a slower decay after the T_g probably due to greater density of hydrogen bonds. Shorter length between urethane groups gives rise to higher density of hydrogen bonds.¹³⁷

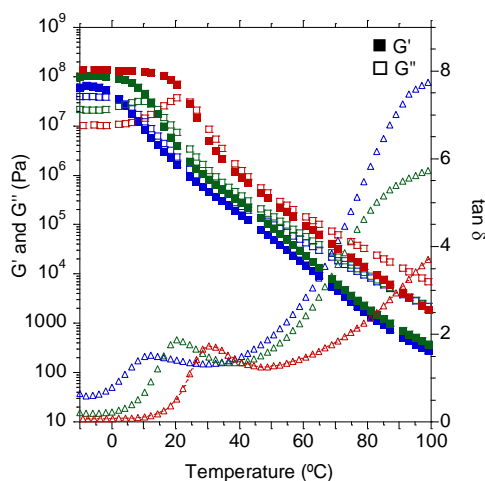


Figure 5.8. G' , G'' and $\tan \delta$ values for 70/30-MXDA (blue), 60/40-MXDA (green) and 50/50-MXDA (red) compositions between -10 and 100 °C.

Further characterization of the adhesives were done through frequency measurements at 10, 25, 50, 80 and 100 °C (Figure 5.9 a and Figure A-II.24). In all the cases moduli of 50/50-MXDA composition were above the corresponding for 70/30-MXDA, confirming the data obtained during temperature sweep measurements. Both compositions presented a liquid-like behavior at low frequencies, where G'' was always higher than G' . For non-structured materials this terminal zone is characterized by -2 and -1 slopes for G' and G'' , respectively, in the double logarithmic representation and corresponds to a flow regime.^{139–142} However, in the case of the PHU adhesives, the slope for the curves differed from these values, even at 100 °C (Figure A-II.25). This alteration means the formation of structured polymer networks through hydrogen bonds of the poly(hydroxyl urethane)s, which hindered the flow of the material. To assess the reversibility of the process a second frequency sweep was carried out for 50/50-MXDA (Figure 5.9 b). G' as well G'' were practically equal when the second frequency sweep was performed, supporting the reversibility of the hydrogen bonds formation.

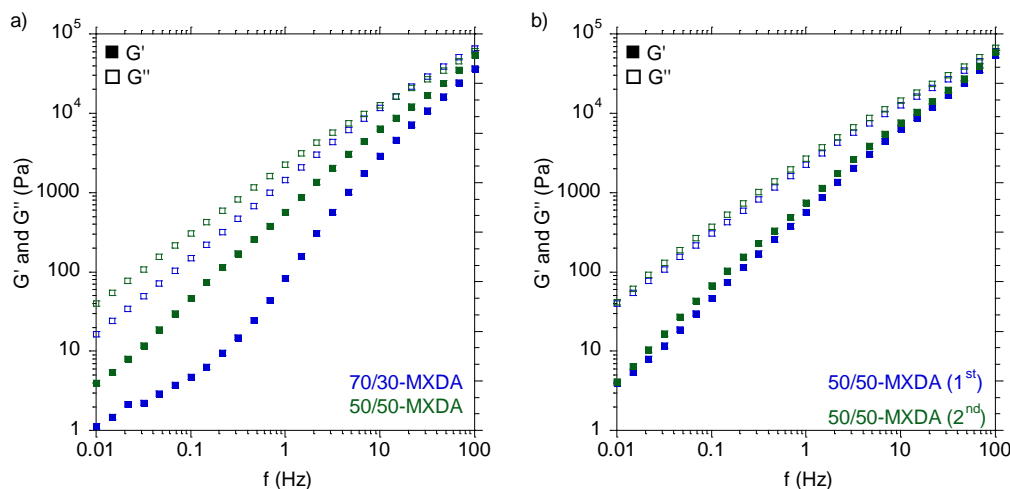


Figure 5.9. a) G' and G'' values between 0.01 and 100 Hz at 100 °C of 70/30-MXDA (blue) and 50/50-MXDA (green) and b) G' and G'' of 50/50-MXDA composition for the first (blue) and the second (green) frequency sweeps to assess reversibility of the hydrogen bond formation of PHU adhesives at 100 °C.

In addition, FTIR spectra at different temperatures were recorded to corroborate this phenomenon (Figure 5.10). It is well established that hydrogen bonding and debonding can be followed through the displacement of the urethane C=O stretching vibration band, N-H bending vibration band as well as O-H stretching vibration bands of the hydroxyl groups.^{94,140,143–145}

Possible intra- and intermolecular hydrogen bonds between PHU polymer chains are depicted in Figure 5.11. C=O stretching band region of the infrared spectra is showed in Figure 5.10 a. At room temperature the band is located at 1705 cm^{-1} indicating that carbonyl groups are taking part in the formation of hydrogen bonds.^{94,143,144} When temperature was increased, the peak of this band blue-shifted to 1720 cm^{-1} resulting from the weakening of hydrogen bond and strengthening of the C=O bond. The remaining shoulder at 1705 cm^{-1} denoted that hydrogen bonds were present even at 130 °C.

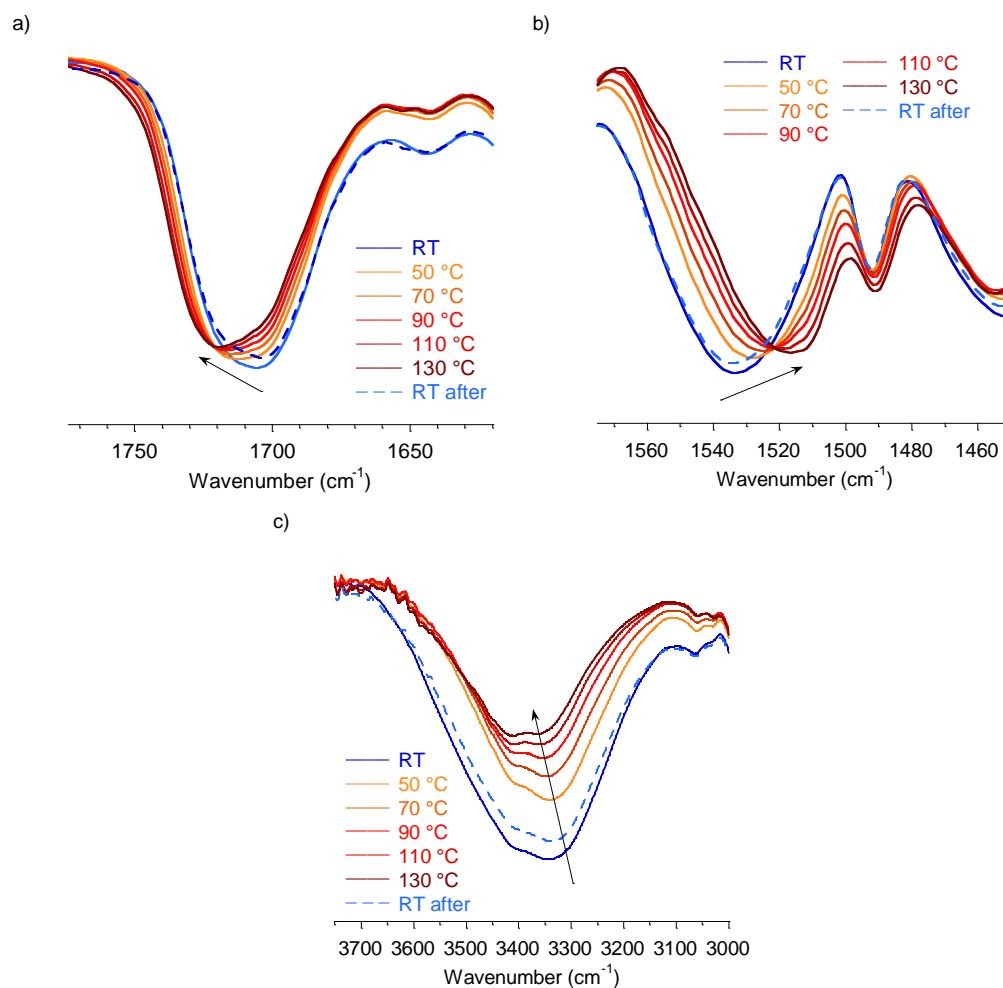


Figure 5.10. Variable temperature FTIR spectra in the region of a) C=O stretching band, b) N-H bending band and c) O-H stretching band of 50/50-MXDA composition.

Following the same trend, N-H bending band red-shifted from 1534 to 1517 cm⁻¹ (Figure 5.10 b) when temperature increased due to the disappearance of the anchoring restriction from hydrogen bonding.¹⁴⁵ Finally, intensity of the maximum OH band at 3344 cm⁻¹ blue-shifts when hydrogen debonding occurred (Figure 5.10 c). A greater energy was necessary to excite the O-H

bonds.¹⁴⁰ Interestingly, when the sample was cooled down the mentioned signals returned to the initial wavenumber values demonstrating the reversibility of the hydrogen bonds.

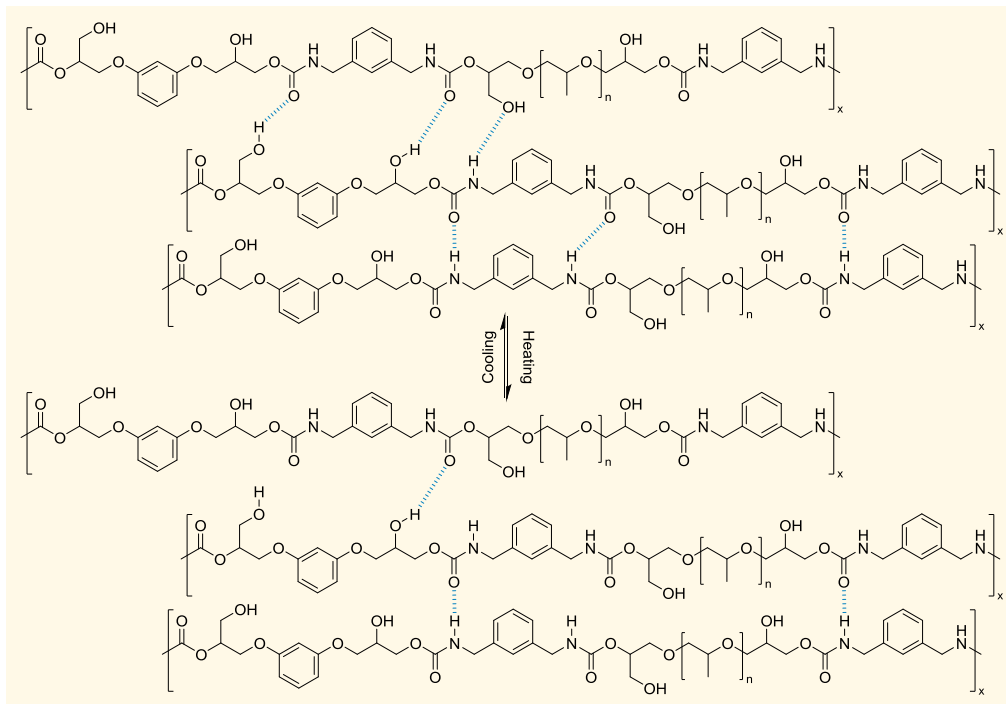


Figure 5.11. Schematic representation of the hydrogen bonding and debonding of the PHU adhesives as function of the temperature. Hydrogen bonds are marked in blue for clarity.

5.3.3. Adhesive properties of PHU hot-melt adhesives

Adhesive properties of the compositions were addressed performing probe tack, lap-shear, shear adhesion failure temperature (SAFT) and shear resistance experiments. Probe tack measurements were carried out using a 5-mm stainless steel cylinder, allowing 10 s contact between the probe and the adhesive at 80 °C and 100 °C, and employing a debonding speed of 300 mm s⁻¹. Stress-strain curves of the compositions at both temperatures are depicted in Figure 5.12.

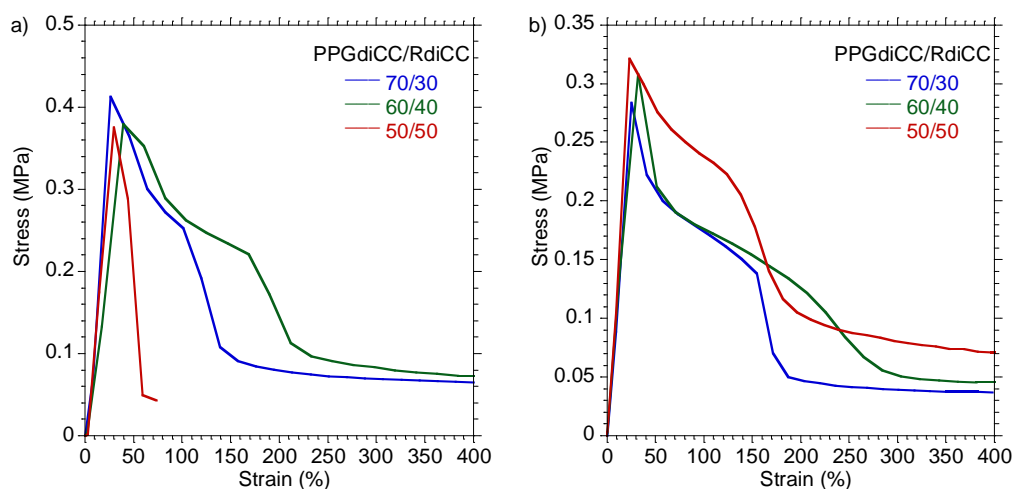


Figure 5.12. Stress-strain curves for 70/30-, 60/40- and 50/50-MXDA compositions at a) 80 and b) 100 °C.

The three formulations had a similar maximum stress, although at 100 °C this values was lower due to the higher liquid-like behavior of the adhesives. 50/50-MXDA presented a sharp decrease after the maximum stress and an adhesive failure after the test. Cohesion of the material was higher than adhesion forces, hindering fibrillation of the adhesive. Therefore, higher temperature would favor application of the adhesive and the wetting of the adherends. On the contrary, 70/30- and 60/40-MXDA showed a slightly stabilization of the stress

(plateau), which was a signature of the creation of a fibrillating structure. The latter presented a greater capacity for fibrillating since a greater plateau was achieved. At 100 °C all compositions exhibited fibrillation due to the viscous deformation that will enhance the wetting of the substrates during the adhesive application. 50/50-MXDA formulation was able to retain a bit more the cohesion, which correlated with the higher G' at 100 °C in the rheological experiments.

After assessing the tackiness of the adhesives, lap-shear strength was determined bonding the stainless steel substrates at 80 °C and 100 °C (Figure 5.13).

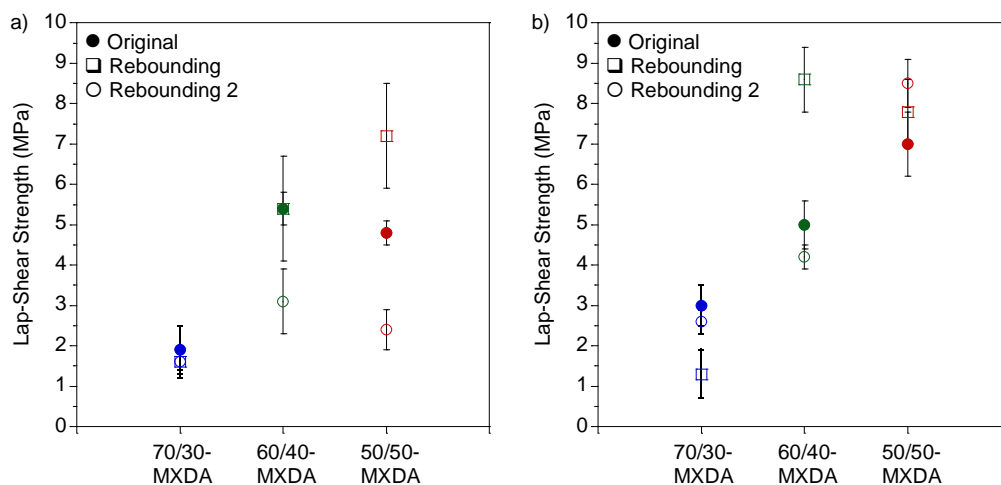


Figure 5.13. Lap-shear strength values for 70/30-, 60/40- and 50/50-MXDA formulations when a) samples were applied onto the substrates at 80 °C and b) samples were applied onto the substrates at 100 °C. Lap-shear strength values are the average of five test specimens and error bar represents the standard deviation.

When materials were applied at 80 °C 70/30-MXDA was characterized with a low lap-shear strength, i.e. 1.9 ± 0.6 MPa, while 60/40-MXDA and 50/50-MXDA showed similar and better performance (Figure 5.13 a). On the other hand, raising the temperature of application up to 100 °C enhanced the performance of the adhesives, specially the 50/50-

MXDA (Figure 5.13 b) indicating the necessity to raise the temperature to 100 °C for the adhesive application. This correlated with probe tack measurements, where 50/50-MXDA exhibited a greater liquid-like behavior and, therefore, a better ability to wet the surface of the adherends. Adhesive failure was predominant for all the compositions regardless the application temperature, indicating greater cohesive forces of the polymer than adhesion between interfaces (Figure A-II.26 a-c and Figure A-II.27 a-c).

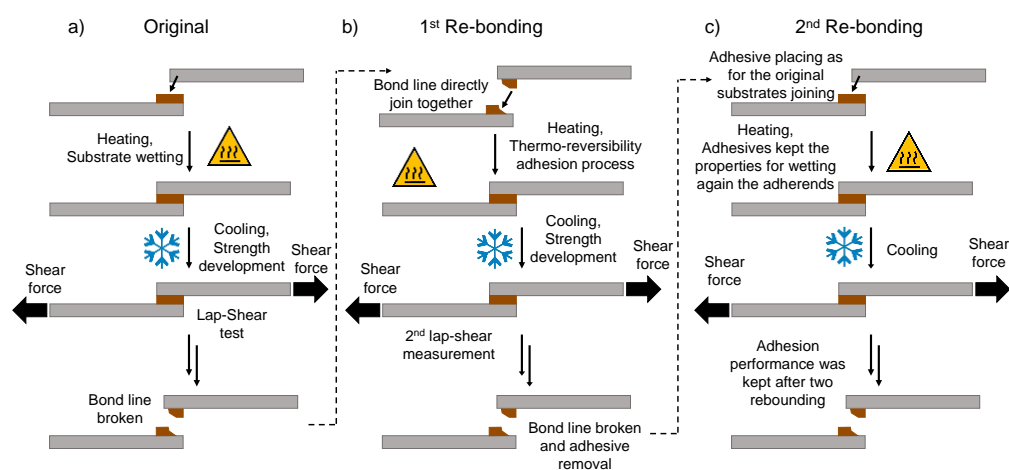


Figure 5.14. Schematic representation of the process for bonding stainless steel adherends for a) first time; b) a first re-bonding after breaking the bond line; and c) a second re-bonding after breaking two times the joint.

Thermo-reversible adhesion of the polymers was addressed by re-bonding adhesives two times (Re-bonding and Re-bonding 2, Figure 5.14 b and c, respectively) after breaking the bond line. In a first re-bonding, substrates were joined together directly and put into the oven at the corresponding temperature to break polymer interactions and allow it flowing. After cooling down the material, substrates were bonded again. In a second re-bonding, adhesives were removed totally from the substrates and applied into new specimens. As a general trend, similar or better lap-shear strength values confirmed the efficiency of the materials for a second

or third used. Adhesive failure after test was predominately observed (Figure A-II.26 d-i and Figure A-II.27 d-i), demonstrating the capacity of the adhesive to regenerate internal forces after several tests.

Lap-shear strength testing measures the ability of a material to withstand stresses set in a plane, which is one of the most common stresses that a bonded joint can face during service. Additional adhesive characterization was performed through shear adhesion failure temperature (SAFT) and shear resistance measurements for determining the temperature at which specimens suffer delamination (service temperature) and the resistance of the materials to creep under static load in shear, respectively.

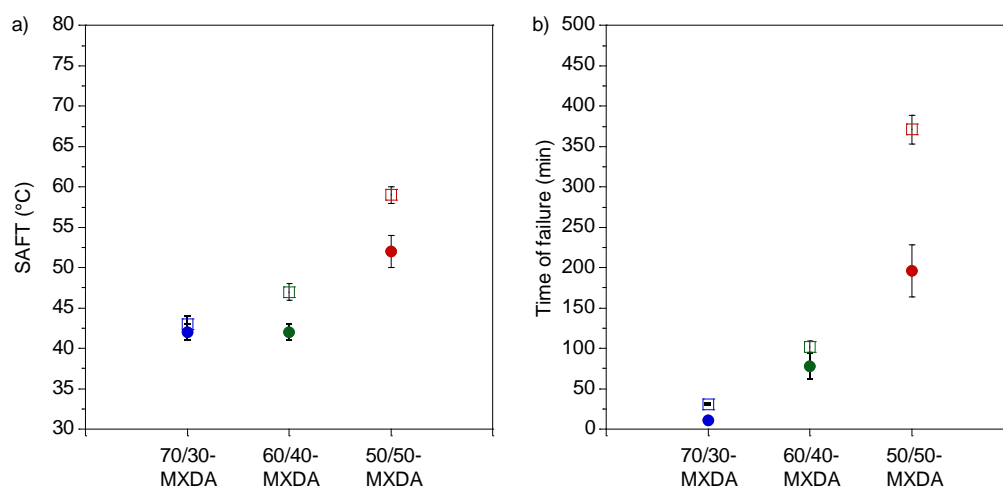


Figure 5.15. a) Average service temperatures values and b) average time values for shear resistance when samples were applied at 80 °C (filled circles) and 100 °C (empty squares) for each composition.

Higher service temperatures as well as creep resistance values were achieved when the proportion of the hard segment, RdiCC, was increased correlating T_g values and the more solid-like behavior manifested in the rheological measurements (Figure 5.15). On the other hand, better results were obtained when the adhesives were applied onto the substrates at 100

°C, especially for 50/50-MXDA bringing to light the necessity of greater temperature for the good wetting of the substrate surfaces. After performing these tests, the nature of adhesion failure was recorded based on visual inspection of the substrates. Cohesive failure (Figure A-II.28) was observed regardless the composition or temperatures of application confirming the liquid-like behavior obtained at low frequencies during frequency sweep measurements (Figure A-II.24).

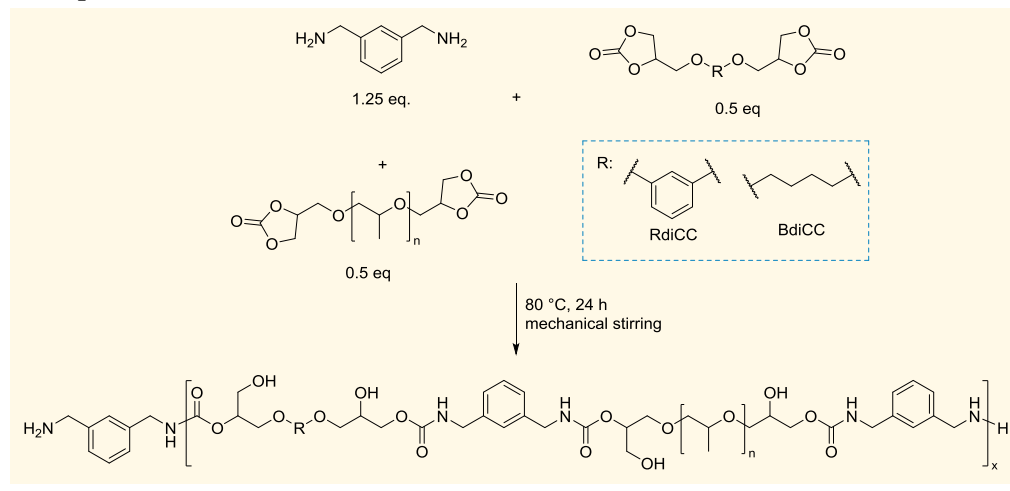
5.4. Influence of the monomer structure in the rheological behavior and adhesives properties of the copolymers

5.4.1. Copolymers based on aliphatic dicyclic carbonates

5.4.1.1. Synthesis and characterization of 50/50BdiCC-MXDA

In order to elucidate if this behaviour was due to the aromaticity of the employed cyclic carbonate which may induce some phase separation, resorcinol dicyclic carbonate was substitute for BdiCC. Thus, only aliphatic dicyclic carbonates were employed in the formulation. The synthesis was performed following the procedure employed for the preparation of the previous copolymers (Scheme 5.3).

Scheme 5.3. Synthesis of the copolymers based on 50/50 PPGdiCC/BdiCC molar ratio and 1.25 equivalents of MXDA.



After 24 h, completion of reaction was confirmed by FTIR-ATR due to total disappearance of C=O stretching band of the cyclic carbonates (1790 cm^{-1} , PPGdiCC and 1780 cm^{-1} , BdiCC) (Figure A-II.29). Further analysis by ^1H NMR characterization showed the signals at 7.6-7.8

ppm of the $-\text{NH}-\text{C}(\text{O})\text{O}$ and the signal of $-\text{CH}_2\text{NH}-$ at 4.15 and 4.17 ppm verifying the formation of the urethane linkage (Figure A-II.30).

Size exclusion chromatography (SEC) was employed for the characterization of the average molar masses of the new copolymer (Table 5.2). The compositions presented very similar weight-average molar masses and polydispersities, in the range of the previous compositions, showing similar reactivity of the monomers.

Table 5.2. Average molar masses and glass transition temperatures of the copolymers based on the polyaddition of MXDA with 50/50 PPGdiCC/BdiCC molar ratio.

Composition PPGdiCC/BdiCC (mol%)	Code	M_n^a kg mol ⁻¹	M_w^a kg mol ⁻¹	PDI ^a kg mol ⁻¹	T_g^b (°C)
50/50*	50/50-MXDA*	2.6 ± 0.1	6.4 ± 0.3	2.5 ± 0.0	30.5
50/50	50/50BdiCC-MXDA	2.5 ± 0.0	5.8 ± 0.1	2.3 ± 0.0	15.5

^aAverage molar masses based on calibration with polystyrene standards ranging from 0.573 to 3,848 kg mol⁻¹; ^b T_g values from rheological temperature sweep measurements done in parallel plates. *It refers to composition of PPGdiCC/RdiCC. Values for 50/50-MXDA were reported again for easier comparison

5.4.1.2. Rheology of 50/50BdiCC-MXDA

Aiming to elucidate the viscoelastic behavior of the copolymer based on aliphatic dicyclic carbonates, temperature and frequency sweep measurements were carried out. In a first step storage and loss moduli as well as loss tangent were evaluated over temperature (Figure 5.16). As expected, substitution of the aromatic RdiCC for the aliphatic BdiCC gave rise to less rigid materials decreasing the glass transition temperature twofold (Table 5.2). Decay of the moduli was also faster showing a greater liquid-like behavior when BdiCC was employed. Frequency sweep measurements corroborated the faster decay of the moduli over the whole range of temperatures and a higher dependency of these moduli with frequency (Figure A-II.31). Nevertheless, although moduli of 50/50-MXDA were higher than 50/50BdiCC-MXDA ones,

similar performance was observed, confirming that in both cases HMAs could be obtained with different properties.

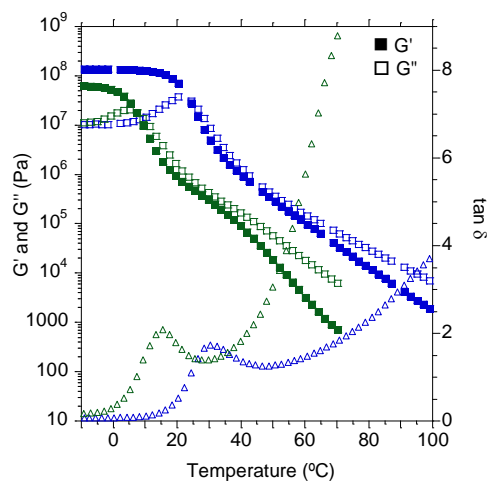


Figure 5.16. G' , G'' and $\tan \delta$ values of 50/50-MXDA (blue) and 50/50BdiCC-MXDA (green). 50/50-MXDA was represented again for easier comparison of the data. Curve of 50/50BdiCC-MXDA was stopped before due to inconsistency of the data.

5.4.1.3. Adhesive properties of 50/50BdiCC-MXDA

After rheological characterization of the BdiCC-based composition, its adhesion performance was addressed by probe tack, lap-shear, SAFT and shear resistance tests. According to the rheological behavior showed by this composition, the adhesion properties were far below from the adhesion performance of 50/50-MXDA in all the measurements (Table 5.3 and Figure A-II.32). Cohesive failure of the adhesive was recorded for all cases showing the lower cohesive forces, according to the greater liquid-like behavior, of the material (Figure A-II.33).

Table 5.3. Lap-shear strength, SAFT and shear resistance values for 50/50BdiCC-MXDA.

Enhanced and Reusable Poly(Hydroxy Urethane)-Based Low-Temperature Hot-Melt Adhesives

Code	Lap-Shear Strength (MPa)			SAFT (°C)	Shear Resistance (min)
	initial	Re-bonding	Re-bonding 2		
50/50-MXDA*	7.0 ± 0.8	7.8 ± 0.8	8.5 ± 0.6	59 ± 1	371 ± 18
50/50BdiCC-MXDA	2.0 ± 0.4	0.5 ± 0.1	1.2 ± 0.1	35 ± 0	9 ± 0

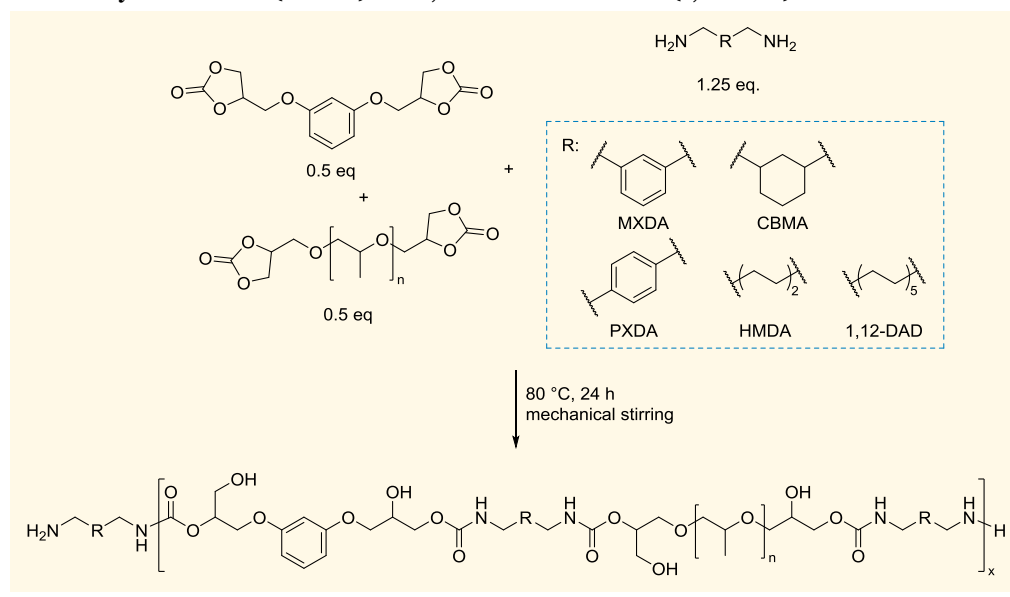
*50/50-MXDA values are showed for easier comparison.

5.4.2. Tuning PHU Hot-Melt adhesives by changing the diamine structure

5.4.2.1. Synthesis and characterization of copolymers based on different diamines

After confirming that HMA could be obtained both with aromatic and aliphatic dicyclic carbonates, we investigated the impact of the diamine in the HMA behaviour. To do so, new copolymers based on a molar ratio 50/50 of the dicyclic carbonates varying the diamine were prepared following the procedure of the MXDA-based copolymers (Scheme 5.4).

Scheme 5.4. Preparation of PHU copolymer compositions reacting 50/50 molar ratio of PPGdiCC/RdiCC with 1.25 equiv of the corresponding diamine, *m*-xylylenediamine (MXDA), *p*-xylylenediamine (PXDA), 1,3-cyclohexanebis(methylamine) (CBMA), hexamethylenediamine (HMDA) and 1,12-diaminododecane (1,12-DAD).



The formation of the PHU was confirmed by FTIR-ATR and ¹H NMR (Figure A-II.34, Figure A-II.35 and Figure A-II.36) and SEC (Table 5.4). SEC of 50/50-HMDA and 50/50-DAD was not possible to be performed since these samples were not soluble either in THF nor in

DMF, which are the common solvents for SEC. On the other hand, average molar masses of compositions based on aromatic and cycloaliphatic diamines were obtained as expected for PHUs being similar to the previous PHUs of this chapter.

Table 5.4. Average molar masses and glass transition temperatures of the copolymers based on the polyaddition of different diamines with 50/50 PPGdiCC/RdiCC molar ratio.

Composition PPGdiCC/RdiCC (mol%)	Diamine	Code	M_n^a kg mol ⁻¹	M_w^a kg mol ⁻¹	PDI ^a kg mol ⁻¹	T_g (°C)	GC ^e (%)
50/50	MXDA	50/50-MXDA	2.6 ± 0.1	6.4 ± 0.3	2.5 ± 0.0	30.5 ^c	^f
	PXDA	50/50-PXDA	3.5 ± 0.7	7.5 ± 0.3	2.2 ± 0.4	26.5 ^c	^f
	CBMA	50/50-CBMA	1.9 ± 0.0	4.3 ± 0.1	2.2 ± 0.0	30.5 ^c	^f
	HMDA	50/50-HMDA	^b	^b	^b	4.9 ^d	65.0 ± 5.0
	1,12-DAD	50/50-DAD	^b	^b	^b	7.2 ^d	60.7 ± 2.2

^aAverage molar masses based on calibration with polystyrene standards ranging from 0.573 to 3,848 kg mol⁻¹; ^bnot determined because samples were not soluble in THF; T_g values from ^crheological temperature sweep measurements done in parallel plates and ^dfrom dynamic mechanical temperature analysis measurements (Figure A-II.37 b); ^egel content after Soxhlet extraction in refluxing THF for 24 h; ^fsoxhlet extraction was not performed since samples presented total solubility in THF (no gel content).

5.4.2.2. Rheology of the copolymers based on different diamines

Temperature sweep experiments were carried out to address the viscoelastic behavior of the materials (Figure 5.17). When using the two aliphatic diamines, HMDA as well as 1,12-DAD we did not observe any HMA behavior as both materials exhibited greater values of the storage than the loss modulus over the whole range of temperatures, which is typical for crosslinked materials (Figure 5.17 a, b). Moreover, when frequency sweeps were carried out G' and G'' exhibited low dependence on frequency demonstrating the permanent elastic behavior of the material (Figure A-II.37 a) as well as samples presented high gel content after soxhlet extractions in refluxing THF (Table 5.4). In our opinion in this case the interaction between the hydroxyl groups and urethanes group are stronger than in the case of aromatic diamines due to the greater mobility and less steric hindrance of the aliphatic chains, avoids the flowing of the

material due to the presence of irreversible hydrogen bonds. As the materials did not present a liquid-like behavior were not further considered for adhesive purposes.

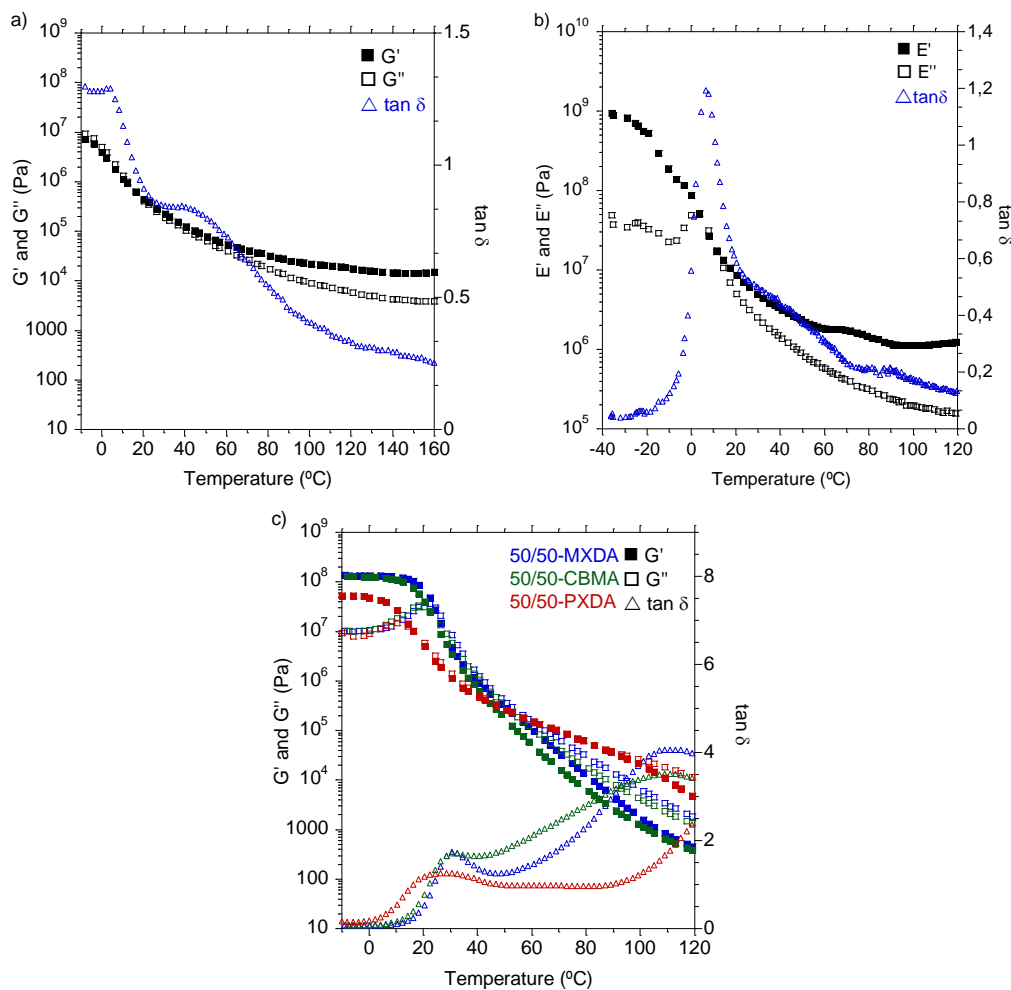


Figure 5.17. a) G' , G'' and $\tan \delta$ values of 50/50-HMDA from temperature sweep measurements; b) E' , E'' and $\tan \delta$ values of 50/50-DAD from DMTA analysis. (This composition was studied through DMTA analysis due to the easier sample preparation); and c) G' , G'' and $\tan \delta$ values of 50/50-MXDA (blue), 50/50-CBMA (green) and 50/50-PXDA (red). 50/50-MXDA was represented again for easier comparison of the data.

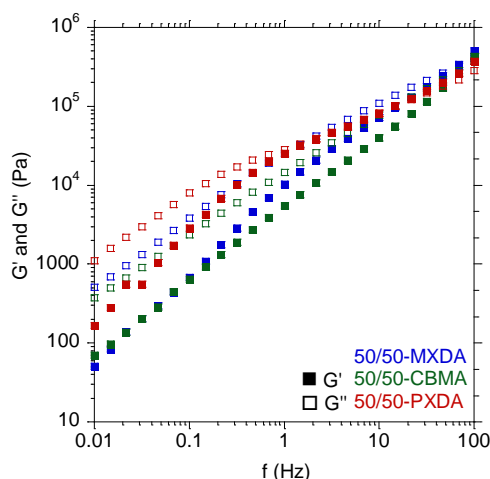


Figure 5.18. G' and G'' values between 0.01 and 100 Hz at 80 °C of 50/50-MXDA (blue), 50/50-CBMA (green) and 50/50-PXDA (red) compositions.

On the other hand, 50/50-CBMA and 50/50-PXDA presented a similar behavior to 50/50-MXDA composition (Figure 5.17 c). After glass transition temperatures both formulations suffered a progressively decay of the moduli. It has to be noted that this decrease of the moduli was a bit more pronounced when cycloaliphatic diamine, CBMA, was employed, whereas when PXDA was used, the moduli remained higher and closer between them showing a stronger interaction of the chains. Frequency sweep measurements were carried out for further analysis of the rheological behavior of the adhesives (Figure 5.18).

Frequency sweep measurement at 80 °C of 50/50-CBMA exhibited a similar decay of the moduli. Thus, possible π - π contributions were discarded. On the other hand, 50/50-PXDA showed a crossover between G' and G'' (Figure 5.18 b, red spots). At high frequencies presented a solid-like behaviour ($G' > G''$) while when low frequencies were applied the adhesive behaved as a liquid ($G'' > G'$). In the whole range of frequencies at 80 °C, adhesives based on PXDA exhibited greater storage as well as loss moduli than MXDA-based materials demonstrating a

key role of the aromatic ring substitution in hydrogen bond interactions. In addition, 50/50-PXDA showed less dependency of the moduli on frequency when temperatures were increased meaning a greater H bonds interaction (Figure A-II.39). FTIR-ATR experiments were performed for 50/50-PXDA for further analysis of hydrogen bonding and debonding. (Figure 5.19).

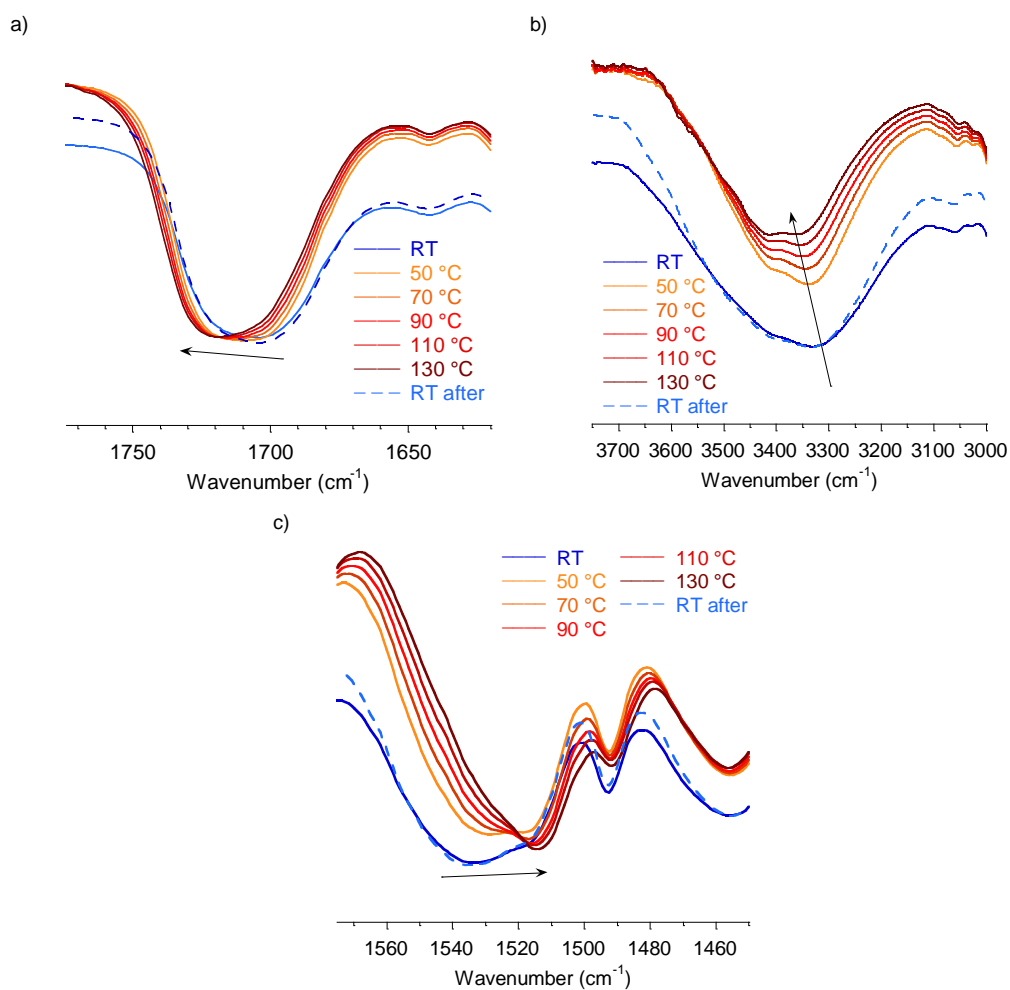


Figure 5.19. Variable temperature FTIR spectra in the region of a) C=O stretching band, b) N-H bending band and c) O-H stretching band of 50/50-PXDA composition.

50/50-PXDA manifested a similar behaviour than its homologous based on MXDA. C=O and maximum of O-H stretching bands blue-shifted while N-H bending band red-shifted when temperature was increased from 25 to 130 °C (Figure 5.19 a, b and c, respectively). The remaining shoulder at 1704 cm⁻¹ denoted that hydrogen bonds were present even at 130 °C. This composition also presented reversible hydrogen bond formation since the vibrational bands recovered the initial position.

5.4.2.3. Diamine influence on adhesion properties of PHU Hot-Melt adhesives

Probe tack, lap-shear strength, SAFT and shear resistance of 50/50-PXDA and 50/50-CBMA were performed for addressing the diamine influence on adhesive properties. Based on rheology and better lap-shear results of the initial study, in this section hot-melt adhesives were applied firstly at 100 °C. Probe tack stress-strain curves of MXDA-, CBMA- and PXDA-based PHUs are depicted in Figure 5.20 a. According to rheology frequency sweeps, 50/50-PXDA composition showed a greater cohesiveness, keeping adhesive properties longer. Due to these higher cohesive forces, adhesive failure was recorded remaining no residue in the stainless steel cylinder probe. As the formulation did not presented liquid-like behaviour at this temperature a further experiment was performed at 120 °C. Tackiness of 50/50-PXDA was slightly lower. However, adhesive failure was recorded and no fibrillation was observed, showing a more solid-like behaviour at these test conditions.

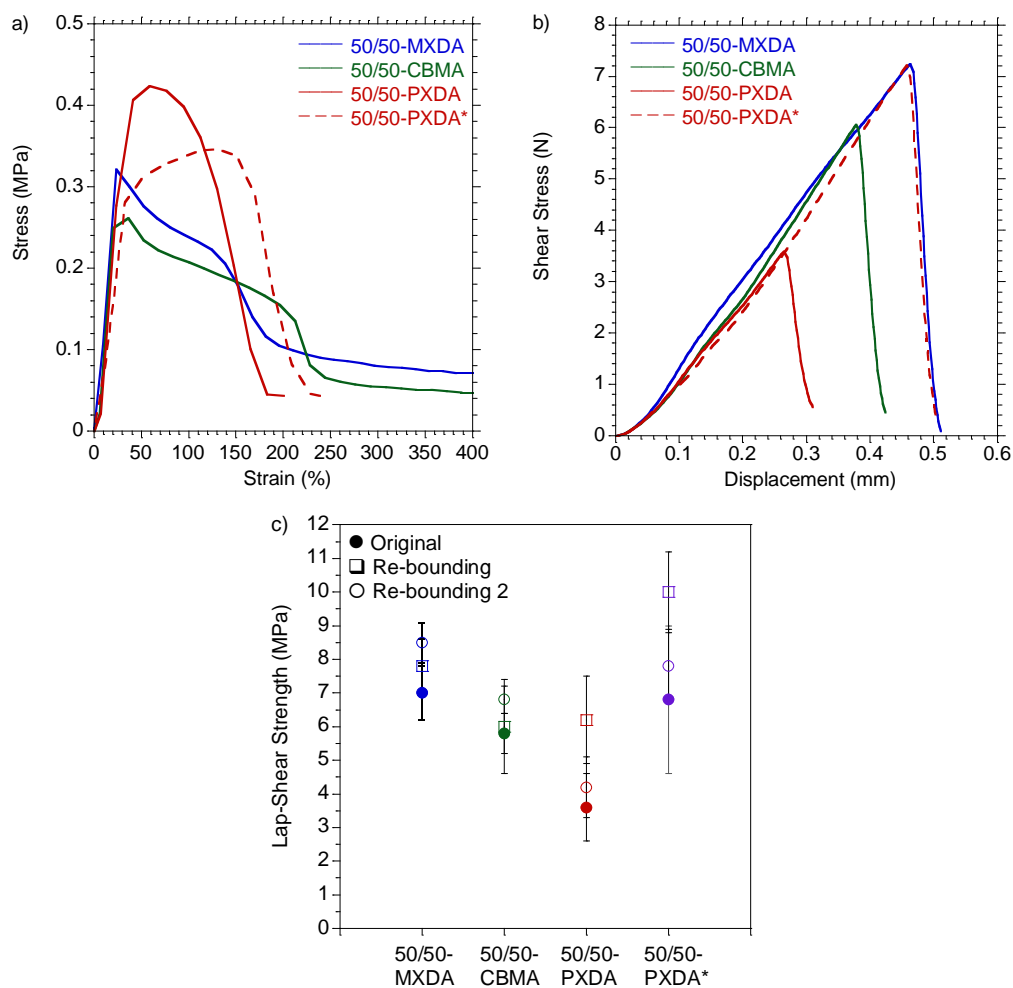


Figure 5.20. a) Probe tack stress-strain curves of 50/50-MXDA, -CBMA and -PXDA compositions performed at 100 °C (solid lines); 50/50-PXDA* was performed at 120 °C (red dash line); b) representative shear stress-displacement curves for the hot-melt adhesives based on MXDA, CBMA and PXDA applying the adhesives at 100 °C (solid lines) and for 50/50-PXDA when it was applied at 120 °C (red dash line); c) lap-shear strength values for 50/50 MXDA-, CBMA- and PXDA-based formulations when samples were applied onto the substrates at 100 °C. 50/50-PXDA* was applied at 120 °C. Lap-shear strength values are the average of five test specimens and error bar represents the standard deviation.

After evaluating tack performance of the adhesives, lap-shear measurements were carried out (Figure 5.20 b). On this test, adhesive failure was registered for all compositions regardless

diamine structure or temperature application (Figure A-II.38). Aromatic-based formulations (50/50-MXDA and -PXDA) presented slightly better lap-shear strength than cycloaliphatic-based composition (50/50-CBMA). Nevertheless, in the case of 50/50-PXDA the temperature of application was increased to 120 °C to obtain a more fluid-like material, according to the rheological measurements, to achieve a good initial wetting of the adhesive providing the maximum adhesion strength. As performed in point 5.3.3, a first and a second re-bonding were carried out to check reversibility of adhesion for these compositions (Figure 5.20 c). Analogous results confirmed the possibility for reusing more than once the PHU hot-melt adhesives. Adhesive failure was registered for all compositions regardless employed diamine or temperature application.

Finally, SAFT and shear resistance of the adhesives was addressed (Table 5.5). Aromatic diamine-based formulations (50/50-MXDA and -PXDA) exhibited greater SAFT as well as shear resistance than cycloaliphatic diamine formulation (50/50-CBMA) corroborating the less tendency to flow showed in the frequency sweep measurements (Figure A-II.39). When the aromatic diamine was *para* substituted, the moduli exhibited higher independency from frequency, therefore, greater resistance to flow, which concurred with the fivefold time in shear resistance experiments (Table 5.5). Cohesive failures were observed after all tests, confirming the liquid-like behavior when long times of experiment are applied (Figure A-II.40).

Table 5.5. Shear Adhesion Failure Temperature (SAFT) and shear resistance values for 50/50 compositions based on MXDA, CBMA and PXDA.

Code	SAFT (°C)	Shear Resistance (min)
50/50-MXDA	59 ± 1	371 ± 18
50/50-CBMA	50 ± 2	160 ± 47
50/50-PXDA	63 ± 1	1941 ± 47

5.4.2.4. Adhesive performance on different substrates

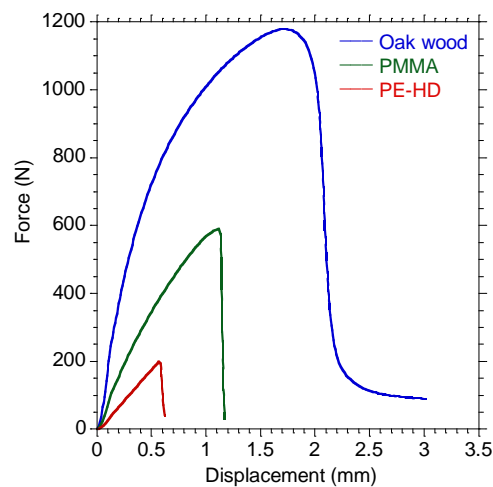


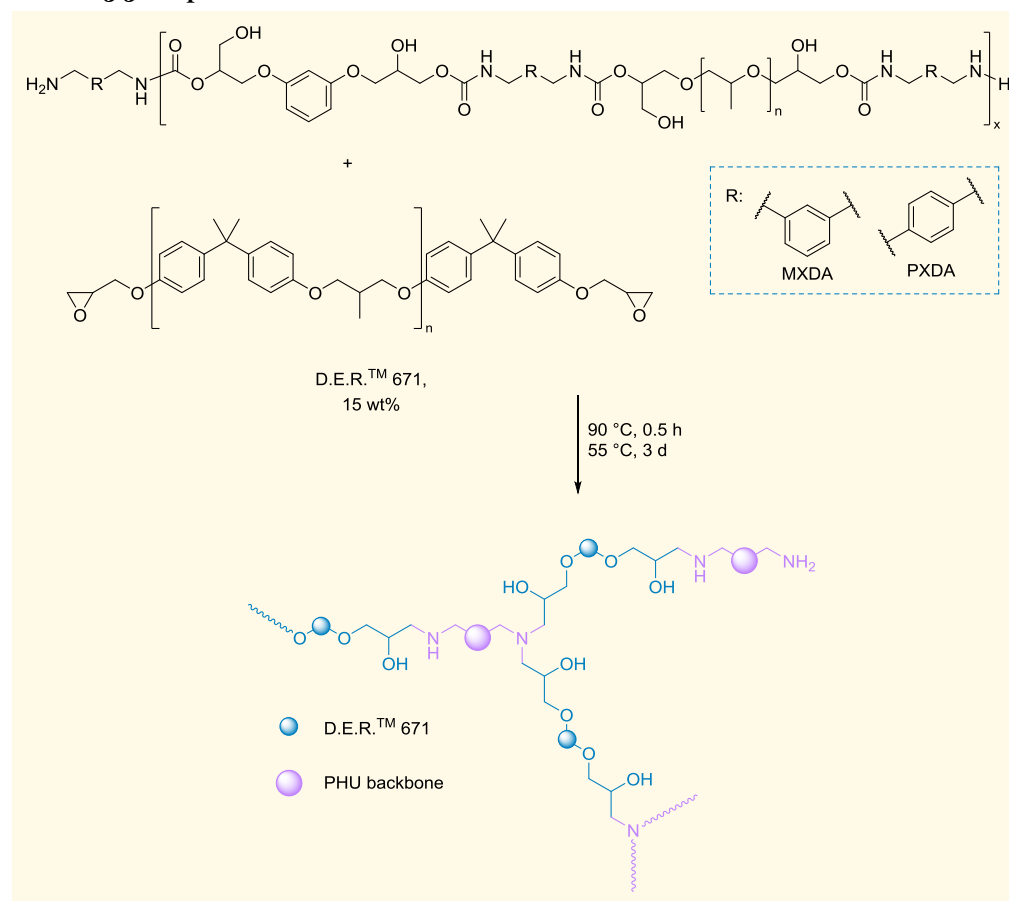
Figure 5.21. Comparison of shear stress-displacement curves of 50/50-MXDA composition on oak wood, poly(methyl methacrylate) (PMMA) and high-density polyethylene (PE-HD).

The ability of the hot-melt adhesives for gluing different substrates was addressed by performing lap-shear strength measurements on oak wood, PE-HD and PMMA. These tests were performed using 50/50-MXDA. As it can be seen in Figure 5.21, low lap-shear strength values were measured when polymeric substrates were glued. Nevertheless, PMMA showed stronger interactions with the adhesive than PE-HD, due to its greater surface energy, as the higher surface energy, the easier wettability of the substrate and therefore stronger attractive forces were created between the adhesive and the substrate. In addition, PMMA can establish hydrogen bonding interactions with the adhesive, while PE-HD was not able to do it. For all polymeric substrates adhesive failure was observed showing the less affinity between adherend and adhesive (Figure A-II.41). In contrast, when a polar substrate like oak wood was bonded, higher lap-shear strength values were obtained. This demonstrates that the adhesives had a

higher interaction with polar substrates, as the hydroxyl groups of the polymer chain had stronger interaction with these surfaces.

5.5. Enhanced hot-melt adhesives

Scheme 5.5. Preparation of enhanced PHU hot-melt adhesives.



As discussed above, hot-melt adhesives are usually composed by more than just one ingredient. Usually commercial HMAs present resins within their formulations, which are used

to enhance the mechanical properties of the compositions. When the resin and the polymer are compatible, they react creating a crosslinked structure that presents stronger mechanical properties than the polymer itself.¹³³ Therefore, attempting to endow the PHU hot-melt adhesives with better static adhesive properties (SAFT) an epoxy resin was incorporated to the 50/50-MXDA and 50/50-PXDA compositions. The incorporation of an additional chemistry to the PHU formulations, in this case epoxy resins, has been demonstrated to thoroughly improve the performance of PHU materials.^{33,51,56,110,115} The excess of diamine employed during the synthesis allowed the further reaction with the epoxy resin. It has been reported that free amine can react twice (two active hydrogen) with an epoxy ring, while already reacted amines with cyclic carbonates are not able to react with the oxirane.⁵¹ Possible final structure of the adhesive is shown in Scheme 5.5. The PHU polymers, 50/50-MXDA and 50/50-PXDA, were heated up to 90 °C and mixed with 15 wt% of solid epoxy resin, D.E.R.TM 671, for 20 minutes. Materials were allowed to react at 55 °C for 3 days to assure the total reaction of the diamines and epoxy groups.

Materials were first characterized by FTIR-ATR showing that the PHU structure was maintained as well as the incorporation of the epoxy due to characteristic band at 829 cm⁻¹. (Figure A-II.42).

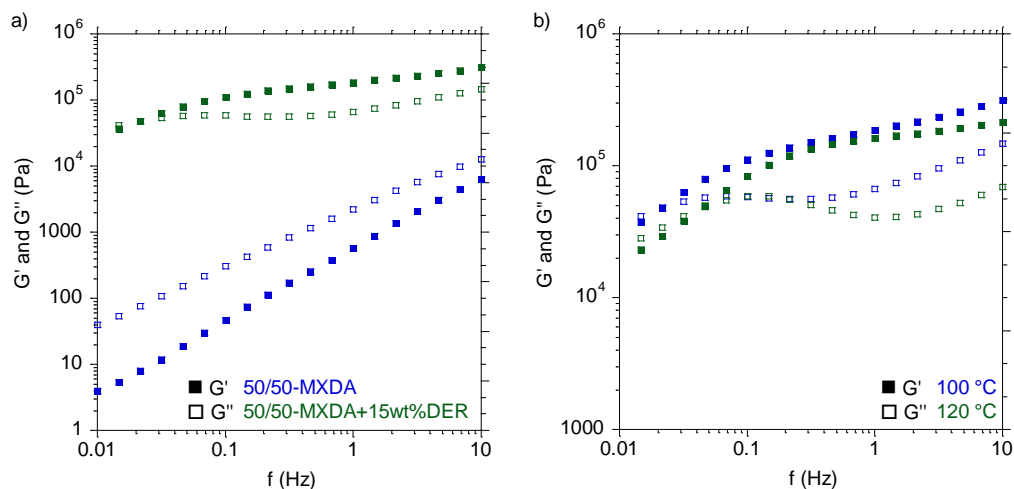


Figure 5.22. G' and G'' values from frequency sweep measurements of a) 50/50-MXDA (blue) and 50/50-MXDA+15wt%DER (green) at $100\text{ }^\circ\text{C}$ and b) 50/50-MXDA+15wt%DER at 100 (blue) and 120 (green) $^\circ\text{C}$.

Frequency sweep measurement at $100\text{ }^\circ\text{C}$ of the 50/50MXDA+15DER composition demonstrated movement restriction of the chains due to the addition of the epoxy resin (Figure 5.22 a). G' as well as G'' presented more independency from frequency than 50/50-MXDA composition, which means greater rubbery behavior. Nevertheless, at low frequencies the crossover of G' and G'' was observed, that is a transition from a solid- to a liquid-like behavior, which allows the material to wet the substrate surface when enough time is employed. In order to save time during application and enhance wettability of the surfaces, adhesives were applied at $120\text{ }^\circ\text{C}$ since the crossover of G'' over G' happens in shorter times at this temperature (Figure 5.22 b).

Lap-shear strength and SAFT values are gathered in Table 5.6. The addition of epoxy resin into the formulation endowed the materials with greater resistance to temperature, enhancing the service temperatures up to almost the double. Moreover, as a signal of cohesive forces reinforcement, adhesive failure in the PXDA-based adhesives was observed (Figure A-II.43 and

Figure A-II.44). On the contrary, lap-shear strength decreased. Nonetheless, values were within the typical lap-shear strengths for hot-melt adhesives³² and reversibility of the bonding was demonstrated through similar, or even better performance after two re-bonding cycles.

Table 5.6. Lap-shear strength and adhesion failure temperatures of the enhanced PHU hot-melt adhesives.

Code	Gel content (%) ^a	Lap-shear strength (MPa)			SAFT (°C)
		Original	Re-bonding	Re-bonding 2	
50/50-MXDA+15wt%DER	3.8 ± 2.8	3.1 ± 0.8	5.5 ± 1.1	8.9 ± 2.0	104 ± 4
50/50-PXDA+15wt%DER	41.3 ± 7.9	2.4 ± 0.8	3.1 ± 0.8	6.7 ± 2.3	119 ± 12

^agel content after Soxhlet extraction in refluxing THF for 24 h.

5.6. Conclusions

To conclude, a palette of non-isocyanate polyurethane-based hot-melt adhesives were synthesized by reacting different molar ratios of dicyclic carbonates (PPGdiCC/RdiCC or PPGdiCC/BdiCC) with aromatic [*m*-xylylenediamine (MXDA), *p*-xylylenediamine (PXDA)], cycloaliphatic [1,3-cyclohexanebis(methyleneamine) (CBMA)] or aliphatic [hexamethylenediamine (HMDA), 1,12-diaminododecane (1,12-DAD)] diamines. FTIR-ATR as well as ¹H NMR characterization showed full conversion of the cyclic carbonates after 24 h at 80 °C under continuous mechanical stirring. Size exclusion chromatography analysis confirmed the expected low weight-average molar masses, which are typical for poly(hydroxy urethane)s due to strong hydrogen bonding of the chains. Rheological characterization of the adhesives showed the increment of rigidity when greater amounts of RdiCC was added. The substitution of RdiCC by BdiCC resulted in a softer material worsening adhesion performance. On the other hand, the incorporation of aliphatic diamines into the formulation gave rise to rubbery materials and absence of any liquid-solid transition or hot-melt behaviour. While similar values in lap-shear strength were obtained for aromatic- and cycloaliphatic-based

compositions, shear adhesion failure temperatures (SAFT) and shear resistance of the materials were superior when aromatic diamines were selected. Incorporation of aromatic diamines improved the temperature resistance of the polymers. Frequency sweep measurements showed that G' and G'' moduli of 50/50-PXDA (*para* aromatic diamine-based formulation) were more independent of frequency than G' and G'' of 50/50-MXDA, corroborating the greater shear resistance under static load. Finally, crosslinked PHU hot-melt adhesives were prepared by adding few amount of epoxy resin (D.E.R.TM 671, 15 wt%). Introduction of the epoxy resin endowed the adhesives with higher service temperatures, due to the permanent crosslinking, without diminishing the thermo-reversibility. Finally, thermo-reversibility adhesion of the copolymers was successfully demonstrated performing lap-shear measurements after two consecutive re-bonding, in which polymers kept the adhesion performance.



Chapter 6.

Conclusions and Outlook

Moved by environmental and lawful obligations, the quest for a sustainable and safer adhesive that can replace isocyanate-based conventional polyurethane adhesives and its application in the automotive industry have been the main goals in this thesis. Thus, the thesis has been oriented to the synthesis of poly(hydroxy urethane)s (PHUs) through the polyaddition of polyamines with poly(cyclic carbonate)s, which had emerged one decade ago as the most appealing and adaptable non-isocyanate polyurethane family for adhesives.

In a first attempt, a monocomponent adhesive based on the combination of NIPU and sol-gel chemistry was developed. Firstly, 5-membered cyclic carbonate monomers based on poly(propylene glycol) (PPG) and resorcinol were successfully synthesized by chemical insertion of CO₂ into the corresponding PPG- and resorcinol-based epoxy resins. Further reaction of an excess of the monomers with a biobased fatty diamine (Priamine™ 1074) conducted to cyclic carbonate-terminated prepolymers. The monocomponent adhesive was prepared by adding 3-(aminopropyl)triethoxysilane (APTES) to this prepolymer, which allowed the curing process to proceed under ambient conditions through a sol-gel process. The system was studied by rheological measurements at different temperatures, which determined the activation energy to be 50 kJ mol⁻¹. The addition of 1 wt% of 1,8-Diazabicyclo[5.4.0]undec-7-ene (DBU) or methanesulfonic acid (MSA) accelerated slightly the curing while the 1 wt% incorporation of HAC decreased fivefold the gel time at 100 °C. Furthermore, using 2.5 wt% of the mild acid, i.e. HAC, permitted the curing at room temperature, although adhesion performance was slightly weakened. Finally, the integration of 40 mol% of resorcinol dicarbonate hard monomer into the composition endowed the adhesive with 2.5 times higher lap-shear strength, bringing to light the relevance of controlling the hard to soft ratio for obtaining well-balanced cohesive and adhesive forces in the adhesion performance.

Seeking for greater lap-shear strengths and the decreasing of gelation times, incorporation of additives into the PHU formulations was taken into account. Thus, combination of an adhesion, i.e. dopamine, and fast-curing, i.e. 3-(aminopropyl)trimethoxysilane, promoters were blended with trimethylolpropane tris(cyclic carbonate) (TMPTC) and *m*-xylylenediamine (MXDA) was performed in order to prepare PHU adhesives. While the formulation containing a 3.9 mol% of dopamine improved the lap-shear strength of the neat PHU-based adhesive, combination of both additives kept the adhesive properties as high as this formulation as well as decreased the gel time fourfold, from more than 3 h to less than 45 min. Nonetheless, TMPTC-based compositions resulted in hard and rigid materials with glass transition temperatures above room temperature. Therefore, we evaluated the integration of the cyclic carbonate soft segment monomer, i.e. PPGdiCC. Adhesives with lower viscosities were obtained and 20 min was set as optimal mixing time possessing an adequate viscosity for application. Less than 30 mol% of trifunctional cyclic carbonate, TMPTC, led to not self-standing materials whereas more than 70 mol% of this compound was employed in the compositions too stiff adhesives were obtained, which did not withstands high deformation forces and exhibited premature failure. Similarly, a minimum 50 mol% of TMPTC was required to be present in the formulations to show superior resistance under shear load and temperature, keeping adhesive properties above 200 °C under 1 kg of load. The addition of PPGdiCC allowed to prepare a palette of adhesive with tunable T_g for different applications depending on the temperature. Adhesion performance of the best composition, 70/30 TMPTC/PPGdiCC molar ratio, was addressed on different adherends such as high-density polyethylene (PE-HD), poly(methyl methacrylate) (PMMA), polyamide, oak wood, aluminium and stainless steel. Adhesion on non-polar substrates (PE-HD, PMMA, polyamide) was characterized with low lap-shear strength values, while excellent adhesion was achieved for polar adherends (oak, aluminium and stainless steel) corroborating the high polarity of the PHU polymers. Finally, the evaluation

of different pre-treatments applied to oak wood laid bare the importance of a good preparation of the materials before gluing thereof, enhancing the adhesion more than twofold.

Despite the good adhesion performance showed by the hybrid PHUs and the capacity of the monocomponent adhesive to cure under ambient conditions, the necessity of high temperature (100 °C) or long times to fully cure moved away both from industrial implementation. Hence, we took advantage of other chemistries, in this case epoxy resins, to enhance curing times and adhesion performance of the poly(hydroxy urethane)-based adhesives at room temperature. Synthesis of amino-terminated PHU was performed by polyaddition of an aliphatic diamine, 1,12-DAD, with a 60/40 molar ratio of PPGdiCC/RdiCC for further mixing with a BPA-based epoxy resin, EPIKOTE™ 828. Rheological characterization showed a gel time higher than 2 h for PHU-epoxy hybrid, while the combination of the PHU with trimethylolpropane tris(3-mercaptopropionate), TMPTMP in a 30/70 equivalent ratio speeded up the curing process to 76 min of gel time in the presence of 0.875 mol% of TMG. Lap-shear measurements in PMMA-SS substrates were performed after 24 h and 1 week exhibiting similar performance, so the adhesives were able to develop maximum shear strength in 24 h. Richer compositions in TMPTMP showed greater lap-shear strength due to less polarity of the polymer. Nonetheless, when stainless steel substrates were bonded 70/30, 50/50 and 30/70 equivalent ratio compositions presented greater lap-shear strengths than fully PHU or TMPTMP formulations as well as higher toughness, which makes adhesives more resistant to vibrations and shock impacts. Besides, the 70/30 PHU/TMPTMP composition showed ability to develop handling strength within 3 h. All compositions displayed excellent service temperatures withstanding 1 kg load for more than 7 h at 217 °C as well as very low equilibrium water contents, diminishing the risk of delamination under humid ambient.

Although the search of structural adhesives was the main goal of this thesis, some hot-melt adhesive formulations were developed. Copolymers made of 70/30, 60/40 and 50/50 molar ratios of PPGdiCC/RdiCC were prepared by polyaddition with *m*-xylylenediamine. The increasing of hard monomer, RdiCC, resulted in adhesives with greater T_g and slower decay of the storage and loss modulus over temperature. Rheological frequency sweep measurements as well as FTIR-ATR spectra at different temperatures confirmed the presence of hydrogen bonds even at high temperatures (100-130 °C). Similar to rheological behaviour, adhesion performance, lap-shear, shear adhesion failure temperature (SAFT) as well as shear resistance, was enhanced with the increment of RdiCC in the formulation. Adhesive failure of all compositions demonstrated greater cohesive strength between the polymer chains than adhesive forces between the adherend and the adhesive. The thermo-reversibility was assessed by consecutive bonding and debonding process exhibiting similar lap-shear strengths in all cases. Substitution of aromatic dicyclic carbonate by aliphatic counterpart gave rise to softer materials with lower T_g , lap-shear strength, SAFT and shear resistance, while replacing the aromatic diamine by aliphatic one produced adhesives, which greater G' than G'' over the temperature due to irreversible hydrogen bonds. Change of the positions in the aromatic ring substitution from *meta* (MXDA) to *para* (PXDA) increased fivefold the shear resistance of the adhesive according to the less dependency of the rheological moduli with the frequency. Finally, hot-melt adhesive compositions based on aromatic diamines were enhanced by addition of a viscous epoxy resin, which reinforced cohesive forces of the materials. Shear adhesion failure temperatures were improved from 60 up to 100 °C, showing a better resistance under load and temperature without reducing their thermo-reversibility character.

Summarizing, poly(hydroxy urethane) adhesive compositions were prepared by polyaddition of dicyclic carbonates with diamines. Study of the adhesive properties

demonstrated the necessity of well-balanced hard to soft ratio of the monomers for obtaining good adhesion performance. Moving forward to design relevant structural adhesives, we showed that the incorporation of additives such as adhesion, dopamine, or fast-curing, alkoxy silane compounds, promoters, dopamine, endowed adhesives with better adhesive properties or faster curing process, respectively. The requirement of high temperatures to achieve desired adhesion performance limited the applications of these adhesives. Thus, combination of PHU with epoxy chemistry was mandatory to reach excellent lap-shear as well as shear properties under load and temperature curing the materials under ambient conditions. Development of PHU thermoplastic polymers opened a new field of applications for this family. Hot-melt adhesives were enhanced by incorporation of a viscous epoxy resin, while thermos-reversibility was not detriment.

Looking ahead to the future, polyaddition of poly(cyclic carbonates) with (poly)amines to produce poly(hydroxy urethane)s postulates as the most appealing alternative to conventional polyurethanes. Nevertheless, the low reactivity of 5-membered cyclic carbonates and the low molar masses represent the main obstacles to their industrial implementation. Optimization of the synthesis of larger size cyclic carbonates (6-, 7- or 8-membered cyclic carbonates) can boost polymerizations at room temperature due to their higher reactivity. On the other hand, combination with other chemistries such as sol-gel or epoxy, are also elegant approaches to overcome limitations at room temperature. More studies in this direction will push the development of relevant PHU formulations. Finally, we think that researchers have to take advantage of the fundamental existing literature in this field for the design of specific catalyst that can speed up the curing process at room temperature to achieve excellent adhesive performance.



Appendix I.

Methods

A-I.1. Instrumentation and characterization techniques

Nuclear Magnetic Resonance (NMR). ^1H spectra were recorded on a Bruker Advance DPX 300 spectrometer at 25 °C. Deuterated chloroform, CDCl_3 , deuterated dimethyl sulfoxide, DMSO-d_6 , and deuterated methanol, $\text{CH}_3\text{OH-d}_4$, were used as solvent.

Fourier Transform Infrared (FT-IR) Spectroscopy. FT-IR spectra were obtained using an FT-IR spectrophotometer (Nicolet is20 FT-IR, Thermo Scientific Inc., USA) equipped with Attenuated Total Reflectance (ATR) with a diamond crystal. Spectra were recorded between 4000 and 600 cm^{-1} with a spectrum resolution of 4 cm^{-1} . All spectra were averaged over 16 scans.

Rheology Measurements. Time, temperature and frequency sweep experiments were performed in a stress-controlled Anton Paar Physica MCR101 rheometer. Time sweep measurements were carried out at different temperatures, at a frequency of 1 Hz and a strain of 1% in order to determine the crossover between loss modulus and storage modulus (gel time). For samples corresponding to Chapter 2, the experiments were carried out using 25 mm parallel plate geometry. For samples corresponding to Chapter 3 and 4, the experiments were carried out using 15 mm disposable parallel plate geometry. Temperature sweep experiments were performed from -10 to 120 °C (some experiments were finished before due to inconsistency of the data), at a frequency of 1 Hz and a strain in the range of viscoelasticity of the materials. For samples corresponding to Chapter 3, the experiments were carried out using 8 mm parallel plate geometry. For samples corresponding to Chapter 5, the experiments were carried out using 15 mm disposable parallel plate geometry. Frequency sweep experiments were carried out at a constant temperature in the viscoelastic regime of the materials, from 0.01 to

100 Hz (0.0628 to 628 rad s⁻¹) using 15 mm disposable parallel plate geometry. Typical terminal behavior of non-structured polymers is characterized with eq 1 and 2.^{141,142}

$$G' \sim \omega^2 \quad (1)$$

$$G'' \sim \omega \quad (2)$$

where G' is the storage modulus, G'' is the loss modulus and ω is the angular frequency in rad s⁻¹.

Therefore, the linear fit of double logarithm plots gives rise to slopes of 1 for G'' and 2 for G' (eq 3 and 4).

$$\log(G') \sim m \log(\omega) \quad (3)$$

where G' is the storage modulus, ω is the angular frequency in rad s⁻¹ and m is equal to 2.

$$\log(G'') \sim m \log(\omega) \quad (4)$$

where G'' is the loss modulus, ω is the angular frequency in rad s⁻¹ and m is equal to 1.

Linear fit of the curves at low frequencies were performed employing the data analysis tools of Origin 2020b.

Dynamic Mechanical Thermal Analysis (DMTA). DMTA experiments were performed using a rectangular sample of the crosslinked materials (2 x 3.5 x 1 mm), using a Triton 2000 DMA from Triton Technology in bending mode. Tests were performed at 1 Hz, at a heating rate of 4 °C min⁻¹ from -35 to 100 °C. Crosslinking density (ν) was calculated on the basis of the

relation between average molecular weight of effective networks chains (M_c) and density of the polymer (ρ) (eq 5).

$$v_e = \frac{\rho}{M_c} \quad (5)$$

From rubber elasticity theory,¹²⁴ the uniaxial stretching were studied on the rubbery plateau at $T_{\alpha+50}$, and at very small deformations. Under these hypotheses, the crosslinking density (v_e), can be obtained from eqs 6 and 7,

$$E' = \frac{3\rho RT}{M_c} \quad (6)$$

$$v_e = \frac{E'_{atTg+50}}{3RT_{g+50}} \quad (7)$$

where E' is the storage modulus in the rubbery plateau (at T_{g+50}), R is gas constant and T_{g+50} is the temperature, in K, 50 K above T_g of transition from vitreous to elastic domain of material determined at the maximum of the $\tan \delta$ curve.¹²⁵

Swelling index. Swelling index was measured after Soxhlet extractions in refluxing THF for 24 h, wiping samples to remove residual THF before weighing. Values were calculated with

$$SI (\%) = \frac{m_s - m_i}{m_i} \times 100 \quad (8)$$

where m_s is the weight of the swollen sample and m_i is the initial weight of the sample.

Gel content. Gel content was measured by Soxhlet extractions in refluxing THF for 24 h. Afterwards, samples were dried in oven at 70 °C for 24 h. Values were calculated with

$$GC (\%) = \frac{m_f}{m_i} \times 100 \quad (9)$$

where m_f is the final weight of the dried sample and m_i is the initial weight of the sample.

Equilibrium water content. Three samples (around 30 mg) of each formulation were immersed separately into 10 mL of deionized water for 96 h. The equilibrium water content was calculated by

$$EWC = \frac{m_s - m_i}{m_i} \times 100 \quad (10)$$

where m_s is the weight of the swollen sample and m_i is the initial weight of the sample.

Differential Scanning Calorimetry (DSC). A differential scanning calorimeter (DSC-Q2000, TA Instruments Inc., USA) was used to analyse the thermal behaviour of the samples. A total of 6–8 mg of samples of Chapter 2 and 3 was scanned from –80 to 100 °C at a heating rate of 20 °C min⁻¹. Samples of Chapter 5 were scanned from –70 to 120 °C at the same heating rate. The glass transition temperatures (T_g) were taken from the inflection point in the heat capacity curve.

Thermogravimetric analyses (TGA). A thermogravimetric analyser (TGA-Q50, TA Instrument Inc., USA) was used to investigate the thermal stability of the samples. A total of 5–10 mg of samples was heated from 30 °C to 800 °C at a heating rate of 10 °C min⁻¹ under N₂ atmosphere (50 mL min⁻¹). The temperature at which the samples lost 5 % of their weight was reported as the onset of degradation of the sample.

Size Exclusion Chromatography (SEC). SEC was performed in THF at 35 °C (flow rate of 1 mL min⁻¹) using a Waters chromatograph equipped with three columns in series (Styragel HR2,

HR4 and HR6) with increasing pore sizes (from 100 to 10^6 Å). Toluene was used as a marker. Polystyrenes of different molar masses, ranging from 573 to 3,848,000 g mol⁻¹, were used for the calibration. The molar masses reported relate to polystyrene. For samples of Chapter 5, three columns in series (Styragel HR1, HR2 and HR4) were employed and polystyrenes of different molar masses, ranging from 106 to 436,000 g mol⁻¹, were used for the calibration, instead the described above.

Shaping of hot-melt adhesives. To prepare the hot-melt adhesive samples of Chapter 5, ~190 mg (rheology), ~90 mg (probe tack), ~250 mg (lap-shear) or ~500 mg (SAFT and shear resistance) of the polymer were shaped in an oven between two substrates (Teflon paper sheets were used to avoid that the adhesive sticks on the substrates) with spacers to control the thickness (0.6-0.8 mm). Circular shape of a 15 mm diameter (rheology), more than 5 mm diameter (tack probe), rectangular shape (12.5 x 25 mm²) and squares of 25 x 25 mm (625 mm²) (SAFT and shear resistance) were prepared. In the case of enhanced hot-melt adhesives by adding 15 wt% of D.E.R.TM 671, 1 kg weight was placed over the second substrate to accelerate the shaping.

Probe Tack Tests. Probe tack measurements were carried out using a TA.HDPlus Texture Analyzer (Texture Technologies, Hamilton, MA, USA) under controlled temperature in an oven. A 5-mm stainless steel cylinder probe was moved downward at a speed of 0.1 mm s⁻¹ until it was brought into contact to the adhesive surface. Immediately after the contact (10 s, with a compressive force of 1 N), the crosshead was allowed to move upward at a speed of 300 mm min⁻¹ until the probe was completely separated from the adhesive.

Lap-Shear Tests. The adhesion properties of the PHUs were evaluated at 298 K and 50% R.H. using an Instron 5569 and applying a parallel force to the adhesive bond with a

displacement rate of 1 mm min⁻¹ (Chapter 2, 3 and 4) and 50 mm min⁻¹ (Chapter 5). Corresponding substrates with dimensions of 100 mm x 25 mm x (thickness of each substrate) mm were used for single lap-shear measurements, and the gripping length on both sides of test specimens was 25 mm, according to DIN EN 1465. Width of aluminium was 20 mm instead of 25 mm. Tests were performed on 5 samples for each formulation to determine the average lap-shear strength. The lap-shear strength was calculated by the equation

$$\tau = \frac{F}{A} \quad (11)$$

where τ is shear stress or lap-shear strength (N mm⁻² or MPa), F is the maximum loading force to remove and break the adhesive (N), and A is the overlapped area of adhesive joint (in all test were 312.5 mm²). The nature of adhesion failure was also recorded based on visual inspection of the sample following the test.

Lap-shear test specimens were prepared as follows. The surfaces of the substrates were cleaned following the procedure described elsewhere³⁸ for stainless steel, PMMA and PE-HD. In the case of oak different surface treatments, described above, was carried out for evaluation on shear strength values. Al-2024 was cleaned as follows: substrates were degreased in an acetone/isopropanol mixture (1:1, V/V) for 5 minutes, followed by a basic treatment in NaOH ($C = 40 \text{ g l}^{-1}$) for 1 min and an acidic treatment in HCl ($C = 1\text{M}$). Between each step, the Al substrates were washed with water. The procedure was repeated 3 times, and then the substrate was wiped with tissue paper and dried at room temperature for 2 h. Adhesive formulations were prepared following the typical procedure of NIPU adhesive preparation for each Chapter described in the experimental part. The adhesive joints were prepared by spreading the viscous material (~50 mg, for samples of Chapter 2; ~35 mg of Chapter 3; ~80 mg of Chapter 4) onto

the cleaned substrates, placing the second substrate into contact and applying light pressure manually. The overlapping area was in all cases 312.5 mm². The adhesive joints were allowed to cure in an oven at 100 °C (Chapter 2 and 3) or at room temperature (Chapter 4) for 24 h. Specimens were prepared five times for each composition to determine the average values.

In Chapter 2, for the evaluation of the performance after water uptake, lap-shear test specimens were first prepared as described above and were then immersed in water for 96 h prior to measuring.

In Chapter 5, lap-shear substrates were cleaned as described above. Hot-melt adhesive samples were applied onto one of the pair of the cleaned substrates and were introduced into an oven (Memmert Vacuum Drying Oven VO200, Thermo Scientific Inc., USA) at the corresponding temperature for 5 min, allowing the softening of the polymer. Afterwards, both substrates were put together and placed again into the oven. Depending on the composition and temperature, samples were left different times to avoid spreading out of the materials from the overlapping area (312.5 mm², 12.5 mm x 25 mm). The adhesive joints were stored at ambient temperature for 24 h prior testing. Specimens were prepared five times for each composition to determine the average values.

For enhanced hot-melt adhesives, polymers were put together with the substrates and directly placed in the oven at 120 °C for 10 min with 1 kg over the glue line to improved wettability of the adhesives.

After finishing the lap-shear test, the thermo-reversible adhesion of the adhesives was tested, to prove the efficiency of the material for repeated use. Each pair of substrates were

stuck again and were placed into the oven at the same conditions of the first application. Following the same procedure, lap-shear measurements were repeated.

Subsequently, a second re-bonding was done. In this case, adhesives were heated and removed from the substrates manually. The test specimens were prepared and lap-shear measurements were carried out following the same procedure, employing the recycled material for shaping the adhesives.

Shear Adhesion Failure Temperature (SAFT) Tests. Shear tests were performed on stainless steel panels using SAFT equipment. Specimens were prepared following the procedure described for lap-shear tests. In this case, ~70 mg (Chapter 3) or ~200 mg (Chapter 4) of the oligomeric mixture was applied onto the panel in an overlapping area of 625 mm² (25 mm × 25 mm). The adhesive joints were cured under same conditions for lap-shear test. In Chapter 5 samples of this area and a thickness of 0.6-0.8 mm were applied onto the substrates as described in lap-shear specimen preparation. A mass of 1000 g was hung to each panel and they were placed into an oven. The temperature was increased from 30 °C to 217 °C at 1°C min⁻¹ rate. The temperature of failure was reported as temperature service of adhesives together with the nature of adhesive failure.

Shear Resistance tests. Shear resistance tests were performed following the same procedure and using the same equipment as the one described for SAFT experiments. Instead of applying a heating rate, temperature was set at 30 °C and the time of failure was recorded. The nature of adhesion failure was also recorded based on visual inspection of the sample following the test.

A-I.2. Materials

Poly(propylene glycol) diglycidyl ether ($M_n \sim 640$ g mol⁻¹) (PPGDGE), Resorcinol diglycidyl ether (RDGE), 1,4-Butanediol diglycidyl ether (BDGE), Trimethylolpropane triglycidyl ether (TMPTE), Tetrabutylammonium iodide (98%) (TBAI), Methanesulfonic acid (99.5%) (MSA), Acetic acid (99%) (HAc), Trimethylolpropane tris(3-mercaptopropionate) ($\geq 95.0\%$) (TMPMP), 1,12-Diaminododecane (98%) (1,12-DAD), *p*-Xylylenediamine (PXDA) (99%), hexamethylenediamine (HMDA) (98%) and 1,1,3,3-Tetramethylguanidine (99%) (TMG) were purchased from Merck KGaA, Germany. 1,3-Cyclohexanebis(methylamine) (*cis*- and *trans*-mixture) (CBMA) (98%) was purchased from TCI Europe N.V, Belgium. Dopamine hydrochloride (99%) (DOP), 1,8-Diazabicyclo[5.4.0]undec-7-ene ($\geq 98\%$) (DBU) and (3-Aminopropyl)trimethoxy silane (97%) (APTMS) were obtained from Alfa Aesar, Germany. (3-Aminopropyl)triethoxy silane (99%) (APTES) and *m*-Xylylenediamine (99%) (MXDA) were purchased from Acros Organics, Belgium. 1,3-Bis(2-hydroxyhexafluoroisopropyl)benzene (97%) (1,3-bis HFIB) was purchased from Fluorochem, United Kingdom. Dimer fatty diamine (trade name: Priamine™ 1074) was received from CRODA, Spain. Solid (trade name: D.E.R.™ 671) and viscous (trade name: EPIKOTE™ Resin 828) epoxy resins, both based on bisphenol A were kindly supply by Oribay Group Automotive S.L., Spain. Deuterated chloroform (CDCl₃) and dimethylsulfoxide (DMSO-d₆) were purchased from Merck KGaA, Germany. Deuterated methanol (MeOH-d₄) were purchased from Eurisotop, France. All reagents were used without further purification.

Al-2024 (thickness of 2 mm), Plexiglas XT 20070 [poly(methyl methacrylate) (PMMA), thickness of 3 mm], wood (oak, thickness of 5 mm), high density polyethylene (PE-HD, thickness of 3 mm) substrates were purchased from Rocholl GmbH, Germany. Stainless steel

AISI 316 (SS, thickness of 1.95 mm) and Polyamide (thickness of 2 mm) substrates were kindly supplied by Oribay Group Automotive S.L., Spain.

A-I.3. Experimental part

A-I.3.1. General

Typical procedure for the synthesis of cyclic carbonates

RGDE (20 g, 90 mmol), TBAI (1.66 g, 4.50 mmol) and 1,3-bis HFIB (1.84 g, 4.50 mmol) were charged to an 80 mL high-pressure autoclave. Subsequently, the cell was closed, the temperature was raised to 80 °C, the CO₂ pressure was adjusted to 100 bar and the reaction was allowed to proceed overnight. RdiCC was obtained quantitatively after depressurization of the reactor and no further purification was required.

Rest of the cyclic carbonates employed in this thesis were synthesized following the same procedure. PPGdiCC was synthesized at kilogram scale.

Titration of the cyclic carbonate by ¹H NMR

A specified amount of cyclic carbonate (PPGdiCC, RdiCC or BdiCC) (around 50 mg) and standard solution of DMSO-d₆ with toluene (around 30 mg of toluene dissolved in 5 mL of DMSO-d₆) were weighed into an NMR tube. Once the ¹H NMR acquisition was completed, characteristic peaks of cyclic carbonate a, b and b' (Figure A-II.5, Figure A-II.6) and CH₃ (2.32 ppm) of toluene were integrated. The integration of CH₃ of toluene was fixed to 300. Carbonate equivalent weight (CEW) of the carbonates was calculated according to eq 12. The CEW values

for each cyclic carbonate were obtained in triplicate determinations and are presented in Table A-II.1.

$$CEW = \frac{m_{C5}}{n_{function\ of\ carbonate}} = \frac{m_{C5} \times I_{CH3}}{(I_a + I_b + I_c) \times n_{toluene}} \quad (12)$$

where m_{C5} is the mass of cyclic carbonate introduced into the NMR tube, $n_{function\ of\ carbonate}$ is the molar amount of function carbonate in cyclic carbonate, I_a , I_b , I_c are the integrations of characteristics peaks a, b and c of carbonate, $n_{toluene}$ is the molar amount of toluene introduced in standard solution and I_{CH3} is the integration of peak CH_3 of toluene.

A-I.3.2. Chapter 2

Typical procedure for PHU prepolymer preparation

PPGdiCC (20.04 g, 0.06 equiv) and Priamine™ 1074 (13.23 g, 0.054 equiv) were added to a 100 mL jacketed glass reactor. The temperature was set at 80 °C for 24 hours with continuous mechanical stirring at 200 rpm. The reaction was cooled down and the polymer stored. For the incorporation of RdiCC, PHU prepolymers were prepared as follows: PPGdiCC (6.58 g, 0.02 equiv), RdiCC (1.87 g, 0.014 equiv) and Priamine™ 1074 (7.26 g, 0.027 equiv) were weighed in a 100 mL jacketed glass reactor. The conditions and time were set up as for the preparation of 100/o PPGdiCC/RdiCC ratio. For the rest of the compositions, quantities of PPGdiCC and RdiCC were adjusted according to the percentages shown in Table 2.2, entries 9-11. In all cases Priamine™ 1074 was kept at 0.9 equivalents regarding to 1 equivalent of carbonate.

Typical procedure for alkoxy silane prepolymer preparation

In a 250 mL three-neck round-bottom flask equipped with a half-moon Teflon helix stirrer 2 g of the PHU prepolymer was weighed. The flask was placed into an oil bath at 40 °C under a N₂ flow for 10 minutes. Then, APTES (2 molar equivalents with respect to the number of cyclic carbonates groups) was added and the mixture was allowed to react for 45 minutes. For the measurements using acid or base catalysts, the catalyst was added at the end of the reaction and stirred for 30 seconds to obtain a homogeneous mixture.

A-I.3.3. Chapter 3

Typical procedure for PHU adhesive preparation

PHU adhesive preparation was followed as described elsewhere.³⁸ DOP (14.6 mg, 0.08 mmol) was dissolved in MeOH (0.3 mL), added to TMPTC (0.700 g, 3.8 10⁻³ equiv) and heated at 60 °C for 5 min. The reaction mixture was stirred at room temperature for 20 minutes and then the solvent was removed under vacuum. Subsequently, a stoichiometric amount (compared to cyclic carbonates) of MXDA (309 μL, 4.7 10⁻³ equiv) and APTMS (13.45 μL, 0.08 mmol) were added into the reaction mixture that was then stirred for 1.5 min at 60 °C and 2 min at room temperature to obtain a homogeneous mixture. Then, the viscous oligomeric solution (~35 mg for lap-shear joints, ~70 mg for SAFT joints) was applied onto the substrates for the preparation of lap-shear or SAFT joints.

For the incorporation of PPGdiCC, NIPU adhesives were prepared as follows: DOP (19.6 mg, 0.10 mmol) was dissolved in MeOH (0.3 mL) and added to a mixture of TMPTC (0.700 g, 3.8 10⁻³ equiv) and PPGdiCC (0.503 g, 1.5 10⁻³ equiv) following the steps described above. After

solvent removal, MXDA (396 μL , $6 \cdot 10^{-3}$ equiv) and APTMS (18.06 μL , 0.10 mmol) were added into the reaction mixture that was then stirred for 20 min at 60 °C and 2 min at room temperature to obtain a homogeneous mixture. For the rest of the compositions, quantities of TMPTC and PPGdiCC were adjusted according to the percentages shown in Table 3.3. In all cases, amine equivalents were kept at stoichiometry values regarding to cyclic carbonate ones.

A-I.3.4. Chapter 4

Typical procedure for amino-terminated PHU oligomer preparation

PPGdiCC (5.3032 g, $15.91 \cdot 10^{-3}$ equiv), RdiCC (2.0212 g, $10.60 \cdot 10^{-3}$ equiv) and 1,12-DAD (5.3119 g, $53.02 \cdot 10^{-3}$ equiv) were added to a 100 mL round-bottom flask equipped with a half-moon Teflon helix stirrer and put into an oil bath at 80 °C. Mechanical stirring at 100 rpm was kept for 5 h. Then, the stir was stopped, the reaction cooled down and amino-terminated PHU oligomers were obtained and used for the further preparation of H-NIPU materials without purification.

Eq 13 was employed for the calculation of the amine mass. Molar ratio between PPGdiCC/RdiCC was fixed to 1.5 and molar ratio of amine regarding cyclic carbonates was fixed to 2 ($r = 2$). The number of active hydrogen of amine was fixed at 1 for one amine function reacting with one cyclic carbonate. The active hydrogen equivalent weight (AHEW) was calculated from eq 15.

$$m_{\text{amine}} = rAHEW_{\text{amine}} \left(\frac{m_{\text{PPGdiCC}}}{CEW_{\text{PPGdiCC}}} + \frac{m_{\text{RdiCC}}}{CEW_{\text{RdiCC}}} \right) \quad (13)$$

Titration of the A-PHUs by ¹H NMR

The Amine Equivalent Weight (AEW) is the amount of resin (in grams) containing one gram-equivalent of amine functions. It was determined using the procedure used for the determination of the CEW. The characteristic signal at 2.65 ppm of the methylene group next to the free amine was chosen (). The AEW is calculated using eq 14.

$$AEW = \frac{m_{A-PHU}}{n_{function\ of\ amine}} = \frac{m_{A-PHU} \times \frac{I_{CH_3}}{3}}{\frac{I_{CH_2}}{2} \times n_{toluene}} \quad (14)$$

where m_{A-PHU} is the mass of A-PHU weighed into the NMR tube, $n_{toluene}$ is the molar amount introduced in the standard solution, I_{CH_2} is the integral of the two methylene protons of the A-PHU next to the free amine, and I_{CH_3} is the integral corresponding to the methyl group of toluene.

The amine hydrogen equivalent weight (AHEW) for amines was calculated from eq 15, taking into account the reactive hydrogens for each type of reaction. For example, in the case of the polyaddition with cyclic carbonates amines present one active hydrogen, while for the preparation of hybrid materials through reaction with epoxy resins, amine has two active hydrogens.

$$AHEW = \frac{AEW}{number\ of\ active\ hydrogen} \quad (15)$$

Typical procedure for the synthesis of hybrid materials

The synthesis of 70/30 composition is described as a typical procedure for the preparation of hybrid materials. A-PHU oligomer (1.0706 g, $4.12 \cdot 10^{-3}$ equiv), TMPTMP (0.2468 g, $1.76 \cdot 10^{-3}$

equiv) and EPIKOTE™ 828 (1.1000 g, $5.88 \cdot 10^{-3}$ equiv) were subsequently weighed in a 26-mL vial. The reactants were stirred for 2 minutes at 50 °C followed by 1 minute at room temperature to obtain an homogeneous mixture. Then, the viscous oligomeric solution was transferred into a plastic 6-mL syringe for applying onto the substrates for the preparation of lap-shear (~80 mg) or SAFT (~200 mg) joints.

For the preparation of 0/100 composition, EPIKOTE™ 828 (1.5535, $8.32 \cdot 10^{-3}$ equiv) was first mixed with TMG (4.56 μ L, $3.64 \cdot 10^{-5}$ equiv, 0.4375 mol%) and then, TMPTMP (1.1631 g, $8.32 \cdot 10^{-3}$ equiv) was added. Mixing was done as previously explained. The homogeneous mixture was applied onto substrates and second substrates were placed after 20 minutes, allowing the adhesive to get enough viscosity to avoid spreading out from the bonding line. The addition of TMG was necessary as epoxy and thiol compound do not react without the presence of a catalyst (Figure A-II.1).

A-I.3.5. Chapter 5

Typical procedure for PHU homopolymer preparation

Homopolymerization of 100/0-MXDA was carried out adding PPGdiCC (2.0196 g, $6.1 \cdot 10^{-3}$ equiv) and MXDA (0.5160 g, $7.6 \cdot 10^{-3}$ equiv) to a 25 mL round bottom flask. The mixture was placed into an oil bath at 80 °C and was left for 24 h under magnetic stirring. Afterwards, the reaction was cooled down and a viscous polymer was obtained.

For the homopolymerization of 0/100-MXDA, RdiCC (1.1554 g, $6.1 \cdot 10^{-3}$ equiv) and MXDA (0.5160 g, $7.6 \cdot 10^{-3}$ equiv) were added to a 25 mL round bottom flask. The mixture was placed into an oil bath at 80 °C and was left for 24 h under magnetic stirring. After cooling down the

reaction a yellowish hard homopolymer was obtained. Polymers were used without further purification.

Typical procedure for PHU copolymer preparation

PPGdiCC (11.1458 g, $33.5 \cdot 10^{-3}$ equiv) and RdiCC (4.2520 g, $22.3 \cdot 10^{-3}$ equiv) were added to a 100 mL jacketed glass reactor. The mixture was allowed to reach 80 °C before adding MXDA (4.7472 g, $69.7 \cdot 10^{-3}$ equiv). The reaction was left for 24 hours under continuous mechanical stirring at 200 rpm and without using any catalyst. Afterwards, the reaction was cooled down and the polymer stored. Polymers were used without further purification.

Eq 13 was employed for the calculation of the amine mass. Molar ratio between PPGdiCC/RdiCC was fixed to according to the different compositions (Table 5.1) and molar ratio of amine regarding cyclic carbonates was fixed to 1.25 ($r = 1.25$). The number of active hydrogen of amine was fixed at 1 for one amine function reacting with one cyclic carbonate. The active hydrogen equivalent weight (AHEW) was calculated from eq 15.

Typical procedure for enhanced hot-melt adhesive preparation

Around 4 g of 50/50-MXDA or 50/50-PXDA composition were heated up to 90 °C and mixed with D.E.R.TM 671 (0.6 g, 15 wt%) for 20 minutes. Afterwards, sample was kept in an oven at 55 °C for 3 days to assure complete reaction of the amine with epoxy groups.

Appendix II.

Supporting Information



A-II.1. General

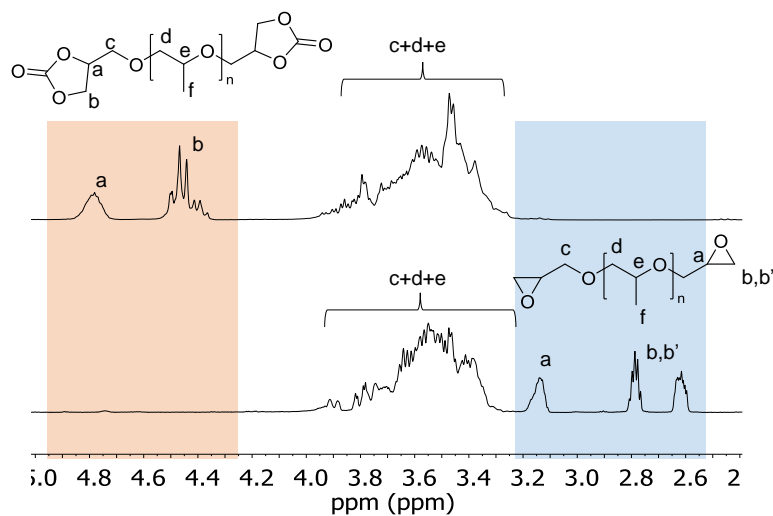


Figure A-II.1. ¹H NMR comparison of the diepoxide (below) and dicarbonate (above) based on poly(propylene glycol). Marked in blue, disappearance of the epoxy signals. Marked in salmon, appearance of cyclic carbonate signals.

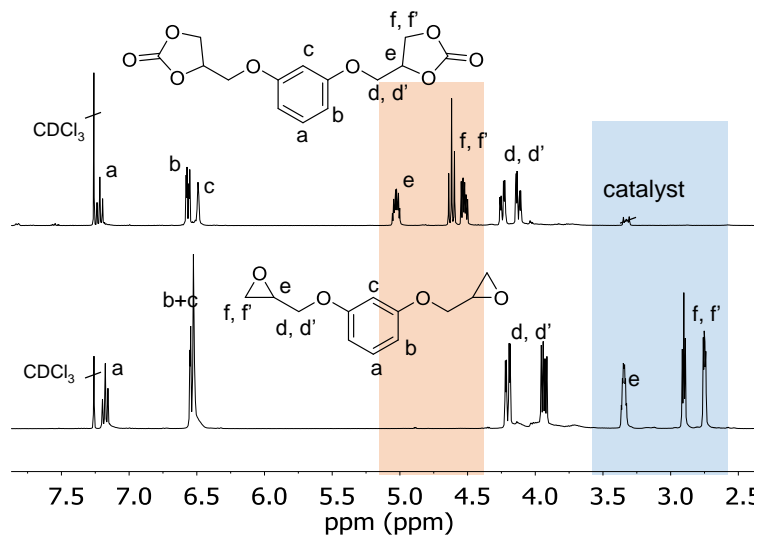


Figure A-II.2. ¹H NMR comparison of the epoxide (below) and dicarbonate (above) based on resorcinol. Marked in blue, disappearance of epoxy signals. Marked in salmon, appearance of cyclic carbonate signals.

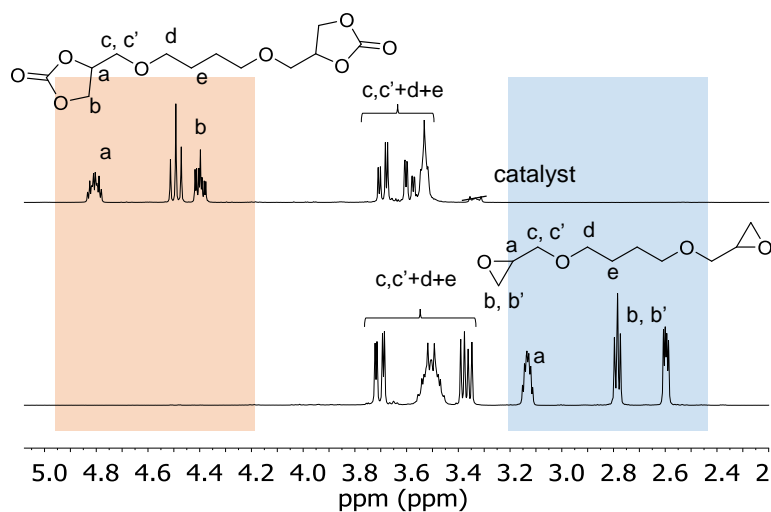


Figure A-II.3. ^1H NMR comparison of the epoxide (below) and dicarbonate (above) based on 1,4-Butanediol. Marked in blue, disappearance of epoxy signals. Marked in salmon, appearance of cyclic carbonate signals.

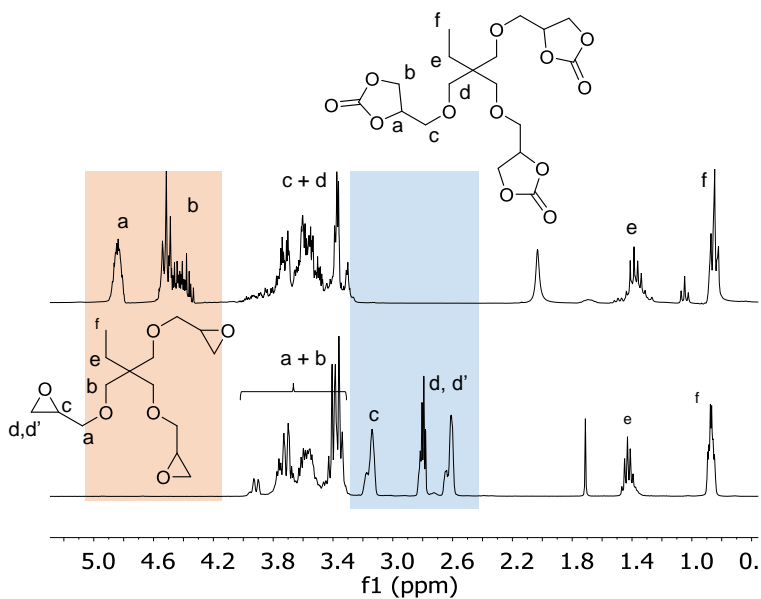


Figure A-II.4. ^1H NMR comparison of the epoxide (below) and dicarbonate (above) based on trimethylolpropane. Marked in blue, disappearance of epoxy signals. Marked in salmon, appearance of cyclic carbonate signals.

Table A-II.1. Carbonate equivalent weight (CEW), amine equivalent weight (AEW), epoxy equivalent weight (EEW) and thiol equivalent weight (TEW) values.

Reactant	CEW (g equiv ⁻¹)	AEW (g equiv ⁻¹)	EEW (g equiv ⁻¹)	TEW (g equiv ⁻¹)
PPGdiCC	190 ± 5	-	-	-
RdiCC	190 ± 5	-	-	-
BdiCC	167 ± 4	-	-	-
TMPTC	182 ± 11	-	-	-
Priamine 1074 TM	-	270 ^a	-	-
DOP	-	189.64	-	-
APTMS	-	179.29	-	-
MXDA	-	68.10	-	-
PXDA	-	68.10	-	-
CBMA	-	71.12	-	-
HMDA	-	58.10	-	-
1,12-DAD	-	100.18	-	-
A-PHU	-	520 ± 5	-	-
EPIKOTE TM 828	-	-	184-190 ^b	-
D.E.R. TM 671	-	-	475-550 ^c	-
TMPTMP	-	-	-	132.85

^aValue provide by Croda; ^bvalue provide by Hexion; ^cvalue provide by Dow Chemical Company. ^{b,c}The media between values was employed for calculations.

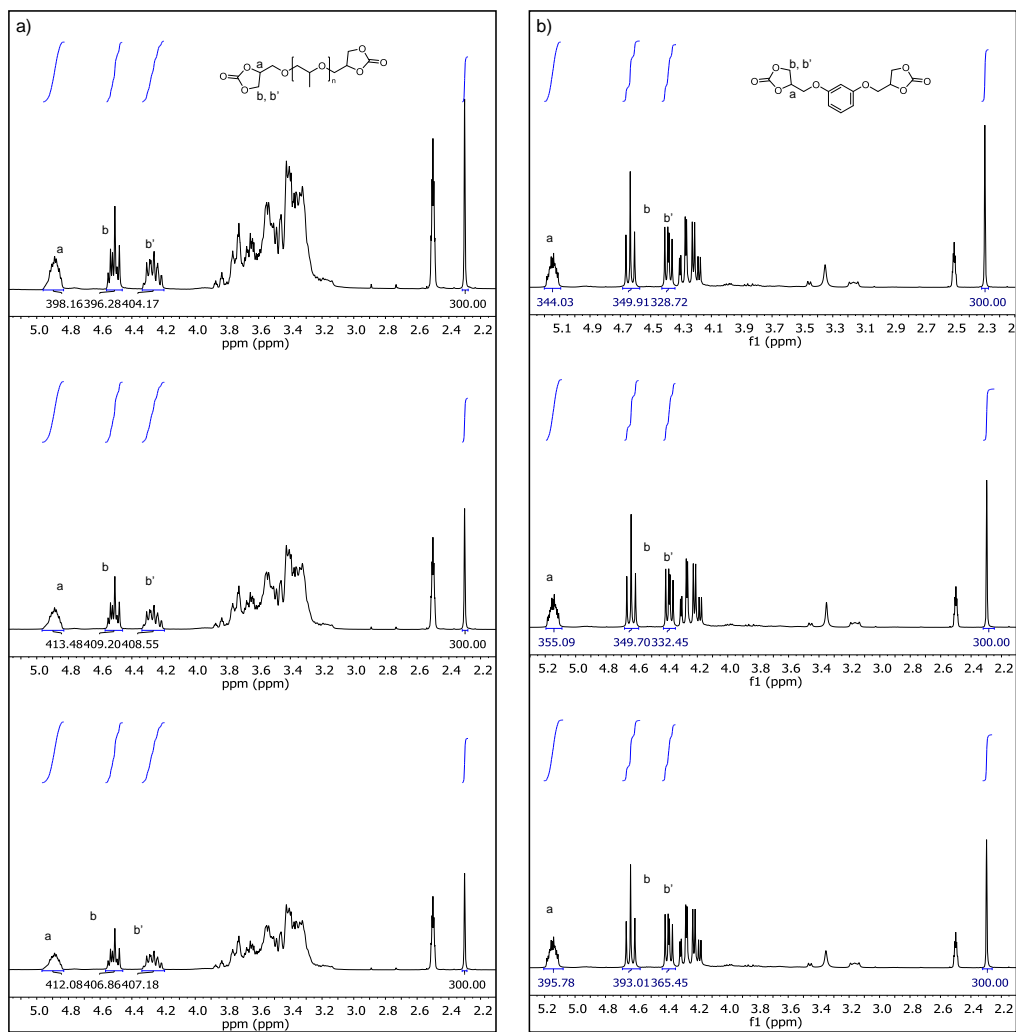


Figure A-II.5. ^1H NMR spectra for triplicate of cyclic carbonate titration of a) PPGdiCC and b) RdiCC. The integration fixed to 300 correspond to the CH_3 signal of toluene added to the DMSO- d_6 standard solution.

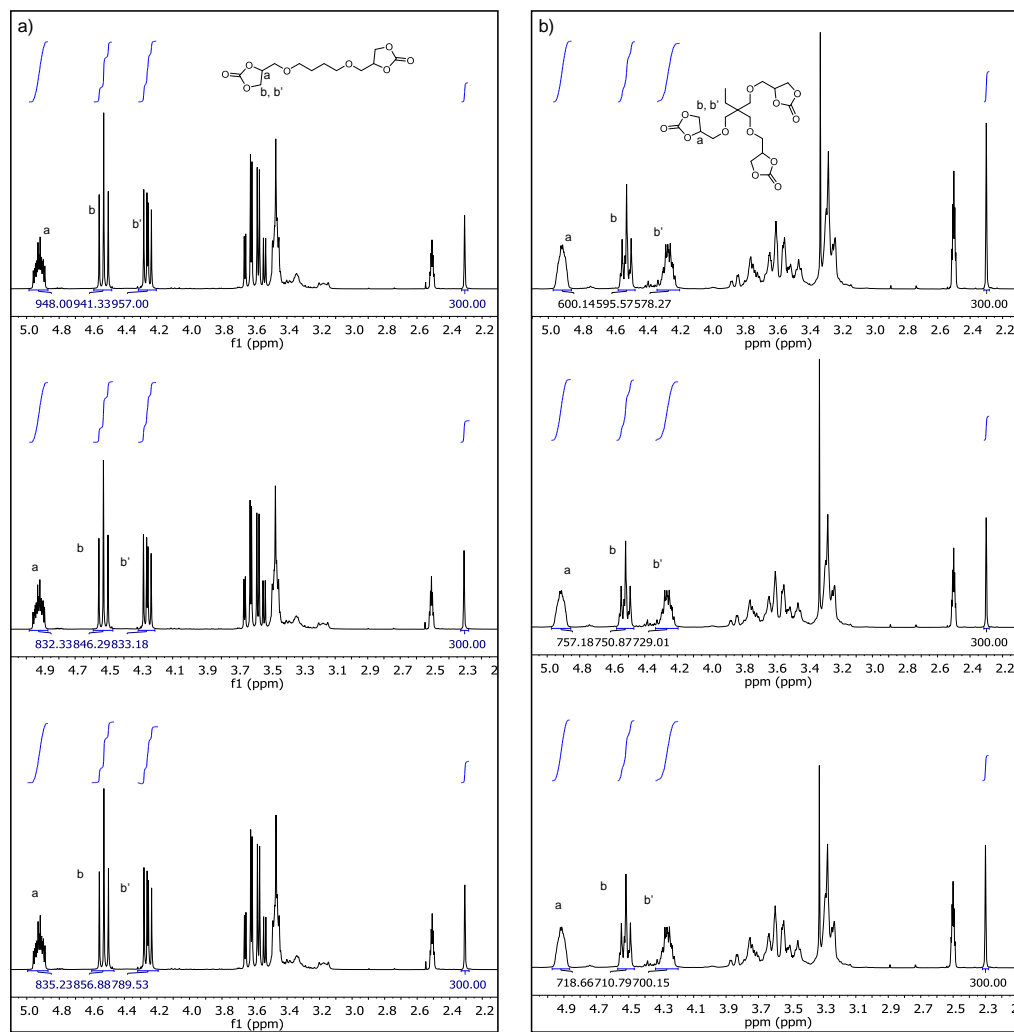


Figure A-II.6. ^1H NMR spectra for triplicate of cyclic carbonate titration of a) BdiCC and b) TMPTC. The integration fixed to 300 correspond to the CH₃ signal of toluene added to the DMSO-d₆ standard solution.

A-II.2. Chapter 2

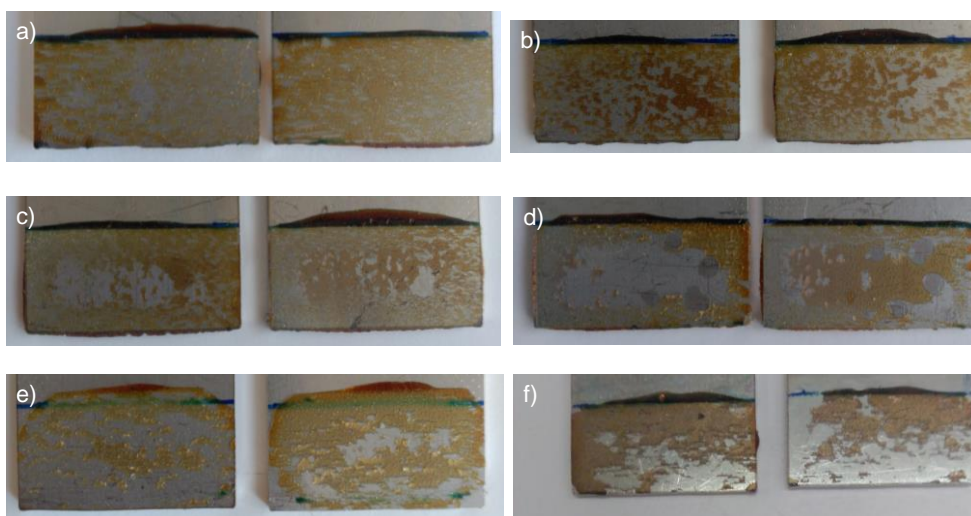


Figure A-II.7. Photos of the representative failure nature of the monocomponent adhesive compositions based on a) 100/0, b) 95/5, c) 90/10, d) 80/20, e) 60/40 and 60/40* PPGdiCC/RdiCC molar ratio. *Lap-shear was performed after 4 days immersed in water.

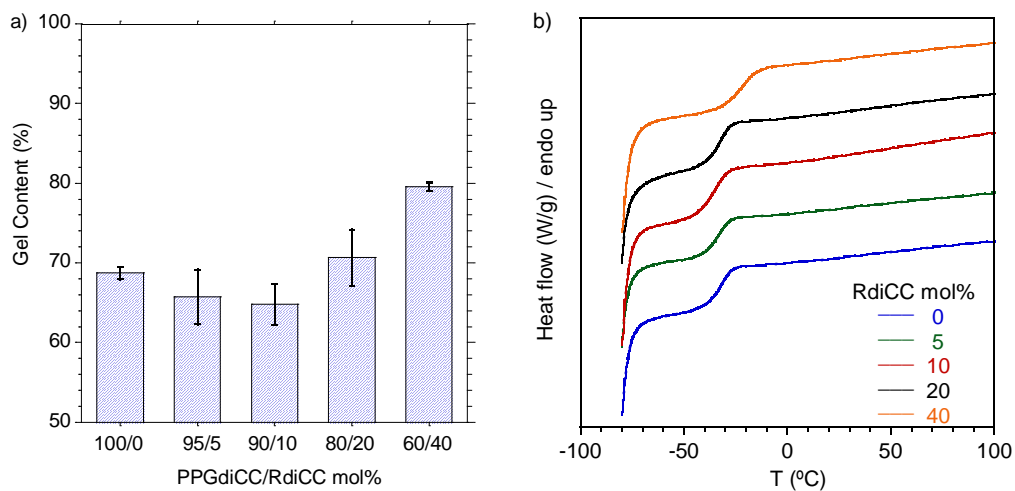


Figure A-II.8. a) Gel content and b) DSC temperature sweeps for the different ratios of PPGdiCC/RdiCC explored.

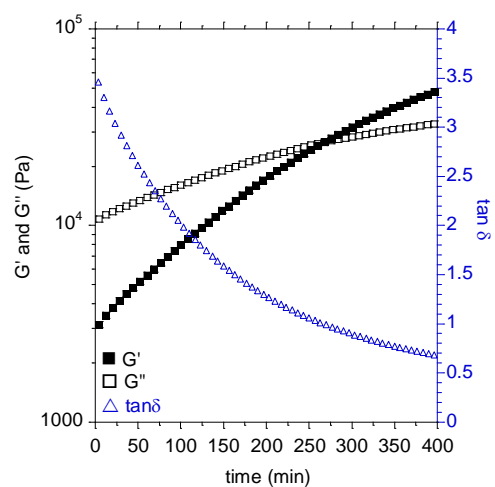


Figure A-II.9. G', G'' and tan δ values for rheological measurements employing 2.5 wt. % of acetic acid for curing at 25 °C 60/40 PPGdiCC/RdiCC-based alkoxy silane-terminated PHU adhesive.

A-II.3. Chapter 3

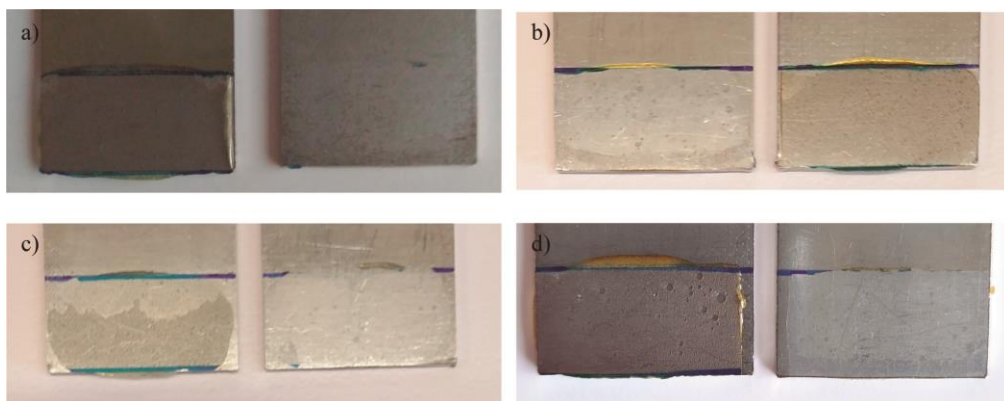


Figure A-II.10. Photos of the representative failure nature of the MXDA-based compositions. a) neat; b) +3.9 mol% DOP; c) +3.9 mol% APTMS and d) +3.9 mol% DOP and APTMS formulation.

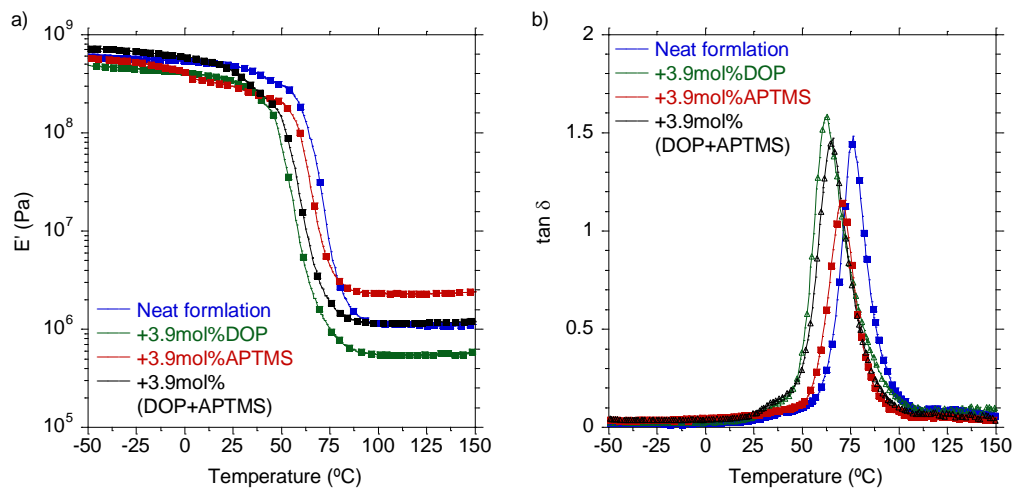


Figure A-II.11. a) Storage moduli and b) $\tan \delta$ from -50 to 150 $^{\circ}\text{C}$ obtained from DMTA measurements of the neat and doped (+3.9 mol% of DOP, APTMS and DOP&APTMS) formulations.

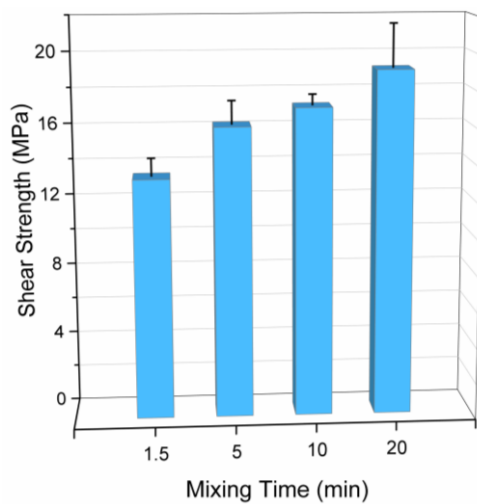


Figure A-II.12. Mixing time influence on the lap-shear strength values of 70/30 TMPTC/PPGdiCC molar ratio composition based on aromatic diamine.

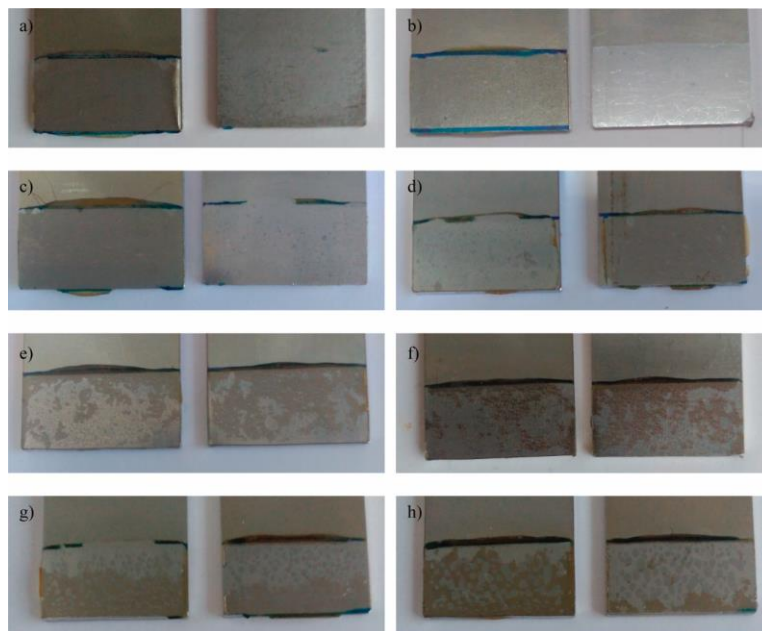


Figure A-II.13. Photos of the representative failure nature of the sweep soft/hard monomer (TMPTC/PPGdiCC) molar ratio based on MXDA. a) 100/0; b) 90/10; c) 80/20; d) 70/30; e) 60/40; f) 50/50; g) 40/60 and h) 30/70 molar ratio composition.

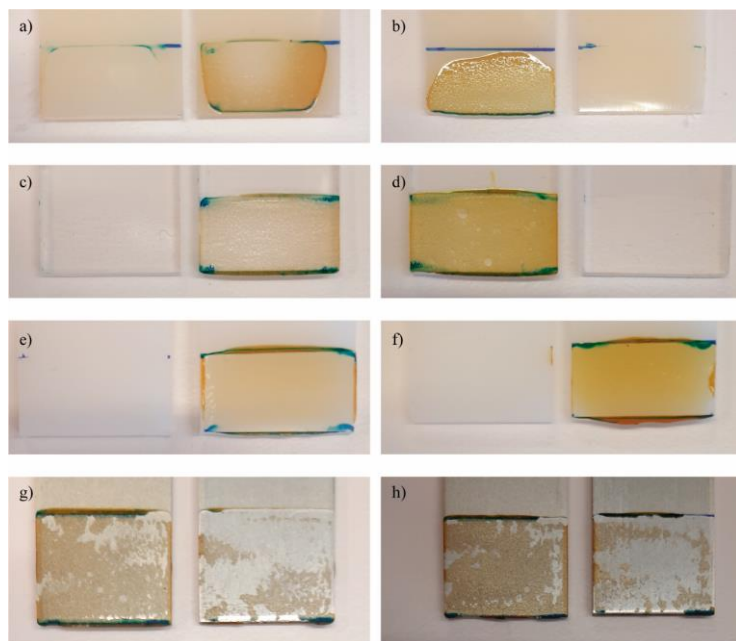


Figure A-II.14. Photos of the representative failure nature on dissimilar substrates of the neat and doped (+3.9 mol% DOP and APTMS) 70/30 molar ratio aromatic diamine-based compositions. a) neat composition and b) doped composition on polyamide; c) neat composition and d) doped composition on PMMA; e) neat composition and f) doped composition on PE-HD and g) neat composition and h) doped composition on aluminium.



Figure A-II.15. Photos of the representative failure nature on oak wood substrates of the neat and doped (+3.9 mol% DOP and APTMS) 70/30 molar ratio aromatic diamine-based compositions depending on the surface treatment applied. a) Surface treatment A; b) Surface treatment B; c) Surface treatment C and d) Surface treatment C' for substrates glued with the neat composition; e) substrate glued with doped composition after surface treatment C'; substrate failure out from gluing line: f) neat composition, surface treatment C'; and g) dope formulation, surface treatment C'. Surface treatment: **A** wood was sanded with sandpaper and wiped with a paper wet in acetone; **B** surface treatment A + (5' in a mixture 1/1 acetone/isopropanol + 2' in water) x3 as reported elsewhere;³⁸ **C** surface treatment B + 1 night at 70 °C; **C'** surface treatment C + more quantity of adhesive (~80 mg).

Table A-II.2. Lap-shear strength values for 70/30 neat and doped with 3.9 mol% of dopamine and APTMS compositions on different substrates.

Entry	Substrate	Composition 70/30 TMPTC/PPGdiCC	Lap-shear strength (MPa)	Adhesive Failure
1	Oak ^a	Neat	12.8 ± 2.4	Subst. F.
2		Doped	11.9 ± 1.2	Subst. F.
3	Polyamide	Neat	2.5 ± 0.6	Adh. F.
4		Doped	2.8 ± 0.7	Adh. F.
5	PMMA	Neat	1.7 ± 0.2	Adh. F.
6		Doped	1.8 ± 0.2	Adh. F.
7	PE-HD	Neat	0.8 ± 0.2	Adh. F.
8		Doped	0.7 ± 0.1	Adh. F.
9	Al	Neat	18.9 ± 1.5	Coadh. F.
10		Doped	20.9 ± 0.9	Coadh. F.

^aBest conditions of surface preparation. Subst. F.: substrate failure; Adh. F.: adhesive failure; Coadh. F.: coadhesive failure.

Table A-II.3. Shear strength values for 70/30 neat compositions for bonding oak wood as function of the surface treatment.

Entry	Surface treatment	Lap-shear strength (MPa)
1	<i>A</i>	7.1 ± 0.6
2	<i>B</i>	5.0 ± 1.5
3	<i>C</i>	10.0 ± 2.7
4	<i>C'</i>	12.8 ± 2.4

Surfaces treatment: *A* wood was sanded with sandpaper and wiped with a paper wet in acetone; *B* surface treatment *A* + (5' in a mixture 1/1 acetone/isopropanol + 2' in water) x3 as reported elsewhere³⁸; *C* surface treatment *B* + 1 night at 70 °C; *C'* surface treatment *C* + more quantity of adhesive (~80 mg)

A-II.4. Chapter 4

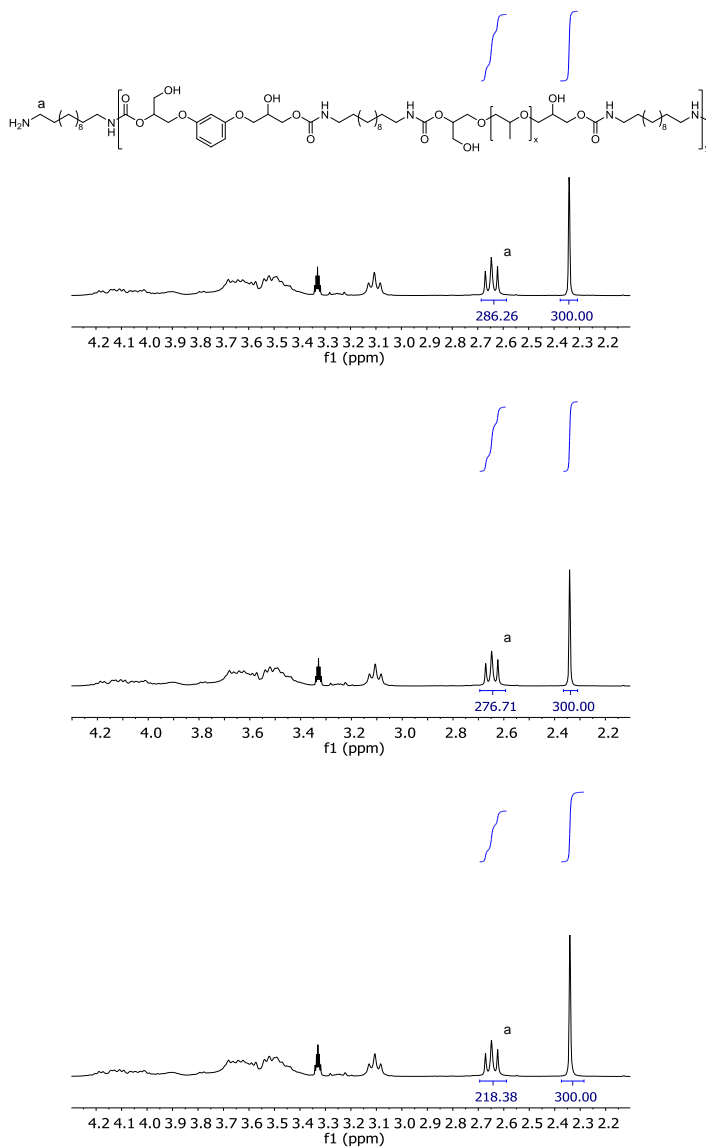


Figure A-II.16. ^1H NMR spectra for triplicate of amine titration of A-PHU. The integration fixed to 300 correspond to the CH_3 signal of toluene added to the DMSO- d_6 standard solution. Rest of the signal of the spectra are assigned in Figure 4.4.

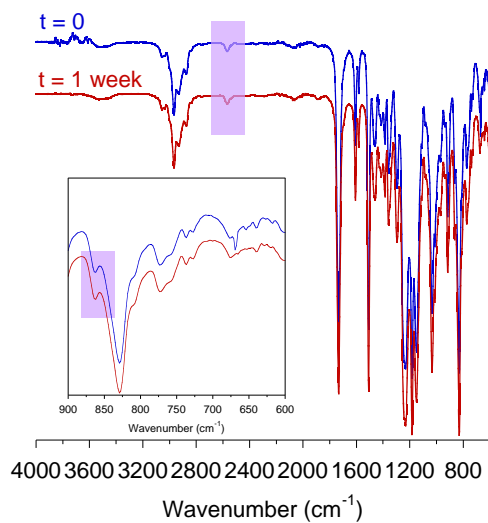
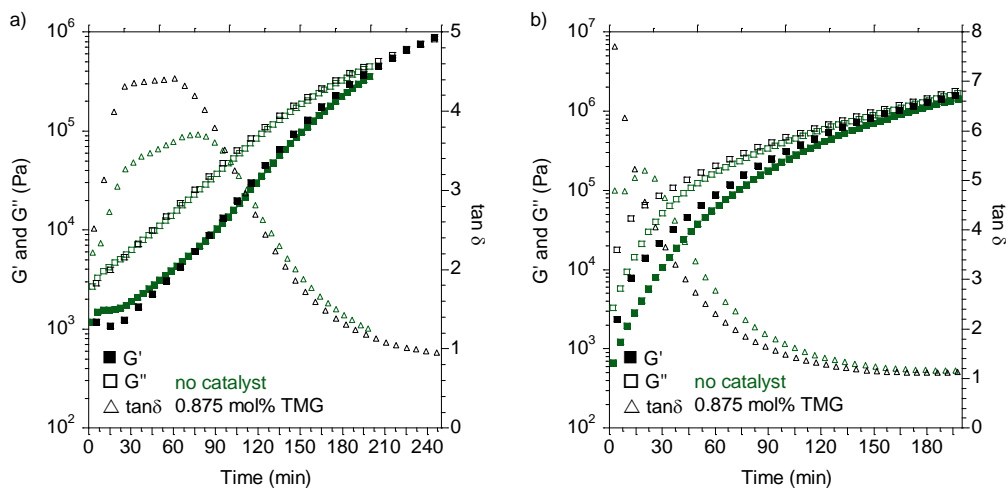


Figure A-II.17. FTIR-ATR spectra of the mixture TMPTMP and EPIKOTE™ 828 at $t = 0$ and after one week. Remaining vibration bands at 2569 cm^{-1} (S-H) and at 862 cm^{-1} (as C-O-C, epoxy), highlighted with purple, showed the stability of the mixture. In the box is zoomed between 900 and 600 cm^{-1} of the spectra.



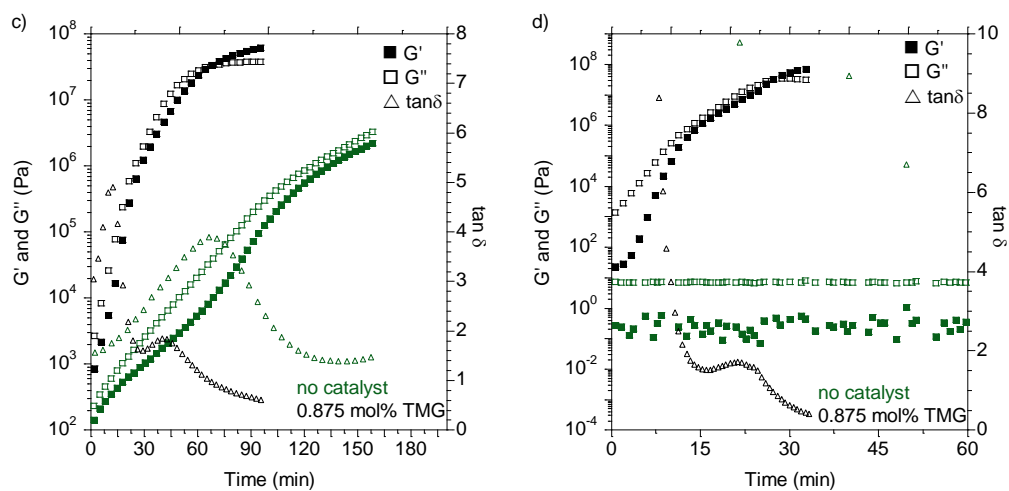


Figure A-II.18. Evolution of G' , G'' and $\tan \delta$ values over time obtained from rheological measurements carried out at 25 °C without catalyst (green spots) and in the presence of 0.875 mol% of TMG (black spots) of a) 100/0, b) 70/30, c) 30/70 and d) 0/100 A-PHU/TMPTMP molar ratio compositions mixed with 1 equiv of EPIKOTE™ 828 regarding total A-PHU/TMPTMP equiv.



Figure A-II.19. Adhesive failure from the PMMA substrate of a) 70/30, b) 50/50 and c) 30/70 A-PHU/TMPTMP equivalent ratio formulations tested after 24 h at room temperature and d) 70/30, e) 50/50 and f) 30/70 equivalent ratio compositions tested after 1 week at the same conditions.

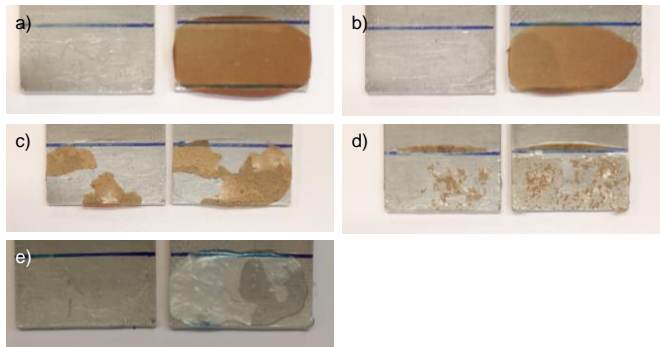


Figure A-II.20. Photos of the representative failure nature of the PHU-epoxy hybrid compositions cured at room temperature for 24 h. a) 100/0, b) 70/30, c) 50/50, d) 30/70 and e) 0/100 A-PHU/TMPTMP equivalent ratios.

A-II.5. Chapter 5

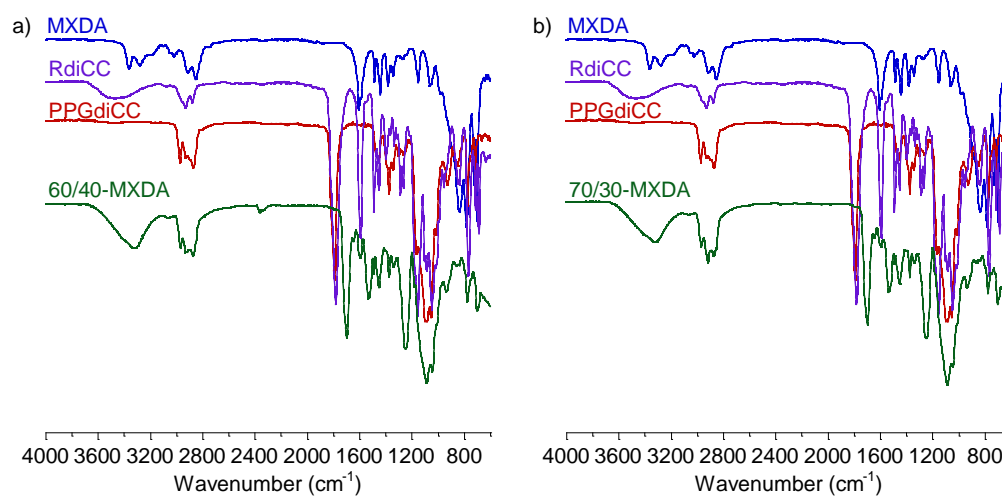


Figure A-II.21. FTIR spectra of a) 60/40-MXDA and b) 70/30-MXDA compositions compared to MXDA, RdiCC and PPGdiCC spectra.

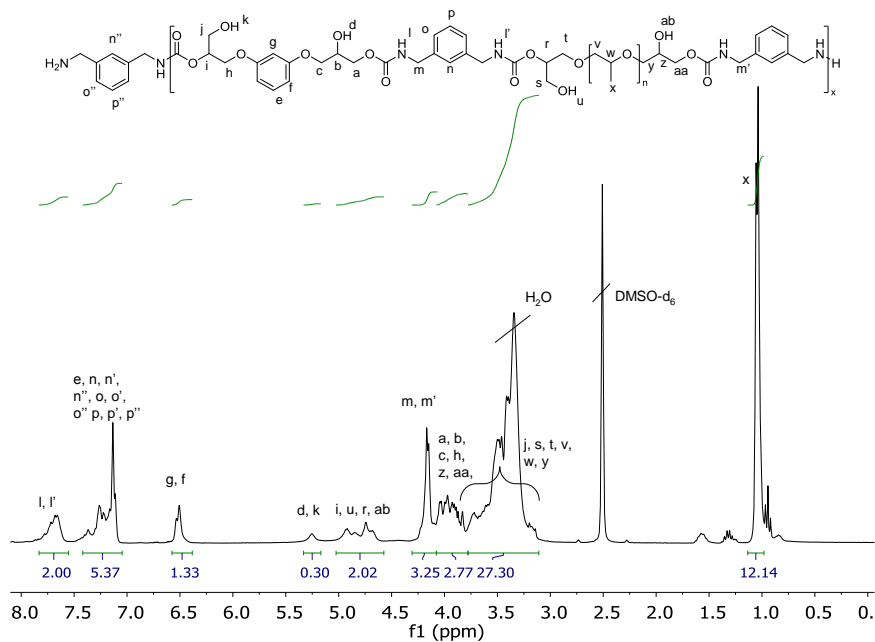


Figure A-II.22. ¹H NMR spectrum of 60/40-MXDA.

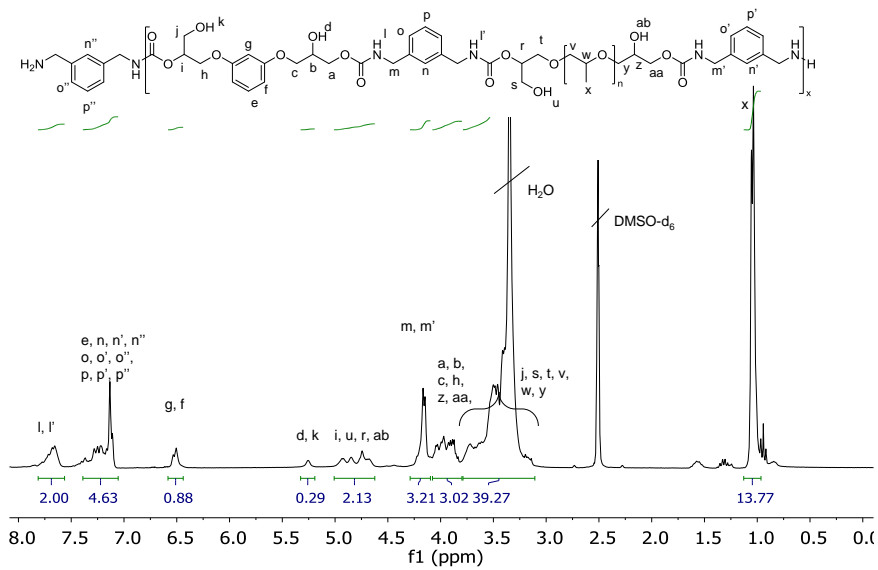


Figure A-II.23. ¹H NMR spectrum of 70/30-MXDA.

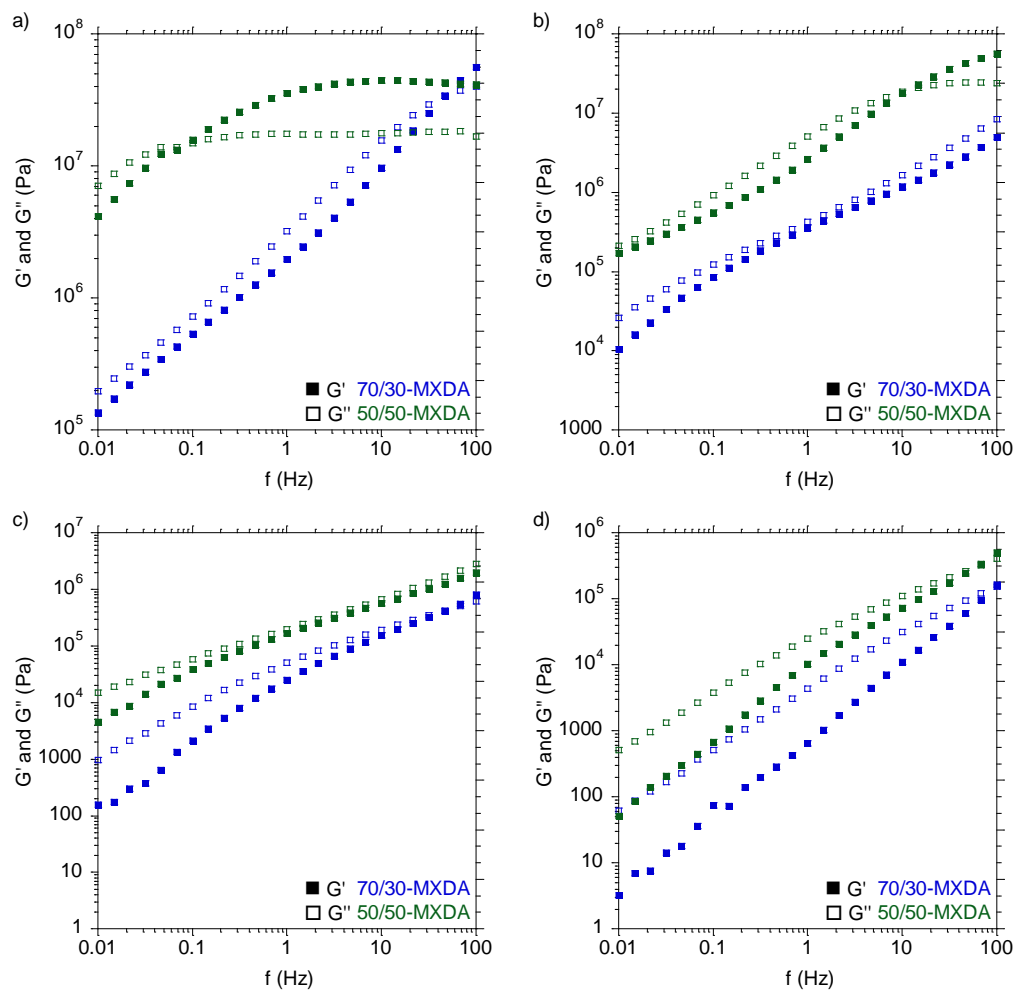


Figure A-II.24. G' and G'' values between 0.01 and 100 Hz at a) 10 °C, b) 25 °C, c) 50 °C and d) 80 °C of 70/30-MXDA (blue) and 50/50-MXDA (green).

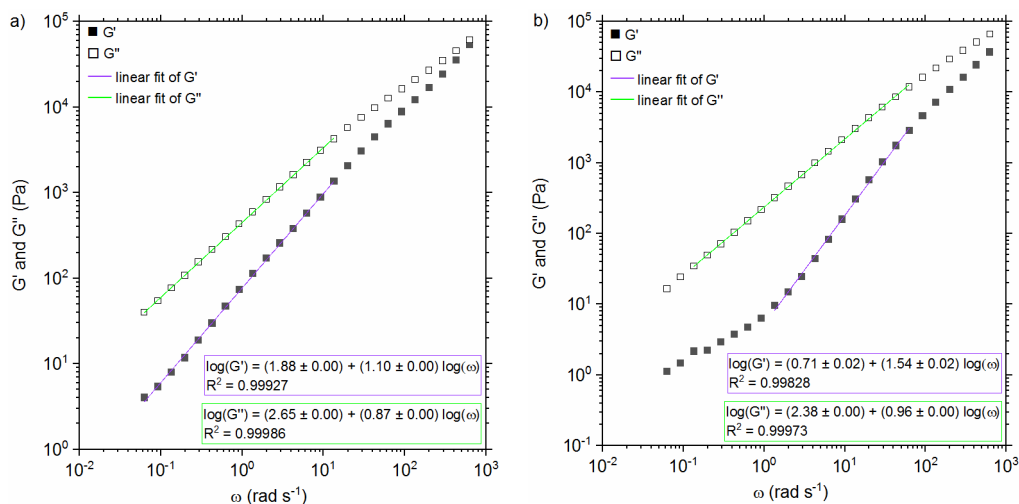


Figure A-II.25. G' and G'' values as a function of ω at 100 °C of a) 50/50-MXDA and b) 70/30-MXDA with the corresponding linear fit. Equations of the linear fit are presented in the boxes and were calculated with analysis tools of Origin 2020b.

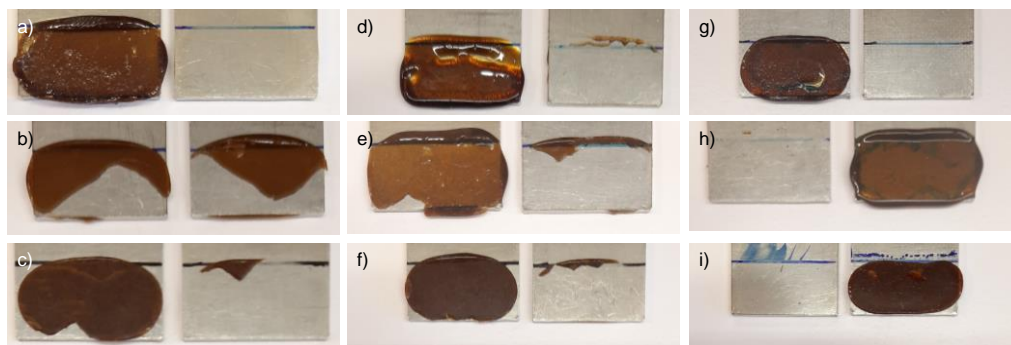


Figure A-II.26. Photos of the representative adhesion failure after lap-shear tests of a) 70/30-MXDA, b) 60/40-MXDA and c) 50/50-MXDA applied at 80 °C; d) 70/30-MXDA, e) 60/40-MXDA and f) 50/50-MXDA after re-bonding at 80 °C; g) 70/30-MXDA, h) 60/40-MXDA and i) 50/50-MXDA and after a second re-bonding at 80 °C.

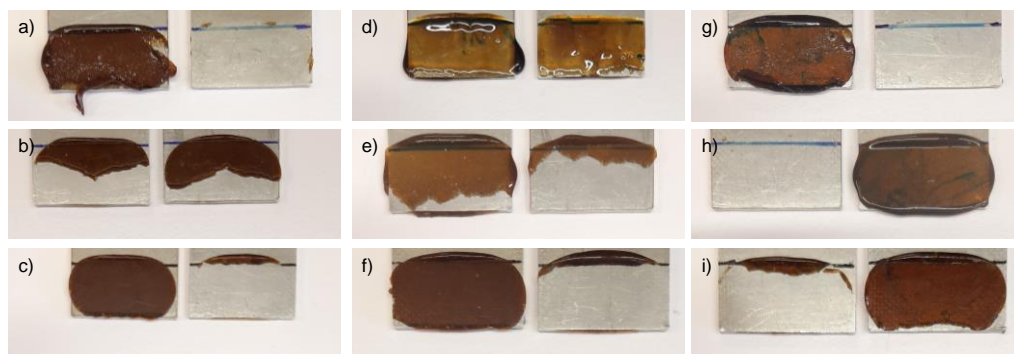


Figure A-II.27. Photos of the representative adhesion failure after lap-shear tests of a) 70/30-MXDA, b) 60/40-MXDA and c) 50/50-MXDA applied at 100 °C; d) 70/30-MXDA, e) 60/40-MXDA and f) 50/50-MXDA after re-bonding at 100 °C; g) 70/30-MXDA, h) 60/40-MXDA and i) 50/50-MXDA after a second re-bonding at 100 °C.

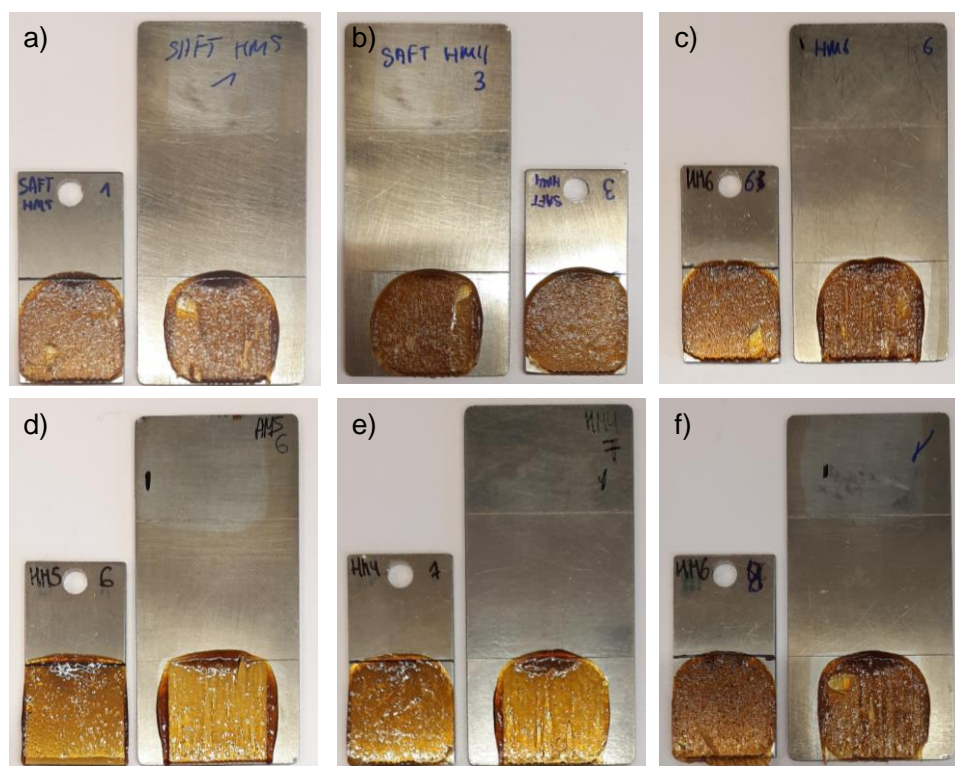


Figure A-II.28. Photos of the representative adhesion failure of a) 70/30-MXDA, b) 60/40-MXDA and c) 50/50-MXDA after SAFT tests and d) 70/30-MXDA, e) 60/40-MXDA and f) 50/50-MXDA after shear resistance measurements.

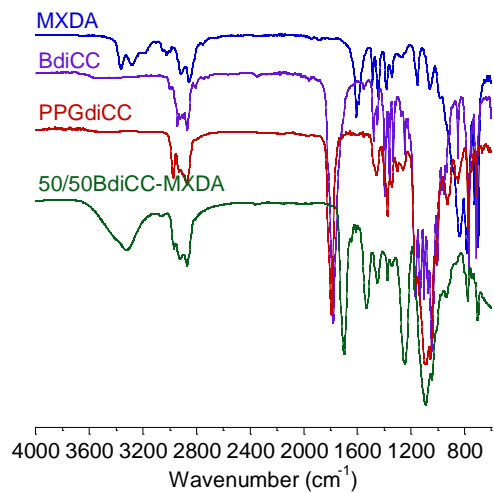


Figure A-II.29. FTIR-ATR spectrum of 50/50BdiCC compared to the initial monomer spectra of MXDA, BdiCC and PPGdiCC.

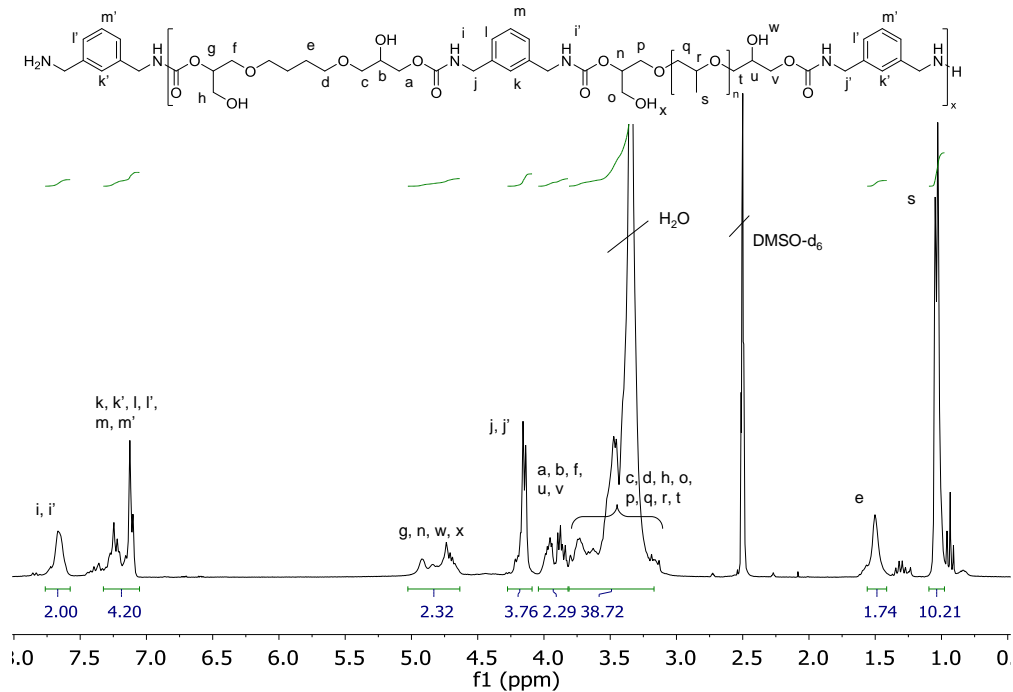


Figure A-II.30. ^1H NMR spectrum of 50/50BdiCC-MXDA composition.

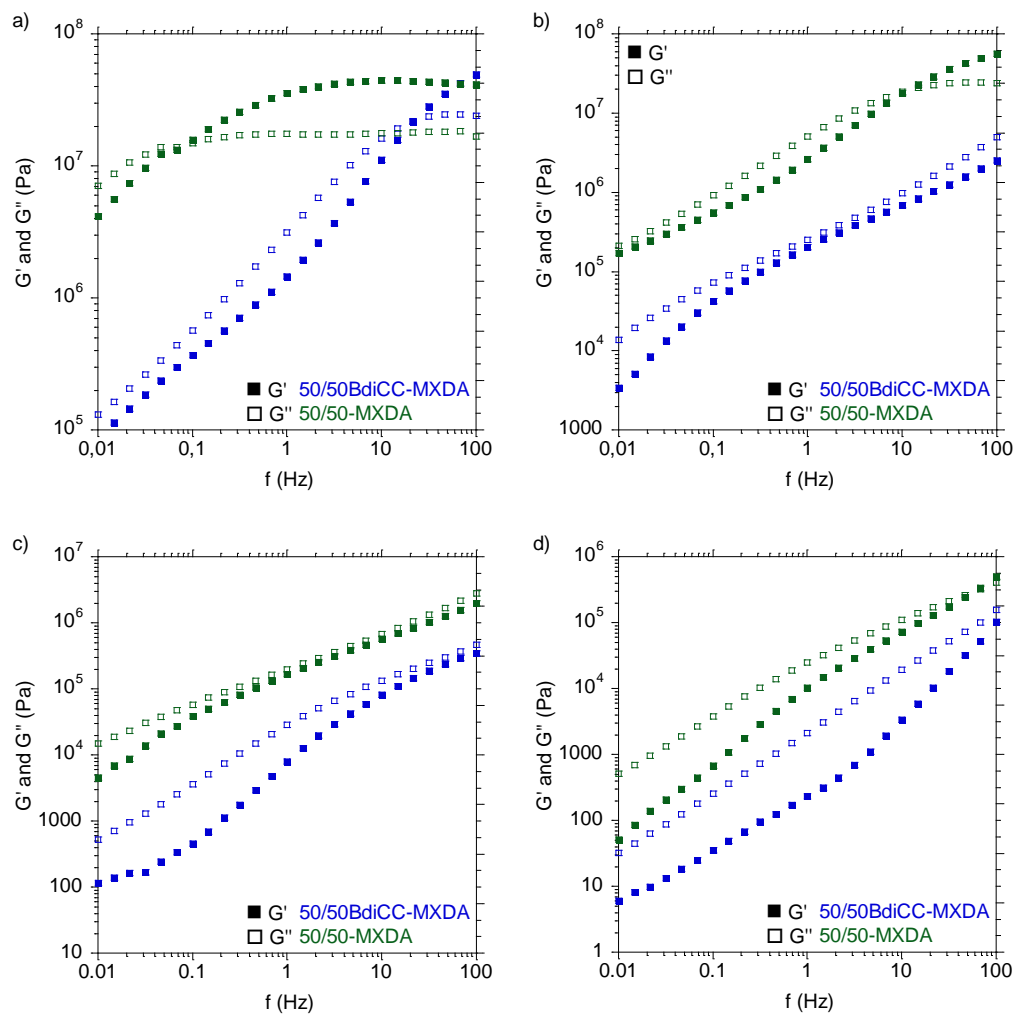


Figure A-II.31. G' and G'' values between 0.01 and 100 Hz of 50/50BdiCC-MXDA and 50/50-MXDA compositions at a) 10 °C b) 25 °C c) 50 °C d) 80 °C. Moduli of 50/50-MXDA are depicted once again for easier comparison.

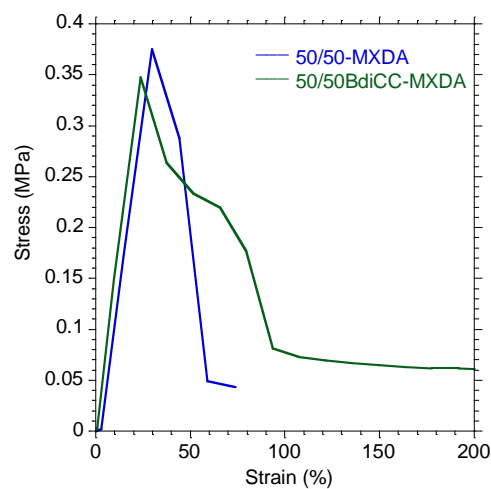


Figure A-II.32. Stress-strain curves for 50/50BdiCC-MXDA and 50/50-MXDA compositions at 80 °C. 50/50-MXDA curve is depicted for easier comparison.

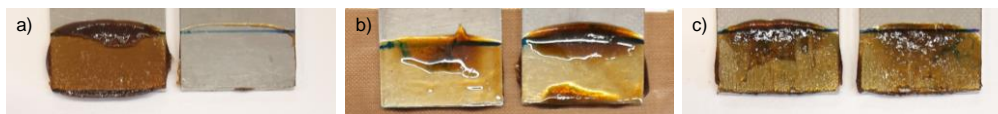


Figure A-II.33. Photos of the representative adhesion failure of 50/50BdiCC-MXDA a) applied at 100 °C, b) after a re-bonding at 100 °C and c) after a second re-bonding at 100 °C.

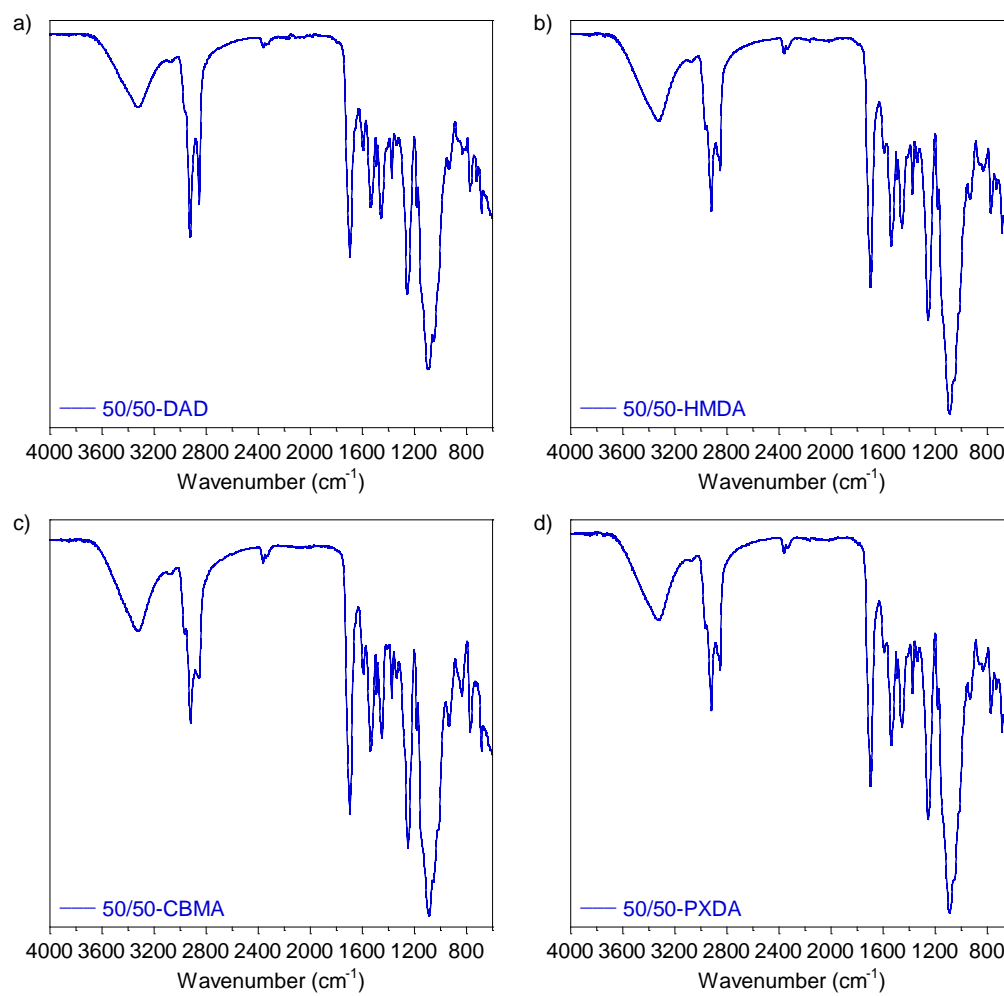


Figure A-II.34. FTIR-ATR spectra of a) 50/50-DAD, b) 50/50-HMDA, c) 50/50-CBMA and d) 50/50-PXDA compositions.

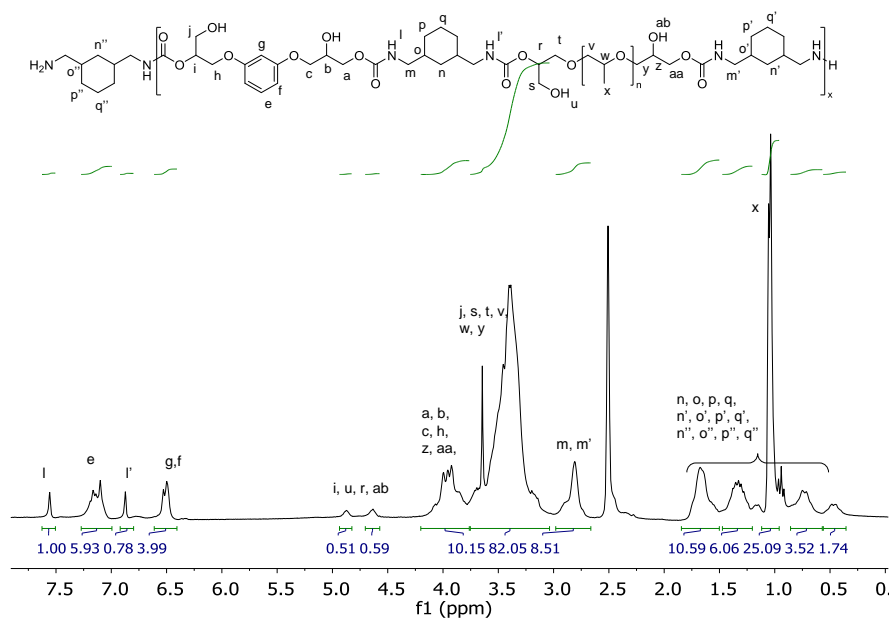


Figure A-II.35. ^1H NMR spectrum of 50/50-CBMA.

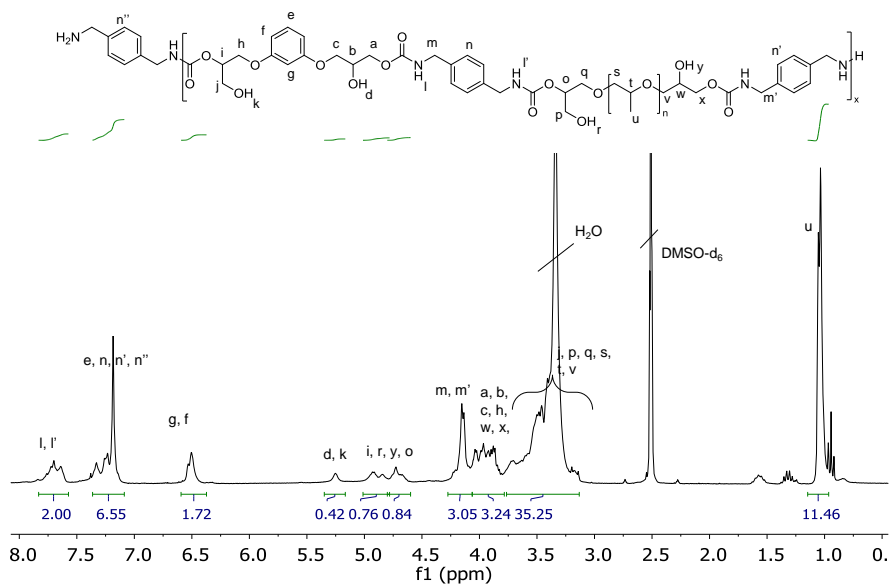


Figure A-II.36. ^1H NMR spectrum of 50/50-PXDA.

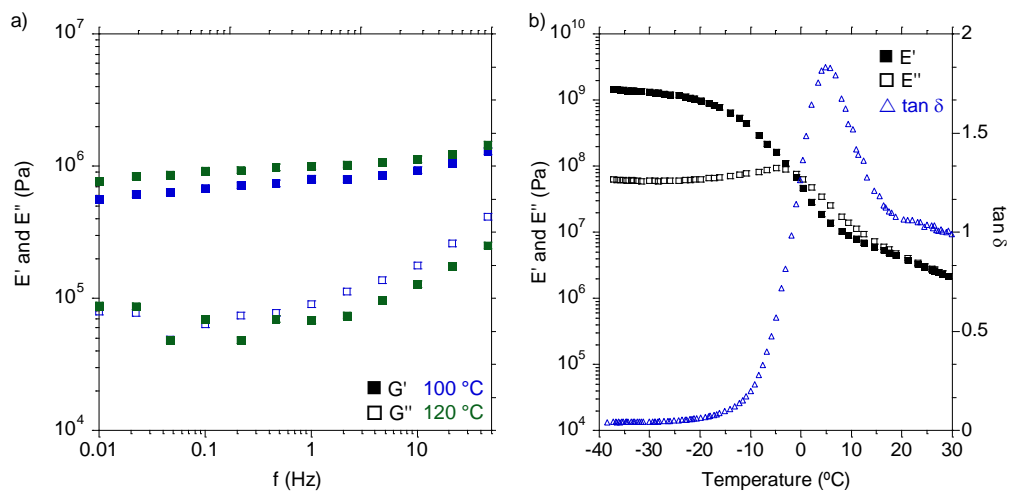


Figure A-II.37. a) E' and E'' values between 0.01 and 50 Hz of 50/50-DAD at 100 (blue) and 120 (green) °C and b) E' , E'' and $\tan \delta$ values of 50/50-HMDA from DMTA analysis. DMTA was employed to determine the glass transition temperature of the material.

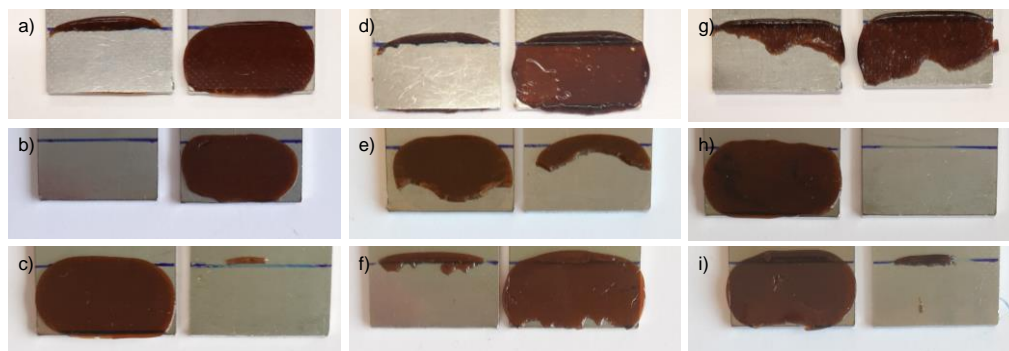


Figure A-II.38. Photos of the representative adhesion failure after lap-shear tests of a) 50/50-CBMA and b) 50/50-PXDA applied at 100 °C; c) 50/50-PXDA applied at 120 °C; d) 50/50-CBMA and e) 50/50-PXDA after a re-bonding at 100 °C; f) 50/50-PXDA after a re-bonding at 120 °C; g) 50/50-CBMA and h) 50/50-PXDA after a second re-bonding at 100 °C; i) 50/50-PXDA after a second re-bonding at 120 °C.

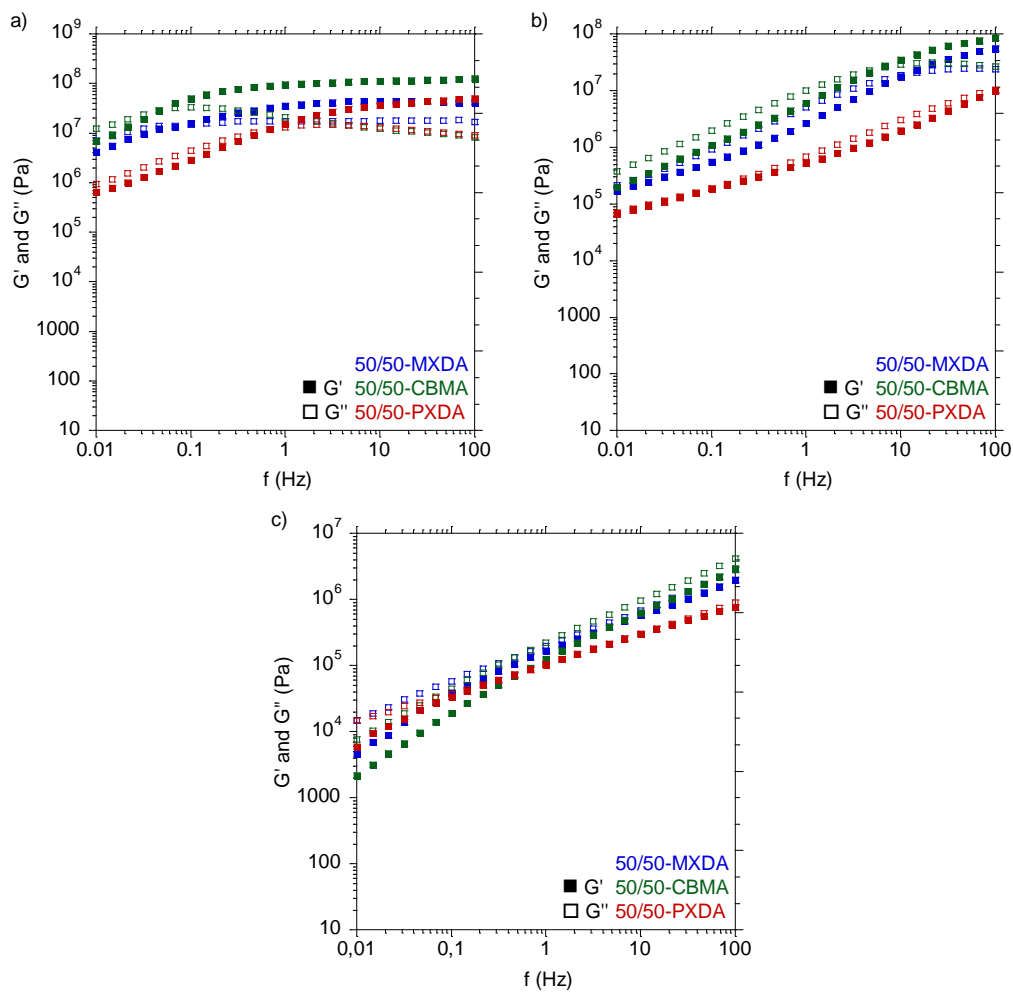


Figure A-II.39. G' and G'' values between 0.01 and 100 Hz of 50/50-MXDA, 50/50-CBMA and 50/50-PXDA compositions at a) 10 °C, b) 25 °C and c) 50 °C.

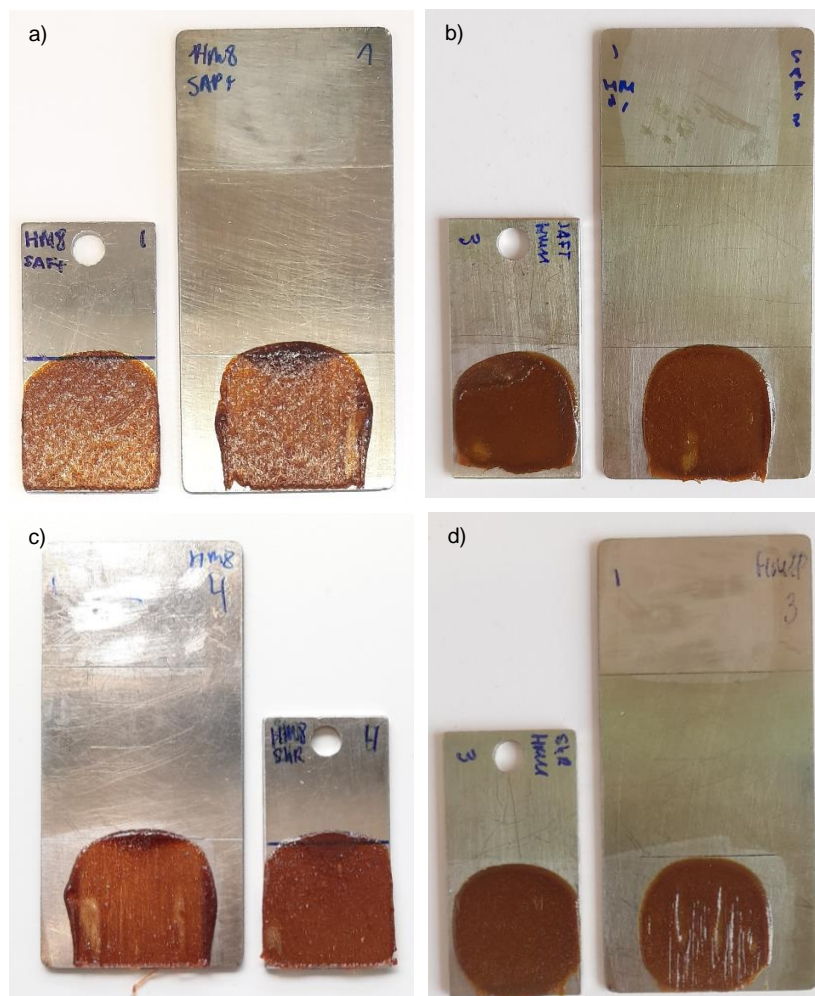


Figure A-II.40. Photos of the representative adhesion failure of a) 50/50-CBMA and b) 50/50-PXDA after SAFT tests and c) 50/50-CBMA and d) 50/50-PXDA after shear resistance measurements.



Figure A-II.41. Photos of the representative adhesion failure after lap-shear tests of 50/50-MXDA when it was applied onto a) oak, b) PE-HD and c) PMMA.

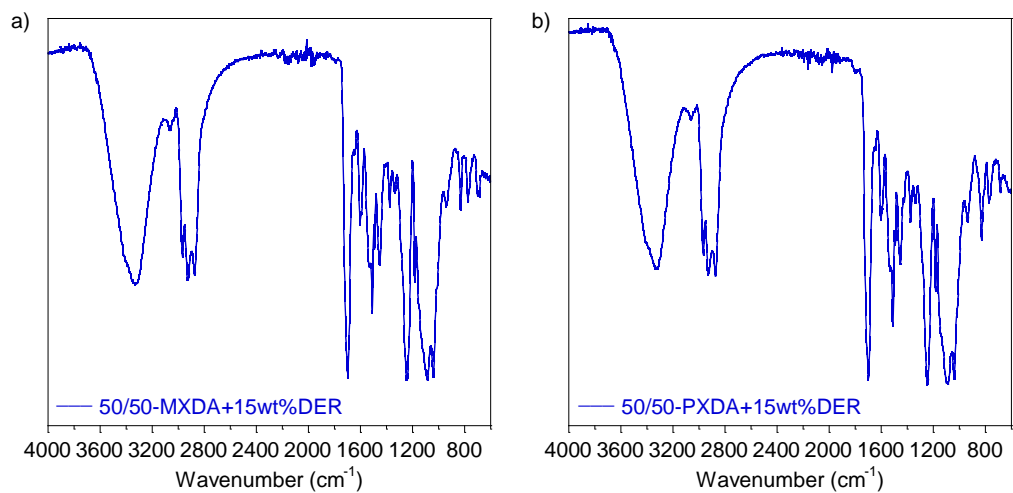


Figure A-II.42. FTIR-ATR spectra of a) 50/50-MXDA+15wt%DER and b) 50/50-PXDA+15wt%DER compositions.

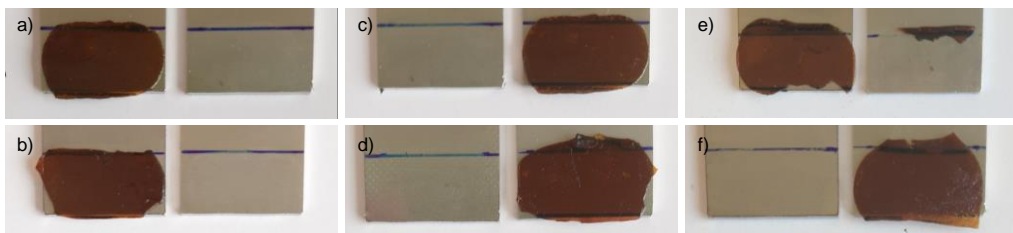


Figure A-II.43. Photos of the representative adhesion failure after lap-shear tests of a) 50/50-MXDA+15DER and b) 50/50-PXDA+15DER applied at 120 °C; c) 50/50-MXDA+15DER and d) 50/50-PXDA+15DER after re-bonding at 120 °C; e) 50/50-MXDA+15DER and f) 50/50-PXDA+15DER after a second re-bonding at 120 °C.

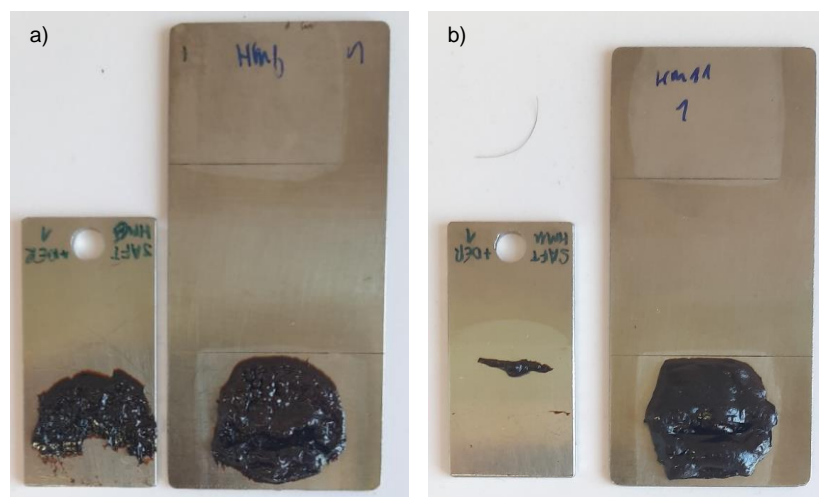


Figure A-II.44. Photos of the representative adhesion failure of a) 50/50-MXDA+15DER and b) 50/50-PXDA+15DER after SAFT tests. Adhesives showed this aspect because were in the oven at 217 °C for more than 7 h (a composition of Chapter 4 was evaluated at the same time in the oven).



References



- (1) Geyer, R.; Jambeck, J. R.; Law, K. L. Production, Use, and Fate of All Plastics Ever Made. *Sci. Adv.* **2017**, *3* (7), e1700782. <https://doi.org/10.1126/sciadv.1700782>.
- (2) MarketsandMarkets. *Polyurethane Adhesives Market by Resin Type (Thermoset & Thermoplastic), Technology (Solvent-Borne, 100% Solids, Dispersion), End-Use Industry (Automotive, Construction, Packaging, Footwear, Industrial, and Furniture), Region - Global Forecast to 2024; 2020*.
- (3) Bayer, O.; Siefken, W.; Rinke, H.; Orthner, L.; Schild, H. A Process for the Preparation of Polyurethanes or Polyureas. *DRP 728981*, 1937.
- (4) Szycher, M. Polyurethane Adhesives. In *Szycher's Handbook of Polyurethanes*; Szycher, M., Ed.; Taylor and Francis Group: Boca Raton, 2013; pp 393–416.
- (5) Karol, M. H.; Kramarik, J. A. Phenyl Isocyanate Is a Potent Chemical Sensitizer. *Toxicol. Lett.* **1996**, *89* (2), 139–146. [https://doi.org/10.1016/S0378-4274\(96\)03798-8](https://doi.org/10.1016/S0378-4274(96)03798-8).
- (6) Dhimiter, B.; Herrick, C. A.; Smith, T. T.; Woskie, S. R.; Streicher, R. P.; Cullen, M. R.; Liu, Y.; Redlich, C. A. Skin Exposure to Isocyanates: Reasons for Concern. *Environ. Health Perspect.* **2007**, *115* (3), 328–335. <https://doi.org/10.1289/ehp.9557>.
- (7) Barbhuiya, M.; Bhunia, S.; Kakkar, M.; Shrivastava, B.; Tiwari, P.; Gupta, S. Fine Needle Aspiration Cytology of Lesions of Liver and Gallbladder: An Analysis of 400 Consecutive Aspirations. *J. Cytol.* **2014**, *31* (1), 20–24. <https://doi.org/10.4103/0970-9371.130634>.
- (8) Slocombe, R. J.; Hardy, E. E.; Saunders, J. H.; Jenkins, R. L. Phosgene Derivatives. The Preparation of Isocyanates, Carbamyl Chlorides and Cyanuric Acid1. *J. Am. Chem. Soc.* **1950**, *72* (5), 1888–1891. <https://doi.org/10.1021/ja01161a009>.
- (9) Dyer, E.; Scott, H. The Preparation of Polymeric and Cyclic Urethans and Ureas from Ethylene Carbonate and Amines. *J. Am. Chem. Soc.* **1957**, *79* (3), 672–675. <https://doi.org/10.1021/ja01560a045>.
- (10) Carré, C.; Ecochard, Y.; Caillol, S.; Avérous, L. From the Synthesis of Biobased Cyclic Carbonate to Polyhydroxyurethanes: A Promising Route towards Renewable Non-Isocyanate Polyurethanes. *ChemSusChem* **2019**, *12* (15), 3410–3430. <https://doi.org/10.1002/cssc.201900737>.

-
- (11) Maisonneuve, L.; Lamarzelle, O.; Rix, E.; Grau, E.; Cramail, H. Isocyanate-Free Routes to Polyurethanes and Poly(Hydroxy Urethane)S. *Chem. Rev.* **2015**, *115* (22), 12407–12439. <https://doi.org/10.1021/acs.chemrev.5b00355>.
- (12) Khatoon, H.; Iqbal, S.; Irfan, M.; Darda, A.; Rawat, N. K. A Review on the Production, Properties and Applications of Non-Isocyanate Polyurethane: A Greener Perspective. *Prog. Org. Coatings* **2021**, *154* (September 2020), 106124. <https://doi.org/10.1016/j.porgcoat.2020.106124>.
- (13) Grignard, B.; Gennen, S.; Jérôme, C.; Kleij, A. W.; Detrembleur, C. Advances in the Use of CO₂ as a Renewable Feedstock for the Synthesis of Polymers. *Chem. Soc. Rev.* **2019**, *48* (16), 4466–4514. <https://doi.org/10.1039/C9CS00047J>.
- (14) Alves, M.; Grignard, B.; Mereau, R.; Jerome, C.; Tassaing, T.; Detrembleur, C. Organocatalyzed Coupling of Carbon Dioxide with Epoxides for the Synthesis of Cyclic Carbonates: Catalyst Design and Mechanistic Studies. *Catal. Sci. Technol.* **2017**, *7* (13), 2651–2684. <https://doi.org/10.1039/C7CY00438A>.
- (15) Kamphuis, A. J.; Picchioni, F.; Pescarmona, P. P. CO₂-Fixation into Cyclic and Polymeric Carbonates: Principles and Applications. *Green Chem.* **2019**, *21* (3), 406–448. <https://doi.org/10.1039/C8GC03086C>.
- (16) Guo, L.; Lamb, K. J.; North, M. Recent Developments in Organocatalysed Transformations of Epoxides and Carbon Dioxide into Cyclic Carbonates. *Green Chem.* **2021**, *23* (1), 77–118. <https://doi.org/10.1039/DoGC03465G>.
- (17) Aomchad, V.; Cristòfol, À.; Della Monica, F.; Limburg, B.; D'Elia, V.; Kleij, A. W. Recent Progress in the Catalytic Transformation of Carbon Dioxide into Biosourced Organic Carbonates. *Green Chem.* **2021**, *23* (3), 1077–1113. <https://doi.org/10.1039/DoGC03824E>.
- (18) Llevot, A.; Meier, M. Perspective: Green Polyurethane Synthesis for Coating Applications. *Polym. Int.* **2019**, *68* (5), 826–831. <https://doi.org/10.1002/pi.5655>.
- (19) Sonnenschein, M. F. Polyurethane Adhesives and Coatings. In *Polyurethanes: Science, Technology, Markets, and Trends*; Sonnenschein, M. F., Ed.; John Wiley & Sons, Ltd: New Jersey, 2015; pp 336–374. <https://doi.org/10.1002/9781118901274.ch10>.
- (20) Szycher, M. Structure-Property Relations in Polyurethanes. In *Szycher's Handbook of*

- Polyurethanes*; Szycher, M., Ed.; Taylor and Francis Group: Boca Raton, 2013; pp 37–86.
- (21) Szycher, M. Waterborne Polyurethanes. In *Szycher's Handbook of Polyurethanes*; Szycher, M., Ed.; Taylor and Francis Group: Boca Raton, 2013; pp 417–448.
- (22) Szycher, M. Radiation-Curable Adhesives and Coatings. In *Szycher's Handbook of Polyurethanes*; Szycher, M., Ed.; Taylor and Francis Group: Boca Raton, 2013; pp 495–522.
- (23) Petrie, E. M. Adhesive Classification. In *Handbook of adhesives and sealants*; Petrie, E. M., Ed.; McGraw-Hill: New York, 2000; pp 279–318.
- (24) Kim, B. K.; Lee, Y. M. Aqueous Dispersion of Polyurethanes Containing Ionic and Nonionic Hydrophilic Segments. *J. Appl. Polym. Sci.* **1994**, *54* (12), 1809–1815. <https://doi.org/10.1002/app.1994.070541204>.
- (25) Wang, H.; Shen, Y.; Fei, G.; Li, X.; Liang, Y. Micromorphology and Phase Behavior of Cationic Polyurethane Segmented Copolymer Modified with Hydroxysilane. *J. Colloid Interface Sci.* **2008**, *324* (1), 36–41. <https://doi.org/https://doi.org/10.1016/j.jcis.2008.04.068>.
- (26) Lee, H.-T.; Wu, S.-Y.; Jeng, R.-J. Effects of Sulfonated Polyol on the Properties of the Resultant Aqueous Polyurethane Dispersions. *Colloids Surfaces A Physicochem. Eng. Asp.* **2006**, *276* (1), 176–185. <https://doi.org/https://doi.org/10.1016/j.colsurfa.2005.10.034>.
- (27) Chattopadhyay, D. K.; Raju, K. V. S. N. Structural Engineering of Polyurethane Coatings for High Performance Applications. *Prog. Polym. Sci.* **2007**, *32* (3), 352–418. <https://doi.org/https://doi.org/10.1016/j.progpolymsci.2006.05.003>.
- (28) Chattopadhyay, D. K.; Webster, D. C. Hybrid Coatings from Novel Silane-Modified Glycidyl Carbamate Resins and Amine Crosslinkers. *Prog. Org. Coatings* **2009**, *66* (1), 73–85. <https://doi.org/https://doi.org/10.1016/j.porgcoat.2009.06.004>.
- (29) Ebnesajjad, S. Adhesives Technology Handbook. In *Adhesives Technology Handbook*; Ebnesajjad, S., Landrock, A. H., Eds.; Elsevier: London, 2009; pp 1–18. <https://doi.org/10.1115/1.3225943>.

-
- (30) Petrie, E. M. Surfaces and Surface Preparation. In *Handbook of adhesives and sealants*; Petrie, E. M., Ed.; McGraw-Hill: New York, 2000; pp 197–252.
- (31) Duncan, B. Developments in Testing Adhesive Joints. In *Advances in structural adhesive bonding*; Dillard, D. A., Ed.; Woodhead Publishing Limited: Cambridge, 2010; pp 389–436.
- (32) Ebnesajjad, S. Characteristics of Adhesive Materials. In *Handbook of adhesives and surface preparation*; Ebnesajjad, S., Ed.; Elsevier Ltd: Oxford, 2011; pp 137–183.
- (33) Ecochard, Y.; Caillol, S. Hybrid Polyhydroxyurethanes: How to Overcome Limitations and Reach Cutting Edge Properties? *Eur. Polym. J.* **2020**, *137*, 109915. <https://doi.org/https://doi.org/10.1016/j.eurpolymj.2020.109915>.
- (34) Leitsch, E. K.; Beniah, G.; Liu, K.; Lan, T.; Heath, W. H.; Scheidt, K. A.; Torkelson, J. M. Nonisocyanate Thermoplastic Polyhydroxyurethane Elastomers via Cyclic Carbonate Aminolysis: Critical Role of Hydroxyl Groups in Controlling Nanophase Separation. *ACS Macro Lett.* **2016**, *5* (4), 424–429. <https://doi.org/10.1021/acsmacrolett.6b00102>.
- (35) Tomita, H.; Sanda, F.; Endo, T. Polyaddition Behavior of Bis(Five- and Six-Membered Cyclic Carbonate)s with Diamine. *J. Polym. Sci. Part A Polym. Chem.* **2001**, *39* (6), 860–867. [https://doi.org/https://doi.org/https://doi.org/10.1002/1099-0518\(20010315\)39:6<860::AID-POLA1059>3.0.CO;2-2](https://doi.org/https://doi.org/https://doi.org/10.1002/1099-0518(20010315)39:6<860::AID-POLA1059>3.0.CO;2-2).
- (36) Schimpf, V.; Heck, B.; Reiter, G.; Mülhaupt, R. Triple-Shape Memory Materials via Thermoresponsive Behavior of Nanocrystalline Non-Isocyanate Polyhydroxyurethanes. *Macromolecules* **2017**, *50* (9), 3598–3606. <https://doi.org/10.1021/acs.macromol.7b00500>.
- (37) Cornille, A.; Michaud, G.; Simon, F.; Fouquay, S.; Auvergne, R.; Boutevin, B.; Caillol, S. Promising Mechanical and Adhesive Properties of Isocyanate-Free Poly(Hydroxyurethane). *Eur. Polym. J.* **2016**, *84*, 404–420. <https://doi.org/10.1016/j.eurpolymj.2016.09.048>.
- (38) Panchireddy, S.; Grignard, B.; Thomassin, J.-M.; Jerome, C.; Detrembleur, C. Catechol Containing Polyhydroxyurethanes as High-Performance Coatings and Adhesives. *ACS Sustain. Chem. Eng.* **2018**, *6* (11), 14936–14944.

- <https://doi.org/10.1021/acssuschemeng.8b03429>.
- (39) Tryznowski, M.; Gołofit, T.; Świdarska, A. Poly(Hydroxyurethane)s with Diethyl Tartrate-Based Amide Backbone by an Isocyanate-Free Route: Use as Adhesives. *Polymer (Guildf)*. **2018**, *144*, 1–6. <https://doi.org/10.1016/j.polymer.2018.04.041>.
- (40) Tryznowski, M.; Świdarska, A.; Gołofit, T.; Zołek-Tryznowska, Z. Wood Adhesive Application of Poly(Hydroxyurethane)s Synthesized with a Dimethyl Succinate-Based Amide Backbone. *RSC Adv.* **2017**, *7* (48), 30385–30391. <https://doi.org/10.1039/c7ra05455f>.
- (41) Xi, X.; Pizzi, A.; Delmotte, L. Isocyanate-Free Polyurethane Coatings and Adhesives from Mono- and Di-Saccharides. *Polymers (Basel)*. **2018**, *10* (4), 1–21. <https://doi.org/10.3390/polym10040402>.
- (42) Xi, X.; Wu, Z.; Pizzi, A.; Gerardin, C.; Lei, H.; Zhang, B.; Du, G. Non-Isocyanate Polyurethane Adhesive from Sucrose Used for Particleboard. *Wood Sci. Technol.* **2019**, *53* (2), 393–405. <https://doi.org/10.1007/s00226-019-01083-2>.
- (43) Sukumaran Nair, A.; Cherian, S.; Balachandran, N.; Panicker, U. G.; Kalambalayil Sankaranarayanan, S. K. Hybrid Poly(Hydroxy Urethane)s: Folded-Sheet Morphology and Thermoreversible Adhesion. *ACS Omega* **2019**, *4* (8), 13042–13051. <https://doi.org/10.1021/acsomega.9b00789>.
- (44) China National Standard GB/T 17657 - Test Methods for Evaluating the Properties of Wood-Based Panels and Surface Decorated Wood-Based Panels. 1999.
- (45) Tanigawa, M.; Kimura, K.; Takahashi, K.; Uruno, M.; Muto, K.; Hanada, K. Polyhydroxyurethane Resin, Polyhydroxyurethane Resin Composition Containing the Resin, and Adhesive. JP 6367769B2, 2018.
- (46) Muto, K.; Kimura, K.; Takahashi, K.; Uruno, M.; Tanigawa, M.; Minami, A. Method for Producing Polyhydroxyurethane Resin. JP 2017222760A, 2017.
- (47) Muto, K.; Kimura, K.; Takahashi, K.; Uruno, M.; Tanigawa, M.; Minami, A. Polyhydroxyurethane Resin, Hot Melt Adhesive Using the Resin, Molded Product and Laminate. JP 2020007406A, 2020.
- (48) Figovsky, O. L.; Shapovalov, L. D. Nonisocyanate Polyurethanes for Adhesives and

-
- Coatings. *First Int. IEEE Conf. Polym. Adhes. Microelectron. Photonics Incorporating POLY, PEP Adhasives Electron.* **2001**, 257–264. <https://doi.org/10.1109/polytr.2001.973291>.
- (49) Figovsky, O.; Shapovalov, L.; Birukova, O.; Leykin, A. Modification of Epoxy Adhesives by Hydroxyurethane Components on the Basis of Renewable Raw Materials. *Polym. Sci. - Ser. D* **2013**, 6 (4), 271–274. <https://doi.org/10.1134/S1995421213040047>.
- (50) Stroganov, I. V.; Stroganov, V. F. Peculiarities of Structurization and Properties of Nonisocyanate Epoxyurethane Polymers. *Polym. Sci. - Ser. C* **2007**, 49 (3), 258–263. <https://doi.org/10.1134/S1811238207030113>.
- (51) Lambeth, R. H.; Rizvi, A. Mechanical and Adhesive Properties of Hybrid Epoxy-Polyhydroxyurethane Network Polymers. *Polymer (Guildf)*. **2019**, 183, 121881. <https://doi.org/https://doi.org/10.1016/j.polymer.2019.121881>.
- (52) Anitha, S.; Vijayalakshmi, K. P.; Unnikrishnan, G.; Kumar, K. S. S. CO₂ Derived Hydrogen Bonding Spacer: Enhanced Toughness, Transparency, Elongation and Non-Covalent Interactions in Epoxy-Hydroxyurethane Networks. *J. Mater. Chem. A* **2017**, 5 (46), 24299–24313. <https://doi.org/10.1039/C7TA08243F>.
- (53) Diakoumakos, C. D.; Kotzev, D. L. Nanocomposites Based on Polyurethane or Polyurethane-Epoxy Hybrid Resins Prepared Avoiding Isocyanates. US 8143346B2, 2012.
- (54) Figovsky, O.; Shapovalov, L. D.; Blank, N.; Buslov, F. Method of Synthesis of Polyaminofunctional Hydroxyurethane Oligomers and Hybride Polymers Formed Therefrom. EP 1070733A1, 2001.
- (55) Figovsky, O.; Shapovalov, L. D.; Blank, N.; Buslov, F. Cyclocarbonate Groups Containing Hydroxyamine Oligomers From Epoxycyclocarbonates. US 6407198B1, 2002.
- (56) Figovsky, O.; Shapovalov, L. D. Preparation of Oligomeric Cyclocarbonates and Their Use in Nonisocyanate or Hybrid Nonisocyanate Polyurethanes. US 7232877B2, 2007.
- (57) Birukov, O.; Figovsky, O.; Leykin, A.; Shapovalov, L. D. Epoxy-Amine Composition Modified with Hydroxyalkylurethane. US 7898553B2, 2011.

- (58) Lammerschop, O.; Kinzelmann, H.-G. Two-Component Binder System with Cyclocarbonate and Epoxy Groups. US 10179871B2, 2019.
- (59) Brinker, C. J.; Scherer, G. W. *Sol-Gel Science: The Physics and Chemistry of Sol-Gel Processing*, 1st ed.; Academic Press, 1990.
- (60) Rossi de Aguiar, K. M. F.; Ferreira-Neto, E. P.; Blunk, S.; Schneider, J. F.; Picon, C. A.; Lepienski, C. M.; Rischka, K.; Rodrigues-Filho, U. P. Hybrid Urethanesil Coatings for Inorganic Surfaces Produced by Isocyanate-Free and Sol-Gel Routes: Synthesis and Characterization. *RSC Adv.* **2016**, *6* (23), 19160–19172. <https://doi.org/10.1039/C5RA24331A>.
- (61) Panchireddy, S.; Thomassin, J. M.; Grignard, B.; Damblon, C.; Tatton, A.; Jerome, C.; Detrembleur, C. Reinforced Poly(Hydroxyurethane) Thermosets as High Performance Adhesives for Aluminum Substrates. *Polym. Chem.* **2017**, *8* (38), 5897–5909. <https://doi.org/10.1039/c7py01209h>.
- (62) Panchireddy, S.; Grignard, B.; Thomassin, J.-M. M.; Jerome, C.; Detrembleur, C. Bio-Based Poly(Hydroxyurethane) Glues for Metal Substrates. *Polym. Chem.* **2018**, *9* (19), 2650–2659. <https://doi.org/10.1039/C8PY00281A>.
- (63) Cornille, A.; Auvergne, R.; Figovsky, O.; Boutevin, B.; Caillol, S. A Perspective Approach to Sustainable Routes for Non-Isocyanate Polyurethanes. *Eur. Polym. J.* **2017**, *87*, 535–552. <https://doi.org/10.1016/J.EURPOLYMJ.2016.11.027>.
- (64) Sardon, H.; Pascual, A.; Mecerreyes, D.; Taton, D.; Cramail, H.; Hedrick, J. L. Synthesis of Polyurethanes Using Organocatalysis: A Perspective. *Macromolecules* **2015**, *48* (10), 3153–3165. <https://doi.org/10.1021/acs.macromol.5b00384>.
- (65) Yuen, A.; Bossion, A.; Gómez-Bengoa, E.; Ruipérez, F.; Isik, M.; Hedrick, J. L.; Mecerreyes, D.; Yang, Y. Y.; Sardon, H. Room Temperature Synthesis of Non-Isocyanate Polyurethanes (NIPUs) Using Highly Reactive N-Substituted 8-Membered Cyclic Carbonates. *Polym. Chem.* **2016**, *7* (11), 2105–2111. <https://doi.org/10.1039/c6py00264a>.
- (66) Gennen, S.; Grignard, B.; Tassaing, T.; Jérôme, C.; Detrembleur, C. CO₂-Sourced α -Alkylidene Cyclic Carbonates: A Step Forward in the Quest for Functional Regioregular Poly(Urethane)s and Poly(Carbonate)s. *Angew. Chemie Int. Ed.* **2017**, *56* (35), 10394–

-
10398. <https://doi.org/10.1002/anie.201704467>.
- (67) Bossion, A.; Aguirresarobe, R. H.; Irusta, L.; Taton, D.; Cramail, H.; Grau, E.; Mecerreyes, D.; Su, C.; Liu, G.; Müller, A. J.; et al. Unexpected Synthesis of Segmented Poly(Hydroxyurea-Urethane)s from Dicyclic Carbonates and Diamines by Organocatalysis. *Macromolecules* **2018**, *51* (15), 5556–5566. <https://doi.org/10.1021/acs.macromol.8b00731>.
- (68) Blain, M.; Jean-Gérard, L.; Auvergne, R.; Benazet, D.; Caillol, S.; Andrioletti, B. Rational Investigations in the Ring Opening of Cyclic Carbonates by Amines. *Green Chem.* **2014**, *16* (9), 4286–4291. <https://doi.org/10.1039/C4GC01032A>.
- (69) Fleischer, M.; Blattmann, H.; Mühlhaupt, R. Glycerol-, Pentaerythritol- and Trimethylolpropane-Based Polyurethanes and Their Cellulose Carbonate Composites Prepared via the Non-Isocyanate Route with Catalytic Carbon Dioxide Fixation. *Green Chem.* **2013**, *15* (4), 934–942. <https://doi.org/10.1039/C3GC00078H>.
- (70) Cornille, A.; Ecochard, Y.; Blain, M.; Boutevin, B.; Caillol, S. Synthesis of Hybrid Polyhydroxyurethanes by Michael Addition. *Eur. Polym. J.* **2017**, *96*, 370–382. <https://doi.org/10.1016/J.EURPOLYMJ.2017.09.028>.
- (71) Türünç, O.; Kayaman-Apohan, N.; Kahraman, M. V.; Menceloğlu, Y.; Güngör, A. Nonisocyanate Based Polyurethane/Silica Nanocomposites and Their Coating Performance. *J. Sol-Gel Sci. Technol.* **2008**, *47* (3), 290–299. <https://doi.org/10.1007/s10971-008-1786-0>.
- (72) Assumption, H. J.; Mathias, L. J. Photopolymerization of Urethane Dimethacrylates Synthesized via a Non-Isocyanate Route. *Polymer (Guildf)*. **2003**, *44* (18), 5131–5136. [https://doi.org/10.1016/S0032-3861\(03\)00530-5](https://doi.org/10.1016/S0032-3861(03)00530-5).
- (73) Figovsky, O. L.; Shapovalov, L. D. Features of Reaction Amino-Cyclocarbonate for Production of New Type Nonisocyanate Polyurethane Coatings. *Macromol. Symp.* **2002**, *187* (1), 325–332. [https://doi.org/10.1002/1521-3900\(200209\)187:1<325::AID-MASY325>3.0.CO;2-L](https://doi.org/10.1002/1521-3900(200209)187:1<325::AID-MASY325>3.0.CO;2-L).
- (74) Sardon, H.; Irusta, L.; Fernández-Berridi, M. J.; Lansalot, M.; Bourgeat-Lami, E. Synthesis of Room Temperature Self-Curable Waterborne Hybrid Polyurethanes Functionalized with (3-Aminopropyl)Triethoxysilane (APTES). *Polymer (Guildf)*.

- 2010**, *51* (22), 5051–5057. <https://doi.org/10.1016/j.polymer.2010.08.035>.
- (75) Sardon, H.; Irusta, L.; Aguirresarobe, R. H.; Fernández-Berridi, M. J. Polymer/Silica Nanohybrids by Means of Tetraethoxysilane Sol–Gel Condensation onto Waterborne Polyurethane Particles. *Prog. Org. Coatings* **2014**, *77* (9), 1436–1442. <https://doi.org/https://doi.org/10.1016/j.porgcoat.2014.04.032>.
- (76) Kathalewar, M.; Sabnis, A. Novel Bis-Urethane Bis-Silane Precursor Prepared via Non-Isocyanate Route for Hybrid Sol-Gel Coatings. *Int. J. Sci. Eng. Res.* **2012**, *3* (8), 1–4.
- (77) Aguiar, K.; Ferreira-Neto, E.; Blunk, S.; Schneider, J.; Picon, C.; Lepienski, C.; Rischka, K.; Rodrigues Filho, U. Hybrid Urethanesil Coatings for Inorganic Surfaces Produced by Isocyanate Free and Sol-Gel Routes: Synthesis and Characterizations. *RSC Adv.* **2016**, *6*, 19160–19172. <https://doi.org/10.1039/C5RA24331A>.
- (78) Decostanzi, M.; Ecochard, Y.; Caillol, S. Synthesis of Sol-Gel Hybrid Polyhydroxyurethanes. *Eur. Polym. J.* **2018**, *109*, 1–7. <https://doi.org/10.1016/J.EURPOLYMJ.2018.08.054>.
- (79) Gennen, S.; Alves, M.; Méreau, R.; Tassaing, T.; Gilbert, B.; Detrembleur, C.; Jerome, C.; Grignard, B. Fluorinated Alcohols as Activators for the Solvent-Free Chemical Fixation of Carbon Dioxide into Epoxides. *ChemSusChem* **2015**, *8* (11), 1845–1849. <https://doi.org/10.1002/cssc.201500103>.
- (80) Licari, J. J.; Swanson, D. W. 3 - Chemistry, Formulation, and Properties of Adhesives. In *Materials and Processes for Electronic Applications*; Licari, J. J., Swanson, D. W. B. T.-A. T. for E. A., Eds.; William Andrew Publishing: Norwich, NY, 2005; pp 95–168. <https://doi.org/https://doi.org/10.1016/B978-081551513-5.50005-X>.
- (81) Froidevaux, V.; Negrell, C.; Caillol, S.; Pascault, J.-P.; Boutevin, B. Biobased Amines: From Synthesis to Polymers; Present and Future. *Chem. Rev.* **2016**, *116* (22), 14181–14224. <https://doi.org/10.1021/acs.chemrev.6b00486>.
- (82) Blain, M.; Cornille, A.; Boutevin, B.; Auvergne, R.; Benazet, D.; Andrioletti, B.; Caillol, S. Hydrogen Bonds Prevent Obtaining High Molar Mass PHUs. *J. Appl. Polym. Sci.* **2017**, *134* (45), 44958. <https://doi.org/https://doi.org/10.1002/app.44958>.
- (83) Peña-Alonso, R.; Rubio, F.; Rubio, J.; Oteo, J. L. Study of the Hydrolysis and Condensation of γ -Aminopropyltriethoxysilane by FT-IR Spectroscopy. *J. Mater. Sci.*

-
- 2007, 42 (2), 595–603. <https://doi.org/10.1007/s10853-006-1138-9>.
- (84) Bechtold, M. F.; Mahler, W.; Schunn, R. A. Polymerization and Polymers of Silicic Acid. *J. Polym. Sci. Polym. Chem. Ed.* **1980**, 18 (9), 2823–2855. <https://doi.org/10.1002/pol.1980.170180907>.
- (85) Colby, M. W.; Osaka, A.; Mackenzie, J. D. Effects of Temperature on Formation of Silica Gel. *J. Non. Cryst. Solids* **1986**, 82 (1), 37–41. [https://doi.org/https://doi.org/10.1016/0022-3093\(86\)90108-0](https://doi.org/https://doi.org/10.1016/0022-3093(86)90108-0).
- (86) Hurd, C. B.; Miller, P. S. Studies on Silicic Acid Gels. II. *J. Phys. Chem.* **1931**, 36 (8), 2194–2204. <https://doi.org/10.1021/j150338a009>.
- (87) Kaupmees, K.; Trummal, A.; Leito, I. Basicities of Strong Bases in Water: A Computational Study. *Croat. Chem. Acta* **2014**, 87 (4), 385–395. <https://doi.org/10.5562/cca2472>.
- (88) Peter, J. Hydrolysis of Esters of Oxy Acids:PKa Values for Strong Acids; Brønsted Relationship for Attack of Water at Methyl; Free Energies of Hydrolysis of Esters of Oxy Acids. *Can. J. Chem.* **1979**, 56 (17), 2342–2354.
- (89) Haynes, W. M. *CRC Handbook of Chemistry and Physics*, 97th ed.; Press., C., Ed.; 2016.
- (90) Coltrain, B. K.; Kelts, L. W. The Chemistry of Hydrolysis and Condensation of Silica Sol–Gel Precursors. In *The Colloid Chemistry of Silica*; Advances in Chemistry; American Chemical Society, 1994; Vol. 234, pp 19–403. <https://doi.org/doi:10.1021/ba-1994-0234.ch019>.
- (91) Gioia, C.; Banella, M. B.; Vannini, M.; Celli, A.; Colonna, M.; Caretti, D. Resorcinol: A Potentially Bio-Based Building Block for the Preparation of Sustainable Polyesters. *Eur. Polym. J.* **2015**, 73, 38–49. <https://doi.org/10.1016/j.eurpolymj.2015.09.030>.
- (92) Besse, V.; Foyer, G.; Auvergne, R.; Caillol, S.; Boutevin, B. Access to Nonisocyanate Poly(Thio)Urethanes: A Comparative Study. *J. Polym. Sci. Part A Polym. Chem.* **2013**, 51 (15), 3284–3296. <https://doi.org/10.1002/pola.26722>.
- (93) Burchardt, B. Advances in Polyurethane Structural Adhesive. In *Advances in structural adhesive bonding*; Dillard, D. A., Ed.; Woodhead Publishing Limited: Cambridge,

- 2010; pp 35–65. <https://doi.org/10.1017/CBO9781107415324.004>.
- (94) Rekondo, A.; Fernández-Berridi, M. J.; Irusta, L. Synthesis of Silanized Polyether Urethane Hybrid Systems. Study of the Curing Process through Hydrogen Bonding Interactions. *Eur. Polym. J.* **2006**, *42* (9), 2069–2080. <https://doi.org/10.1016/j.eurpolymj.2006.03.024>.
- (95) Burchardt, B. R.; Merz, P. W. Elastic Bonding and Sealing in Industry. In *Adhesives and Sealants*; Cognard, P. B. T.-H. of A. and S., Ed.; Elsevier Science Ltd: Oxford, 2006; Vol. 2, pp 355–xlii. [https://doi.org/https://doi.org/10.1016/S1874-5695\(06\)80017-5](https://doi.org/https://doi.org/10.1016/S1874-5695(06)80017-5).
- (96) SikaTack® DRIVE Product Data Sheet. Sika Schweiz AG: Zurich 2016.
- (97) Zhang, Y.; Hasegawa, K.; Kamo, S.; Takagi, K.; Ma, W.; Takahara, A. Enhanced Adhesion Effect of Epoxy Resin on Metal Surfaces Using Polymer with Catechol and Epoxy Groups. *ACS Appl. Polym. Mater.* **2020**, *2* (4), 1500–1507. <https://doi.org/10.1021/acsapm.9b01179>.
- (98) Tran, N. T.; Flanagan, D. P.; Orlicki, J. A.; Lenhart, J. L.; Proctor, K. L.; Knorr, D. B. Polydopamine and Polydopamine–Silane Hybrid Surface Treatments in Structural Adhesive Applications. *Langmuir* **2018**, *34* (4), 1274–1286. <https://doi.org/10.1021/acs.langmuir.7b03178>.
- (99) Patil, N.; Jérôme, C.; Detrembleur, C. Recent Advances in the Synthesis of Catechol-Derived (Bio)Polymers for Applications in Energy Storage and Environment. *Prog. Polym. Sci.* **2018**, *82*, 34–91. <https://doi.org/https://doi.org/10.1016/j.progpolymsci.2018.04.002>.
- (100) Hurd, C. B. Theories for the Mechanism of the Setting of Silicic Acid Gels. *Chem. Rev.* **1938**, *22* (3), 403–422. <https://doi.org/10.1021/cr60073a001>.
- (101) Gottardi, V.; Guglielmi, M.; Bertoluzza, A.; Fagnano, C.; Morelli, M. A. Further Investigations on Raman Spectra of Silica Gel Evolving toward Glass. *J. Non. Cryst. Solids* **1984**, *63* (1), 71–80. [https://doi.org/https://doi.org/10.1016/0022-3093\(84\)90387-9](https://doi.org/https://doi.org/10.1016/0022-3093(84)90387-9).
- (102) Chen, K. C.; Tsuchiya, T.; Mackenzie, J. D. Sol-Gel Processing of Silica: I. The Role of the Starting Compounds. *J. Non. Cryst. Solids* **1986**, *81* (1), 227–237.

[https://doi.org/https://doi.org/10.1016/0022-3093\(86\)90272-3](https://doi.org/https://doi.org/10.1016/0022-3093(86)90272-3).

- (103) Saiz-Poseu, J.; Mancebo-Aracil, J.; Nador, F.; Busqué, F.; Ruiz-Molina, D. The Chemistry behind Catechol-Based Adhesion. *Angew. Chemie Int. Ed.* **2019**, *58* (3), 696–714. <https://doi.org/10.1002/anie.201801063>.
- (104) Knorr, D. B.; Tran, N. T.; Gaskell, K. J.; Orlicki, J. A.; Woicik, J. C.; Jaye, C.; Fischer, D. A.; Lenhart, J. L. Synthesis and Characterization of Aminopropyltriethoxysilane-Polydopamine Coatings. *Langmuir* **2016**, *32* (17), 4370–4381. <https://doi.org/10.1021/acs.langmuir.6b00531>.
- (105) Viana, G.; Costa, M.; Banea, M. D.; da Silva, L. F. M. Water Diffusion in Double Cantilever Beam Adhesive Joints. *Lat. Am. J. Solids Struct.* **2017**, *14* (2), 188–201. <https://doi.org/10.1590/1679-78253040>.
- (106) Van Krevelen, D. W.; Te Nijenhuis, K. *Properties of Polymers*, 4th ed.; Elsevier B.V., 2009. <https://doi.org/10.1016/b978-0-08-054819-7.00027-3>.
- (107) Burchardt; Schulenburg, J. O.; Linnenbrink, M. New Building Blocks for Lightweight Structures. *Adhes. Adhes.* **2009**, *6* (4), 22–27. <https://doi.org/10.1007/BF03250462>.
- (108) Schulenburg, J. O.; Kramer, A. Structural Adhesives: Improvements in Vehicle Crash Performance. *SAE Trans.* **2004**, *113* (5), 111–114.
- (109) Figovsky, O. L.; Sklyarsky, L. S.; Sklyarsky, O. N. Polyurethane Adhesives for Electronic Devices. *J. Adhes. Sci. Technol.* **2000**, *14* (7), 915–924. <https://doi.org/10.1163/156856100742979>.
- (110) Figovsky, O.; Shapovalov, L.; Buslov, F. Ultraviolet and Thermostable Non-Isocyanate Polyurethane Coatings. *Surf. Coatings Int. Part B Coatings Trans.* **2005**, *88*, 67–71. <https://doi.org/10.1007/BF02699710>.
- (111) Figovsky, O.; Shapovalov, L.; Axenov, O. Advanced Coatings Based upon Non-Isocyanate Polyurethanes for Industrial Applications. *Surf. Coatings Int. Part B Coatings Trans.* **2004**, *87* (2), 83–90. <https://doi.org/10.1007/BF02699601>.
- (112) Figovsky, O.; Leykin, A.; Shapovalov, L. Non-Isocyanate Polyurethanes – Yesterday, Today and Tomorrow. *Altern. Energy Ecol.* **2016**, *4* (3–4), 95–108. <https://doi.org/10.15518/isjaee.2016.03-04.009>.

- (113) Ma, Z.; Li, C.; Fan, H.; Wan, J.; Luo, Y.; Li, B.-G. Polyhydroxyurethanes (PHUs) Derived from Diphenolic Acid and Carbon Dioxide and Their Application in Solvent- and Water-Borne PHU Coatings. *Ind. Eng. Chem. Res.* **2017**, *56* (47), 14089–14100. <https://doi.org/10.1021/acs.iecr.7b04029>.
- (114) Asemani, H.; Zareanshahraki, F.; Mannari, V. Design of Hybrid Nonisocyanate Polyurethane Coatings for Advanced Ambient Temperature Curing Applications. *J. Appl. Polym. Sci.* **2019**, *136* (13), 1–10. <https://doi.org/10.1002/app.47266>.
- (115) Lambeth, R. H. Progress in Hybrid Non-Isocyanate Polyurethanes. **2020**, No. July. <https://doi.org/10.1002/pi.6078>.
- (116) Ehlers, J.-E.; Rondan, N. G.; Huynh, L. K.; Pham, H.; Marks, M.; Truong, T. N. Theoretical Study on Mechanisms of the Epoxy–Amine Curing Reaction. *Macromolecules* **2007**, *40* (12), 4370–4377. <https://doi.org/10.1021/ma070423m>.
- (117) Rozenberg, B. A. Kinetics, Thermodynamics and Mechanism of Reactions of Epoxy Oligomers with Amines BT - Epoxy Resins and Composites II; Dušek, K., Ed.; Springer Berlin Heidelberg: Berlin, Heidelberg, 1986; pp 113–165.
- (118) Tcharkhtchi, A.; Nony, F.; Khelladi, S.; Fitoussi, J.; Farzaneh, S. 13 - Epoxy/Amine Reactive Systems for Composites Materials and Their Thermomechanical Properties; Boisse, P. B. T.-A. in C. M. and P. D., Ed.; Woodhead Publishing, 2015; pp 269–296. <https://doi.org/https://doi.org/10.1016/B978-1-78242-307-2.00013-0>.
- (119) Ramsdale-Capper, R.; Foreman, J. P. Internal Antiplasticisation in Highly Crosslinked Amine Cured Multifunctional Epoxy Resins. *Polymer (Guildf)*. **2018**, *146*, 321–330. <https://doi.org/https://doi.org/10.1016/j.polymer.2018.05.048>.
- (120) Hoyle, C. E.; Lowe, A. B.; Bowman, C. N. Thiol-Click Chemistry: A Multifaceted Toolbox for Small Molecule and Polymer Synthesis. *Chem. Soc. Rev.* **2010**, *39* (4), 1355–1387. <https://doi.org/10.1039/B901979K>.
- (121) Konuray, A. O.; Fernández-Francos, X.; Ramis, X. Analysis of the Reaction Mechanism of the Thiol–Epoxy Addition Initiated by Nucleophilic Tertiary Amines. *Polym. Chem.* **2017**, *8* (38), 5934–5947. <https://doi.org/10.1039/C7PY01263B>.
- (122) Carioscia, J. A.; Stansbury, J. W.; Bowman, C. N. Evaluation and Control of Thiol-Ene/Thiol-Epoxy Hybrid Networks. *Polymer (Guildf)*. **2007**, *48* (6), 1526–1532.

<https://doi.org/10.1016/j.polymer.2007.01.044>.

- (123) Jin, K.; Heath, W. H.; Torkelson, J. M. Kinetics of Multifunctional Thiol-Epoxy Click Reactions Studied by Differential Scanning Calorimetry: Effects of Catalysis and Functionality. *Polymer (Guildf)*. **2015**, *81*, 70–78. <https://doi.org/https://doi.org/10.1016/j.polymer.2015.10.068>.
- (124) Hill, L. W. Calculation of Crosslink Density in Short Chain Networks. *Prog. Org. Coatings* **1997**, *31* (3), 235–243. [https://doi.org/10.1016/S0300-9440\(97\)00081-7](https://doi.org/10.1016/S0300-9440(97)00081-7).
- (125) Hill, L. Structure/Property Relationships of Thermoset Coatings. *J. Coatings Technol.* **1992**, *64*, 28–42.
- (126) Ströbech, C. Polyurethane Adhesives. *Int. J. Adhes. Adhes.* **1990**, *10* (3), 225–228. [https://doi.org/https://doi.org/10.1016/0143-7496\(90\)90108-A](https://doi.org/https://doi.org/10.1016/0143-7496(90)90108-A).
- (127) MarketsandMarkets. *Hot Melt Adhesives (HMA) Market by Type (EVA, SBC, MPO, APAO, Polyamides, Polyolefines, Polyurethanes), Application (Packaging Solutions, Nonwoven Hygiene Products, Furniture & Woodwork, Bookbinding), and Region - Global Forecast to 2022*; 2017.
- (128) Utekar, P.; Gabale, H.; Khandelwal, A.; Mhaske, S. T. Hot-Melt Adhesives from Renewable Resources: A Critical Review. *Rev. Adhes. Adhes.* **2016**, *4* (1), 104–118. <https://doi.org/10.7569/RAA.2016.097303>.
- (129) Li, W.; Bouzidi, L.; Narine, S. S. Current Research and Development Status and Prospect of Hot-Melt Adhesives: A Review. *Ind. Eng. Chem. Res.* **2008**, *47* (20), 7524–7532. <https://doi.org/10.1021/ie800189b>.
- (130) Dahmane, H. Development of Environmentally Friendly Warm-Melt Adhesives for the Packaging Industry. *Int. J. Adhes. Adhes.* **1996**, *16* (1), 43–45. [https://doi.org/https://doi.org/10.1016/0143-7496\(96\)88485-5](https://doi.org/https://doi.org/10.1016/0143-7496(96)88485-5).
- (131) Paul, C. W. Hot-Melt Adhesives. *MRS Bull.* **2003**, *28* (6), 440–444. <https://doi.org/DOI:10.1557/mrs2003.125>.
- (132) Wongsamut, C.; Demleitner, M.; Suwanpreedee, R.; Altstädt, V.; Manuspiya, H. Copolymerization Approach of Soft Segment towards the Adhesion Improvement of Polycarbonate-Based Thermoplastic Polyurethane. *J. Adhes.* **2020**, 1–17.

- <https://doi.org/10.1080/00218464.2020.1786370>.
- (133) Gharde, S.; Sharma, G.; Kandasubramanian, B. Hot-Melt Adhesives: Fundamentals, Formulations, and Applications: A Critical Review. *Rev. Adhes. Adhes.* **2020**, *8* (1), 1–28. <https://doi.org/10.7569/RAA.2020.097301>.
- (134) Aguirresarobe, R. H.; Nevejans, S.; Reck, B.; Irusta, L.; Sardon, H.; Asua, J. M.; Ballard, N. Healable and Self-Healing Polyurethanes Using Dynamic Chemistry. *Prog. Polym. Sci.* **2021**, *114*, 101362. <https://doi.org/https://doi.org/10.1016/j.progpolymsci.2021.101362>.
- (135) Beniah, G.; Uno, B. E.; Lan, T.; Jeon, J.; Heath, W. H.; Scheidt, K. A.; Torkelson, J. M. Tuning Nanophase Separation Behavior in Segmented Polyhydroxyurethane via Judicious Choice of Soft Segment. *Polymer (Guildf)*. **2017**, *110*, 218–227. <https://doi.org/https://doi.org/10.1016/j.polymer.2017.01.017>.
- (136) Beniah, G.; Heath, W. H.; Torkelson, J. M. Functionalization of Hydroxyl Groups in Segmented Polyhydroxyurethane Eliminates Nanophase Separation. *J. Polym. Sci. Part A Polym. Chem.* **2017**, *55* (20), 3347–3351. <https://doi.org/https://doi.org/10.1002/pola.28722>.
- (137) Beniah, G.; Fortman, D. J.; Heath, W. H.; Dichtel, W. R.; Torkelson, J. M. Non-Isocyanate Polyurethane Thermoplastic Elastomer: Amide-Based Chain Extender Yields Enhanced Nanophase Separation and Properties in Polyhydroxyurethane. *Macromolecules* **2017**, *50* (11), 4425–4434. <https://doi.org/10.1021/acs.macromol.7b00765>.
- (138) Benedek, I. *Pressure-Sensitive Adhesives and Applications - Second Edition, Revised and Expanded*, 2nd ed.; Dekker, M., Ed.; CRC Press: Boca Raton, 2004. <https://doi.org/10.1201/9780203021163>.
- (139) Chirila, T. V.; Lee, H. H.; Oddon, M.; Nieuwenhuizen, M. M. L.; Blakey, I.; Nicholson, T. M. Hydrogen-Bonded Supramolecular Polymers as Self-Healing Hydrogels: Effect of a Bulky Adamantyl Substituent in the Ureido-Pyrimidinone Monomer. *J. Appl. Polym. Sci.* **2014**, *131* (4). <https://doi.org/https://doi.org/10.1002/app.39932>.
- (140) Osterwinter, C.; Schubert, C.; Tonhauser, C.; Wilms, D.; Frey, H.; Friedrich, C. Rheological Consequences of Hydrogen Bonding: Linear Viscoelastic Response of

-
- Linear Polyglycerol and Its Permethylated Analogues as a General Model for Hydroxyl-Functional Polymers. *Macromolecules* **2015**, *48* (1), 119–130. <https://doi.org/10.1021/ma501674x>.
- (141) Pan, Y.; Schubert, D. W.; Ryu, J. E.; Wujick, E.; Liu, C.; Shen, C.; Liu, X. Dynamic Oscillatory Rheological Properties of Polystyrene/Poly(Methyl Methacrylate) Blends and Their Composites in the Presence of Carbon Black. *Engineered Science*. 2018, pp 86–94. <https://doi.org/10.30919/es.180402>.
- (142) Santinath Singh, S.; Aswal, V. K.; Bohidar, H. B. Internal Structures of Agar-Gelatin Co-Hydrogels by Light Scattering, Small-Angle Neutron Scattering and Rheology. *Eur. Phys. J. E* **2011**, *34* (6), 62. <https://doi.org/10.1140/epje/i2011-11062-3>.
- (143) Irusta, L.; Iruin, J. J.; Fernández-Berridi, M. J.; Sobkowiak, M.; Painter, P. C.; Coleman, M. M. Infrared Spectroscopic Studies of the Self-Association of Ethyl Urethane. *Vib. Spectrosc.* **2000**, *23* (2), 187–197. [https://doi.org/https://doi.org/10.1016/S0924-2031\(00\)00059-X](https://doi.org/https://doi.org/10.1016/S0924-2031(00)00059-X).
- (144) Irusta, L.; L'Abée, M.; Iruin, J. J.; Fernández-Berridi, M. J. Infrared Spectroscopic Studies of the Urethane/Ether Inter-Association. *Vib. Spectrosc.* **2001**, *27* (2), 183–191. [https://doi.org/https://doi.org/10.1016/S0924-2031\(01\)00133-3](https://doi.org/https://doi.org/10.1016/S0924-2031(01)00133-3).
- (145) Zhang, K.; Chen, M.; Drummey, K. J.; Talley, S. J.; Anderson, L. J.; Moore, R. B.; Long, T. E. Ureido Cytosine and Cytosine-Containing Acrylic Copolymers. *Polym. Chem.* **2016**, *7* (43), 6671–6681. <https://doi.org/10.1039/C6PY01519K>.

List of Publications, Collaborations and Contributions



Part of this thesis has been published or will be published in a near future. The list of articles that would be issued from this work is as follows (the authors list and/or article title might be changed).

1. Monocomponent Non-Isocyanate Polyurethane Adhesives Based on a Sol–Gel Process. **Álvaro Gómez-López**, Bruno Grignard, Iñigo Calvo, Christophe Detrembleur and Haritz Sardon. *ACS Applied Polymer Materials*, **2020**, 2 (5), 1839-1847. <https://doi.org/10.1021/acsapm.0c00062>.

2. Synergetic Effect of Dopamine and Alkoxysilanes in Sustainable Non-Isocyanate Polyurethane Adhesives. **Álvaro Gómez-López**, Bruno Grignard, Iñigo Calvo, Christophe Detrembleur and Haritz Sardon. *Macromolecular Rapid Communications*, **2020**, 2000538, 1-9. <https://doi.org/10.1002/marc.202000538>.

3. Poly(Hydroxyurethane) Adhesives and Coatings: State-of-the-Art and Future Directions. **Álvaro Gómez-López**, Satyannarayana Panchireddy, Bruno Grignard, Iñigo Calvo, Christine Jérôme, Christophe Detrembleur and Haritz Sardon. *ACS Sustainable Chemistry and Engineering*, **2021**, 9 (29), 9541-9562. <https://doi.org/10.1021/acssuschemeng.1c02558>.

4. Trends in Non-Isocyanate Polyurethane (NIPU) Development. **Álvaro Gómez-López**, Fermin Elizalde, Iñigo Calvo and Haritz Sardon. Submitted.

5. Enhanced and Reusable Poly(Hydroxy Urethane)-Based Low-temperature Hot Melt Adhesives. **Álvaro Gómez-López**, Bruno Grignard, Lourdes Irusta, Iñigo Calvo, Alejandro J. Müller, Christophe Detrembleur, Haritz, Sardon. In preparation.

6. Fast-Curing Room Temperature Poly(Hydroxy Urethane)-Epoxy hybrid Adhesives. **Álvaro Gómez-López**, Bruno Grignard, Iñigo Calvo, Christophe Detrembleur and Haritz Sardon. In preparation.

Some other collaborations have been carried out and published or will be published soon.
(The authors list and/or article title might be changed)

1. 3D-Printed Bioplastics with Shape-Memory Behavior Based on Native Bovine Serum Albumin. Eva Sanchez-Rexach, Patrick T. Smith, **Álvaro Gómez-López**, Maxence Fernandez, Aitziber L. Cortajarena, Haritz Sardon and Alshakim Nelson. *ACS Applied Materials & Interfaces*, **2021**, 13 (16), 19193-19199. <https://doi.org/10.1021/acsami.0c22377>.

2. Insights on the Atmospheric-Pressure Plasma-Induced Free-Radical Polymerization of Allyl Ether Cyclic Carbonate Liquid Layers. Edyta M. Niemczyk, **Álvaro Gómez-López**, Jean R. N. Haler, Gilles Frache, Haritz Sardon and Robert Quintana. *Polymers*, **2021**, 13 (17), 2856. <https://doi.org/10.3390/polym13172856>.

3. Atmospheric-Pressure Plasma-Induced Free-Radical Polymerization of Allyl Ether 8-membered Cyclic Carbonate. Edyta M. Niemczyk, **Álvaro Gómez-López**, Haritz Sardon and Robert Quintana. In preparation.

Part of this work has been presented in national and international conferences.

Oral communications

1. Sustainable Adhesives Based on Non-Isocyanate Polyurethanes (NIPUs). Álvaro Gómez-López, Lourdes Irusta, Iñigo Calvo, Haritz Sardon. *6th Young Polymer Scientist Conference*, Donostia-San Sebastian, Spain, 2018.

2. Curing Process and Adhesive Properties of Sustainable Hybrid Non-Isocyanate Polyurethanes. Álvaro Gómez-López, Lourdes Irusta, Iñigo Calvo, Haritz Sardon. *VII International Baekeland Symposium*, Tarragona, Sapin, 2019.

Poster presentation

1. Sustainable Adhesives Based on Non-Isocyanate Polyurethanes (NIPUs). Álvaro Gómez-López, Lourdes Irusta, Iñigo Calvo, Haritz Sardon. *10th ECNP International Conference on Nanostructured Polymers and Nanocomposites*, Donostia-San Sebastian, Spain, 2018.

2. Curing Process of Sustainable Monocomponent Adhesive Based on Hybrid Non-Isocyanate Polyurethanes (NIPUs). Álvaro Gómez-López, Lourdes Irusta, Iñigo Calvo, Haritz Sardon. *13th International Conference on Advanced Polymers via Macromolecular Engineering*, Stellenbosch, South Africa, 2019.